MODELLING VEGETATION DYNAMICS AND THEIR FEEDBACKS OVER SOUTHERN AFRICA IN RESPONSE TO CLIMATE CHANGE FORCING

BY

GILLIAN DREW

Thesis Presented for the Degree of

DOCTOR OF PHILOSOPHY

in the Department of Environmental and Geographical Science

UNIVERSITY OF CAPE TOWN

2004

ABSTRACT

The importance of vegetation feedbacks to the atmosphere has been highlighted in many recent research studies. The influence of climate on vegetation has long been established, and climate has regularly been used to predict vegetation distribution. However, the influence of vegetation on climate is a relatively new research area. The need to understand vegetation-atmosphere interactions is growing in light of the increasing atmospheric carbon dioxide concentrations and the change in climate associated with these increases. These linkages are analysed over southern Africa with the use of sophisticated computer models of the climate and vegetation. The models are used to explore some of the vegetation-atmosphere interactions for this region, but without attempting a definitive study of either system. This study is therefore an initial exploration of what is a very complex issue that requires a vast amount of research.

The sensitivities of the vegetation and climate models to their input are tested. The MM5 regional climate model shows a significant sensitivity to a 20% change in surface albedo. This results in reduced transport of moisture into the interior of the sub-continent, which contributed towards increased temperatures over the interior. The Sheffield Dynamic Global Vegetation Model has been shown to accurately predict the vegetation distribution over southern Africa. The importance of fire is shown to influence the distribution of C_4 Grassland and Deciduous Broadleaf Trees, which are the main plant functional types found in savannahs. Increasing precipitation favours tree plant functional types, while decreasing precipitation allows for the expansion of C_4 Grasslands and desert encroachment. Increasing temperatures had a dramatic effect on the C_3 Grassland/Shrubland, causing a contraction of their spatial extent. However, the most important factor that will influence future vegetation distribution has been shown to be carbon dioxide. The increased carbon dioxide concentrations predicted for 2070-2099 will result in a dramatic encroachment of woody vegetation into the grasslands and savannahs of southern Africa.

At the moment, none of the current climate change predictions include a dynamic vegetation component that can respond to climate changes and feedback to the climate model. The changes in vegetation predicted here suggest that there will be changes in the feedbacks from the vegetation to the atmosphere, which will affect the climate. Future research should therefore focus on incorporating dynamic vegetation into climate models, preferably at a regional scale to assist impact studies. Policy makers and climate change impact researchers should therefore ensure that they use the most up-to-date climate change predictions available.

ACKNOWLEDGEMENTS

My sincerest thanks go to my supervisors:

- Assoc. Prof. Bruce Hewitson,
- Dr Guy Midgley

I would also like to thank the following people for their assistance:

- Prof. Ian Woodward and Dr Mark Lomas, University of Sheffield, for providing the SDGVM model and for all their guidance on aspects of running the model;
- Dr. Peter Holmes for advice at the beginning of my thesis;
- Mrs Shirley Butcher for help with the GIS work;
- Martin Ward for help with the data conversions;
- Ruwani Walawege and Chris Jack, for help with the MM5 climate model.
- My colleagues in CSAG, past and present, and especially Anne Barrable.

I am grateful to the National Research Foundation (NRF) for financial assistance, and to the Department of Arts, Culture, Science and Technology (DACST) for funding provided through the Seasonal Forecasting through Innovative Computing project. The Water Research Council (WRC) of South Africa also provided financial assistance through project K5/114

Finally, I would like to thank my family, especially Dad, Mineen and Tong, for all their support and encouragement throughout my academic career. This thesis is dedicated to my Dad, and to my grandfathers who would have been so proud.

CONTENTS

SECTION 1:

BACKGROUND

CHAPTER 1: CLIMATE AND VEGETATION INTERACTIONS

1.1 Introduction

The African continent is characterised by a high diversity of both its climates and vegetation. Dissected by the equator and spanning the tropics in both hemispheres, the continent is therefore characterised by a range of different climates, ranging from the dry, hot deserts of the Sahara and Namib, to the moist tropical climates of the central region, where rainforests flourish (White, 1983). It is however, hampered by poverty and war, making African society particularly vulnerable to additional impacts from changing climates. Appropriate responses to changing conditions are not possible due to the limitations of these developing economies (Pronk, 2002). Furthermore, the lack of technological development in many areas means that Africa's people are heavily reliant on natural resources for survival; for example, agriculture is often on a subsistence basis, without any technology such as fertilisers or irrigation, and most often energy needs are met from biomass such as wood and cattle dung (Tyson *et al*, 2002), which can have a devastating impact on the natural vegetation.

The southern African regional climate system in particular displays a high degree of inter-annual variability, with consequent societal vulnerability. The January 2000 floods in Mozambique and northern South Africa, and the widespread drought of the early 1980s clearly demonstrate the extremes that the sub-continent is prone to, and it is these extremes that scientists predict will increase in the future (Tyson *et al*, 2002). Of the contributing processes principally focussed on by atmospheric scientists, the El Niño Southern Oscillation (ENSO) phenomenon is the primary forcing agent, and is known to explain up to 25% of rainfall variability over South Africa (Tyson and Preston-Whyte, 2000). The role of sea surface temperatures, and, in particular, a temperature dipole in the Indian Ocean, in modulating rainfall over Africa has been the focus of recent studies (Tyson and Preston-Whyte, 2000; Behera and Yamagata, 2001; Reason, 2001). Warm sea surface temperatures

south of Madagascar, coupled with cool sea surface temperatures off western Australia, are linked to enhanced rainfall over south eastern Africa (Reason, 2001). The dipole pattern has been shown to explain a further 12% of the total variance in southern Africa rainfall (Behera and Yamagata, 2001). The remaining large uncertainties on what contributes to rainfall variability remain largely unknown.

One possible further cause of rainfall variability is the feedback from the land-surface and vegetation to the atmosphere. The importance of vegetation feedbacks at sub-continental scales has been recognised by the Intergovernmental Panel on Climate Change (IPCC) (IPCC, 2001). For example, studies in the Sahel suggest that the land-surface may have played a role in the dessication of the region (Charney, 1975; Charney *et al*, 1975, 1977). A more recent study of biosphere-atmosphere interactions in the Sahel is that of Zeng *et al* (1999), which undertook a series of model experiments aimed at determining the contribution of three processes to climate variability, namely, oceanic forcing (sea surface temperatures), land-surface processes (soil moisture and hydrology) and vegetation processes. Their results show that only the experiment that includes all three processes accurately captures the inter-annual variability of precipitation in the region, and the interactive vegetation feedback enhances the rainfall variability originating from sea surface temperature variations.

At finer scales, Marshall *et al* (2003) have shown that the change from wetland to agricultural land in South Florida has resulted in the increase in frequency of crop damaging freeze events. Stohlgren *et al* (1998) have shown that increasing the amount of land under irrigated crops in north-central Colorado, United States, resulted in decreased summer temperatures and increased precipitation. The change from natural vegetation (grassland) and dryland crops to irrigated crops decreased surface albedo, and increased roughness length and soil moisture. This enhanced exchanges of energy and moisture between the atmosphere and the land surface. However, as the albedo was lower, less heat was transferred to the

atmosphere, but the increased soil moisture allowed more water vapour to evaporate and transpire, resulting in cooler and moister conditions. Further evidence for the influence of local land use changes on regional climate can be found in Chase *et al* (1999), Eastman *et al* (2001) and Pielke (2001a)

In response to the above issues this thesis seeks to enhance current understanding of the coupled atmosphere-biosphere systems over Africa south of the equator. This is done by using both vegetation and climate models to explore the dynamics of these systems. This thesis does not attempt a definitive study of either of them, as such a study is beyond the scope of this work, but rather elucidates initial understanding of these issues in order to lay a foundation for further research.

The balance of this chapter describes the current vegetation and climate of the region and highlights the dominant factors influencing interactions between these two systems. Using this as a framework, the objectives of the thesis are then outlined.

1.2 African Climate: Past, Present and Future

1.2.1 Present Climate

As noted above, the African climate is characterised by a high degree of variability, in both space and time. The climate varies from temperate in the far south, through sub-tropical, tropical, equatorial and even deserts. A detailed description of the climate of southern Africa can be found in Tyson and Preston-Whyte (2000).

The atmospheric processes over Southern Africa are dominated by a belt of subsiding air from the Hadley cell, which is situated between the South Atlantic and the Indian Ocean high-pressure cells. Temperatures are generally high, with large diurnal variations (Nicholson, 2001), but it is the region's rainfall that is particularly subject to both spatial and temporal variations. The southern tip of Africa experiences winter rainfall, related mainly to the passage of mid-latitude cyclones, or

cold fronts. Further north, and to the east, rainfall is concentrated to the summer months, most often in the form of large convective thunderstorms (Tyson, 1986). The western regions of South African and Namibia are considerably drier than the eastern regions. West African rainfall is strongly influenced by the movement of a Monsoon Trough, and therefore displays many similarities to the climate of south Asia (Barry and Chorley, 2003). The equatorial and tropical regions are strongly influence by the presence and movement of the Inter-Tropical Convergence Zone (ITCZ), which produces two rainy seasons (Semazzi and Song, 2001).

Rainfall over much of southern Africa is particularly prone to large inter-annual variations, and the processes underlying this variability have been the subject of much research recently, but are still not well understood. It has been suggested that the oceans (sea surface temperatures and the El Niño Southern Oscillation) and the land-surface both play a prominent role, but both are not fully understood and are poorly represented in general circulation model (GCM) predictions of African climate (Hulme *et al*, 2001).

In terms of contributions to global climate variability, only the seasonal cycle and monsoon systems contribute more than the El Niño Southern Oscillation (ENSO) phenomenon (Allan, 2000), but the relationship between the ENSO and southern African climate is more complex. The ENSO phenomenon is known to have a particularly strong influence on the climates of equatorial east Africa (high rainfall during a warm ENSO event) and southern Africa (low rainfall during a warm ENSO event), but the link between ENSO events and west African rainfall is not as clear (Nicholson, 2001). The ENSO phenomenon does show a strong correlation with southern African rainfall, but does not explain all the variability that is seen in regional precipitation patterns. The Atlantic and Indian Oceans adjacent to the continent also strongly affect the climate of the continent. Recent research has shown a link between south central African precipitation and a temperature dipole in the Indian Ocean. A warm anomaly to the south of Madagascar, coupled with cooler

sea surface temperatures off western Australia results in increased rainfall over south eastern Africa (Behera and Yamagata, 2001; Reason, 2001). However, the interactions between the oceans and the atmosphere do not explain all the variability seen in southern African rainfall patterns.

While the above gives a clear picture of the large scale governing processes, the smaller scale interactions between the land-surface and the atmosphere are increasingly seen as important in contributing to the precipitation variability in the region, and have been shown to be particularly important over West Africa, where considerable information exists suggesting a feedback between the land and the atmosphere that may play a significant role in determining rainfall for this region (Nicholson, 1997). Albedo changes, caused by the exposure of highly reflective soils after the destruction of vegetation, have been suggested as far back as the 1970s (for example, Charney, 1975) as possible causes of extended drought in the region. A study by Semazzi and Song (2001), where the tropical rainforest in central Africa was replaced by savannah grassland, showed that deforestation caused a significant reduction in rainfall, and delayed the onset of the rainy seasons. Through the process of teleconnection, the deforestation in the equatorial regions was also found to affect rainfall over southern Africa. Within the deforestation region, increases in temperature were also noted due to the reduction in evapotranspiration. Although this is an extreme case of vegetation cover change, is does indicate the important role that vegetation plays in the climate system, over Africa, and parallels the findings of Lawton *et al* (2001), who showed that deforestation of a montane cloud forest in Costa Rica resulted in a reduction in the amount of cumulus cloud that developed over the deforested areas. This was caused by the reduction of evapotranspiration, which lowered the atmospheric moisture content and lifted the cloud base. Similar results were found by Dirmeyer and Shukla (1994) for South America, where rainforest was replaced by grassland in a modelling simulation.

Recently, studies focussing on the relationship between vegetation and climate over South Africa have indicated a significant sensitivity of vegetation to precipitation forcing (Shannon, 2000). Furthermore, a strong feedback role on regional atmospheric moisture processes is suggested, especially over the summer rainfall region, but this study was limited by the weak representation of vegetation types, the absence of CO_2 fertilisation effects on vegetation growth and evapotranspiration, and the lack of a disturbance sub-model (most notably fire) in the vegetation model. Despite these limitations, the linkages suggested are particularly important when considered in the context of the highly variable climate system, and especially regional vulnerability to predicted climate change scenarios. This serves to emphasise the critical need to understand the role of the landscape, and vegetation in particular.

It is commonly perceived that sea-surface temperature is the major driver of precipitation across the subcontinent, with probable marginal control by feedback from vegetation to regional climate. Recent research has shown that local vegetation change at a scale as small as the landscape can influence the local and regional development of weather systems (Betts *et al*, 1997; Chase *et al*, 2000; Zhao *et al*, 2001). These views represent an important contrast that needs to be resolved before accurate medium and long-range predictions of southern African climate can be made, and emphasise the need for modelling systems incorporating feedbacks between the atmosphere, the ocean and the land-surface/vegetation.

1.2.2 Past Climate Change

Modelling studies of past climates can be used to evaluate model accuracy, as past climate changes are fairly well documented, depending on how far back one goes. During the mid-Holocene, vegetation changes over North Africa were shown to have an affect on the monsoons in the region (Kutzbach *et al*, 1996), and ocean and vegetation processes are needed to introduce the feedbacks necessary to explain observed monsoon changes (McAvaney *et al*, 2001). The expansion of the boreal

forests during the mid-Holocene caused an increase in both temperature and precipitation by changing the albedo and radiation absorption (Foley *et al*, 1994). Without the expansion of the boreal forests, the warming in the mid-Holocene predicted by models is not in line with evidence from palaeo-studies. The inclusion of the boreal forest expansion in modelling studies was shown to increase the temperature to a value much closer to the evidence (Foley *et al*, 1994). Studies have also shown that the southward migration of the boreal forest/tundra boundary changed the albedo of the region and may have been involved in the initiation of the last ice age 115 000 years ago (Noblet *et al*, 1996). The importance of vegetation in influence climate, even in the past, is shown by these studies, and further shows that the biosphere-atmosphere interactions are not confined to the present, but have occurred in the past, and will continue in the future.

1.2.3 Current and Future Climate Changes

In light of the fact that atmosphere-biosphere interactions occurred in the past, and currently occur, it is useful to consider how they might interact in the future, and we must therefore first have some indication of how climate is changing, and how it may change in the future. Global mean warming for the twentieth century has been calculated at 0.6°C, with a distinct anthropogenic signal (IPCC, 2001). However, this global figure does not fully express the regional variations. According to Hulme *et al* (2001), the African climate is warmer than it was 100 years ago, and has been warming at a rate of 0.5°C per century through the 20th century. The six warmest years on record have all occurred since 1987, with 1998 being the warmest. These figures are consistent with global warming figures. Most of the continent displays this warming trend, apart from some coastal areas (Nigeria/Cameroon and South Africa) where some cooling is evident (Hulme *et al*, 2001). Equatorial Africa has experienced an increase in rainfall of up to 10% per century over the last 100 years, but most of the continent has seen a decrease in rainfall, particularly in the Sahel, and the region around Botswana, Zimbabwe and northern South Africa. According

to Nicholson (2001), rainfall across most of Africa was below normal throughout the 1980s and 1990s.

For the future, calculations by Hulme *et al* (2001) of temperature change suggest warming over Africa of 0.2 – 0.5°C per decade for the period leading up to 2071-2100. The greatest warming will occur in the semi-arid regions of the Sahel and southern Africa, with the least warming in the equatorial regions and coastal zones. Minimum temperatures are expected to increase more than maximum temperatures (Giorgi *et al*, 2001).

Predictions of future rainfall changes are more complex than predictions of temperature change, and vary between different GCMs used for the predictions. This may be partly because the GCMs do not appear to simulate ENSO events very accurately, which in turn affects the models' ability to simulate rainfall variability. The complexity of relationships between African rainfall, ocean process and the land-surface is also not fully understood, and can therefore not be accurately modelled by current GCMs. This increases uncertainty in model projections of future climate change. For example, it is generally believed that a warmer atmosphere will result in increased atmospheric water vapour, thereby increasing cloud cover and possibly inducing more rainfall (Dickinson, 1986), but many other factors may have a stronger influence. However, there are three predictions that can be made. Firstly, summer precipitation will increase in tropical Africa; secondly, any increases in precipitation will very likely lead to an increase in precipitation variability; and finally, the frequency of extreme events (droughts and floods) is likely to increase and they may become more intense (IPCC, 2001). However, the impact of land surface processes on the climate has not been included into any of the current climate change scenarios, which could result in significant changes to current predictions.

1.3 African Vegetation

In view of the potential of vegetation to strongly modulate regional climates, a baseline current distribution of vegetation is required before one can assess how the change in climate could give rise to new patterns of vegetation in the future. White (1983) states that Africa has a more diversified flora than any other region of equivalent area, and studies in regions such as the Eastern Arc, Tanzania, western Cape and semi-arid Namib regions, and tropical forests have shown that these areas support extremely high regional plant species richness (e.g. Cowling and Hilton-Taylor, 1997). South Africa alone contains about 20 000 plant species, and thus renders the task of characterising African vegetation according to floristic categorisations extremely difficult (Cowling *et al,* 1997).

There have been several studies that attempted to classify the vegetation of Africa, but many of them cover different spatial domains. The area of these studies is usually confined to political boundaries, such as the work of Acocks (1988), which describes the vegetation of South Africa. The study by White (1983) is one of the few published maps that describes the vegetation of the whole of Africa (Figure 1.1). As the domain for this study includes the whole of Africa south of equator, an accurate, up-to-date description of the vegetation of this entire domain is hard to come by. The vegetation descriptions that are available will be discussed below.

White (1983) describes the distinguishing features of sixteen major vegetation types in Africa. Acocks (1988) describes the vegetation of South Africa in terms of veld types, which is a unit of vegetation whose range of variation is small enough to permit the whole of it to have the same farming potentialities. Thus, the primary aim behind this work was to describe vegetation in terms of its agricultural potential, in order to facilitate farm management. Acocks (1988) recognised 7 broad vegetation types, divided into 70 veld types, with 75 variations. Such a scheme is not useful in the context of this study, as it is too complex.

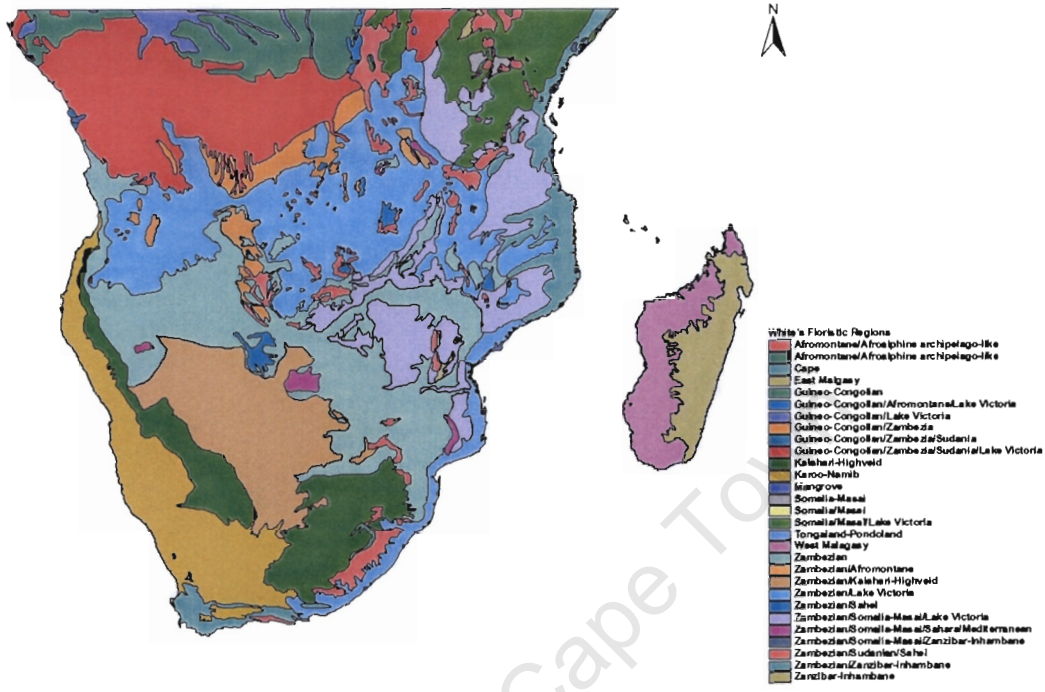

Figure 1.1: The distribution of floristic kingdoms in Africa south of the Equator according to White (1983).

The concept of biomes has also been widely used. Rutherford and Westfall (1994) used biomes to classify the vegetation of southern Africa, and define a biome as a broad ecological unit that represents a major life zone extending over a natural area. This is essentially a structural characterisation, in which a link between structure and function is seen as the underlying principle. In this approach, the vegetation of southern Africa may be divided into six biomes, namely Forest, Savannah, Grassland, Nama Karoo, Succulent Karoo and Fynbos. The work of Low and Rebelo (1996) provides a broad overview of the vegetation types in South Africa, Lesotho and Swaziland. This work contains an additional biome to those described by Rutherford and Westfall (1994), the Thicket Biome, which describes the vegetation that replaces forest where rainfall is low. The most recent and comprehensive account of vegetation in southern Africa is that of Cowling *et al*

(1997), which again uses the concept of biomes. Table 1.1 shows a comparison of the nomenclature used in these works. The classifications shown reveal that there are several vegetation types that are important in the region. Following this approach, a brief description of each biome is given below.

1.3.1 Biomes of southern Africa

In order to describe the structure of the dominant biomes in this region effectively, it is important to highlight the two dominant photosynthetic functional types that occur in this region, distinguished by the pathway used to fix carbon during photosynthesis. These functional types provide important insights into the relative performance of different structural types across the subcontinent. Plants using the Calvin-Benson (C_3) photosynthesis pathway form a 3-carbon compound during primary fixation of carbon (Jones, 1992). The complete photosynthesis process occurs in all cells in a leaf, with a consequent loss of carbon during the reverse process, photorespiration, which also occurs in all cells. Because of this limitation, the C_3 pathway is relatively inefficient, except under high atmospheric CO_2 concentrations, when photorespiration is suppressed. The C_3 pathway is the pathway used by virtually all woody plants in southern Africa, and is common in grasses only in cool, moist and temperate habitats (Jones 1992). Plants following the Hatch-Slack (C_4) pathway, by contrast, form a 4 carbon organic acid during photosynthesis. This compound is transported within the system to specialised cells where final photosynthesis occurs and any CO_2 released during photorespiration is re-fixed, making this a more efficient system (Jones, 1992). The C_4 pathway is common in tropical and semi-arid environments, due mainly to its increased efficiency at higher temperatures.

Table 1.1: The nomenclature used in publications describing the vegetation of Africa and southern Africa.

	Acocks (1988)	**White (1983)**	**Rutherford and Westfall (1994)**	**Low and Rebelo (1996)**	**Cowling *et al* (1997)**
1	Coastal tropical forest types	Afroalpine vegetation	Desert		Desert
2	Inland tropical forest types	Anthropic landscapes	Forest	Forest	Forest
3	Tropical bush and savannah types (bushveld)	Bamboo	Fynbos	Fynbos	Fynbos
4	False bushveld types	Bushland	Grassland	Grassland	Grassland
5	Karoo and Karroid types	Desert	Nama-Karoo	Nama-Karoo	Nama-Karoo
6	False Karoo types	Forest	Savannah	Savannah	Savannah
7	Temperate and transitional forest and scrub types	Grassland	Succulent Karoo	Succulent Karoo	Succulent Karoo
8	Pure grassveld types	Halophytic vegetation		Thicket	Coastal vegetation
9	False grassveld types	Herbaceous fresh-water swamp and aquatic vegetation			
10	Sclerophyllous bush types	Mangrove			
11	False sclerophyllous bush types	Scrub forest			
12		Scrub woodland			
13		Shrubland			
14		Thicket			
15		Transition woodland			
16		Wooded grassland			
17		Woodland			

Savannahs are the dominant vegetation type in Africa and occupy 60% of sub-Saharan Africa (Scholes, 1997). They are characterised by the co-existence of trees and C_4 grasses. The ratio of trees to grasses is used to define various types of savannah (Chidumayo, 2001). The co-existence of the grasses and trees appears to be made possible partly by the difference in timing of growth. Savannahs are generally confined to summer rainfall regions, and so the trees begin shoot growth in the dry season, prior to the growth of grasses at the onset of the rainy season (Chidumayo, 2001). However, the persistence of savannah vegetation is also reliant on herbivory and, importantly, fire (Low and Rebelo, 1996; Scholes, 1997). The thicket biome of Low and Rebelo (1996) differs from the Savannah biome by the absence of a conspicuous grassy ground layer, and is described as "a closed shrubland to low forest dominated by evergreen, sclerophyllous or succulent trees, shrubs and vines."

The miombo woodlands of central, southern and eastern Africa consist of mature trees (10-20m) forming a partly closed canopy with an understory of broadleaf shrubs and a lower herbaceous layer of forbs, small sedges and C_4 grasses (Frost, 1996). The defining property of miombo woodlands is the dominance of the *Brachystegia*, *Julbernardia* and/or *Isoberlinia* generas. There has been considerable debate as to whether the miombo woodlands are in fact savannah, woodland or forest, but it is generally accepted that they can be considered as part of the spectrum of savannahs (Campbell *et al*, 1996). Local variations in the vegetation occur in response to changes in the nature of soils and disturbances, such as fire, land use and herbivory.

The Succulent Karoo Biome has the highest species richness recorded for semi-arid vegetation, with a high level of endemism (Rutherford and Westfall, 1994; Low and Rebelo, 1996; Cowling and Hilton-Taylor, 1997). The Fynbos Biome is roughly the same as the Cape Floristic Kingdom, which is recognised as one of the world's six floristic kingdoms. Approximately 80% of the species in the region are endemic

(Rutherford and Westfall, 1994; Low and Rebelo, 1996; Scholes, 1997). The Succulent Karoo Biome is predicted to virtually disappear within 50-100 years and the Fynbos Biome will be severely threatened during this time period (Midgley *et al*, 2001). It is highly likely that these changes in vegetation will in turn affect the climate of the region. Accurate predictions of future vegetation distributions are thus needed in order to facilitate modelling of future climate changes.

1.4 Vegetation Response to Climate

Having discussed the current distribution of vegetation for southern Africa, some of the important influences of climate on vegetation are now highlighted. It is now widely accepted that the atmosphere cannot be modelled on its own, and that it is strongly linked to land-surface, ocean and vegetation processes (McAvaney *et al*, 2001). The exchanges of moisture and heat between the land-surface and the atmosphere have an important impact on climate. Water fluxes from the land-surface to the atmosphere move through vegetation. Land-surfaces are more variable than oceans, so the exchanges of heat and moisture between land and atmosphere are less consistent (Dickinson, 1992). There is also strong evidence that vegetation distribution is strongly influenced by climate, precipitation and temperature in particular (Woodward and Williams, 1987).

The African climate has a strong influence on not only on current vegetation, but also on soils and land use (Nicholson, 2001). In order for plants to survive and flourish in a given region, they must be adapted to the prevailing climate and CO_2 conditions. Changes in climate and CO_2 will therefore affect vegetation distribution and ecosystem composition (Woodward, 1987a). Most studies have focussed on the role of precipitation, due to the critical role of water as a resource for agriculture and other economic activities. Increasing the supply of water to plants directly increases growth and leaf mass, while decreasing the water supply has the opposite effect (Woodward and Williams, 1987).

Furthermore, there is also a growing body of evidence showing that temperature exerts a vital control on important physiological processes, such as reproduction (Woodward and Williams, 1987; Desanker and Justice, 2001). Minimum temperatures are often critical in defining the limits of plant survival. Woodward and Williams (1987) attempted to predict the distribution of global vegetation using only minimum temperature. The results were promising for zones of tundra, conifers and some deciduous and evergreen forests, but the arid regions were not very well predicted. The incorporation of precipitation in defining vegetation distribution vastly improved the results, suggesting that both temperature and precipitation play a vital role in defining vegetation distribution. The study by Chidumayo (2001) demonstrated that the interaction between minimum and maximum temperature was responsible for most of the variations in monthly Normalised Difference Vegetation Index (NDVI, a remotely sensed index that gives an indication of vegetation growth), over the savannah regions of Botswana and Zambia. The effect of temperature on vegetation is particularly important in light of the findings by the IPCC (2001), which indicate that temperatures are increasing and will continue to do so.

Woodward (1988) describes the different responses of annual and perennial vegetation to climate. For annual vegetation, the temperature during the growing season is critical, while perennial vegetation is sensitive to temperature during both the growing season and the dormant season. During the dormant season, perennial vegetation may be subjected to extremes such as very low temperatures, drought or water logging. Vegetation survives these periods by either endurance or avoidance. Endurance involves a period of non-growth but with characteristics of productivity, such as green leaves, remaining on the plant. Avoidance is characterised by marked changes in the plant, for example, the loss of its leaves (Beerling and Woodward, 2001). However, the IPCC (2001) predicts an increase in extreme events, such as droughts and flooding, which may cause conditions beyond the survival limits of current vegetation and ecosystems.

Therefore, given the strong dependence of vegetation on climate, in order for plant species to survive under a changing climate, they must either adapt or migrate. Studies of past climate changes show that vegetation can migrate, but the current warming of the climate is unprecedented in the Earth's history and is therefore considered too rapid for species to adapt (Woolhouse, 1988). One study in North America predicts that beech trees will have to migrate 40 times faster than they have ever done in the past (Roberts, 1989), however, migration rates vary greatly between species, making general predictions difficult. More mature trees may be able to continue to survive in an area where the climate is now unsuitable for them, but they may be unable to reproduce, so as these mature trees die that species will become less and less common in the region. However, as most ecosystems are comprised of many species, it is likely that some species will be able to survive under the new conditions, thereby preserving some part of the ecosystem. On the other hand, an entirely different type of vegetation may become dominant (Woodward and Williams, 1987). Any change in plant species composition is likely to have further effects; for example, the change of forest composition will affect the birds and animals living in the forest. Many of the studies of vegetation response to changing climates and CO_2 concentrations have focussed on individual species or were undertaken at a small scale, due to the inherent difficulties in analysing large areas. The long-term effects of such changes on large ecosystems are thus poorly understood (Woodward and Williams, 1987; Cao *et al*, 2001). The use of models, however, does allow an analysis of changes over large areas and many biomes.

The IPCC (2001) also predicts future changes in atmospheric CO_2, which will not only alter temperature and precipitation, but will also enhance the effects on vegetation, through its effect on photosynthesis and growth. Vegetation types will respond independently to changes in CO_2 and climate. Plants that follow the Calvin-Benson (C_3) photosynthesis pathway are widely believed to initially respond positively to increased CO_2 by enhanced photosynthesis and water-use efficiency, but this saturates as the plants become acclimatised to the new CO_2 level (Cao and

Woodward, 1998). Plants following the Hatch-Slack (C_4) pathway do not respond to higher CO_2 levels, as they use a CO_2 concentrating mechanism that makes them more efficient at photosynthesis, as discussed above. The competition between C_3 plant and C_4 plants is largely controlled by climate and atmospheric CO_2 concentration. C_4 plants perform optimally in warm, dry conditions with low CO_2 concentrations, and are therefore common over many parts of the African savannahs. According to Teeri (1988) temperature is the only climate variable consistently linked to C_4 grass abundance in numerous studies throughout the world, although precipitation was also found to be important. Studies of past climates suggest that C_3 plants should dominate during more humid periods (Schefuss *et al*, 2003). The linkages between climate, ocean and vegetation are further emphasized by this study, as the aridity over the continent can be associated with colder SST (which reduces evaporation). This increased aridity favours the growth of C_4 plants over C_3 plants, and is suggested by Schefuss *et al* (2003) to be the dominant control of C_4 abundance on a continental scale.

The concentration of CO_2 in the atmosphere is linked to changes in the density of stomata on leaves, and can therefore also influence plant water use efficiency. An increase in the CO_2 concentration will decrease the stomatal density, which would help to reduce water loss, thereby increasing water use efficiency (Woodward, 1987b). The increase in water use efficiency would result in higher production values in vegetation (Cao and Woodward, 1998). When climate change is considered on its own, vegetation production increases in the high latitudes, but decreases in the tropics and temperate regions, resulting in very little net global change. When considered together, CO_2 and climate change will increase productivity in the high latitudes and the CO_2 change counterbalances the decrease in productivity caused by climate change in the tropics and temperate regions. Any increase in productivity due to increased CO_2 will be limited by the availability of other nutrients (Warrick *et al*, 1986); in other words, a forest ecosystem that has a

low nutrient content will not be able to increase productivity as much as one with a high nutrient content.

As a consequence of this increase in water use efficiency by vegetation under enhanced CO_2, there is a decrease in the amount of moisture transpired by vegetation, which has a strong influence on the hydrological budget of the region. The hydrological budget and soil moisture will also be directly affected by climate changes (for example, a decrease in precipitation would decrease soil moisture), emphasising the fact that the climate and land-surface are too strongly linked to be considered individually.

As soil moisture has a strong effect on both vegetation and climate, the linkages outlined above are of importance. Soil moisture is the main moisture storage facility available for plants, and plants transfer the soil moisture to the atmosphere through transpiration. According to Schulze (1990), 91% of all precipitation that falls in southern Africa is evaporated or transpired, making it a significant factor in the hydrological budget for the region. Climate plays a direct role in determining soil moisture, by determining the evaporative demand of the atmosphere (Chapin, 2003). Shukla and Mintz (1982) analysed the effect of evapotranspiration by running two model scenarios, one where evapotranspiration was set to potential evapotranspiration (where soil is moist and covered by vegetation) and the other where no evapotranspiration took place. The experiment with no evapotranspiration resulted in a precipitation decrease and decreased cloudiness. The reduction in cloud cover also influenced the temperature, with the no evapotranspiration scenario being generally warmer than the evapotranspiration scenario.

1.5 The Carbon Budget

The effect of carbon dioxide (CO_2) on vegetation has been touched on above but it is also the most prevalent greenhouse gas in the atmosphere, and is therefore one of the main foci for controlling global climate warming by controlling the increasing

concentrations in the atmosphere. In order to control the amount of CO_2 in the atmosphere, it is necessary to determine where it is produced (sources) and where it may be absorbed from the atmosphere (sinks). Current estimates agree that the sources are greater than the known sinks, creating an imbalance in the carbon budget. The known sources of CO_2 are mainly anthropogenic, resulting from activities such as fossil fuel burning and deforestation. The two main sinks are thought to be the oceans and the land-surface, but the imbalance in the carbon budget suggests a "missing sink".

Recent studies suggest that the "missing sink" may be situated in the tropical rainforests, but that it is has been concealed by the release of carbon from deforestation in these regions (Cao and Woodward, 1998). Schlindler (1999) suggests a number of small sinks are responsible and together constitute the "missing sink". He suggests that the role of the oceans may have been underestimated; secondly, that the increased nitrogen emissions may have enhanced growth in previously nitrogen limited areas in northern temperate forests; and also that the longer growing seasons in the boreal regions may have resulted in more productivity and therefore greater carbon absorption in this region. Another suggestion is that the missing sink includes large areas of forest regrowth that have not been considered before (Pacala *et al*, 2001). Vegetation can therefore act as both a source and a sink, and is possibly underestimated as a sink. Vegetation will consume CO_2 during photosynthesis, but destruction of vegetation will release any carbon stored in the vegetation into the soils and atmosphere.

Large-scale destruction of forests, particularly tropical forests (such as the Amazon) where large amount of carbon are stored, will therefore have an important impact on the climate. According to Nepstad *et al* (1999) logging and fires in the Amazon forest has the potential to double net carbon emissions from land-use, particularly during severe El Niño episodes, which produce droughts in the region and increase the possibility of fires. A study by Page *et al* (2002) concluded that the amount of

carbon released by forest fires in Indonesia during a 1997 El Niño dry season was equivalent to Europe's annual carbon emissions from fossil fuel burning. Forests are therefore an important consideration when seeking to control carbon dioxide emissions.

Afforestation is sometimes suggested as one way to control CO_2 concentrations in the atmosphere, as there will then be more trees available to absorb CO_2 from the atmosphere (carbon sequestration). Trees accumulate more carbon when they are young, and so as they mature, the benefit from planting them will be lost (Cao and Woodward, 1998). The planting of trees will also have an influence on the albedo of the land-surface, which has a strong influence on climate. For example, the decreased albedo resulting from a change from agriculture to forest has a positive radiative forcing on climate (Betts, 2000). The climate response to the changed albedo can possibly be greater than the response from lowered CO_2 caused by afforestation. Furthermore, any forests planted would probably increase evapotranspiration and thereby the amount of water vapour in the atmosphere, affecting clouds and precipitation. Water vapour itself is a greenhouse gas, so increases in its concentration in the atmosphere will enhance global warming (Pielke, 2001b). Warmer climates also stimulate soil respiration, which would act as a further source of carbon (Cao and Woodward, 1998), possibly counteracting the benefits from forestation. Cox *et al* (2000) used a coupled carbon cycle and climate model to show that the land surface will change from a weak sink to a strong source of carbon at about 2050, based on a business as usual scenario. The results from six dynamic global vegetation models described by Cramer *et al* (2001) also revealed that the carbon sink would decrease after 2050. This emphasises that the terrestrial carbon sink cannot be relied on to absorb the excess CO_2 produced by anthropogenic activities.

Furthermore, carbon cycling in Africa remains relatively understudied, despite the potential for large impacts on climate and the vulnerability of African societies. The

recently observed changes in the climate of Africa, particularly the warming and the increased aridity in areas such as the Sahel, must have some influence on the carbon cycle by influencing plant growth (Cao *et al*, 2001). Studies of past changes in the carbon budget are based on CO_2 concentrations in ice cores, and can be used to infer the interactions among processes. These studies reveal that the carbon budget and the climate are too strongly linked to be modelled independently (Sundquist, 1993). The importance of accurate carbon cycle modelling, particularly over Africa, is therefore imperative for predicting future climate change scenarios.

Cao *et al* (2001), using a biogeochemical model, established that climate change reduces plant production and soil carbon stocks, thereby releasing CO_2 into the atmosphere. This is counteracted by the increase in photosynthesis caused by increased CO_2 leading to carbon accumulation in vegetation. The net result of carbon accumulation is, however, not seen in measurements of carbon fluxes for Africa, which suggest that the area is a carbon sink. Cao *et al* (2001) conclude that changes in land use over the region are resulting in carbon release into the atmosphere, which hides the carbon uptake by vegetation. These models are just one of a number of methods than can be used to analyse the sources and sinks of carbon.

Recent advances in satellite technology have improved our understanding of terrestrial carbon sinks. The moderate resolution imaging spectroradiometer (MODIS) on board the NASA Terra satellite is providing data suitable for carbon cycle assessment. Potter *et al* (2003) used this data to calculate Net Ecosystem Productivity (NEP) for 2001 and linked the results to observed climate patterns. Positive NEP fluxes (net sink fluxes) were associated with above average temperatures and heavy rainfall, while negative NEP fluxes (new source fluxes) were associated with droughts. These results show that terrestrial carbon fluxes may show large interannual variation, changing between source and sinks from one year to the next. This adds complexity to the carbon budget debate, and

emphasises the need for more studies on the role of vegetation in the carbon budget.

1.6 Vegetation and Fire

Climate and carbon dioxide are important controlling factors in the distribution of southern African vegetation, but fires are a frequent occurrence in the region and also impact on the type of vegetation found here. Fire is possibly the most important type of disturbance, particularly in the savannahs of Africa, and is likely to be affected by climate change. For example, a region that will be affected by a decrease in precipitation and a temperature increase is likely to experience more fires under such a scenario. Fire regimes are therefore strongly linked to climate, but may also be affected by vegetation type and man. An area that has a plentiful water supply is likely to be too moist for frequent fire, but an area that is too dry will not support much vegetation, so there will be little fuel to support fires. The ideal conditions for fires are therefore neither too wet nor too dry (Vazquez *et al*, 2002), or an area characterised by alternate wet and dry seasons. Weather may also cause the onset of fires, through lightning. Anthropogenic activities tend to alter the nature of the vegetation and land-surface, and may also be the cause of igniting fires, and will thereby affect the fire regime of the area (Bond *et al*, 2003a).

Acocks (1988) recognised the importance of fire in South African vegetation when he described several 'false' grasslands. Acocks suggests that these areas have the climate to support forest ecosystems, but the fire regime started by Iron Age farmers had destroyed the forests and resulted in these grasslands. The modelling study by Bond *et al* (2003a) proved that most of the higher rainfall regions of South Africa would be able to support forests in the absence of fire. This includes parts of the Fynbos biome and the grasslands of the interior, where the rainfall is sufficient to support forests. Bond *et al* (2003b) also suggest that lower atmospheric CO_2 during the late Tertiary and Quaternary periods would have slowed growth of C_3 forests after fire episodes, and therefore allowed the C_4 grasses to dominate. There is

therefore strong evidence that changes in atmospheric CO_2 concentrations may affect rates of plant recovery after fires, which could change the structure of the vegetation and the ecosystem (Bond *et al,* 2003b).

Fire can be both beneficial and destructive to vegetation. Certain species require the heat from fires for germination, but others are unable to survive the damage caused by fire. A study by Wells (1965) showed that the presence of isolated scarp woodlands in a generally treeless flat landscape was mainly due to fire. The high winds associated with the flat landscape helped to spread fires that destroyed all woody plants. The scarps act as natural fire breaks, and therefore protect the woodlands from damage. D'Antonio and Vitousek (1992) showed that the introduction of grasses into a forest increased the frequency of fires due to the greater availability of fuels associated with grasses, and resulted in the conversion of the forest into a savannah.

As a more recent example of the effects of fire, Vazquez *et al* (2002) compared fire regime characteristics and potential natural vegetation in Spain. They found that higher fire incidence was related to areas of higher vegetation productivity, which corresponded to deciduous vegetation, while warm and humid Mediterranean climates enhanced fire propagation. They concluded that conditions ideal for plant growth were more important than favourable conditions for fire. As plant growth itself is closely linked to climatic conditions (Woodward, 1987a), changing climates will affect plant growth, and through this, fire regimes, and we therefore need some indication of how fire regimes may change in the future.

At present, there are no models available to predict future fire regimes globally, and it is therefore not possible to assess how they might change in future, particularly in light of predicted climate change and possible vegetation response to climate change (e.g. Bond and Midgley, 2000; Bond *et al*, 2003a). Furthermore, fire is clearly more closely related to weather than to climate, as an extended period of dry

weather is all that is necessary to dry out vegetation and for fires to ignite (Nepstad *et al*, 1999). This is particularly important in view of the already stated prediction that extreme events, such as droughts, are expected to increase with global climate change (IPCC, 2001), as well as the importance of fire in sustaining many ecosystems in southern Africa (Cowling *et al*, 1997).

The interactions between climate and vegetation over southern Africa can be seen as highly complex, and there therefore is a strong need for more research into these interactions and how they might change.

1.7 Aims and Objectives

This work aims to facilitate current understanding of the interactions between the land surface and the atmosphere over southern Africa, particularly in relation to vegetation response to temperature and rainfall variability. It will also aid in the understanding of the projected influences of climate change on vegetation and enhance ongoing research in climate forecasting. Consideration is also given to some of the factors already discussed that may influence the interactions of coupled atmosphere-biosphere systems.

The primary objective is thus to consider the relationship between vegetation and climate in terms of the land-surface response to projected climate scenarios, complimented by an initial exploration of the attributes of the feedback from the land-surface to the atmosphere. Sophisticated computer models of the land-surface will be used to investigate the dynamics of the vegetation response to different atmospheric CO_2 scenarios, and different projections of precipitation and temperature changes. Complementing this will be an evaluation of how land-surface change influences the moisture cycle, with special focus on the evapotranspiration of moisture back to the atmosphere. However, this work does not attempt to be a definitive study of either vegetation or climate modelling, but rather uses these

methods as tools to explore the basic dynamics of coupled systems, seeking to lay the broad framework from which more detailed and focused research may develop.

1.8 Structure of the dissertation

In order to achieve these aims, a series of experiments were undertaken using the computer models. However, to prevent these experiments appearing isolated and unrelated, a review of the relevant literature places these models and the techniques used within the context of current research. This dissertation is therefore divided into five sections.

Section one serves as an introduction by providing the background information about the study region, namely Africa south of Equator, and introduces some of the important relationships between vegetation and climate (Chapter 1). The various computer models and techniques used are also outlined. Chapter 2 describes the climate models used and attempts to place them within the context of current climate modelling studies. Chapter 3 reviews the development of vegetation modelling and discusses the current vegetation models available, followed by a detailed description of the vegetation model used in this study. The various vegetation classification schemes available are also discussed, followed by an attempt to develop a classification more suited to the study region and the techniques used here. The final chapter in section one (chapter 4) discusses the various techniques and methodologies used in this study.

Section two introduces some of the effects of vegetation on climate, and discusses the role of vegetation/land-surface in climate models. This is achieved by presenting some initial results from a regional climate model study showing some effects of changing land surface characteristics within a regional climate model.

Section three introduces the effects on current vegetation distribution by validating the vegetation model used in later experiments.

Section four attempts to predict how future climate changes may effect vegetation distribution. Within this section are two sets of experiments. The first set examines hypothetical changes in climate (chapter 7), while the second series of experiments uses predicted climate changes to model future vegetation changes (chapter 8).

The final section (section five) ties together the vegetation and climate interactions and discusses the implications of future changes. Suggestions for future research are also presented.

CHAPTER 2: CLIMATE MODELLING

2.1 Introduction

Climate models are mathematical representations of the various processes that shape global and regional climate. The relationships between these processes are preferably calculated using basic physical principles or simplifications, as opposed to empirically-derived relationships (IPCC, 1997). This is due to the uncertainty as to whether such empirically-derived relationships would hold under future climate conditions. The calculations of these processes are based on five sets of equations, as described by Chase and Barry (2003):

1. The three dimensional equations of motion (i.e. conservation of momentum).
2. The equation of continuity (i.e. conservation of mass or the hydrodynamic equation).
3. The equation of continuity for atmospheric water vapour (i.e. conservation of water vapour).
4. The equation of energy conservation (i.e. the thermodynamic equation derived from the first law of thermodynamics).
5. The equation of state for the atmosphere.
6. Conservation equations for other atmospheric constituents such as sulphur aerosols may be applied in more complex models.

The calculations of thermal energy involve detailed analysis of the vertical radiative transfer of radiation (solar and longwave), and the methods of transportation (moist and dry, convective or turbulent). The water vapour equation usually has two components, a source (evapotranspiration from the Earth's surface) and a sink (precipitation) (Dickinson, 1986). The climate model is usually initialised with a set of boundary conditions and is then set to run at a timescale determined by the requirements of the study. The horizontal resolution is either several degrees latitude by longitude, or it is represented by a series of two-dimensional sine and

cosine functions, known as a spectral model (Chase and Barry, 2003). The number of vertical levels typically varies between ten and twenty levels.
There are several different types of climate models and their complexity varies. One-dimensional models are either averaged horizontally or vertically, and are designed to examine a specific dimension of the climate, most commonly radiation and convection or the energy balance (IPCC, 1997). Two-dimensional models provide further complexity and produce a more physically based computation of horizontal heat transport.

The simplest three-dimensional climate model is a representation of only the processes that occur in the atmosphere (atmospheric general circulation model or AGCM)[1]. Other important processes, such as those in the oceans and land-surface, are usually prescribed by a fixed set of variables (parameterisation), usually sea surface temperatures, albedo, roughness length, and so on. A slightly more complex system would be to couple an AGCM to a 'slab' ocean. Here, the ocean is modelled as a layer of water of constant depth, with heat transport through this layer specified and kept constant. The next level would be to couple an AGCM with an ocean general circulation model (OGCM), often referred to as an atmosphere-ocean GCM (AOGCM). The OGCM is a three-dimensional representation of the ocean, sea ice and oceanic processes. In the AOGCM, atmospheric variables, such as wind speed, are fed into the OGCM, which in turn provides constantly changing sea surface temperatures and other oceanic variables back to the AGCM. With each level of complexity, the number of explicitly modelled processes grows, with fewer processes being parameterised. The most complex models include atmospheric chemistry models, and sometimes carbon cycle models (terrestrial and oceanic carbon). These models are particularly important for modelling responses to changes in CO_2 concentrations. However, fully coupled models with dynamic vegetation included are rare, and should at this stage still be considered experimental (IPCC, 2001).

[1] http://www.meto.gov.uk/research/hadleycentre/models/modeltypes.html

The complexity of the atmosphere and its interactions with the land surface and oceans must therefore limit the accuracy of the GCM (Hulme, 1996). Climate models require sophisticated computing equipment with large amounts of processing power and storage. This can make it very expensive to run climate models, and often requires compromises. Despite these limitations, climate models are the best instruments available for large-scale studies of the atmosphere and possible changes in the climate. Grassl (2000) suggests a set of four capabilities that are necessary for improved confidence in predictions of future climates by GCMs. These are:

i. Adequate representation of the present climate;
ii. Reproduction of the changes since the start of the instrumental record for a given history of external forcings, within typical interannual and decadal time-scale climate variability;
iii. Reproduction of a different climate episode in the past as derived from palaeo climate records for given estimates of the history of external forcings; and
iv. Successful simulation of the gross features of an abrupt climate change even from the past.

Currently, many GCMs adequately reproduce present climate, as well as the climate variability, and therefore, most current GCMs pass steps one and two. Evaluating a model's ability to successfully simulate a past climate event is limited by the availability of palaeo-climate data, and is therefore limited to well-known events such as the last glacial maximum. Despite this, Grassl (2000) suggests that many GCMs are fairly successful in achieving this task (step three), but are only partially successful in achieving step four, the simulation of an abrupt climate change.

The reason for this is that global climate can be affected by many processes, such as changes in solar energy received, changes in the Earth's orbit, volcanic eruptions, changes in atmospheric composition, change in cloudiness, albedo and

atmosphere - land surface – ocean interactions, all of which can act independently or together, and should all be considered within a global climate model (Bolin *et al*, 1986). However, the incorporation of all these processes requires adequate computing power, which is usually limited, so the exact processes incorporated differ for each climate model, often depending on the developers' research aims.

For Africa, the oceans and the land surface both play a prominent role in affecting the region's climate, but both are not fully understood and are poorly represented in general circulation model (GCM) predictions of African climate (Hulme *et al*, 2001), especially since most current GCMs are developed in the northern Hemisphere, and are therefore biased towards the processes that occur there. GCM predictions of regional climate over southern Africa are still fairly poor, particularly predictions of precipitation (Hewitson and Joubert, 1998). The El Niño Southern Oscillation (ENSO) phenomenon, which has an important impact on southern African climate, is still not fully understood, and is therefore not well modelled by many climate models, which has a strong influence on the models' ability to accurately predict rainfall over Africa. Furthermore, few of the current GCMs include a dynamic vegetation/land cover component as standard, the inclusion of which may improve model simulations, particularly over Africa where the role of the land surface is increasingly proving to be important (e.g. Shannon, 2000).

This study is an initial attempt at examining the biosphere-atmosphere feedbacks over southern Africa, using both climate and vegetation models, but does not attempt to be a definitive study of either. This chapter will now discuss the climate models and the climate change scenarios used in this thesis.

2.2 The Global Climate Models

When using climate models, one must remember that although all GCMs share the common aim of attempting to model global climate and its variability, they are developed by different scientists, and the methods and parameterisations

programmed into each model are different (Gutowski *et al*, 1991). The results from each model will therefore be different. For this reason, four GCMs are used in this study, providing some estimate of the envelop of possible future climate change. The vegetation model requires three climate variables, temperature, precipitation and relative humidity, as input parameters. The four GCMs used were selected as they provided the necessary climate variables for the vegetation model used later in this study. The data from these GCMs are available from the IPCC Data Distribution Centre[2]. These four GCMs are described below and their main differences are highlighted in Table 2.1.

2.2.1. HadCM3 General Circulation Model

The HadCM3 General Circulation Model (GCM) is a coupled ocean-atmosphere model, based on the previous version of the climate model (HadAM2b), both of which were developed at the Hadley Centre, United Kingdom (Pope *et al*, 2000). The model has a horizontal resolution of 2.5° latitude by 3.75° longitude, with 19 levels in the vertical and a 30-minute timestep. The resolution has a range comparable to 417 km x 278 km at the equator reducing to 295 km x 278 km at 45° latitude (Gordon *et al*, 2000). A full description of the model can be found in Gordon *et al* (2000), and Pope *et al* (2000) have validated the performance of the model.

The affects of both the major (CO_2, water vapour and ozone) and minor greenhouse gases are included in the radiation scheme, which has 6 spectral bands in the shortwave, and 8 spectral bands in the longwave (Edwards and Slingo, 1996). The model uses a prognostic cloud scheme originally described by Smith (1990) and modified by Gregory and Morris (1996). The precipitation scheme used was described by Senior and Mitchell (1993) and the evaporation of precipitation follows the approach described by Gregory (1995). The mass-flux schemes of Gregory and Rowntree (1990) and Gregory and Allen (1991) are used to model moist and dry convection.

[2] http://ipcc-ddc.cru.uea.ac.uk/dkrz/dkrz_index.html

Table 2.1: A brief description of the four climate models used in this study (modified from IPCC, 2001, Table 8.1).

	Model Name	Centre	Main reference	Atmospheric Resolution	Ocean Resolution	Land Surface	Sea Ice	Flux Adjust
1	CGCM2	CCCMa	Flato and Boer (2001)	T32 (3.8x3.8) L10	1.8x1.8 L29	M,BB	T,R	H,W
2	ECHAM4/ OPYC2	DKRZ	Roeckner *et al* (1996)	T42 (2.38x2.8) L19	2.8x2.8 L11*	C	T,R	H,W*
3	HadCM3	UKMO	Gordon *et al* (2000)	2.5x3.75 L19	2.0x2.0 L31	C	(d)	-
4	DOE PCM	NCAR	Washington *et al* (2000)	T42 (2.8x2.8) L18	0.67x0.67 L32	C	T,R	-

Atmospheric resolution: Horizontal resolution expressed as degrees latitude x longitude or as a spectral truncation with a rough translation to degrees latitude x longitude in brackets. Vertical resolution is expressed as "Lxx", where xx is the number of vertical levels.
Ocean resolution: Horizontal resolution expressed as degrees latitude x longitude. Vertical resolution is expressed as "Lxx", where xx is the number of vertical levels. An asterisk indicates enhanced horizontal resolution near the Equator.
Land surface scheme: BB = modified bucket scheme with spatially varying soil moisture capacity and/or a surface resistance; M = multi-layer temperature scheme; and C = a complex land surface scheme usually including multi-soil layers for temperature and soil moisture, and an explicit representation of canopy processes.
Sea ice model: T = thermodynamic ice model only; R = ice rheology included; and (d) = ice extent/thickness determined diagnostically from ocean surface temperature.
Flux adjustment: H = heat flux and W = fresh water flux. An asterisk indicates annual mean flux adjustment only.

The oceanic component of the model has a resolution capable of representing the important details of oceanic currents, namely 20 levels with a horizontal resolution of 1.25° x 1.25°. Johns *et al* (1997) described the basic model and the recent changes were detailed in Gordon *et al* (2000).

A new land surface scheme for the HadCM3 was described by Cox *et al* (1999), and includes the representation of soil processes, such as freezing and melting of soil moisture, surface runoff and soil drainage. The formulation of evaporation includes the dependence of stomatal resistance on temperature, vapour pressure and CO_2 concentration. Surface albedo is a function of snow depth, vegetation type and the temperature over snow and ice.

2.2.2. NCAR PCM General Circulation Model

The Parallel Climate Model (PCM) is a fully coupled ocean-atmosphere model with a sea ice model, developed in the United States. It includes the National Center for Atmospheric Research (NCAR) Community Climate Model version 3 (CCM3), the Los Alamos National Laboratory (LANL) Parallel Ocean Program and the Naval Postgraduate School (NPG) sea ice model[3]. The different components are coupled using the interpolation scheme of Jones (1999) because the horizontal grids are different and it is necessary to preserve total global energy exchange between the components (Washington *et al*, 2000).

The atmospheric component, the CCM3, has a horizontal resolution at T42 (approximately 2.9° in latitude and longitude) with 18 hybrid vertical levels (Washington *et al*, 2000). The greenhouse gases that affect longwave radiation in the CCM3 are CO_2, O_3, H_2O, CH_4, N_2O, CFC11 and CFC12. The parameterisation of convection follows the method of Zhang and McFarlane (1995) for penetrative convection, and the method of Hack (1994) for shallow convection. Kiehl *et al* (1998) describe the computation of cloud fraction and optical properties, and the boundary layer turbulent fluxes of heat, moisture and momentum are described by Holtslag and Boville (1993). Further details of the CCM3 can be found in Kiehl *et al* (1998), Hack *et al* (1995), Hurrell *et al* (1998) and Briegleb and Bromwich (1998).

A land surface model (LSM) developed by Bonan (1996) is incorporated into the CCM3 climate model, which accounts for exchanges of energy, momentum and water between the atmosphere and the land surface. The LSM is a one-dimensional representation with prescribed vegetation types and soil properties.

The ocean component is the LANL Parallel Ocean Program (POP) model described by Dukowicz and Smith (1994), Maltrud *et al* (1998) and Smith *et al* (1995). It has an average resolution of 2/3° latitude and longitude with increased latitudinal resolution

[3] http://www.cgd.ucar.edu/pcm/main.html

near the equator of approximately 1/2°. The increased resolution at the equator, along with low values of vertical mixing coefficients have improved El Niño-La Niña cycle over previous versions (Meehl *et al*, 2000). The sea-ice component (Zhang and Hibler, 1997) predicts ice thickness and concentration, snow thickness and surface ice temperature in response to winds, ocean currents, air and ocean temperatures, humidity, radiation and internal ice stresses at a resolution of 27km (Washington *et al*, 2000). The resolution of the ocean and sea-ice component in the PCM is substantially higher than most coupled climate models (Washington *et al*, 2000).

2.2.3. CCCma Coupled General Circulation Model

The Canadian Centre for Climate Modelling and Analysis (CCCma) Coupled General Circulation Model (CGCM) contains an atmospheric and an oceanic component. The atmospheric component is essentially the AGCM2 described by McFarlane *et al* (1992), which is a spectral model with triangular truncation at wave number 32, producing a surface grid resolution of approximately 3.7° x 3.7°. The atmospheric component has 10 vertical levels. The model has an interactive cloud scheme, moist convection and the radiative heating formulation described by Fouquart and Bonnel (1980). The moisture variable in the model is specific humidity. A full description of the model can be found in McFarlane *et al* (1992), as well as a description of the sea-ice component, which calculates growth and melt.

The land-surface component includes a one-dimensional soil layer with varying soil properties (Flato *et al*, 2000). The surface grid includes land, oceans and inland seas, which are treated at 50 m layers of quiescent sea water. The inland seas included are the Baltic, Black, Caspian and Red Seas. Sub-grid scale lakes are not included.

This is the first version of the model to incorporate a complete three-dimensional ocean component (Flato *et al*, 2000). The ocean model used is the GFDL MOM

version 1 of Pacanowski *et al* (1993) with some modifications. The oceanic component has a horizontal resolution of approximately 1.8° x 1.8° and 29 vertical levels. This means that each atmospheric grid cell corresponds to four ocean grid cells.

2.2.4. The ECHAM4/OPYC3 General Circulation Model

The atmospheric general circulation model ECHAM is based on the weather forecast model of the European Centre for Medium Range Weather Forecasts (ECMWF) and was developed in Hamburg, Germany. The current version is the fourth generation model and is described in Roeckner *et al* (1996b). The standard version of the model has 19 vertical sigma levels and a horizontal resolution at T42, although the model is set up to use resolutions ranging from T21 to T106. A new semi-Lagrangian scheme has been added to ECHAM4 for the transport of water vapour and cloud water, and is described by Williamson and Rasch (1994). The prognostic variables are vorticity, divergence, temperature, logarithm of surface pressure, specific humidity and mixing ratio of total cloud water[4]. The radiation scheme of previous versions has been replaced by the two-stream method of Fouquart and Bonnell (1980) for shortwave radiation and by the method of Morcrette (1991) for longwave radiation.

The OPYC ocean model derives its name from Ocean and isoPYCnal coordinates, and uses isopycnals as the vertical coordinate system. The model is described by Oberhuber (1993).

Heat and water budgets, as well as snow effects, in the soil are included in the soil model. Vegetation effects, such as interception by the canopy and evapo-transpiration are parameterised in a highly idealised way. The fraction of vegetation cover was based on the Wilson and Henderson-Sellers (1985) data, with the land-surface parameters compiled by Claussen *et al* (1994).

[4] http://www.mpimet.mpg.de/en/extra/models/echam/index.php

The range of uses for global climate model output is limited by their coarse resolution that they are usually run on. Regional climate models are therefore frequently used for studies that require finer scale data, particularly impact studies. A regional climate model is used in this study to explore the sensitivity of the southern African climate to vegetation inputs. This regional climate model and some of the issues surrounding regional climate modelling are discussed below.

2.3 Regional Climate Modelling

2.3.1. Introduction

According to Vaughan *et al* (2001) the current GCMs are able to capture the large-scale changes in surface temperatures during the last 100 years, but the regional variations are still inadequately modelled. Regional climates are strongly influenced by features such as local topography, which need to be represented at a scale appropriate for the study. There are therefore two main types of climate models. Global climate models run at a resolution appropriate to the large domain covered, and do not necessarily include fine details, especially of features such as topography. Regional climate models (RCMs) are run at a finer resolution in order to capture the regional variation. RCMs are usually run over a smaller domain and for shorter time periods, as they are far more computational expensive than the global models. RCMs cannot be run independently however, and must be given lateral boundary fields, such as sea surface temperatures. The source of these input boundary fields is often global climate models or observed data.

The common practice of using GCM or reanalysis data to provide boundary fields for RCMs is referred to as nesting, and is a one-way process. In other words, no feedback from the RCM to the driving data occurs. Denis *et al* (2002) recognise nine issues that occur as a result of the nesting of RCMs in coarser scale data sets. Firstly, the methods used to nest the models should accurately map the two datasets without creating any errors that could contaminate the nested model results. The

second issue is the maximum resolution jump that can be used between the nested model and the driving data. There is a considerable range in the values used, but one suggestion is the use of multiple nesting to decrease the jump between each nest. Thirdly, the spin-up period of the RCM needs to be considered, as different components of the model may take different times to reach equilibrium. The temporal, vertical and horizontal resolutions as well as the physical parameterisations of the nested model and the driving data may also be different, leading to errors close to the boundaries of the nested region. The domain size of the nested region also needs to be considered, as a change in the domain size can alter the results. The quality of the driving data is important, as any errors in this data will be transferred to the nested model and result in further errors (garbage in, garbage out). Finally, RCMs have been designed for short term, high resolution studies, but it is not certain that if RCMs were run for longer time scales, they would not generate systematic errors or climate drifts. All these issues can lead to errors in RCM results and should be carefully considered during RCM modelling studies. These issues, however, are not limitations, and should merely be considered when running a RCM. Furthermore, it has been shown that RCMs can be used in climate simulations and that they improve the spatial detail of model outputs when compared to GCMs, and produce results similar to other regionalisation techniques, such as statistical downscaling (Giorgi *et al*, 2001). The MM5 regional climate model that is used later in this study is now discussed.

2.3.2. The MM5 Regional Climate Model

The fifth-generation Mesoscale Model (MM5) was jointly developed by the Pennsylvania State University (Penn State) and the National Center for Atmospheric Research (NCAR), both based in the United States. A full description of the MM5 model can be found in Grell *et al* (1994). The model has multiple nest and four-dimensional data assimilation capabilities. The initial boundary fields that need to be supplied to MM5 are horizontal winds, temperature, pressure, and moisture fields (Dudhia *et al*, 2000). The source of these boundary fields is usually either from a

global climate model or observed data, such as the NCEP reanalysis data (Kalnay *et al*, 1996). There is a choice of three map projections, namely Lambert Conformal (for mid-latitudes), Polar Stereographic (for high latitudes) and Mercator (for low latitudes).

In addition to the climatological boundary fields that are needed to run MM5, land-use and topography datasets are also required. The MM5 has recently been altered to include an advanced land surface model (LSM), in recognition of the important role that the land surface plays in influencing regional climates (Chen and Dudhia, 2001a, 2001b). The LSM included in the MM5 was developed at Oregon State University, and is used to provide surface sensible and latent heat fluxes as lower boundary conditions to the atmospheric model. It has a single canopy layer and calculates soil variables (soil moisture and temperature), as well as snow storage and water stored in the canopy. A hydrology sub-model is used to determine evaporation and runoff (Chen and Dudhia, 2001a).

In order to use climate models for studies of future climate, a description of the variables that may cause climate change is needed. There are several such descriptions, which are known as climate change scenarios. The climate change scenarios that are relevant to this study are discussed below.

2.4 Climate Change Scenarios

Hulme (1996) described climate change scenarios as presenting coherent, systematic and physically plausible descriptions of future climate that may be used as an input into climate change assessments. Most climate change scenarios are based on assumptions about population growth, economic growth and future energy use. These scenarios are then used to estimate future growth of greenhouse gas concentrations, which can then be used to predict the response of both the climate and vegetation to these changed concentrations. Most of the older studies have focussed either on the climate or the vegetation, but there are a growing number of

studies attempting to predict how climate and vegetation may change, and the knock-on effects of those changes. This study uses climate change scenarios to examine the possible change in vegetation under future climate.

Only two climate change scenarios were available from the IPCC Data Distribution Centre (IPCC-DDC) that provided the necessary climate variables needed for this study for all of the four global climate models. These scenarios are the IPCC Special Report on Emission Scenarios (SRES) A2 and the B2 scenarios (Nakićenović *et al*, 2000). These emissions scenarios are based on assumptions about the future evolution of major drivers of emissions, namely technology, economics, energy and population (Desanker and Justice, 2001). Therefore, the scenarios do not describe the actual climate of the future, but rather how the factors that will affect the atmospheric chemistry may change, such as technology, and how these will affect greenhouse gas emissions. The two scenarios used in this research are described as (Nakićenović *et al*, 2000):

> *"A2*: The A2 storyline and scenario family describes a very heterogeneous world. The underlying theme is self-reliance and preservation of local identities. Fertility patterns across regions converge very slowly, which results in continuously increasing population. Economic development is primarily regionally oriented and per capita economic growth and technological change more fragmented and slower than other storylines.
>
> *B2*: The B2 storyline and scenario family describes a world in which the emphasis is on local solutions to economic, social and environmental sustainability. It is a world with continuously increasing global population, at a rate lower than A2, intermediate levels of economic development, and less rapid and more diverse technological change than in the A1 and B1 storylines. While the scenario is also oriented towards environmental protection and social equity, it focuses on local and regional levels."

Together, these two scenarios and the other IPCC scenarios that are not used in this work provide an envelope of possible future greenhouse gas emissions, which can be used to simulate a range of possible future climate changes. As an example, Figure 2.1 shows the atmospheric concentration of four greenhouse gases from the six SRES scenarios up to 2100, with the outdates IS92a scenario included for comparison.

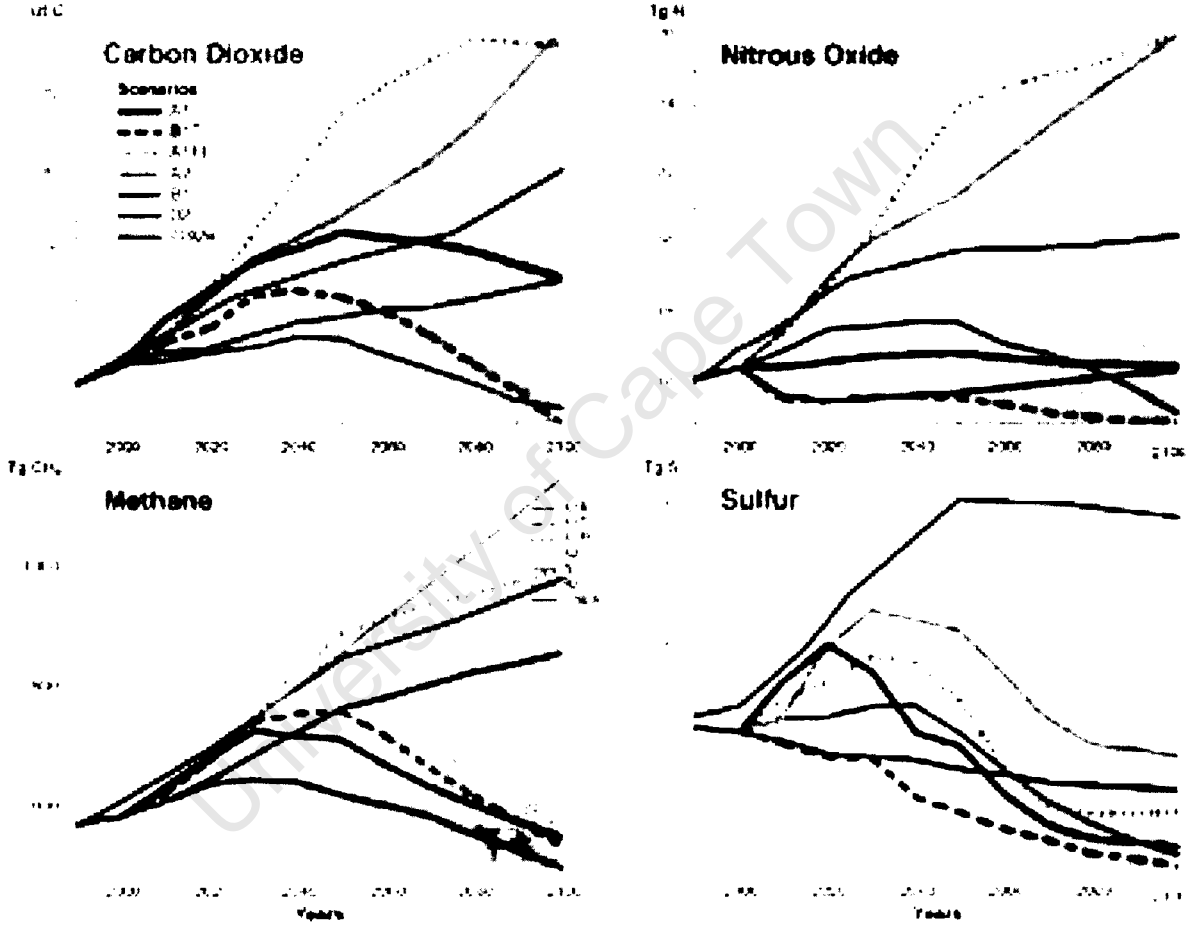

Figure 2.1: Atmospheric concentrations of Carbon Dioxide, Nitrous Oxide, Methane and Sulphur for the six SRES scenarios (IPCC, 2001).

2.5 Conclusion

This chapter has described the some of the principles used in climate modelling, as well as the various models used in this study. Although there are inherent biases

and problems with climate models, they are still the best method of studying climates and climate change. Continual research and development insures that the number of problems is decreasing, and the predictions are therefore improving. One of the important limitations of current climate models is the inclusion of vegetation as a dynamic component. The following chapter will discuss the principles of vegetation and land surface modelling, as well as some of the land surface classification schemes that are currently used by climate modellers.

CHAPTER 3: LAND SURFACE MODELS

3.1 Introduction

Recognition of the importance of the land-surface in climate modelling (e.g. Copeland *et al*, 1996; Pielke *et al*, 1991 and 1998; Henderson-Sellers, 1993) has been a strong factor in driving the improvement of the land-surface models that are coupled with climate models (Henderson-Sellers *et al*, 2003). This incorporation of biophysical land surface models into general circulation models (GCMs) has markedly improved the results from the GCMs. The main improvements include the ability to simulate a more realistic surface energy balance, improved diurnal temperature ranges and relative humidity variation, and more realistic evaporation and precipitation rates (Sellers, 1991). This chapter discusses a range of vegetation and land surface models that are currently used, as well as the principles behind them and some of the important contributions they have made to atmospheric modelling.

Incorporation of vegetation-atmosphere feedbacks has also improved the accuracy of simulations of past climatic conditions (e.g. Foley *et al*, 1994; Noblet *et al*, 1996), as well as current climatic simulations. Zeng *et al* (1999) showed that the inclusion of interactive vegetation in a GCM simulation of rainfall in the Sahel resulted in noticeable increases in the inter-decadal rainfall variability, which closely matched observed patterns of variability in the region.

In terms of dynamics, the Land Surface Models (LSMs) are designed to model fluxes of energy, momentum, water and heat between the land surface and the atmosphere. These fluxes have a direct impact on surface winds, air temperature and precipitation (Sellers, 1991). Perhaps the principal component controlling surface fluxes is albedo, determined by the vegetation and soil colour. This determines the amount of incident radiation reflected from the surface, and therefore directly impacts on energy fluxes between the land surface and the atmosphere

(Dickinson, 1992). Secondly, the latent heat and moisture are transferred from the land surface to the atmosphere through evapotranspiration, in turn having a direct impact on local air temperature and humidity, and through these, an indirect impact on other climate variables. This evapotranspiration is in part dynamically variable as a function of vegetation processes and available soil moisture, with most of the moisture flux moving through vegetation as a by-product of photosynthesis (Dickinson, 1992).

Additionally, the roughness length of natural land surfaces is determined by the height and structure of the vegetation, and determines the amount of turbulence in the lower atmosphere, which controls the speed of moisture and energy fluxes between the land surface and the atmosphere. Larger roughness lengths result in higher turbulence. Finally, the exchange of trace gases is important to both the land surface and the atmosphere (Sellers, 1991). Gases such as carbon dioxide and nitrogen are essential for plant growth, but are also important greenhouse gases needed to warm the atmosphere.

The first generation of LSMs were simple "bucket" models often based on Manabe (1969), where the land surface was defined only in terms of surface temperature and soil moisture held in a "bucket", which were used to calculate potential surface evaporation. Once the "bucket" was full, it overflowed to produce runoff. However, this system has been found to over-estimate evaporation rates over land in almost all situations (Sellers, 1987). The second generation of LSMs included a vegetation canopy, which addressed many of the inadequacies of the older models (Cox *et al*, 1999). The Simplified Biosphere Model (SiB) of Sellers *et al* (1986) is an example of a second generation LSM. The second generation LSMs emphasised canopy parameterisation with fixed vegetation distribution. These models tended to under-estimate evapotranspiration rates (Henderson-Sellers *et al*, 2003), and the static vegetation patterns limits their applicability to future global change studies (Foley *et al*, 1998). More recent models have begun to include models of vegetation cover,

pioneered by Henderson-Sellers (1993), but have mainly used asynchronous coupling methods, where the vegetation input is in equilibrium with the climate.

The complementary global biogeochemical models have developed independently of LSMs, and are designed to study carbon cycling by the terrestrial biosphere. These models assume a constant distribution of global vegetation, but the recognition that climate change should lead to a change in vegetation distribution has led to the development of vegetation models that include both global biogeochemical cycles and a dynamic vegetation component (Cramer *et al*, 2001). These Dynamic Global Vegetation Models (DGVMs) have been developed with the primary aim of predicting *vegetation and vegetation change*. The land surface models on the other hand were developed to provide estimates of processes that influence climate, with the aim of improving *climate* predictions.

In order to further this aim of improving climate predictions, recent research has begun to explore methods to couple LSMs with DGVMs to provide dynamic vegetation input for climate models, thereby providing a complete internally consistent carbon balance (Moorcroft, 2003). One of the first attempts at coupling dynamic vegetation to atmospheric models was that of Cox *et al* (2000), who used a fully coupled, three-dimensional carbon climate model to model the response of climate and vegetation to increased atmospheric CO_2 concentrations. Their results showed that vegetation could change from a net sink of carbon to a carbon source by about 2050. It is now known that the terrestrial biosphere serves as a significant moderator of global atmospheric CO_2 change (Cao and Woodward, 1998; Schindler, 1999), despite the fact that the terrestrial surface acts as a lower boundary field for only 30% of the atmosphere (Dickinson, 1992). This kind of model could therefore be important for climate change studies that run over longer time scales when carbon cycle-climate interactions could significantly influence the rate of atmospheric CO_2 increase, the nature and extent of the physical climate response, and ultimately, the response of the biosphere itself to global change (Stocker *et al*, 2001). This will

eventually show the influence of the climate system on the terrestrial carbon cycle and vice versa.

Despite the increased interest in vegetation-atmosphere modelling studies, integrated modelling assessments of climate change impacts for southern Africa are still fairly rare, particularly since the models available are not well calibrated for this region. However, studies of other parts of the world have emphasised the need for accurate, integrated modelling of the atmosphere, ocean and land surface processes (e.g. Charney *et al*, 1975; Nobre *et al,* 1991; Pielke *et al*, 1998; Chase *et al*, 1999; Zeng *et al*, 1999). The aim of this study is to use vegetation and climate models to explore the dynamics of coupled atmosphere-biosphere systems in southern Africa.

With the aim of improving current understanding of vegetation-atmosphere feedbacks over southern Africa in mind, the first step is to examine the possibilities of coupling a dynamic vegetation model, the Sheffield Dynamic Global Vegetation Model (SDGVM), with a regional climate model. Prior to this, it is necessary to test the SDGVM over this region, to determine if it will prove a valid model for inclusion in the regional climate model as the dynamic vegetation component. The development of appropriate base maps of vegetation lies at the core of the atmosphere-vegetation interaction modelling techniques developed in this thesis. Accurate and up-to-date vegetation maps are needed to act not only as input for climate models, but also to validate the vegetation model output before it can be used as input for the climate model. For optimal application, such base maps need to be described at a spatial scale relevant to the needs of the climate modelling envisaged, and they need to class vegetation into units that adequately represent the key functional characteristics simulated by the climate model. In addition, the base map needs to capture with fidelity the spatial distribution of vegetation units within the area of interest. The datasets currently available need improvement, as many have not been recently updated, and the classifications designed to simplify the structural

complexity of the vegetation do not achieve this aim. This chapter discusses the vegetation model used later in this study, as well as land surface models and the classifications currently used by both climate and vegetation modellers.

3.2 Vegetation Modelling

3.2.1 Introduction

One of the first attempts at predicting vegetation distribution using climate data was undertaken by Holdridge (1947), who developed a diagram of expected vegetation under different temperature and moisture conditions. The Holdridge diagram (Figure 3.1) contains 37 named "life zones", which are defined by locating the area of coincidence of at least two primary climate variables. However, the Holdridge scheme is based on currently observed correlations between climate and vegetation distribution, and is therefore unable to simulate transient changes in vegetation distribution in response to changing climate (Foley *et al*, 1998). Box (1981) developed a simple predictive model based on the broad correlations between climate and vegetation distribution, but this has been criticised, as the fundamental physiological basis for these correlations is not apparent (Woodward and Williams, 1987). This makes the Box (1981) model, like the Holdridge scheme, unsuitable for predicting future changes in vegetation in response to changing climate conditions.

The inadequacies of these earlier models resulted in a series of newer vegetation models, which were developed based on plant physiology, and use the understanding of these processes to predict not only vegetation distribution, but also variables such as Net Primary Production (NPP), Leaf Area Index (LAI) and biomass production. These dynamic vegetation models (for example, Foley *et al*, 1996; Woodward *et al*, 1995; and Prentice *et al*, 1992) are based more on the relationships between climate and vegetation dynamics, as opposed to the older models that were based on correlations between climate and vegetation distribution. The newer models are therefore better suited to climate change scenario studies as the

interactions between climate and vegetation will most likely not be the same as at present (Foster, 2001).

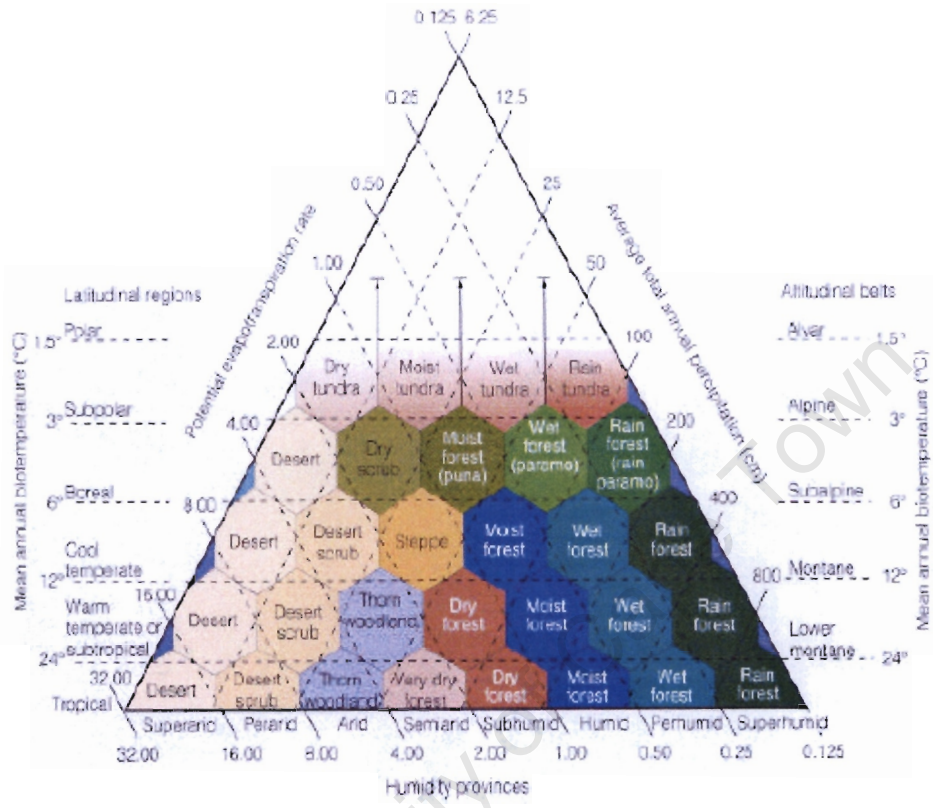

Figure 3.1: The Holdridge life zones. Annual potential evapo-transpiration ratio is defined as the annual potential evapo-transpiration divided by the annual total precipitation. Biotemperature represents the conditions important for plant growth.

As these newer models share many of the same characteristics, the general structure of a Dynamic Global Vegetation Model (DGVM) is shown in Figure 3.2 (Lomas and Woodward, 2003). DGVMs all simulate physiological, biophysical and biogeochemical processes, which include representations of processes such as photosynthesis, respiration, and canopy energy balance, as well as the controls of stomatal conductance and canopy boundary-layer conductance, and the allocation of carbon and nitrogen within the plant (Cramer *et al*, 2001). These processes are represented by a core set of coupled modules, which run at timescales appropriate for the process (see Figure 3.2).

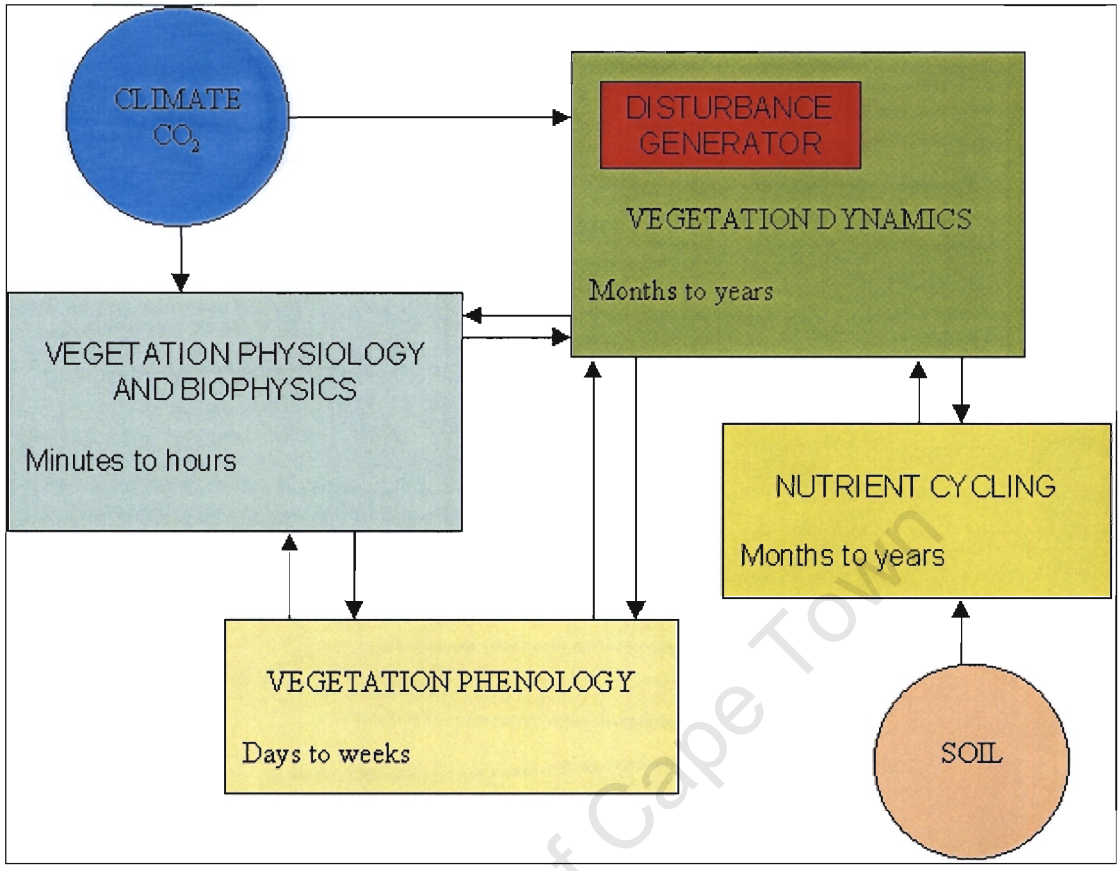

Figure 3.2: The general structure of a Dynamic Global Vegetation Model (from Lomas and Woodward, 2003). H_2O_{30} is the H_2O leached below 30cm.

The concept of Net Primary Production (NPP) is used to model the process of carbon cycling within vegetation. NPP is defined as the net amount of carbon captured by land plants, and is affected by the interactions of photosynthesis, respiration, decomposition and nutrient cycling (Melillo *et al*, 1993). The variation in NPP seen between different biomes appears to be directly related to climate (dry or cold climates have lower NPP than warm and moist climates), but in reality, it is as a result of the climate's affect on the length of the growing season and the productivity of the vegetation. Larger plants and evergreen trees support more leaf area than do smaller plants and deciduous trees (Chapin, 2003). This can be directly related to NPP, with more leaves corresponding to higher production. The NPP and the leaf area are related to the type of vegetation that occurs, and are used to predict the dominant vegetation.

Most vegetation models are limited as to the number of vegetation types that can be simulated, and it is therefore not possible to model at the species level. The concept of Plant Functional Types (PFTs) is commonly used, for example C_3 and C_4 plants, and deciduous and evergreen, and trees and grasses. Specific ranges of climate variables define the PFTs, and a disturbance generator is usually included to simulate the effects of fire and disease on the PFTs. Each site within the model will be assigned a fractional coverage of the PFTs that can survive there, and the combination of PFTs defines the structural characteristics of the vegetation (Cramer *et al*, 2001).

In addition, soil processes are usually included as they are essential in calculating the available nutrients (e.g. nitrogen) and moisture for vegetation. Evaporation is strongly dependent on the soil moisture content and on plant canopy cover, and affects the amount of water vapour in the atmosphere. The highest rates of soil evaporation occur when the soil is saturated. As the soil dries, surface resistance will increase, which will decrease the amount of evaporation from the soil (Jones, 1992). Once the soil is dry, the only source of moisture for the combined process of evapotranspiration is vegetation. The depth to which plant roots penetrate the soil (rooting depth) also determines the amount of water the plants can access. If the soil is totally dry, the moisture reservoir for vegetation is exhausted and this will cause stress on the vegetation (Jones, 1992). Soil texture and depth are given as prescribed inputs to the models and are used to determine soil hydrology. Soil hydrology is frequently based on a simple bucket model, where each soil layer represents a bucket. When the first bucket is full, it overflows into the next bucket, and so on. The number of soil layers and modifications to this simple scheme varies between the different vegetation models. Although the importance of soil moisture is generally recognised by both climate and vegetation modellers, soil processes are still generally not fully developed within the models themselves.

The Sheffield Dynamic Global Vegetation Model (SDGVM) was selected for this study, as it contains the necessary sub-models required to model vegetation dynamics over southern Africa. The SDGVM and its components are described below.

3.2.2 The Sheffield Dynamic Global Vegetation Model

The following section outlines the internal details and attributes of the Sheffield Dynamic Global Vegetation Model (SDGVM).

The SDGVM is a mechanistic model that has been constantly developing since the first version of the model was presented by Woodward (1987a). It was first developed as the Dynamic Global Phytogeography Model (DOLY), described by Woodward *et al* (1995). The DOLY model was later restructured to incorporate the CENTURY model of Parton *et al* (1992) for carbon and nitrogen cycles, and became known as the SDGVM (Woodward *et al*, 2001). The SDGVM was developed to address the inadequacies of DOLY, and is still under constant revision (Woodward, *pers. comm.*).

In order to run SDGVM a set of inputs are required, namely, a constant atmospheric carbon dioxide value, soil texture and depth (by default set to 1m), air temperature, relative humidity, and precipitation. The default climate dataset used to run SDGVM was provided by the Climate Research Unit (CRU), University of East Anglia as described by New *et al* (1999). This dataset provides monthly averages of mean air temperature, relative humidity and precipitation for 1901 to 1995. A rain generator is used in SDGVM to predict the number of wet days in a month from the monthly precipitation averages. The precipitation is then divided equally between the wet days. Minimum temperatures are estimated by SDGVM from the monthly averages.

The resolution and domain of a SDGVM run is determined by the climate input data. SDGVM is, in principle, a point model, as there is no area assigned to each point

that is modelled and there are no interactions between the points (Lomas and Woodward, 2003). Each point is defined by a latitude and longitude, and is referred to as a site. The sites can, in practice, be considered to have an area assigned to them, usually based on the resolution of the climate data used as inputs. For example, the default climate dataset (New *et al*, 1999) has a resolution of 0.5° latitude x 0.5° longitude, and the results from this dataset would have this resolution. Latitude is also used to determine the radiation and daylight hours at the site (Lomas and Woodward, 2003).

One of the most important inputs into SDGVM is the atmospheric CO_2 input data, which is provided by the Hadley Centre, and consists of an average for each year from 1830 to 2100, given as a partial pressure (Lomas and Woodward, 2003). Currently, atmospheric CO_2 is the only greenhouse gas that is taken into account by the SDGVM and affects the photosynthetic pathways of vegetation (Lomas and Woodward, 2003).

A further input file for SDGVM is the soil texture taken from the International Satellite Land Surface Climatology Project (ISLSCP) soil texture map (ISLSCP CD-ROM, published March 1995), which gives the soil texture as a percentage of clay, sand and silt. These are used to determine the soil hydrological characteristics, as well as in the calculation of soil carbon and nitrogen dynamics (Lomas and Woodward, 2003). The soil texture map has a resolution of 1° x 1°, and has five categories (Table 3.1). The field capacity and wilting point fractions are multiplied by soil depth (which is set to 1m by default) in order to obtain the actual capacities.

Table 3.1: ISLSCP soil texture classifications

Classification	Index	Percentage			Field capacity fraction (fc)	Wilting point fraction (wp)
		Clay	Sand	Silt		
Loamy sand	1	7	80	13	0.1179	0.0439
Sandy loam	2	12	62	26	0.1667	0.0737
Loam	3,7	18	42	40	0.2217	0.1130
Sandy clay loam	4	27	63	10	0.1963	0.1136
Clay loam	5	30	35	35	0.2526	0.1520

There are no prescribed values for the vegetation variables given as input files (cover, biomass, leaf area index, net primary productivity, etc.) or soil nutrient values. The DOLY model is therefore used within SDGVM to initialise soil nitrogen and soil carbon. DOLY, as the forerunner of SDGVM, has many of the same features, except that it does not model vegetation biomass or vegetation functional types (Lomas *et al*, 2001). The SDGVM is then run for an extended period of time (usually 200 years) as a spin up to calculate the initial equilibrium values of the vegetation variables such as Net Primary Productivity (NPP) and Leaf Area Index (LAI), as well as the cover of each functional type. The third and final stage of any SDGVM run uses the output from the spin-up as the initial state of the system. A list of all the variables calculated and their description can be found in Table 3.2.

Once these variables have been calculated, SDGVM can determine the dominant vegetation type at each site. This is done using the concept of Plant Functional Types (PFTs) rather than individual species. This is aimed at decreasing the complexity of the model due to the limitation of computing resources, while still producing useful output. SDGVM models six PFTs, namely C_3 Grassland/Shrubland (C_3), C_4 Grassland (C_4), Evergreen Broadleaf Forest (EvBl), Evergreen Needleleaf Forest (EvNl), Deciduous Needleleaf Forest (DcNl) and Deciduous Broadleaf Forest (DcBl). Only four of the six PFTs occur in southern Africa, as the climate is generally unsuitable for natural Needleleaf forests.

Table 3.2: The state variables of the SDGVM (Lomas *et al*, 2001)

Soil Variables:	
Soil moisture	The soil moisture profile is given as depths of water in a series of layers. Six separate pools are modelled: four soil layers, a snow pool and a liquid snow pool.
Soil carbon	Eight soil carbon pools are modelled: surface and soil structural material, active soil organic matter, surface microbes, surface and soil metabolic material, slow and passive soil organic material.
Soil nitrogen	Eight soil nitrogen pools are modelled, as for soil carbon.
Vegetation Variables:	
Cover	A site contains a proportion of each PFT, which is further divided into age in years. The total fraction of cover taken up by each PFT is given by summing the contributions at each age. A cover element refers to an element of cover corresponding to a specific age and PFT.
Biomass	The carbon equivalent biomass of each cover element is partitioned into leaf, stem (or trunk for trees) and root biomass.
Leaf Area Index (LAI)	A dimensionless number that specifies the area of leaf per area of vegetation. All cover elements of a particular PFT have the same LAI.
Net Primary Productivity (NPP)	The net annual carbon gain through photosynthesis after allowing for respiration. All cover elements of a particular PFT have the same NPP.
Number density	The number of plants per m^2 for each cover element (trees only).
Height	Tree trunks are modelled as cylinders, whose height is given by this variable. No height is assigned to grass.

The vegetation modelled by SDGVM is the potential natural vegetation, as there is no accounting for processes such as anthropogenic modifications of the land surface included in the model. For each site, the fraction covered by each PFT is calculated. Area not covered by vegetation is assigned to Bare Ground (BG), and is then available for growth by the PFTs if the climate is suitable for growth (Lomas and Woodward, 2003). The PFTs are characterised by a set of properties (Table 3.3). The properties are defined as follows (Lomas and Woodward, 2003):

Life-span: The maximum age that a PFT can attain. Vegetation dies once it reaches this age.

Specific leaf area (SLA): The cost, in terms of carbon, to produce a leaf of unit area is inversely proportional to the SLA.

Leaf life-span: The maximum age that a leaf can live to. A leaf dies once it reaches this age.

Seeding density: The initial number density of new cover elements.

Water potential: The maximum water potential across the full height of a tree, before cavitation sets in and disrupts the water column.

Table 3.3: Plant functional type properties.

PFT	Life-span (years)	Wood density (t C m^{-3})	Xylem conductivity (10^{-9} m^3 s^{-1})	Water potential (MPa)	Photo-synthesis route	Specific leaf area (m^2 kg^{-1})	Leaf life-span (days)
C_3	1	0.0	0.0	0.0	C_3	0.017	360
C_4	1	0.0	0.0	0.0	C_4	0.017	360
EvBl	200	0.4	7.0	2.2	C_3	0.007	3600
EvNl	200	0.2	1.5	3.6	C_3	0.007	3600
DcBl	200	0.4	7.0	2.2	C_3	0.017	360
DcNl	200	0.2	1.5	3.6	C_3	0.017	360

There are five main components in SDGVM that are used to calculate these properties and the other output files. The interactions of these five components are shown in Figure 3.3 (Lomas and Woodward, 2003). The NPP, hydrology and phenology models are run daily, in that order. The carbon and nitrogen model is run monthly and the growth model is run at the end of each year.

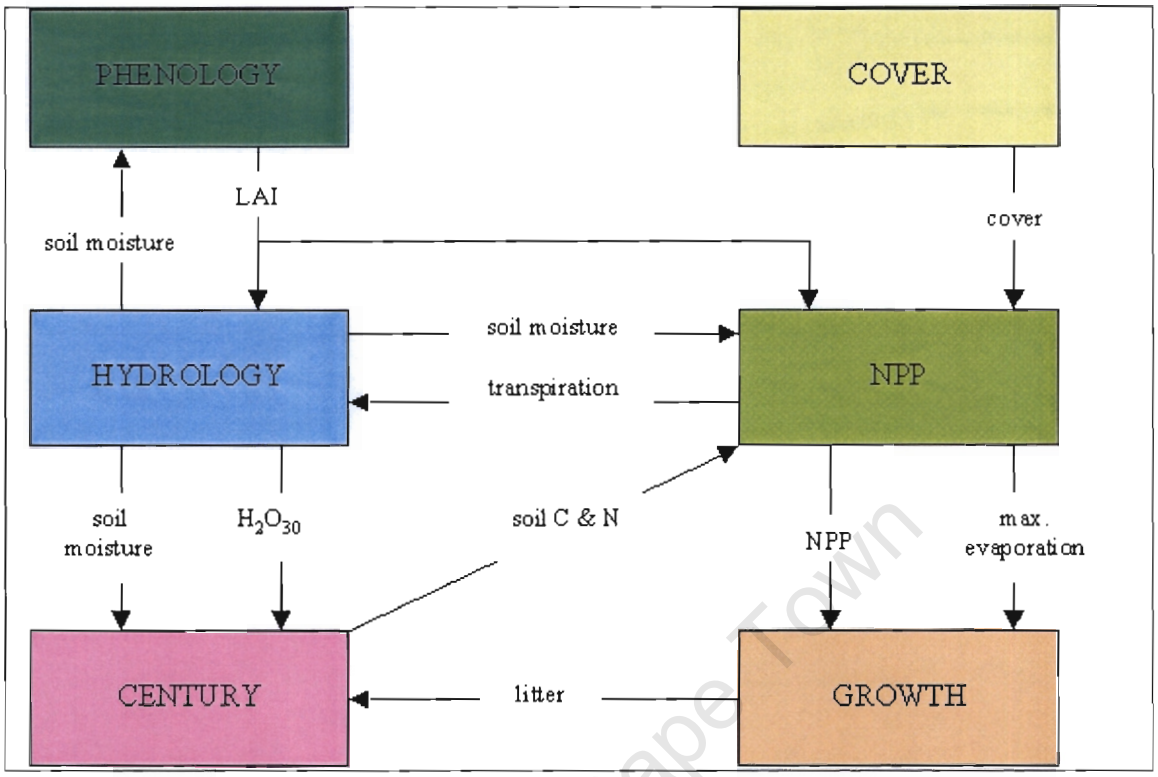

Figure 3.3: The interactions between the five main components of the Sheffield Dynamic Global Vegetation Model (from Lomas and Woodward, 2003).

The components are described as (Lomas *et al*, 2001):

Soil carbon and nitrogen dynamics are based on the CENTURY model of Parton *et al* (1992). The carbon stock is assumed to exist in eight separate pools that interact with each other on varying timescales, with the nitrogen model operating in the same general manner.

The hydrology model is a simple 'bucket' model with four buckets or layers, and a total depth currently set to 1m. The top layer is 5cm in depth, and the other three buckets are of equal depth. When a bucket is full to its field capacity, any further water will flow into the bucket below it until all buckets are full when runoff occurs. Water loss is represented through bare soil evaporation, sublimation, transpiration and interception.

The NPP model was described by Woodward *et al* (1995) and is used to determine photosynthesis. Stomatal conductance, which is dependent on temperature and soil moisture, influences the exchange of gasses. Canopy

conductance controls transpiration. NPP is calculated daily and assigned to roots, leaves and stems on an annual basis.

The phenology model controls the production and senescence of leaves. This is currently a simple procedure that determines when leaves are produced or dropped. These processes occur instantaneously, and are determined by temperature and soil moisture.

The growth model allocates the annual NPP to biomass, calculates the new ground and assigns it to PFTs, and calculates the litter produced in the year. This initialises the state of the system at the beginning to the year, based on the results from the previous year. The sequence of events is as follows:

- Age the vegetation by one year. Some vegetation is lost due to PFTs reaching their maximum age. This occurs annually with grasses as they have a maximum age of 1 year. The cover lost is available for new growth and the released biomass is converted into litter.
- Compute the probability of fire, using an empirical function that depends on the monthly precipitation and temperature. A portion of the biomass lost goes into litter, and the remainder is released into the atmosphere. This fire module has been shown to improve the prediction of vegetation over southern Africa (Bond *et al*, 2003a).
- Compute the probability of other disturbances, such as disease. All the biomass lost is transformed into litter.
- Calculate the cover proportions assigned to the forest cover elements after the disturbances have occurred.
- Determine the forest functional type proportions in the new ground based on the minimum annual temperature and the days off (the number of days when no photosynthesis occurs).
- Assign the remaining bare ground is assigned to grasses and calculate the C_3/ C_4 split, using linear weighting of the functional type NPP values.

- Impose natural thinning on the trees and reduce the number density if necessary, to allow a minimum growth rate. The biomass of thinned trees goes into litter.
- Assign the NPP to biomass.
- Compute the litter.

A further important consideration with all models is the limitations inherent in that model. Two problems do exist with the SDGVM that have particular relevance to the current study area. Firstly, SDGVM does not include plants that use the Crassulacean acid metabolism (CAM) photosynthesis pathway. These are plants that open their stomata at night and close them during the day, allowing them to minimise water loss (Jones, 1992). These include many succulents and other arid plants, and these are therefore not modelled by SDGVM. These types of plants are common in the arid and semi-arid regions of Africa, all of which are assigned to Bare Ground by SDGVM. There is therefore no distinction between true bare ground and areas such as the Karoo region of South Africa that is in fact covered by sparse vegetation as described by Acocks (1988), Cowling *et al* (1997), Low and Rebelo (1996), and Rutherford and Westfall (1994). However, vegetation change in the arid zone, while of concern in terms of biodiversity, is arguably of secondary importance in terms of feedback mechanisms due to the sparse coverage in the arid zones.

Secondly, SDGVM does not distinguish between shrubs and C_3 grasses in the C_3 functional type. The most species-rich biome in southern Africa, the Fynbos Biome, is dominated by shrubs, and can therefore not be accurately modelled by SDGVM. The reason for not modelling shrubs is due to the lack of a comprehensive understanding as to what defines a shrub (Woodward, *pers. comm.*). It would be simple to define shrubs as shorter trees, but it would then not be possible to distinguish between young trees and shrubs. However, the C_3 plant functional type does represent both C_3 grassland and C_3 shrubland (Beerling and Woodward,

2001). Despite these problems, SDGVM does appear to simulate current vegetation distribution over southern Africa with reasonable fidelity.

3.3 Climate Model Land Surface Schemes

Whilst the SDGVM forms the basis of investigating the vegetation response, the data used to drive the SDGVM under climate change scenarios is itself a product of a model – the GCM – which has it's own dependencies on the internal land surface scheme used. Similarly, when investigating the response of the atmosphere to vegetation perturbations, this is predicated in part on the sophistication of the land surface scheme in the regional climate model (RCM), in this case the MM5. Consequently it is important to understand the Land Surface Model (LSM) approach adopted by the different GCMs and RCMs from which data is used in this thesis, and these are outlined below.

During the same period that vegetation models were being developed, the recognition of the biosphere - atmosphere feedbacks led climate modellers to the develop their own set of parameterisations of the land surface for inclusion in climate models, usually in terms of albedo, roughness length and moisture availability. These properties vary with different vegetation and soil types, as well as with the amount of vegetation cover and the soil depth. In fact, the distribution of vegetation in most climate models is simply the basis of look-up tables for the surface characteristics that are demanded (Henderson-Sellers, 1993). Some of these land surface parameterisations and the land surface models are discussed below.

3.3.1 Land Surface Models in Regional Climate Models

Most climate models, be they RCMs (e.g. MM5) or GCMS (e.g. HadCM3, NCARPCM, CCCMa CGCM, etc), use a land surface parameterisation that has been developed in the Northern Hemisphere, and there is thus a bias towards northern hemispheric conditions, especially in terms of land surface descriptions.

For example, there are several classes for snow cover and tundra that are irrelevant in the southern African context. Land surface processes have been greatly simplified in GCMs (Trenberth, 1992), reducing the need for a high degree of resolution in distinguishing between major vegetation types and reducing the computing power necessary to run such models. There is therefore a need to assess the characteristics of the land-surface boundary fields used in this study.

Focusing first on the MM5 RCM, the original vegetation map available described only 4 vegetation classes for Southern Africa, namely desert, range-grassland, savannah and tropical/sub-tropical forest (Figure 3.4). As described in the first chapter, sub-Saharan Africa contains one of the highest levels of floristic diversity in the world, and it is not surprising to expect a high degree of functional diversity associated with this, which is reflected in many different types of vegetation assemblages found throughout the continent. Vegetation types here range from simple grasslands and shrublands, through unique succulent-leaved shrublands of the arid south-west coast, to the many savannah and woodland types and finally deciduous woodlands, forests and even evergreen tropical rainforest (White, 1983). The four classes in the original vegetation map used by the MM5 model therefore strongly underestimated the vegetation structural diversity of the region, and probably compromised model accuracy, especially as it is a regional scale model.

In an attempt to improve this, the MM5 was altered to include an advanced land surface model (LSM), in recognition of the important role that the land surface plays in influencing regional climates (Chen and Dudhia, 2001a, 2001b). The LSM now included in the MM5 was developed at Oregon State University, and is used to provide surface sensible and latent heat fluxes as lower boundary conditions to the atmospheric model. It has a single canopy layer and calculates soil variables (soil moisture and temperature), as well as snow storage and water stored in the canopy. A hydrology sub-model is used to determine evaporation and runoff (Chen and

Dudhia, 2001a). Within the LSM, soils and vegetation are represented as annually fixed maps, with vegetation based on three sets of land-use categorisations. These have 13, 16 or 24 categories, with the 24-category set most frequently used. This legend is based on one developed by the United States Geological Survey (USGS), where the data was developed (Figure 3.5). This base map is an improvement on the original 4 classes, and provides some potential to map the many classes found in southern Africa with some level of fidelity.

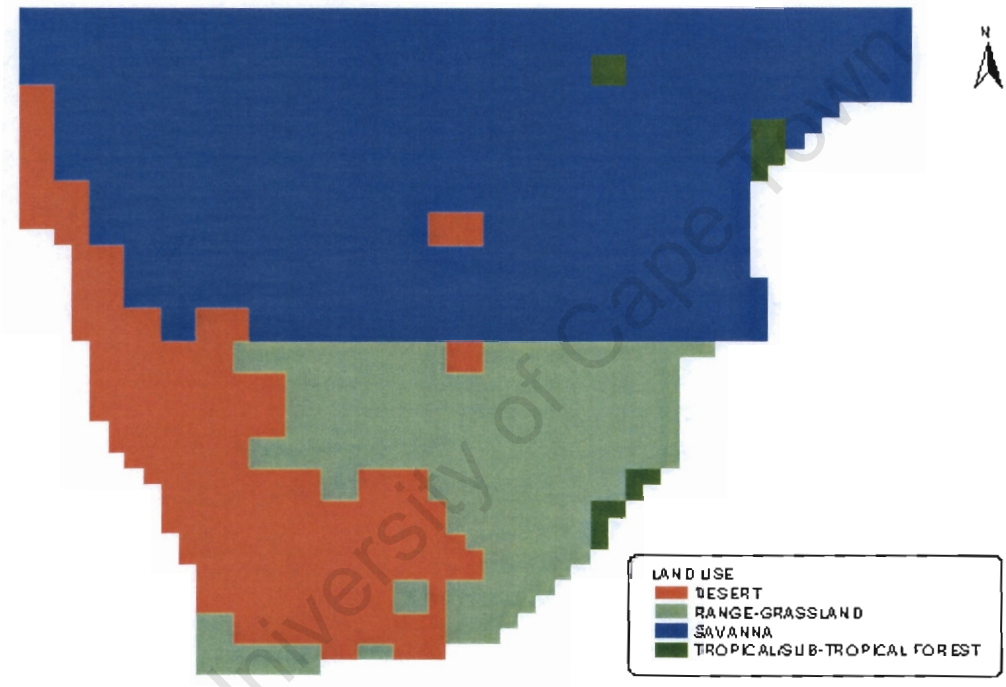

Figure 3.4: The original MM5 model vegetation map

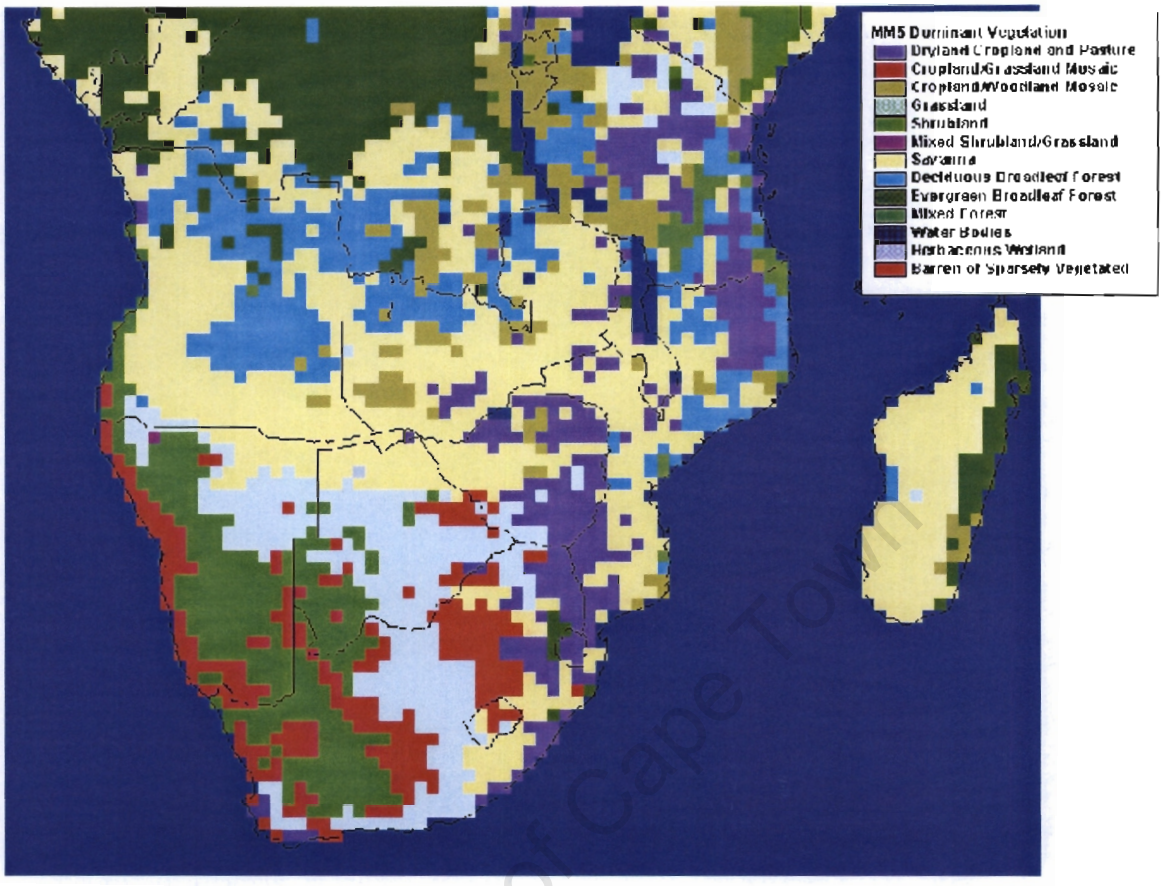

Figure 3.5: The new land-surface USGS dataset used in the MM5 model.

3.3.2 Alternative Land Surface Schemes in Climate Models

An alternative land surface model used in the climate modelling community is the Biosphere-Atmosphere Transfer Scheme (BATS) of Dickinson (1984), which has been used in a first attempt to incorporate an interactive vegetation component into a climate model by Henderson-Sellers (1993). The BATS model has been modified by Dickinson *et al* (1992) and incorporates a single canopy layer and multiple soil layers. The fraction of vegetation varies seasonally based only on minimum temperature and neglects the influence of soil moisture (Henderson-Sellers, 1993). BATS uses 18 vegetation classes based on several data sets, including Matthews (1983) and Wilson and Henderson-Sellers (1985). Albedo values are specified for each vegetation type in the ultraviolet/visible and near-infrared wavelengths. Soil

albedo depends on soil colour and moisture content. A simple carbon cycle calculation is included, which simulates photosynthesis, respiration and litter decay. Table 3.4 shows a comparison between the USGS land surface scheme and the BATS classes (Henderson-Sellers, 1993). For most of the classes, the USGS scheme has a higher albedo, except for the snow or ice class. There are also significant differences in the roughness lengths assigned to the classes. The trees in the BATS all have higher roughness lengths than in the USGS scheme, but for all the other classes the USGS values are higher.

The Simple Biosphere Model (SiB) of Sellers *et al* (1986) is another land surface model frequently used by climate modellers and was one of the first second generation LSMs that recognised the importance of vegetation in the transfer of moisture from the soil to the atmosphere. SiB consists of three sub-models, each based on the three important parameters identified for vegetation-atmosphere interactions, namely albedo, roughness length and surface resistance. The three sub-models therefore describe processes of radiative transfer, turbulent transport and biophysical control of evapotranspiration (Dorman and Sellers, 1989). Table 3.5 shows a comparison of the surface roughness length from SiB and Matthews (1983). These values show the great variation in parameters used in land surface models. The SiB2 model (Sellers *et al*, 1996a) incorporates land surface parameters directly derived from satellite imagery, as opposed to those inferred from land surface classes in SiB (Sellers *et al*, 1996b). Vegetation was also reduced to a single layer and a simpler model of soil moisture stress was used in SiB2. A further improvement is the calculation of photosynthesis in SiB2, which was not calculated in SiB (Sellers *et al*, 1996b).

Table 3.4: The comparison between the USGS classification scheme and the BATS model as used by Henderson-Sellers (1993).

USGS	BATS	Summer Albedo (%)		Rougness Length (cm)	
		USGS	BATS	USGS	BATS
Urban and built-up land		18		60	
Dryland cropland and pasture	Crop	17	10	18	6
Irrigated cropland and pasture	Irrigated crop	18		18	
Mixed dryland/irrigated cropland and pasture		18		18	
Cropland/grassland mosaic		18		16.8	
Cropland/woodland mosaic		16		24	
Grassland	Short grass	19	10	14.4	2
Shrubland	Evergreen shrub	22		12	
Mixed shrubland/grassland	Tall grass	20	8	13.2	10
Savannah	Deciduous shrub	20		18	
Deciduous broadleaf forest	Deciduous broadleaf tree	16	8	60	80
Deciduous needleleaf forest	Deciduous needleleaf tree	14	5	60	100
Evergreen broadleaf forest	Evergreen broadleaf tree	12	4	60	200
Evergreen needleleaf forest	Evergreen needleleaf tree	12		60	
Mixed forest	Mixed woods	13	6	60	80
Water bodies		8		0.012	
Herbaceous wetland		14		24	
Wooded wetland	Bog or marsh	14		48	
Barren or sparsely vegetated	Desert	25	20	12	5
Herbaceous tundra		15		12	
Wooded tundra		15		35	
Mixed tundra	Tundra	15	9	18	4
Bare ground tundra		25		12	
Snow or ice	Ice cap/glacier	55	80	6	1
	Semi-desert		17		10

Table 3.5: The roughness length from Matthews (1984) in comparison to that predicted by SiB (Sellers *et al*, 1986).

Vegetation Type	**Matthews (1984)**	**SiB**
Broadleaf-evergreen trees (tropical forest)	200.0	265.0
Broadleaf-deciduous trees	32.0	83.0
Broadleaf and needleleaf trees (mixed forest)	66.0	118.0
Needleleaf-evergreen trees	100.0	88.0
Needleleaf-deciduous trees (larch)	100.0	73.0
Broadleaf trees with ground cover (savannah)	1.8	86.0
Groundcover only (perennial)	1.0	8.0
Broadleaf shrubs with perennial groundcover	1.0	6.0
Broadleaf shrubs with bare soil	0.8	6.0
Dwarf trees and shrubs with groundcover (tundra)	0.5	7.0
Bare soil	0.5	1.0
Winter wheat and broadleaf deciduous trees	N/a	31.0

As knowledge about land surface-atmosphere interactions has grown, the land surface schemes have evolved to incorporate the latest findings. One of the schemes that has evolved is the new land surface scheme that has recently been incorporated into the HadCM3 climate model, known as the Meteorological Office Surface Exchange Scheme (MOSES) (Cox *et al*, 1999). MOSES is used to calculated moisture, energy and CO_2 fluxes between vegetation and the atmosphere. The incorporation of CO_2 fluxes will improve future climate change predictions under increased atmospheric CO_2 conditions. The new scheme also includes a new interactive representation of stomatal control of transpiration (Cox *et al*, 1998). The soil in the model has four layers, with thicknesses of 0.1, 0.25, 0.65 and 2.0m, from top to bottom. These are used to define the amount of soil moisture available for plants, as root depth is taken into account (Cox and Best, 1999). The land cover dataset used in the model is that of Wilson and Henderson-Sellers (1985), where each land cover class if defined by a standard set of parameters (roughness length, albedo, etc). Only a single surface type is simulated at each site.

The NCAR PCM (described in Chapter 2), which is also used later in this study, is a system of models including an atmospheric component and an oceanic component. The atmospheric model, Community Climate Model version 3 (CCM3), includes the

land surface model known as the Community Land Model (CLM), which has been modified and the second version (CLM2) is now being used. The CLM2 has four components[1]:

1. Biogeophysics: this module is responsible for the instantaneous exchanges of energy, water and momentum with the atmosphere. These surface fluxes influence the simulated surface climate.
2. Hydrological cycle: this module simulates the hydrological cycle over land and includes interception of water by plant foliage and wood, throughfall and stemflow, infiltration, runoff, soil water and snow, which influence atmospheric temperature, precipitation and runoff.
3. Biogeochemistry: the instantaneous exchanges of chemical constituents with the atmosphere.
4. Dynamic vegetation: the module simulates the carbon cycle, and vegetation community compositions and structure, in response to changes such as disturbance (e.g. fire and land use change) and climate change. This module is based on the Lund-Potsdam-Jena (LPJ) model (Sitch *et al*, 2002), but has been greatly modified.

Currently, only the biogeophysics and hydrological cycle modules are used, with the other two modules still under development.

The land surface in the NCAR CLM2 is divided into five land use categories, namely glacier, lake, wetland, urban and vegetated, with the vegetated areas further defined according to twelve plant functional types (PFTs). To account for mixed ecosystems, each site may have up to four PFTs growing there. The combination of PFTs allows the definition of 28 mixed ecosystems or biomes (Table 3.6); for example, savannah consists of 70% C_4 grasses and 30% tropical trees (Bonan *et al*, 2002). The PFTs are associated with a set of parameters, which defines their structure and interactions with the atmosphere. Soil texture and colour are also included to determine soil thermal and hydraulic properties, and soil albedo.

[1] http://www.cgd.ucar.edu/tss/clm

Table 3.6: The biomes of the NCAR LSM (Bonan *et al*, 2002).

	Biome
1	Glacier
2	Desert
3	Needleleaf evergreen forest, cool
4	Needleleaf deciduous forest, cool
5	Broadleaf deciduous forest, cool
6	Mixed forest, cool
7	Needleleaf evergreen forest, warm
8	Broadleaf deciduous forest, warm
9	Mixed forest, warm
10	Broadleaf evergreen forest, tropical
11	Broadleaf deciduous forest, tropical
12	Savannah
13	Forest tundra, evergreen
14	Forest tundra, deciduous
15	Forest crop, cool
16	Forest crop, warm
17	Grassland, cool
18	Grassland, warm
19	Tundra
20	Shrub land, evergreen
21	Shrub land, deciduous
22	Semidesert
23	Irrigated crop, cool
24	Crop, cool
25	Irrigated crop, warm
26	Crop, warm
27	Wetland, forest
28	Wetland, nonforest

Another model used in this study is the Canadian Climate Centre Coupled General Circulation Model, which uses the Canadian Land Surface Scheme (CLASS) to model both soil and vegetation processes. The soil profile consists of three layers with depths of 0.10, 0.25 and 3.75m (Verseghy, 1991). Soil albedo values are based on the soil texture, which is derived from Wilson and Henderson-Sellers (1985). Each grid square divided into four separate subareas: bare soil, snow-covered, vegetation-covered and vegetation and snow-covered. The vegetation cover is modelled as a single layer with four broad vegetation types, namely

needleleaf and broadleaf trees, crops and grass. The assigned parameters, such as albedo and roughness length for each grid square is then calculated as the weighted average of the parameters based on the cover types represented in the grid square (Verseghy *et al*, 1993).

The land surface and vegetation models discussed above frequently require vegetation maps or maps of vegetation parameters, either as input data or for validation of the results. The classifications used in these datasets are discussed in the next section.

3.4 Alternative Classifications and Schemes

The use of plant functional types (PFTs) has been advocated by many authors, especially those working in vegetation modelling and prediction (e.g. Box, 1996; Smith *et al*, 1993, 1997). However, increasingly climate model land surface classifications are using the concept of PFTs as well, as can be seen in NCAR LSM (Bonan *et al*, 2002). This follows the increasing trend of climatologists and vegetation scientists working together and coupling their models together, for example, the Lund-Potsdam-Jena (LPJ) model (Sitch *et al*, 2002) has been incorporated into the NCAR LSM (Bonan *et al*, 2002), and the coupling of an atmospheric model, an ocean model and a DGVM by Cox *et al* (2000). The concept of biomes has also been used to describe vegetation distribution, but biomes are by definition mixed ecosystems and are therefore complex and difficult to quantify in terms of parameters required by climate model, e.g. photosynthesis, stomatal conductance, and LAI (Bonan *et al*, 2002). PFTs provide a single plant type that can be easily quantified in these terms and are therefore much more useful. The fractional cover of PFTs can then be used to calculate combinations of PFTs at a site to determine the changes in a mixed system.

Although the concept of PFTs and biomes provide a simple method of summarising species distributions, the wide variety of land-surface classifications that are

currently available creates some confusion for the vegetation or land surface modeller. Table 3.7 show some of the various legends discussed here and shows the wide range of nomenclature used. Three datasets that have been regularly used in both climate and carbon modelling studies, namely the global datasets of Matthews (1983), Olson and Watts (1982) and Wilson and Henderson-Sellers (1985). These datasets were compiled from existing datasets and are all more than 15 years old.

The increasing availability of satellite data has begun to improve the accuracy of land surface datasets. Satellite imagery can also be used to monitor the land surface and detect changes, e.g. deforestation or the effects of a drought. Examples currently used include advanced very high resolution radiometer (AVHRR), Moderate-Resolution Imaging Spectroradiometer (MODIS) and SPOT-VGT.

Satellite imagery has been used by the International Satellite Land Surface Climatology Project (ISLSCP), which has collected together various datasets to describe the land surface, namely vegetation; hydrology and soils; snow, ice and oceans; radiation and clouds; and near-surface meteorology (Meeson *et al*, 1995). These datasets have a common resolution of 1° x 1°, and are based on more recent data than the three datasets described above. The vegetation dataset uses a legend of 15 vegetation types and uses the Normalised Difference Vegetation Index (NDVI) as the basis for the classification of the 4km AVHRR data generalised to the 1° x 1° resolution (DeFries and Townshend, 1994). Beerling and Woodward (2001) used this dataset to validate the global vegetation distribution modelled by the Sheffield Dynamic Global Vegetation Model (SDGVM). The model predictions show a general agreement with the ISLSCP vegetation distribution, apart from some areas in southern Africa where the ISLSCP data show more desert than the SDGVM predicts, but the resolution of this dataset is still fairly coarse, especially for regional studies.

Table 3.7: Comparison of nomenclature in various land cover datasets and models.

SDGVM PFTs	Class	BOX	IGBP	USGS	MATTHEWS	WHS	NCARLSM	SIB	ISLSCP
Evergreen Broadleaf Forest	1	Tropical evergreen broad-leaved trees	Evergreen broadleaf forests	Evergreen broadleaf forest	Tropical evergreen rainforest, mangrove forest	Tropical broadleaf tree	Broadleaf evergreen forest, tropical	Broadleaf-evergreen trees (tropical forest)	Broadleaved evergreen forest
	1a	Extra-tropical evergreen broadleaf trees (mainly laurophyll)			Tropical/subtropical evergreen seasonal broadleaf forest	Evergreen broadleaf tree			
	1b				Subtropical evergreen rainforest				
	1c				Temperature evergreen seasonal broadleaf forest, summer rain				
	1d				Evergreen broadleaved sclerophyllous forest, winter rain				
	1e				Evergreen broadleaved sclerophyllous woodland				
Deciduous Broadleaf Forest	2	Tropical deciduous broadleaved trees/arborescents	Deciduous broadleaf forests	Deciduous broadleaf forest	Tropical/subtropical drought-deciduous forest	Deciduous broadleaf tree	Broadleaf deciduous forest, tropical	Broadleaf-deciduous trees	Broadleaf deciduous forest and woodland
	2a	Temperate deciduous broadleaf trees			Cold-deciduous forest, without evergreens		Broadleaf deciduous forest, cool		

	2b				Tropical/subtropical drought deciduous woodland		Broadleaf deciduous forest, warm		
	2c				Cold-deciduous woodland				
Evergreen Needleleaf Forest	3	Temperate/boreal needleleaved evergreen trees	Evergreen needleleaf forests	Evergreen needleleaf forest	Temperate/subpolar evergreen rainforest	Evergreen needleleaf tree	Needleleaf evergreen forest, cool	Needleleaf evergreen trees	Coniferous forest and woodland
	3a				Temperate/subpolar evergreen needleleaved forest		Needleleaf evergreen forest, warm		
	3b				Tropical/subtropical evergreen needleleaved forest				
	3c				Evergreen needleleaved woodland				
Deciduous Needleleaf Forest	4	Boreal/cool-temperate deciduous needle-leaved trees	Deciduous needleleaf forests	Deciduous needleleaf forest		Deciduous needleleaf tree	Needleleaf deciduous forest, cool	Needleleaf-deciduous trees (larch)	High latitude deciduous forest and woodland
	5		Mixed forests	Mixed forest	Cold-deciduous forest, with evergreens		Mixed forest, cool	Broadleaf and needleleaf trees (mixed forest)	Mixed coniferous and broadleaf deciduous forest and woodland
	5a						Mixed forest, warm		

C4 Grassland	6	Grasses and related graminoids	Grassland	Grassland	Tall grassland, no woody cover	Long grass	Grassland, warm	Groundcover only (perennial)	C4 grassland
C3 Plants	6a				Medium grassland, no woody cover		Grassland, cool		C3 grassland
	6b				Meadow, short grassland, no woody cover	Short grass and forbs			
	6c	Ephemeral herbs			Forb formations				
	7		Wetland	Herbaceous wetland			Wetland, nonforest		
	7a			Wooded wetland		Swamp	Wetland, forest		
	8	Short-season broad-leaved dwarf-shrubs		Mixed tundra	Arctic/alpine tundra, mossy bog	Tundra	Tundra	Dwarf trees and shrubs with groundcovr (tundra)	Tundra
	8a			Herbaceous tundra	Cold-deciduous subalpine/subpolar shrubland, cold-deciduous dwarf shrubland		Forest tundra, deciduous		
	8b			Wooded tundra			Forest tundra, evergreen		
	8c			Bare ground tundra					
	9	Deciduous shrubs/dwarf-shrubs	Closed shrublands	Shrubland	Drought-deciduous shrubland/thicket	Deciduous shrub	Shrubland, deciduous	Broadleaf shrubs with perennail groundcover	C3 wooded grassland

	9a	Sclerophyll trees/arborescents	Open shrublands	Mixed shrubland/grassland	Tall/medium/short grassland with shrub cover	Evergreen broadleaf shrub	Shrubland, evergreend		
	9b	Sclerophyll /coriaceous shrubs/dwarf-shrubs			Evergreen broadleaved shrubland/thicket, evergreen dwarf-shrubland	Thorn shrub			
	9c				Evergreen needleleaved or microphyllous shruland/thicket				
	10	Diurnally active tuft-arborescents/frutescents/forbs			Xeromorphic forest/woodland		Semi-desert	Broadleaf shrubs with bare soil	Shrubs and bare ground
	10a	Stress-tolerant succulents			Xeromorphic shrubland/dwarf shrubland				
	11		Savannas	Savanna	Tall/medium/short grassland with <10% woody tree cover or tuft plant cover		Savanna	Broadleaf trees with ground cover (savanna)	Wooded C4 grassland
	11a		Woody savannas		Tall/medium/short grassland with 10-40% woody tree cover				
	12	Stress-tolerant lower plants, especially mosses, lichens	Barren or sparse	Barren or sparsely vegetated	Desert	Soil	Desert	Bare soil	Desert, bare ground
	13			Urban and built-up land		Urban			
	14			Water bodies		Water			Water

	14a					Inland lake			
	15		Snow and ice	Snow and ice	Ice	Ice	Glacier	Perpetual ice	Ice
	16		Cropland	Dryland cropland and pasture	Cultivation	Arable	Crop, warm		Cultivation
	16a		Crop and other vegetation	Cropland/grassland mosaic		Maize	Crop, cool		
	16b			Irrigated cropland and pasture		Irrigated crop	Irrigated crop, cool		
	16c			Mixed dryland/irrigated cropland and pasture		Rice	Irrigated crop, warm		
	16d			Cropland/woodland mosaic		Sugar	Forest crop, cool	Winter wheat and broadleaf deciduous trees	
	16e					Cotton	Forest crop, warm		

As an alternative, the IGBP-DIS dataset was developed to improve on the datasets above and uses a biome-based classification (Loveland *et al*, 2000). It was developed using an unsupervised classification of the 1 km AVHRR NDVI data. The legend has 17 land cover classes. Each continent was treated separately, which captures the diversity of each continent more accurately. Several issues affect the accuracy of this data (Loveland *et al*, 2000). Firstly, the impact of atmospheric contamination and the occurrence of cloud affect the classification, as with all satellite imagery. The seasonal changes in cultivated land created difficulties in distinguishing between crops and natural vegetation, and there were limitations in the reference data used to distinguish between these two classes.

A further problem relating to these approaches to representing the land surface in climate models is that the vegetation is frequently static, with only the parameters used to define each vegetation type varying for summer and winter, for example the USGS scheme (Table 3.8). This is a major problem when simulating future climate, as the major anthropogenic changes in climate expected will certainly impact on the spatial distribution of vegetation types. What is needed is an approach that simulates vegetation structure at the appropriate coarse functional type scale, but which allows the generation of a vegetation component that is responsive to climate change. Furthermore, the scheme was developed at the United States Geological Survey (USGS), and therefore has a northern hemisphere bias, along with many of the other classifications discussed. For example, there are four types of tundra and a snow or ice class, none of which occur in Africa. In fact, only 13 of the 24 USGS classes actually occur in the study region (see Figure 3.5). There is also only one savannah class in this legend, but African savannahs are known to be quite varying, and savannah could be subdivided into several classes (Scholes, 1997; Scholes *et al*, 1997). There are also few data available for Africa to compare with the defined values for each of the parameters, and to validate the seasonal changes. The validity of using such a legend for Africa is therefore questionable.

Table 3.8: The parameters defining the vegetation types within the MM5 Land Surface Model (S=summer, W=winter), based on the USGS 24 class categorisation.

Vegetation Class	Albedo		Soil Moisture		Surface Emmissivity		Roughness Length		Thermal Inertia		Snow Effect Factor		Surface Heat Capacity	
	S	W	S	W	S	W	S	W	S	W	S	W	S	W
1 Urban and Built-Up Land	18	18	0.10	0.10	0.88	0.88	60	60	3	3	0.52	0.52	1.89E+06	1.89E+06
2 Dryland Cropland and Pasture	17	23	0.30	0.60	0.92	0.92	18	6	4	4	0.60	0.60	2.50E+06	2.50E+06
3 Irrigated Cropland and Pasture	18	23	0.50	0.50	0.92	0.92	18	6	4	4	0.60	0.60	2.50E+06	2.50E+06
Mixed Dryland/Irrigated														
4 Cropland and Pasture	18	23	0.25	0.50	0.92	0.92	18	6	4	4	0.60	0.60	2.50E+06	2.50E+06
5 Cropland/Grassland Mosaic	18	23	0.25	0.40	0.92	0.92	16.8	6	4	4	0.60	0.60	2.50E+06	2.50E+06
6 Cropland/Woodland Mosaic	16	20	0.35	0.60	0.93	0.93	24	24	4	4	0.60	0.60	2.50E+06	2.50E+06
7 Grassland	19	23	0.15	0.30	0.92	0.92	14.4	12	3	4	0.60	0.60	2.08E+06	2.08E+06
8 Shrubland	22	25	0.10	0.20	0.88	0.88	12	12	3	4	0.62	0.62	2.08E+06	2.08E+06
9 Mixed Shrubland/Grassland	20	24	0.15	0.25	0.90	0.90	13.2	12	3	4	0.60	0.60	2.08E+06	2.08E+06
10 Savanna	20	20	0.15	0.15	0.92	0.92	18	18	3	3	0.00	0.00	2.50E+06	2.50E+06
11 Deciduous Broadleaf Forest	16	17	0.30	0.60	0.93	0.93	60	60	4	5	0.56	0.56	2.50E+06	2.50E+06
12 Deciduous Needleleaf Forest	14	15	0.30	0.60	0.94	0.93	60	60	4	5	0.50	0.50	2.50E+06	2.50E+06
13 Evergreen Broadleaf Forest	12	12	0.50	0.50	0.95	0.95	60	60	5	5	0.00	0.00	2.92E+06	2.92E+06
14 Evergreen Needleleaf Forest	12	12	0.30	0.60	0.95	0.95	60	60	4	5	0.50	0.50	2.92E+06	2.92E+06
15 Mixed Forest	13	14	0.30	0.60	0.94	0.94	60	60	4	6	0.54	0.58	4.18E+06	4.18E+06
16 Water Bodies	8	8	1.00	1.00	0.98	0.98	0.012	0.012	6	6	0.00	0.00	9.00E+25	9.00E+25
17 Herbaceous Wetland	14	14	0.60	0.75	0.95	0.95	24	24	6	6	0.55	0.55	2.92E+06	2.92E+06
18 Wooded Wetland	14	14	0.35	0.70	0.95	0.95	48	48	5	6	0.58	0.58	4.18E+06	4.18E+06
19 Barren or Sparsely Vegetated	25	25	0.02	0.05	0.85	0.85	12	12	2	2	0.62	0.62	1.20E+06	1.20E+06
20 Herbaceous Tundra	15	60	0.50	0.90	0.92	0.92	12	12	5	5	0.60	0.00	9.00E+25	9.00E+25
21 Wooded Tundra	15	50	0.50	0.90	0.93	0.93	35	36	5	5	0.60	0.00	9.00E+25	9.00E+25
22 Mixed Tundra	15	55	0.50	0.90	0.92	0.92	18	18	5	5	0.60	0.00	9.00E+25	9.00E+25
23 Bare Ground Tundra	25	70	0.02	0.95	0.85	0.95	12	6	2	5	0.62	0.00	1.20E+06	1.20E+06
24 Snow or Ice	55	70	0.95	0.95	0.95	0.95	6	6	5	5	0.00	0.00	9.00E+25	9.00E+25

Box (1996) developed a model of approximately 50 dominant plant types that were based on major climatic factors and current global vegetation distribution. These 50 classes were then group into 15 major plant types, which Box (1996) suggests could be used as a minimal set of PFTs for modelling studies (Table 3.9). An examination of the legend in Table 3.8 revealed that most could be summarised into 14 classes, namely evergreen broadleaf and needleleaf forests, deciduous broadleaf and needleleaf forests, mixed forests, shrubland, savannah, grassland, desert or sparsely vegetated, cultivation, snow or ice, water, urban areas and tundra.

Table 3.9: Dominant plant types and biomes suggest by Box (1996)

	Dominant Plant Type	**Biome Type(s)**
1	Tropical evergreen broad-leaved trees	Tropical rainforests
2	Tropical deciduous broad-leaved trees/arborescents	Raingreen forests, woodlands, scrub
3	Extra-tropical evergreen broad-leaved trees (mainly laurophyll)	Evergreen broad-leaved forests, temperate rainforests
4	Temperature deciduous broad-leaved trees	Summergreen broad-leaved forests and woodlands
5	Temperate/boreal needle-leaved evergreen trees	Needle-leaved evergreen forests/open woodlands
6	Boreal/cool-temperate deciduous needle-leaved trees	Deciduous boreal needle-leaved forests/open woods
7	Sclerophyll trees/arborescents	Subhumid woodlands/scrub
8	Sclerophyll/coriaceous shrubs/dwarf-shrubs	Shrublands, krummholz, semi-deserts
9	Deciduous shrubs/dwarf-shrubs	Shrublands, krummholz, semi-deserts
10	Short-season broad-leaved dwarf-shrubs	Tundra: dwarf-shrubs, graminoid, etc
11	Diurnally active tuft-arborescents/frutescents/forbs	Tropical alpine scrub
12	Grasses and related graminoids	Grasslands and savannas
13	Stress-tolerant succulents	Semi-desert scrub
14	Ephemeral herbs	Semi-desert scrub
15	Stress-tolerant lower plants, especially mosses, lichens	Tundra, cold-desert

Using the ideas of Bonan *et al* (2002) and the summarised classes discussed above, the fractional cover of PFTs had been used to develop a classification of biomes

from the output from the Sheffield Dynamic Global Vegetation Model (SDGVM). This classification is based on the ISLSCP legend and refers to the biomes that occur in southern Africa, based on published descriptions of vegetation in the region (Cowling *et al,* 1997; Rutherford and Westfall, 1994; Low and Rebelo, 1996). This classification takes into account the vegetation types that are found in the region, and excludes those that do not occur in southern Africa, such as tundra (Table 3.10). It is also an effective tool for analysing the fractional cover of the SDGVM output, as opposed to just the dominant vegetation type. As this classification was developed based on vegetation model output, it does not include classes that are not composed of natural vegetation, for example croplands or urban areas. These can be added as required. This classification will be used later to validate the accuracy of the vegetation distribution predicted by SDGVM over southern Africa.

Table 3.10: The Modified Classification of SDGVM output.

Class	Description	Name
1	BG > 90%	Desert
2	C3s > 60%	C3 Grassland/Shrubland
3	C4s > 60%	C4 Grassland
4	EvBl > 60%	Evergreen Broadleaf Forest
5	DcBl > 60%	Deciduous Broadleaf Forest
6	DcBl and C4 > 20% and <60%	Savannah
7	EvBl and DcBl mix together < 60%	Mixed Forest
8	DcBl > 30%, with C4s or C3s > 20%	Shrubland/Savannah
9	BG > 30% and < 90%, with C3s or C4s	Arid Shrubland

3.5 Conclusions

There are a large number of land surface classifications and land surface models currently being used in land-surface – atmosphere interactions studies. Several of these have been discussed, focussing on those that have impacted this study. For example, the MM5 regional climate model is used in Chapter 5 to assess the response of a regional climate to its vegetation inputs, so the land surface classification of the MM5 model has been discussed. In general, most of the

classifications used have been developed in the northern hemisphere, and therefore do not accurately reflect the diversity of southern African vegetation. However, these classifications can be adapted to better suit the region with reference to the published descriptions of the vegetation of southern Africa.

Furthermore, the land surface models used in climate models are being updated, and there are recent attempts to couple land surface models with DGVMS to achieve the aim of a dynamic component in climate models.

The following chapter explains the methods used to prepare the input data for these models, as well as the techniques used to analyse the output from the models.

CHAPTER 4: TECHNIQUES AND DATA DESCRIPTION

4.1. Introduction

All models represent a simplification of reality, and will therefore have biases based on the decisions made by the developer on how to simplify the processes being modelled. In order to evaluate a model's performance, a dataset that represents reality is needed, against which the model can be validated. For a climate model, there are several data sources that provide the spatial and temporal scales that are required to validate the climate model under current conditions. Examples of these include observed and reanalysis datasets. Climate and weather are continually monitored and recorded, providing extensive datasets available for validation, and also as input for reanalysis projects. A reanalysis project uses observed data in the initial data assimilation scheme of a fixed global weather forecasting model. This creates a dynamically consistent set of historical atmospheric analyses (Kalnay *et al*, 1996).

Vegetation distribution, on the other hand, changes at a much slower pace than climate and is therefore not being constantly monitored. The result is that many of the datasets and descriptions of vegetation for Africa south of the Equator are not recent. The most comprehensive description currently available is White (1983), which is now more than 20 years old. More recent descriptions of the vegetation of South Africa and some of its neighbouring states are available (Cowling *et al*, 1997; Low and Rebelo, 1996; Rutherford and Westfall, 1994), but further north, there is a distinct lack of recent data. Most of these vegetation descriptions do not consider the change from natural vegetation to agriculture or other uses. However, this can be considered an advantage, as the vegetation model used in this study (along with several other vegetation models) only predicts potential natural vegetation, and would thus exclude agriculture and man-made land uses.

This chapter therefore describes the preparation of a dataset that will be used to validate the vegetation model, as well as some of the preparation of datasets for use in the experiments presented in later chapters. The vegetation validation dataset has been created from several different sources, in an attempt to provide the most up-to-date vegetation map possible for the study region. As this dataset relies on such a variety of sources, it was decided to use satellite imagery in addition to the validation dataset, as well as a published dataset, the ISLSCP vegetation distribution map (DeFries and Townshend, 1994). The satellite data chosen is from the SPOT-VGT[1] system, which is specifically designed to monitor vegetation and is described below. These datasets are described in the next two sections.

4.2. Validation Data Description

4.2.1. Version 1

In order to create a dataset to validate the results from the vegetation model, the United States Geological Survey (USGS) land cover classification was used to define a regional grid in a Geographical Information System (GIS), at a 0.25° resolution. The classification defines 24 land cover classes (Table 4.1), including urban areas, cropland and pasture, and a range of natural vegetation structural types (such as savanna, grassland and forest). As this classification was designed to be used with climate models, each land surface class is associated with a set of characteristics, such as surface roughness, height and albedo, which are the model inputs. These characteristics vary seasonally, having different values for "summer" and "winter". A number of different data sources were used to complete the GIS dataset, so the USGS classification was used to unify the different classifications that accompany these data sources.

[1] http://www.vgt.vito.be/

The first data set used to create version 1 of the GIS database was the public domain UNESCO/AETFAT/UNSO Vegetation Map of Africa (White, 1983), which has well defined structural units, more or less analogous to the USGS classification (Figure 4.1). Table 4.2 shows how the White's structural types were fitted into the USGS Classification.

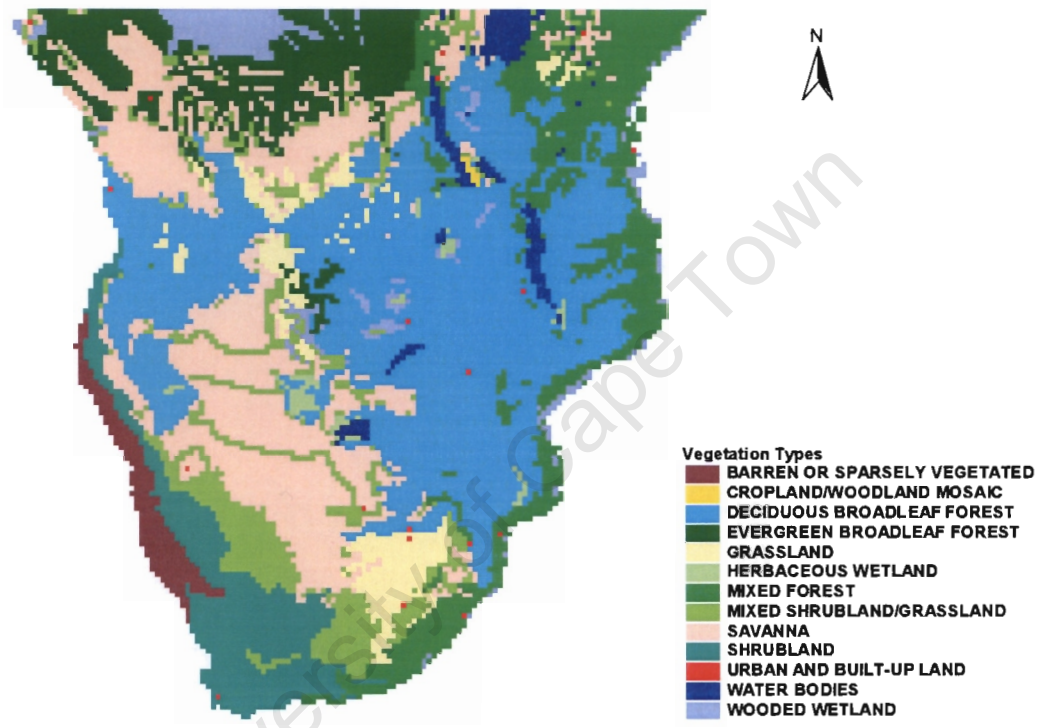

Figure 4.1: Version 1 of the NBI validation dataset

Table 4.1: USGS Land Cover Classes and variables defining each class for summer.

Class	Albedo	Soil Moisture	Surface Emmissivity	Surface Roughness Length	Thermal Inertia	Snow Effect Factor	Surface Heat Capacity	Land Cover Type
1	18	0.10	0.88	60.000	3	0.52	1.89E+06	Urban and Built-Up Land
2	17	0.30	0.92	18.000	4	0.60	2.50E+06	Dryland Cropland and Pasture
3	18	0.50	0.92	18.000	4	0.60	2.50E+06	Irrigated Cropland and Pasture
4	18	0.25	0.92	18.000	4	0.60	2.50E+06	Mixed Dryland/Irrigated Cropland and Pasture
5	18	0.25	0.92	16.800	4	0.60	2.50E+06	Cropland/Grassland Mosaic
6	16	0.35	0.93	24.000	4	0.60	2.50E+06	Cropland/Woodland Mosaic
7	19	0.15	0.92	14.400	3	0.60	2.08E+06	Grassland
8	22	0.10	0.88	12.000	3	0.62	2.08E+06	Shurbland
9	20	0.15	0.90	13.200	3	0.60	2.08E+06	Mixed Shrubland/Grassland
10	20	0.15	0.92	18.000	3	0.00	2.50E+06	Savanna
11	16	0.30	0.93	60.000	4	0.56	2.50E+06	Deciduous Broadleaf Forest
12	14	0.30	0.94	60.000	4	0.50	2.50E+06	Deciduous Needleleaf Forest
13	12	0.50	0.95	60.000	5	0.00	2.92E+06	Evergreen Broadleaf Forest
14	12	0.30	0.95	60.000	4	0.50	2.92E+06	Evergreen Needleleaf Forest
15	13	0.30	0.94	60.000	4	0.54	4.18E+06	Mixed Forest
16	8	1.00	0.98	0.012	6	0.00	9.00E+25	Water Bodies
17	14	0.60	0.95	24.000	6	0.55	2.92E+06	Herbaceous Wetland
18	14	0.35	0.95	48.000	5	0.58	4.18E+06	Wooded Wetland
19	25	0.02	0.85	12.000	2	0.62	1.20E+06	Barren or Sparsely Vegetated
20	15	0.50	0.92	12.000	5	0.60	9.00E+25	Herbaceous Tundra
21	15	0.50	0.93	36.000	5	0.60	9.00E+25	Wooded Tundra
22	15	0.50	0.92	18.000	5	0.60	9.00E+25	Mixed Tundra
23	25	0.02	0.85	12.000	2	0.62	1.20E+06	Bare Ground Tundra
24	55	0.95	0.95	6.000	5	0.00	9.00E+25	Snow or Ice

Table 4.2. White's (1983) structural types versus USGS vegetation classes.

USGS Vegetation Number and Type		White's Structural Type
6	Cropland/woodland mosaic	Cultivation and secondary grassland replacing upland and montane forest.
7	Grassland	Highveld grassland; Edaphic and secondary grassland on Kalahari sand; Altimontane vegetation in South Africa.
8	Shrubland	Cape shrubland (Fynbos); Bushy Karoo-Namib shrubland; Succulent Karoo shrubland; Dwarf Karoo shrubland.
9	Mixed shrubland/grassland	Transition from Afromontane scrub forest to Highveld grassland; Semi-desert grassland and shrubland; The Kalahari/Karoo-Namib transition; Grassy shrubland; Altimontane vegetation in tropical Africa.
10	Savannah	Mosaic of lowland rain forest and secondary grassland; Mosaic of dry deciduous forest and secondary grassland with wooded grassland; Mosaic of Afromontane scrub forest, Zambezian scrub woodland and secondary grassland; Mosaic of wetter Zambezian woodland and secondary grassland; Transition from undifferentiated woodland to Acacia deciduous bushland and wooded grassland; Transition from Colophospermum mopane scrub woodland to Karoo-Namib shrubland; *Acacia polyacantha* secondary wooded grassland; Kalahari deciduous Acacia wooded grassland and bushland; Mosaic of West African evergreen bushland and secondary Acacia wooded grassland; Mosaic of Malagasy deciduous thicket and secondary grassland; Mosaic of Brachystegia bakerana thicket and edaphic grassland; Tugela basin wooded bushland.
11	Deciduous broadleaf forest	Malagasy dry deciduous forest; Wetter Zambezian miombo woodland; Drier Zambezian miombo woodland; *Colophospermum mopane* woodland and scrub woodland; Undifferentiated woodland.

13	Evergreen needleleaf forest	Guineo-Congolian rain forest drier types; Transitional rain forest; Malagasy moist montane forest; Zambezian dry evergreen forest.
15	Mixed forest	West African coastal mosaic; East African coastal mosaic; Undifferentiated montane vegetation; South African evergreen and semi-evergreen bushland and thicket; Itigi deciduous thicket; Malagasy deciduous thicket; Somalia-Masai Acacia-Commiphora deciduous bushland and thicket.
17	Herbaceous wetland	Herbaceous swamp and aquatic vegetation; Halophytic vegetation.
18	Wooded wetland	Swamp forest; Mosaic of swamp forest and wetter lowland rain forest (Guineo-Congolian); Mosaic of edaphic grassland and semi-aquatic vegetation; Mangrove.
19	Barren or sparsely vegetated	The Namib Desert.

The Environmental Potential Atlas (ENPAT) CD-ROM (DEAT, 1997) was also used in version 1 and contains data that defines urban areas for South Africa as polygons. This data set also contains a land use coverage that was used to improve the definition of cropland over South Africa. The ENPAT land use coverage contains 10 land use classes. These represent the USGS classes as shown in Table 4.3. Unfortunately, similar datasets are not available for other countries in the study region, so the ESRI[2] point coverage of urban areas was used to pinpoint the location of other major cities. Only those urban areas that are capitals of a country, or those which have a population greater than 1 000 000 were used. A polygon coverage of inland water bodies, supplied by the NBI, was used in conjunction with a lake coverage from ESRI[2] to define the position of inland water bodies.

Table 4.3. ENPAT classes versus USGS classes

ENPAT Class		USGS Vegetation Type	
1	Cattle and game farming		Natural vegetation
2	Conservation/Protected area		Natural vegetation
3	Forestry	14	Evergreen needleleaf forest
4	Mixed farming	2	Dryland cropland and pasture
5	Natural area		Natural vegetation
6	Sheep farming		Natural vegetation
7	Subsistence farming		Natural vegetation
8	Sugar cane	3	Irrigated cropland and pasture
9	Urban area	1	Urban and built-up land
10	Wheat and maize	3	Irrigated cropland and pasture

Conservation International (CI, 1999) has created a dataset for the island of Madagascar, which is regarded as the most up-to-date vegetation description for Madagascar, and was therefore also included in the first version of the NBI validation dataset. Table 4.4 shows how the CI vegetation classes were reclassified into the USGS land use classes.

[2] Part of the World dataset that accompanies the ArcView GIS 3.x software

These datasets were combined to create version 1 of the GIS database, but these datasets do not all represent the most recent surveys of southern African vegetation. It was therefore decided to create a newer version.

Table 4.4: Classification of CI data into USGS classification.

CI Vegetation Type	USGS Vegetation Type	
Dunes and salty sands	19	Barren or sparsely vegetated
Limestone formation	8	Shrubland
Degraded limestone formation	19	Barren or sparsely vegetated
Galery formation	13	Evergreen broadleaf forest
Dense humid/moist mountain forest	13	Evergreen broadleaf forest
Dense evergreen rainforest	13	Evergreen broadleaf forest
Dense evergreen rainforest seasonal	13	Evergreen broadleaf forest
Dry forest	15	Mixed forest
Litural forest	15	Mixed forest
Schlerophylous lowland forest (very degraded)	15	Mixed forest
Secondary formation	10	Savannah
Philippia scrub	8	Shrubland
Dense scrub	8	Shrubland
Dense dry scrub	8	Shrubland
Marshes	18	Wooded wetland
Forest/savannah mosaic	10	Savannah
Scrub/bare soil mosaic	19	Barren or sparsely vegetated
Savannah/agriculture/secondary forest mosaic	6	Cropland/woodland mosaic
Savannah/agriculture/plantation mosaic	6	Cropland/woodland mosaic
Plantation	15	Mixed forest
Rice paddies	17	Herbaceous wetland
Savannah	10	Savannah
Wooded savannah	10	Savannah
Savannah on highlands	10	Savannah
Bare soil	19	Barren or sparsely vegetated
Water	16	Water bodies
Mangrove	18	Wooded wetland

4.2.2. Version 2

In order to create the most up-to-date GIS database, the most accurate data needed to be included. The National Botanical Institute (NBI) of South Africa was involved in

the Safari 2000 project[3], which resulted in a dataset of the species composition of southern African vegetation, south of the equator. The dataset was developed from a number of sources, including published and unpublished species lists from field surveys, published travellers accounts, and species lists and descriptions associated with mapped units through out the region. The datasets used as sources include those by White (1983) and Low and Rebelo (1996). This dataset therefore represents the most up-to-date distribution of vegetation for Africa south of the equator at this time and was used to create Version 2 (Figure 4.2) of the validation dataset. The next section outlines the techniques used to create this version.

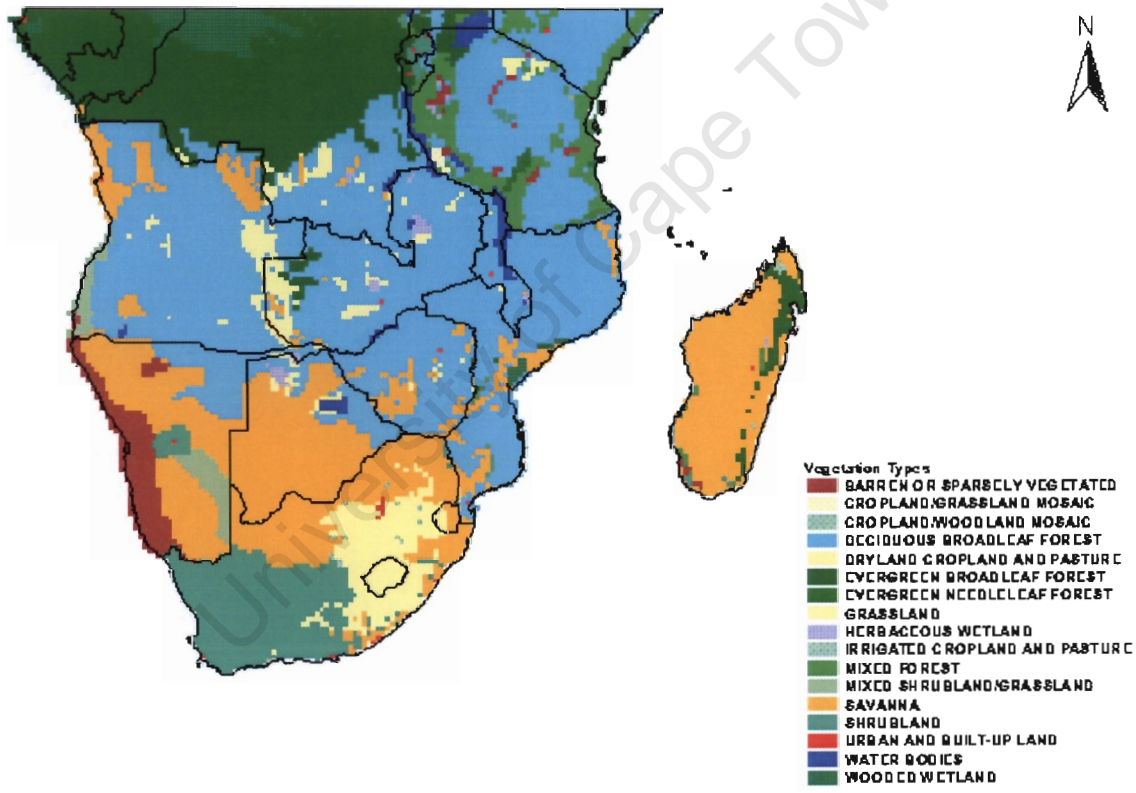

Figure 4.2: Version 2 of the NBI validation dataset

[3] http://www.safari2000.org

4.2.3. Geographical Information System (GIS) Techniques

The initial grid polygon coverage was created in a GIS, with a spatial domain of 0° to 35°s, and 8.5°E to 51°E and a grid cell size of 0.25° by 0.25° (138 columns and 140 rows). The grid cells were first classified by selecting the grid cells that fell within each structural type in the White's classification. The selected grid cells were then classified as the USGS class that corresponds to the White's (1983) class. The water body's coverage was overlaid on the grid and were given preference over the vegetation type. Urban areas were limited to one 0.25° pixel each, which is the limit of resolution of this version. The land cover information from the ENPAT CD-ROM was compared with the vegetation grid and the grid cells were updated in the GIS.

A second classification was performed to validate the first and correct any mistakes. The attribute tables associated with the spatial data were imported into an Excel spreadsheet and used to create pivot tables. Using nested "IF" functions, the vegetation field with the highest area in each grid cell was found. The resulting table was imported into the GIS and joined to the existing attribute table as the new vegetation classification of the grid. This methodology was found to be more accurate than the first and was therefore used for all future classifications of the grid.

4.3. SPOT-VGT data

4.3.1. Introduction to the SPOT-VGT Data

The SPOT Vegetation (SPOT-VGT) sensor was launched on the SPOT 4 satellite in 1998[4]. The sensor was specifically designed for seasonal and long-term monitoring of land-surface properties, such as albedo and surface roughness (which can either be directly determined or inferred from the data). The imagery produced has a resolution of 1 km in the red, blue, near-infrared and short-wave infrared bands. The red band incorporates the absorption peak of chlorophyll (0.665 μm), while the short-

[4] http://www.spot.com

wave infrared band aids in the measurement of the water content in the canopy and its structure. The near-infrared band measures the maximum vegetation spectral reflectance, which is related to the structural properties of the canopy and the amount of bare soil between vegetation. The blue band is included as this is the band were atmospheric aerosol diffusion is at its maximum. The blue band can therefore be used for atmospheric corrections and characterisation of the aerosols.

The dataset available is daily synthesis images (SPOT-VGT S1), covering the fourteen months from November 1999 to December 2000. The original SPOT-VGT S1 data covers the whole of Africa and was subsetted to a new set of co-ordinates. The co-ordinates are:

- 20^0N - 34^0S
- 14^0W - 50^0E

A composite of all 14 images was created using the BAND MATH FUNCTION, available in the ENVI image processing software package. Four images were created, one for each band. Each band had an individual specific mask applied to it in order to eradicate cloud cover, which would have dominated the final image. Once all the bands had been masked, the fourteen monthly images for each of the 4 bands were merged. The expression used to sum and then average all the bands was as follows:

(float(b1)+float(b2)+float(b3)+float(b4)……..+float(b14))/14

This expression added each pixel of each band to its coincident pixel, and then divided the total by 14. This however did not solve the problem of cloud or the satellite path. The final image (Figure 4.3) when viewed as a colour composite clearly shows that the satellite paths and the masked areas can still be seen and will thus influence the final classification.

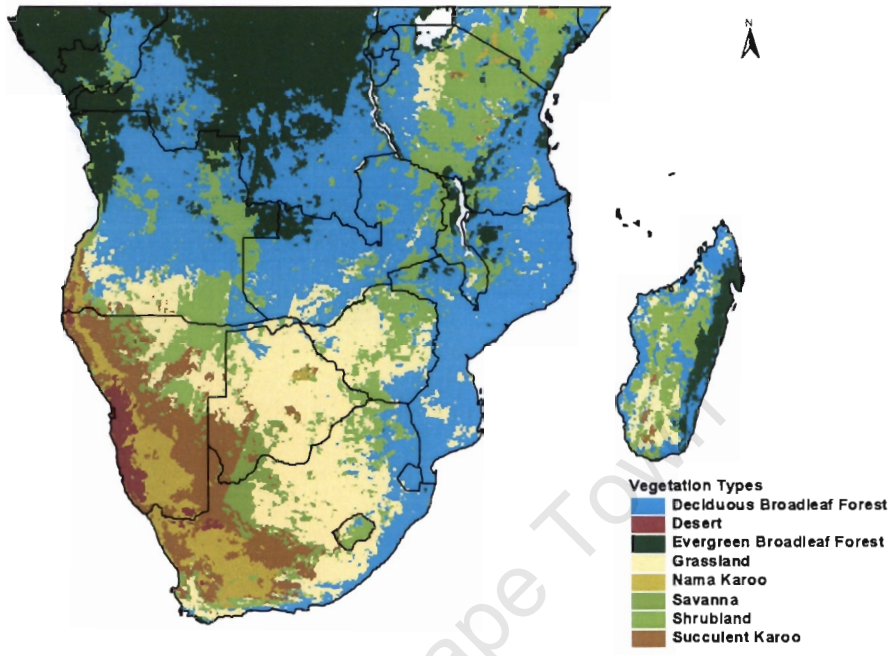

Figure 4.3: SPOT-VGT composite image

4.3.2. Classification procedures

Regions of interest (ROIs) were chosen using map co-ordinates from White's (1983) vegetation map of Africa. Major vegetation zones were classified by choosing a number of ROIs within each vegetation category. The ROI selection was based on the choice of a number of sites within each vegetation category to try and obtain the spectral variability present in each category. The areas were first chosen from the map using geographic co-ordinates and these co-ordinates were then found on each of the satellite images to ensure an accurate location for each of the regions of interest chosen to represent each vegetation category.

The vegetation categories are as follows:

- Fynbos

- Succulent Karoo
- Nama Karoo
- Desert
- Grassland
- Evergreen Forest
- Savanna
- Deciduous Forest
- Cloud (not a vegetation category)

A maximum likelihood classification algorithm was used to classify each image into the nine classes. Each of the fourteen images had to be classified individually due to the changes needed in the ROI's because of the variation in cloud cover. The cloud cover varies considerably and the ROI's needed to be changed in the areas where the cloud is covering the original ROI's. A number of classification iterations were performed on each image to produce a best overall classification output.

4.3.3. Transferring the data to a GIS database

The classification was filtered using a median filter with a kernel size of 15 pixels. This was done to reduce the patchiness of each vegetation class slightly, which helped when each image was converted into the GIS database. The classification was converted from a raster file format into a vector file format and then exported into the GIS. A legend was created for the dataset showing the vegetation classes. The classification was then analysed and compared to the original map so that slight improvements could be made to areas where there were slight misclassifications. The final dataset was used to validate the results from the vegetation model (SDGVM).

4.4. Incorporating Model Results into the GIS Database

4.4.1. Vegetation Model Results

The Sheffield Dynamic Global Vegetation Model (SDGVM) produces ASCII files as its output. These files can be analysed through a number of methods, but the methods chosen in this study use a spreadsheet and a GIS database. The spreadsheet was used for simple statistical analyses and to prepare the raw output from the model so that it can be imported into the GIS database. The same grid polygon coverage used in the NBI validation dataset is also used to assign a spatial dimension within the GIS database to the spreadsheet. The new dataset can then be used to create maps based on the attributes (the model output) or for further analysis.

4.4.2. Climate Model Results

The results from the climate models are produced in a binary format. The results are firstly converted into ASCII format. These results are then processed through the same route as the vegetation model results, and incorporated into the GIS.

4.5. General Circulation Model (GCM) Data Preparation

4.5.1. Conversion to Vegetation Model Input Format

The General Circulation Models (GCMs) used later in this study are all used by the IPCC, which provides access to data from these GCMs through its Data Distribution Centre (DDC)[5]. The DDC aims to provide up-to-date scenarios of climate changes for use in climate change studies. The sets of variables available for each scenario and model are different and are provided as monthly mean values. The GCMs used in this study were selected because they provided the variables required to run the vegetation model, namely temperature, precipitation and relative humidity, or an

[5] http://ipcc-ddc.cru.uea.ac.uk/dkrz/dkrz_index.html

associated variable that could be used to calculate the required variable. However, it should be noted that only the results from these GCMs was used in this study, and that there was attempt to model the feedbacks from the predicted vegetation to the GCMs. The four GCMs selected (CCCMa CGCM2, ECHAM4/OPYC3, UKMO HadCM3 and NCAR PCM, see chapter 2) all provided monthly mean precipitation (mm/day) and temperature in degrees Kelvin. The temperature data was therefore first converted into degrees Celsius as required for the vegetation model. Only the HadCM3 model provided relative humidity (percentage) as required by the vegetation model. Relative humidity was calculated using the following equations for the other three models:

- CCCMa CGCM2 and NCAR PCM Models:
  Given temperature (T°C), pressure (P) and specific humidity (q), calculate

$$e_s = 610.78 * 10^{(T°C/(T°C+238.3)*17.2694)}$$

$$q_s = (0.622 * e_s)/(P-0.378*e_s)$$

$$Rh = q/q_s * 100$$

  Where Rh = relative humidity, e = vapour pressure and the subscript *s* refers to the saturation value at the same temperature.

- ECHAM4/OPYC3 Model:
  Given temperature (T°C) and dew point temperature (Td), calculate

$$e_{s1} = 610.78 * 10^{(T°C/(T°C+238.3)*17.2694)}$$

$$e_{s2} = 610.78 * 10^{(Td/(Td+238.3)*17.2694)}$$

$$Rh = e_{s2}/e_{s1} * 100$$

  Where Rh = relative humidity, e = vapour pressure and the subscript *s* refers to the saturation value at the same temperature.

The GCM scales are still relatively coarse, due to the large time scales of ocean processes that are linked to the atmosphere in these models and the computing power that is needed to run such computationally expensive models (Giorgi *et al*, 2001). The model resolutions of the GCMs used vary considerably, so in order to provide some consistency, all the GCM data was regridded to a resolution 0.5° x 0.5° (latitude x longitude). These datasets were then converted from binary format to ASCII prior to the calculation of the anomalies.

4.5.2. Calculation of the Anomalies

In order to remove the inherent, and different, biases within each GCM, the difference between current and future climate for each GCM was used to drive SDGVM. Two methods were used to calculate these anomalies:

- *Anomaly 1 (An1):* Assumes observed current interannual variability, and is calculated as:

  $An1 = (MFA - MCA) + O_i$,

  where: MFA is the Modelled Future Monthly Average,
  MCA is the Modelled Current Monthly Average,
  O_i is thirty years of current Observed monthly data,
  and i = 1966 to 1995.

- *Anomaly 2 (An2)*: Assumes the modelled future interannual variability, and is calculated as:

  $An2 = (F_i - MCA) + OA$

  where: F_i is thirty year of future modelled monthly data,
  i = 2070 to 2099,
  MCA is the Modelled Current Monthly Average,
  and, OA is the current Observed Monthly Average.

The anomalies were calculated using a computer script, which provided the output in the ASCII format required by the vegetation model. Table 4.5 describes each of the

sixteen experiments and the abbreviations used to refer to each. After the calculation of the anomalies, the GCM data could be used to drive the vegetation model.

Table 4.5: An explanation of the experiment abbreviations.

ABBREVIATION	MODEL	SCENARIO	ANOMALY
CTL	Observed Climate Data		
CA2An1	CCCMa CGCM2	A2	1
CA2An2	CCCMa CGCM2	A2	2
CB2An1	CCCMa CGCM2	B2	1
CB2An2	CCCMa CGCM2	B2	2
EA2An1	ECHAM4/OPYC3	A2	1
EA2An2	ECHAM4/OPYC3	A2	2
EB2An1	ECHAM4/OPYC3	B2	1
EB2An2	ECHAM4/OPYC3	B2	2
HA2An1	HadCM3	A2	1
HA2An2	HadCM3	A2	2
HB2An1	HadCM3	B2	1
HB2An2	HadCM3	B2	2
NA2An1	NCAR PCM	A2	1
NA2An2	NCAR PCM	A2	2
NB2An1	NCAR PCM	B2	1
NB2An2	NCAR PCM	B2	2

4.6. Conclusion

This chapter has described the two datasets, namely the validation dataset and the SPOT-VGT classification, which were used to validate the output from the vegetation model. The preparation of the GCM data for incorporation into the vegetation model has also been discussed. The next section begins the discussion of the modelling experiments, by presenting the results of a sensitivity analysis of the MM5 regional climate model.

SECTION 2:

EFFECTS OF VEGETATION ON CLIMATE

CHAPTER 5: SENSITIVITY EXPERIMENTS I: THE MM5 MODEL

5.1. Introduction

The early chapters established the importance of biogeophysical feedbacks in climate modelling and discussed some of the methods used to incorporate the land-surface into climate models. This chapter shows the results of changing the land surface scheme in a regional climate model, the MM5 (described in chapter 2), by changing some of the parameters that define its vegetation scheme within the model. The objectives of this climate sensitivity experiment were to observe the regional atmospheric model's response to perturbed vegetation parameters, in order to gain some understanding of the processes behind this response, and to determine the relative importance of vegetation parameters for future model integrations.

A modelling study that also changed the vegetation parameters was that of Charney *et al* (1975) where an increase in surface albedo over the Sahara resulted in decreased rainfall. The albedo was increased from 14% to 35%, representing a Sahara covered by vegetation and a Sahara devoid of vegetation, respectively. The albedo increase resulted in a decrease in rainfall by up to 40% and a decrease in cumulus cloud cover. Rainfall distribution shifted south into the Sahel, which also suggests a southward shift of the Intertropical Convergence Zone (ITCZ) over Africa. Furthermore, it was suggested that the decrease in rainfall could cause further vegetation decline, which could further alter the climate, resulting in a cycle of processes. The mechanism suggested for this decrease in rainfall (Charney *et al*, 1975, 1977) is based on the fact that deserts reflect more radiation than surrounding vegetated surfaces, turning the desert into a radiative sink where air must descend. This decreases the relative humidity of the area and so precipitation declines.

Shukla *et al* (1990) found a similar result for deforestation in the Amazon. The increase in albedo caused by the change in vegetation resulted in increased

temperatures and increased outgoing longwave radiation. There was therefore less energy available for latent heat fluxes. The soil temperatures were also found to be higher, which reduced moisture storage and therefore reduced evapotranspiration. The end result was a decrease in precipitation due to the drier air.

A more recent study of the effects of vegetation on climate is that of Henderson-Sellers (1993) who used a climate model to generate vegetation classes based on the Holdridge classification (Holdridge, 1947), in conjunction with the Biosphere-Atmosphere Transfer Scheme (BATS) (Dickinson *et al*, 1986). The Holdridge classification uses a minimum of two climate variables to predict vegetation type. This study involved several disturbances of the vegetation pattern, one of which was deforestation of tropical rainforest in South America and Asia. After five years, the models predicted the recovery of part of the Asian forests, but in South America the deforestation had disturbed the regional climate (by decreasing rainfall) to such an extent that the forests could no longer be supported in this region (Henderson-Sellers, 1993). This supports the suggestion by Charney *et al* (1975, 1977) that vegetation decline and decreasing rainfall form a cycle of processes.

Henderson-Sellers (1993) also made a first attempt to incorporate continental vegetation as an interactive component of a global climate model. The changes in mean global climates resulting from the incorporation of the interactive vegetation are not highly significant, but some regional climates do show significant sensitivity to this change. For example, temperature increases were seen of up to 10°C, with the largest changes occurring in the northern hemisphere during summer.

The studies above have used Global Climate Models (GCMs), but regional climate models (RCMs) consistently out-perform GCMs in simulating climate because they are better at representing sub-GCM grid scale forcings, especially in regard to the surface hydrological budget. However, regional climates do not occur in isolation, but are strongly influenced by forcings and circulations at other spatial (planetary

and local) and time scales (sub-daily to multi-decadal), as well as by other systems such as the biosphere, the hydrosphere and the cryosphere (Giorgi *et al*, 2001). This component of the thesis serves to support complementary modelling research currently being undertaken (Hewitson, *pers. comm.*) by elucidating some insight into the first-order sensitivity of the atmosphere to land surface perturbations such as may be manifest under global climate change. The results presented below are thus only an initial attempt at a very complex issue and should only be considered as an introduction to a much larger study, but these results do serve to introduce some of the feedbacks from the vegetation to the regional climate.

5.2. MM5 Sensitivity to Vegetation Parameters

The default land surface sub-model component of MM5 model defines vegetation types according to a set of parameters, and it is the model's sensitivity to these parameters that is tested here. Several studies have shown that surface albedo and roughness length can be regarded as the two most important parameters (Charney *et al*, 1975; Shukla and Mintz, 1982; Henderson-Sellers, 1993). It was subjectively decided to initially perturb these two parameters by 20% to gauge the model sensitivity. The magnitude of the perturbation (20%) was selected to be comparable to natural interannual variation (Midgley, *pers. comm.*). The land surface sub-component in many climate models is often simply a set of table listing the values of the defining parameters for each vegetation type (Henderson-Sellers, 1993). Similarly, the MM5 model does not simulate albedo or roughness length, so the changes were merely applied to the prescribed default values for each vegetation type. The distribution of the default vegetation in the model was not changed. Table 5.1 shows these two parameter values for each vegetation type before and after the 20% change had been applied.

A control simulation (with default vegetation parameters) was also run and used for comparison. The model run spans a 3-month period (December 1998 to February 1999), over a domain of Africa south of the equator. This was during a La Nina

period[1], which would have produced higher than normal rainfall. The model was run at a 60km grid-cell resolution, using NCEP reanalysis data (Kalney *et al*, 1996) as the boundary forcing. Thirty days prior to December (i.e. the month of November) were used as a spin up period, and an ensemble of 3 simulations was undertaken, with each ensemble member starting on consecutive days. The use of the ensemble modelling technique is important to account for some level of uncertainty related to model performance. As the climate system has an inherently non-linear, chaotic nature, it is possible to get varying results if the initial conditions for a series of model experiments are even slightly different. By using 3 ensemble members, the results can be averaged to get a mean result, and therefore account for some of this uncertainty.

Table 5.1: The albedo and roughness length changes for summer applied in the MM5 sensitivity runs for the vegetation types that occur within the study region.

VEGETATION	OLD ALBEDO	NEW ALBEDO	OLD ROUGHNESS	NEW ROUGHNESS
Dryland cropland and pasture	17	20.4	15	18
Cropland/grassland mosaic	18	21.6	14	16.8
Cropland/woodland mosaic	16	19.2	20	24
Grassland	19	22.8	12	14.4
Shrubland	22	26.4	10	12
Savannah	20	24	15	18
Deciduous broadleaf forest	16	19.2	50	60
Evergreen broadleaf forest	12	14.4	50	60
Water bodies	8	9.6	0.01	0.012
Herbaceous woodland	14	16.8	20	24
Barren or sparsely vegetated	25	30	10	12

5.2.1. Roughness Length

The first experiment analysed the sensitivity of the MM5 model to a change in roughness length. Roughness length is directly related to vegetation height. Taller vegetation can exchange gasses with the atmosphere more readily than short vegetation, due to the deeper layer of the canopy. It was therefore felt that an

[1] http://www.cpc.ncep.noaa.gov/products/analysis_monitoring/ensostuff/ensoyears.html

increase in roughness length, which would simulate taller vegetation, would have a significant impact on the regional moisture fluxes. However, the analysis of the results showed that the intra-ensemble differences were as large as the anomalies between the perturbation and control simulations. It was therefore not possible to identify a clear, visible signal in the results that could be related to the change in roughness length. Consequently, it was concluded that the MM5 model is not overly sensitive to a 20% increase in roughness length, although a larger perturbation would perhaps show more significant results. However, in the context of this initial sensitivity analysis, no further simulations with a roughness length change have been undertaken.

5.2.2. Albedo

In contrast to the roughness length perturbations, the intra-ensemble differences for the albedo perturbation experiment were small compared to the perturbation anomalies. Given the small intra-ensemble differences, the ensemble members were averaged to generate a single control and single perturbation result data set. The important results are discussed below.

An increase in albedo would intuitively be expected to cause a cooling at the surface due to increased reflection of short-wave incoming radiation. In line with this, the regions of the west coast of South Africa and Mozambique show a cooling, but over the interior of South Africa, a noticeable warming was evident in both the ground temperature and the 2m air temperature (Figure 5.1) – a warming comparable to the seasonal mean difference between a normal season and an unusually warm season. The control run shows that most of South Africa has lower ground and 2m air temperatures than the rest of the sub-continent. The anomaly pattern shows an increase in temperature over large parts of this region. A similar pattern was seen over Madagascar, where the interior of the island became warmer, and the coast became cooler. Further investigation of the results revealed that there was a strong reduction in cloud over the interior (Figure 5.2) and a small increase in cloud cover

over the coastal parts of Mozambique. Coupled with this, the anomaly map in Figure 5.3 suggests a long-shore anomaly on the east coast, which represents a small reduction in the flux of lower tropospheric moisture off the ocean into the interior of the continent. These patterns were also reflected by reductions over the interior in specific humidity (Figure 5.4). This suggests a reduced moisture flux into the interior from the moisture source of the Indian Ocean. The net reduction in cloud resulting from reduced moisture availability over the interior of southern Africa thus allows increased short-wave radiation over this region, thereby increasing surface air temperatures. This explains why the cooling over the interior, expected from a simple increase in albedo, did not occur.

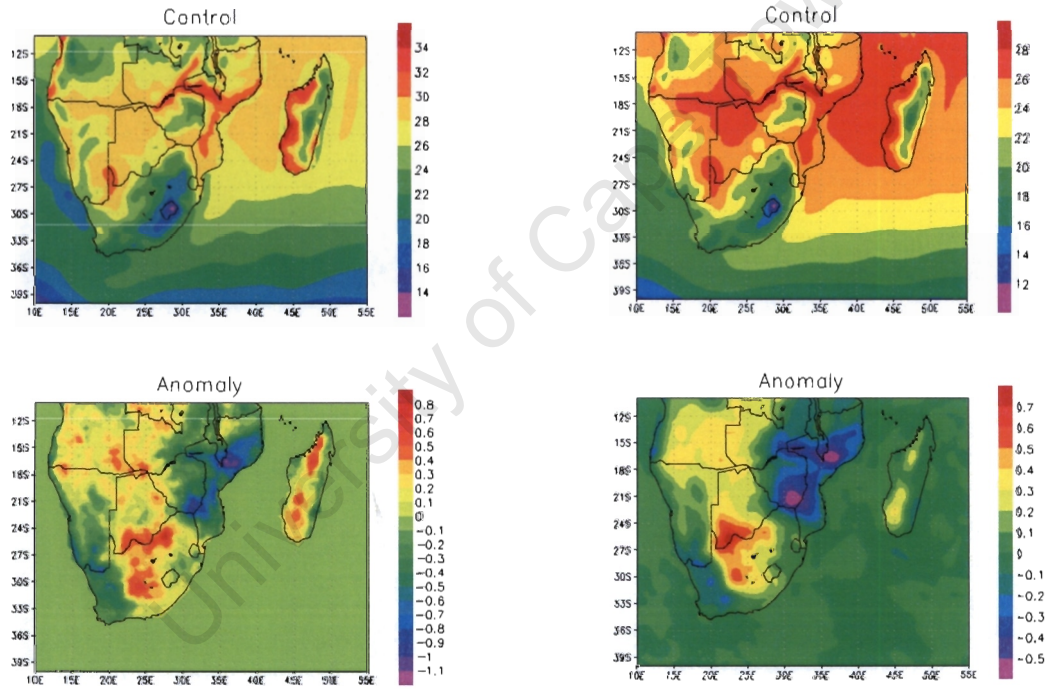

Figure 5.1: a) Ground Temperature (°C) and b) The 2m Air Temperature (°C) for the control run (top) and the difference between the control run and the perturbed albedo run (bottom). These results represent the average of the three ensemble members run from December 1998 to February 1999.

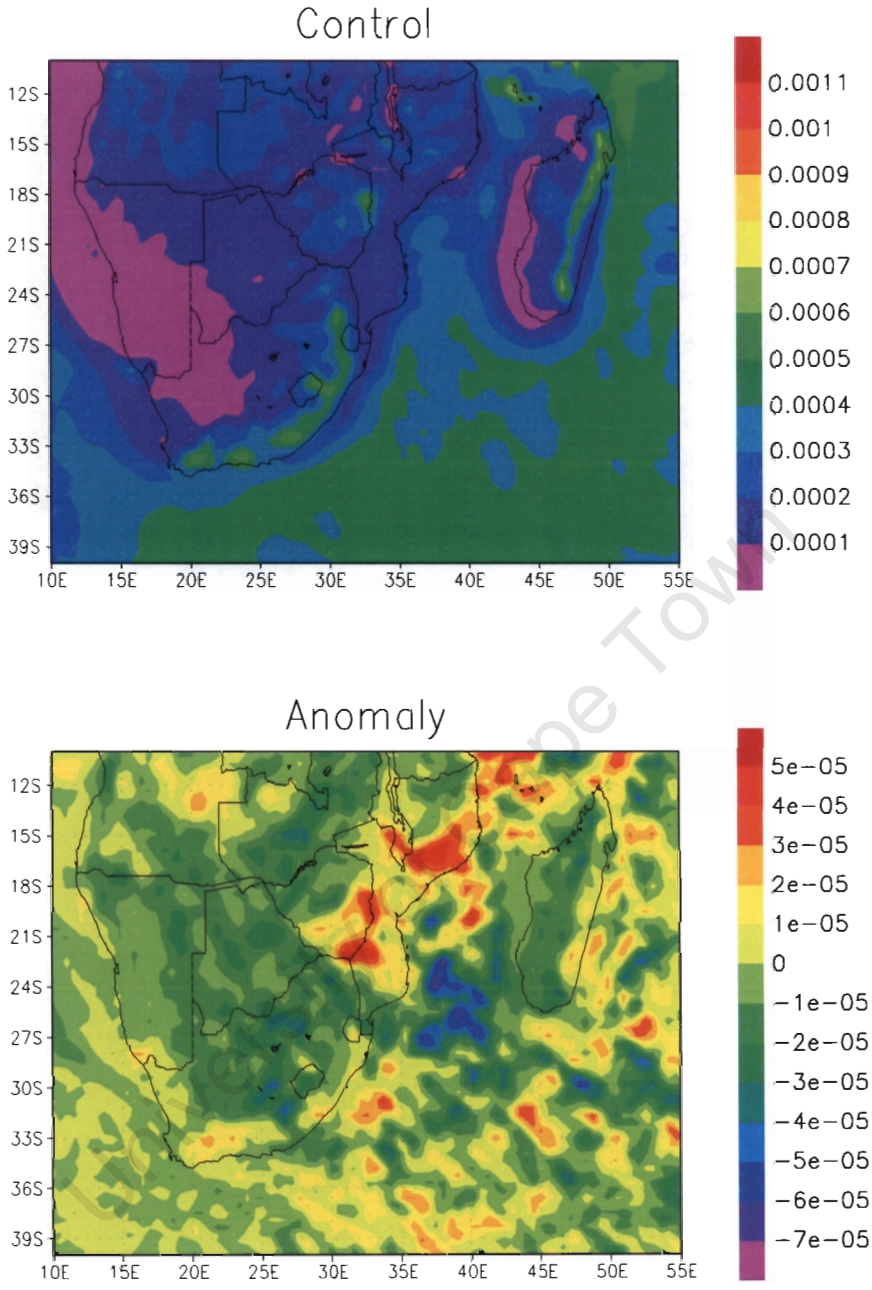

Figure 5.2: The liquid water field (kg/kg) for the control run (top) and the difference between the control run and the perturbed albedo run (bottom). This is a proxy for the amount of cloud in the region.

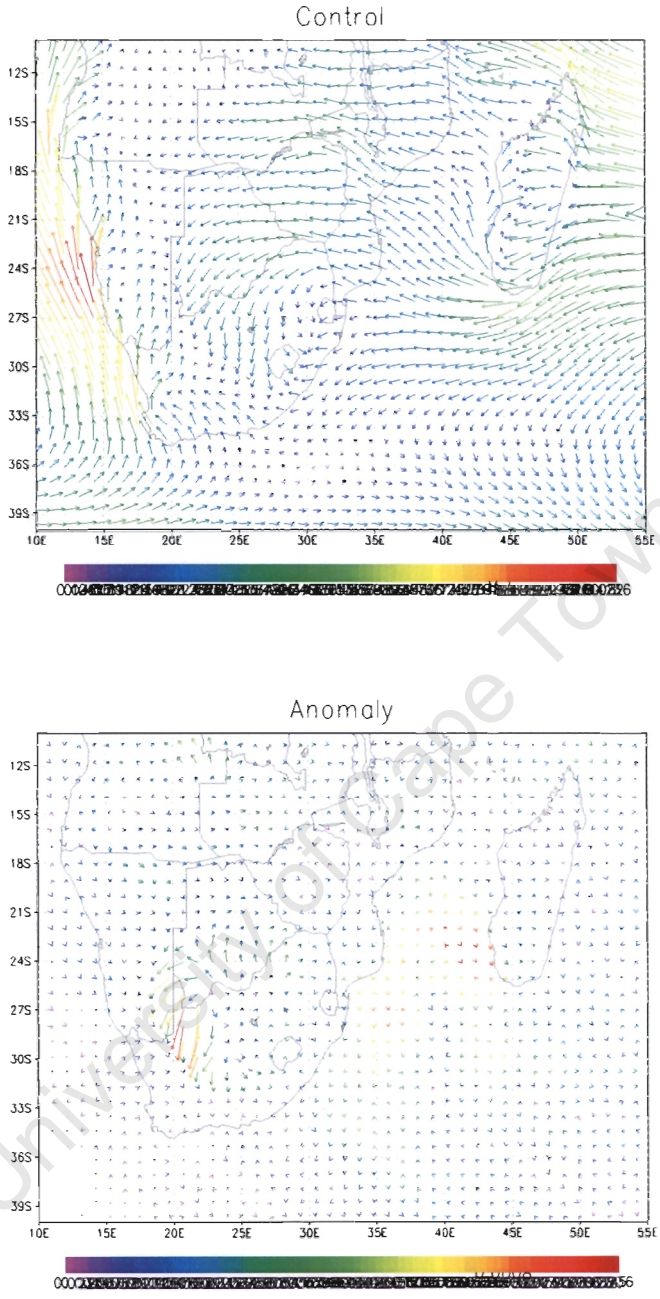

Figure 5.3: The Moisture Flux for the control run (top) and the difference between the control run and the perturbed albedo run (bottom). The lower anomaly map suggests a long-shore anomaly along the east coast, representing a reduced moisture flux from the ocean into the interior.

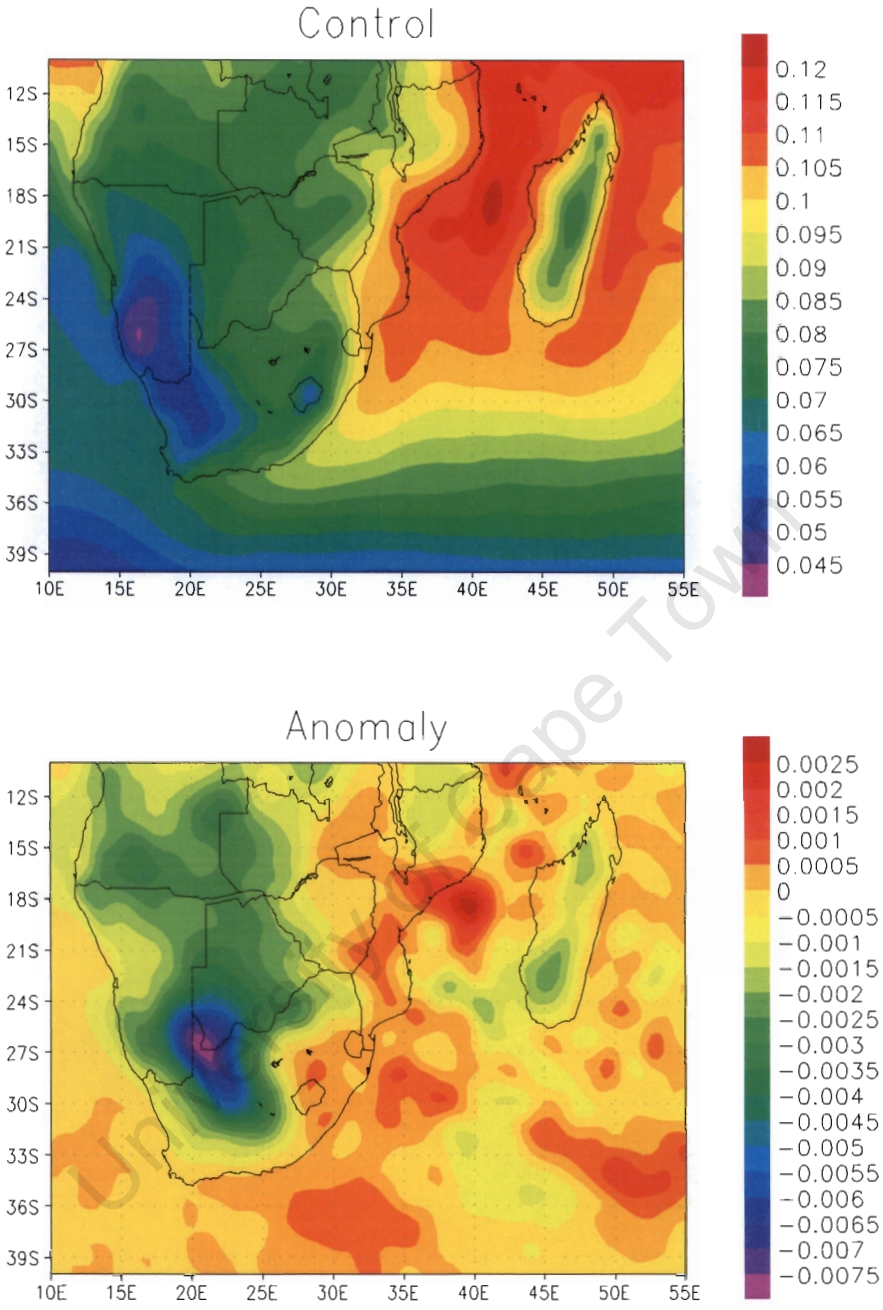

Figure 5.4: The Specific Humidity (kg/kg) for the control run (top) and the difference between the control run and the perturbed albedo run (bottom)

5.3. Conclusion

It has been shown that moderate changes in surface albedo readily lead to changes in magnitude of surface climate of a magnitude comparable to projected changes

resulting from global warming. There is therefore a strong likelihood of interactive feedback processes between climate and vegetation in this region modulating climate changes due to anthropogenic forcing, and suggests that any climate change responses taken in ignorance of this feedback may miss a sizable component of the climate change signal. In this simulation a spatially uniform perturbation was applied. This resulted in the reduced transport of moisture into the interior of the sub-continent, reducing clouds, and increasing incoming short-wave radiation, which contributed towards increased temperatures over the interior. In reality, the vegetation response to climate change will most likely result in a more complex spatial albedo response, with commensurate complexity in how the change is manifest in the atmospheric circulation. Nonetheless, it is apparent that the feedback may readily induce significant changes in regional atmospheric processes.

Furthermore, according to Gutowski *et al* (1991), the surface energy balance is determined primarily by surface absorption of solar radiation and exchanges of longwave radiation, latent heat and sensible heat between the surface and the atmosphere. Any change in radiation, such as will occur with a change in albedo, will therefore affect the surface energy balance. An analysis of several experiments by Nicholson (2001) led to the conclusion that if a very large change in surface albedo occurs in semi-arid regions, such as the Sahel or the Karoo, a significant decrease in rainfall should occur over that region. Changes in albedo are generally linked to vegetation changes, apart from in urban areas.

The suggestion by Charney *et al* (1975, 1977) that increasing albedo and the resulting decrease in precipitation becomes a cyclical process has some importance for southern Africa, in light of the results presented here. The albedo increase in these experiments over southern Africa also resulted in decreased rainfall, as predicted by Charney *et al* (1975) for the Sahel. There is therefore the implication that should albedo increase over southern Africa, Charney's cyclical process could be initiated over this region.

The importance of the vegetation parameters, and especially surface albedo, shown by these experiments and highlighted in Chapter 3, suggest that more research is needed in this area. Accurate and up-to-date albedo maps are needed to validate the land surface classification look-up tables, and these could also be used as direct input into climate models. The most obvious source for these maps is satellite imagery. Most current analyses of satellite imagery focus on ratios such as Normalised Difference Vegetation Index (NDVI), which gives an indication of the "greenness" of the earth. Satellite imagery is now being used to derive vegetation parameters such as albedo, which can be directly incorporated into climate models. The International Satellite Land Surface Climatology Project second initiative (ISLSCP Initiative II) has collated a number of these datasets and at three resolutions (1 degree, half degree and quarter degree)[2]. This collection of datasets includes not only vegetation parameters (such as albedo and leaf area index), but also meteorological, soils and topography data. The datasets are based on several years of data, and the timescales do not always overlap. It is therefore not always possible to find the data that has the same temporal scale that may be required for a particular study. Future studies should look at using satellite imagery as real-time inputs for climate models.

As a parallel focus to the use of satellite imagery, dynamic global vegetation models should also be tested and incorporated into climate models, as they provide a useful tool for predicting vegetation under future climate change. Satellite imagery is only available as past observations, so vegetation models provide the only method of simulating future vegetation patterns. The Sheffield Dynamic Global Vegetation Model (SDGVM) will therefore be tested in the next three chapters with the ultimate aim being to couple the SDGVM and the MM5.

[2] http://islscp2.sesda.com/ISLSCP2_1/html_pages/islscp2_home.html

SECTION 3:

PRESENT EFFECTS OF CLIMATE ON VEGETATION

CHAPTER 6: VEGETATION MODEL VALIDATION

6.1. Introduction

Model validation is a key step in assessing the fidelity of simulation results, especially when outputs are to be used as input for further modelling exercises. In the case of vegetation models, the task of validating model output against "real world" characteristics appears simple, but is in fact fraught with difficulty due to problems which include vegetation patchiness at several scales. Nonetheless, validation is essential, especially as an understanding of successful and unsuccessful simulation of current conditions enhances our understanding of model simulation of future changes (Giorgi *et al*, 2001).

The Sheffield Dynamic Global Vegetation Model (SDGVM) has been extensively tested on a global scale, particularly in terms of the Net Primary Productivity and Leaf Area Index outputs from the model (Woodward *et al*, 1995; Beerling and Woodward, 2001; Woodward *et al*, 2001; Cramer *et al*, 2001). The model was designed so that it could be run at any scale over any domain size. This is achieved by treating each site as independent from all other sites. However, SDGVM is usually still run on a global scale and the results are analysed as global averages. It must also be pointed out that among the many simplifications needed to conduct global modelling, and in the absence of appropriate data, soil depth is assumed to be constant all over the globe, leading to potential errors in soil moisture calculations for particularly deep (e.g. deep Kalahari sands) or shallow soils (e.g. desert soils). The domain for this study covers Africa, south of the equator, and it was therefore necessary to test model performance at a regional level. This was achieved by first analysing the decadal variation in modelled vegetation distribution, followed by comparing the model output to various vegetation databases, namely the validation dataset, the SPOT-VGT classification and the ISLSCP vegetation dataset (DeFries and Townshend, 1994). These datasets were described in Chapters 3 and 4.

A control experiment was undertaken to serve as a comparison for all the SDGVM perturbation or change runs. The control run uses the default climate dataset provided by the Climate Research Unit (CRU), University of East Anglia as described by New *et al* (1999). This dataset comprises monthly averages of mean temperature, precipitation and relative humidity, the climate variables needed as input for SDGVM. The dataset covers 1901 to 1995, and this time period was therefore the period over which the control experiment was run. This run was done on all 3530 sites, with a resolution of 0.5 x 0.5 degrees. The age at which trees escape fires was set at 25 years.

6.2. Time series of SDGVM with CRU data

6.2.1. Decadal Variation

An initial analysis was done on the control run, in order to gauge how accurate SDGVM was predicting current vegetation distribution over Africa, south of the equator. The frequency of occurrence of each Plant Functional Type (PFT) within each of the 95 years was calculated and graphed (Figure 6.1). The graph shows that the number of sites that are predominantly Bare Ground or C_4 Grassland displays the largest fluctuations. On further examination, it was revealed that the success of these two PFTs is inversely related, with the one increasing in years that the other decreases. Calculation of the correlation between the cover fraction of these two PFTs gave a value of –0.97, which confirms a close, negative correlation. The correlations between all the PFTs are shown in Table 6.1. The C_3 Grassland/Shrublands show a correlation of –0.65 with Bare Ground and 0.52 with C_4 Grassland. Therefore, the C_3 Grassland/Shrublands tends to increase when Bare Ground decreases (and vice versa) and also to increase at the expense of C_4 Grasslands. The Evergreen Broadleaf and Deciduous Broadleaf Forests have a negative correlation of –0.66, suggesting possible direct competition between these types.

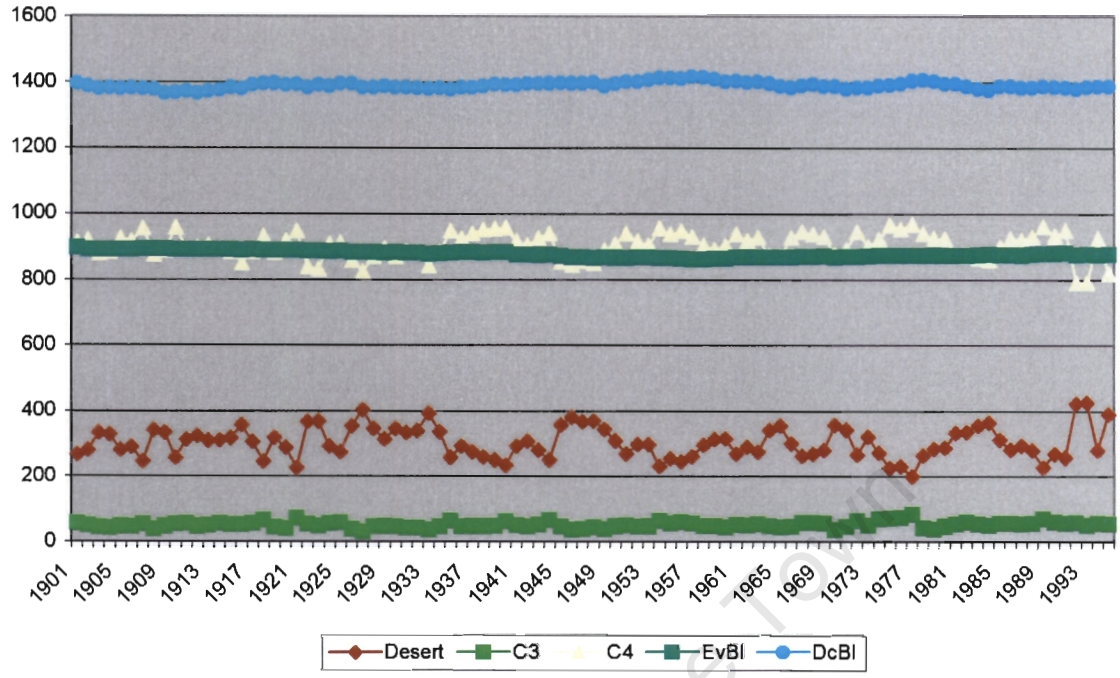

Figure 6.1: The number of sites dominated by each of the Plant Functional Types (the needleleaf woodlands are excluded because they do not dominate any sites).

Table 6.1: Correlations between the PFTs

	Desert	***C3 Grassland/ Shrubland***	***C4 Grassland***	***Evergreen Broadleaf Woodland***	***Deciduous Broadleaf Woodland***
Desert	1				
C3 Grassland/ Shrubland	-0.65	1			
C4 Grassland	-0.97	0.52	1		
Evergreen Broadleaf Woodland	0.03	-0.04	-0.10	1	
Deciduous Broadleaf Woodland	-0.32	0.13	0.25	-0.66	1

The graph (Figure 6.1) furthermore shows that the Deciduous Broadleaf Forest PFT dominates the highest number of sites. C_3 Grassland/Shrubland dominates the

lowest number of sites (apart from Evergreen Needleleaf Forest and Deciduous Needleleaf Forests, which are not predicted to occur in the region at all).

The Evergreen Broadleaf Forests show a general decline in the number of sites they dominate over the 95 years, although, the decline is fairly small (from 897 sites in 1901 to 877 sites in 1995). Deciduous Broadleaf Forests remain fairly consistent throughout the 95 years, with the minimum number of sites dominated by Deciduous Broadleaf Forests being 1366 (in 1912), and the maximum being 1417 (in 1957).

A series of maps showing the distribution of the PFTs for approximately every 10 years can be found in Appendix 6.1. These maps reflect the patterns shown by the statistical changes. The most noticeable changes are shown by the Bare Ground and C_4 Grassland PFTs, which can be seen to interchange, particularly along the borders of the Namib Desert in Namibia and Botswana, and the Karoo semi-desert region in South Africa. Most of the Karoo (as defined by Rutherford and Westfall, 1994) is classified as Bare Ground by SDGVM. This is because SDGVM does not model succulents, and therefore, the climate of this region will either produce Bare Ground or C_4 Grassland (with some C_3 Grassland/Shrubland) in the SDGVM model. Changes can also be seen at the boundaries between the Evergreen Broadleaf Forests and the Deciduous Broadleaf Forests, as well as between the Deciduous Broadleaf Forests and the C_4 Grasslands. Figure 6.2 shows the change in the percentage of sites dominated by each PFT for the years shown by the maps.

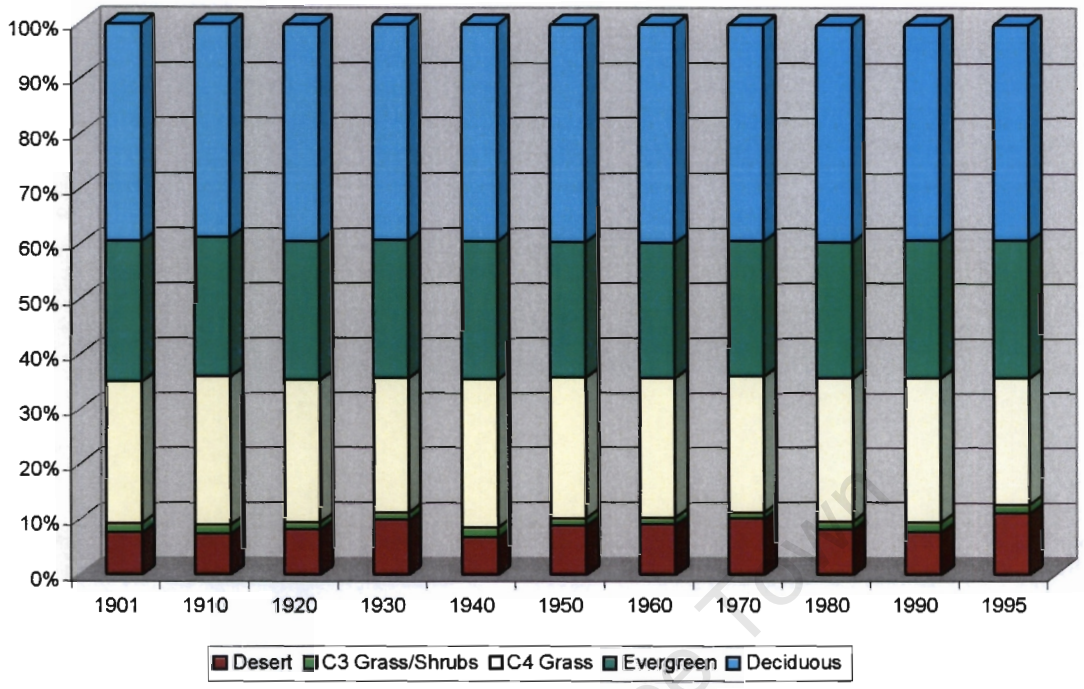

Figure 6.2: The change in percentage of sites dominated by each PFT for selected years (approximately every 10 years).

6.2.2. Annual Variation

Two datasets are be used for validation of the vegetation model output, namely the GIS database developed from the NBI data, and the classification from the SPOT-VGT satellite imagery. The development of these datasets was described in Chapter 3. The NBI data was updated in 2000 and the SPOT-VGT data was acquired for November 1999 through to December 2000. The ideal would therefore be to compare the output from the vegetation model for the year 2000. The default climate dataset (the CRU data) used to run SDGVM is only available up to 1995, and so the SDGVM control run thus ends in 1995. It was therefore decided to examine the annual variation in SDGVM output for the last 10 years of the control run, namely 1986 through to 1995. However, it should be noted that SDGVM was not designed to model inter-annual variability, but rather the long-term changes in vegetation dynamics, and the analysis of inter-annual variation here merely serves to illustrate the acceptability of using the average of ten years of model output for

further analyses. Furthermore, many ecosystems, and forests in particular, do not show large inter-annual variations, due to a time lag in the response of vegetation to climate change. Changes in the spatial distribution of vegetation types are usually only observed over a number of years or even decades (Woodward, 1987b)

The examination of annual variation is based on the number of sites dominated by each Plant Functional Type (PFT). The average number of sites dominated by each PFT was calculated for the 10-year period. The variation from this average was then calculated by subtracting the average number of sites dominated by the PFT from the actual number of sites for each year. This was then converted to a percentage of the total number of sites. The variation between each year was also calculated by subtracting the number is sites dominated for each PFT for year 2 from that of year 1, for example, the number of sites in 1987 minus the number of sites in 1986. This was again converted to a percentage of the total number of sites. These results are shown in Table 6.2. It can be seen that the annual variation for all PFTs across the 10 years is less than 3.5%. As with the decadal variations (see above), the two PFTs that vary the most are the C_4 Grasslands and the Bare Ground. The variation in the other three PFTs is less than 0.5% across all 10 years. This suggests that interannual rainfall variability exerts fine control over the relative cover of C_4 types in marginal semi-arid regions, but has few other short-term effects in southern Africa. The highest inter-annual variation over the 10-year period is less than 5% for all PFTs, with the inter-annual variation for the C_3 Grassland/Shrublands and the forest PFTs being less than 0.4%. Forests and shrubs have longer life-spans than grasses and respond slower to change, so we do not expect to see large interannual variations. The life cycle of grasslands (annual vegetation) is much shorter, and so they respond much quicker to changes (Woodward, 1987b). It is therefore not surprising that the greater inter-annual variability is shown by the annual PFT, the C_4 Grassland, while the PFTs with longer life cycles show less variability.

Table 6.2a: The annual variation from the average (in percentage) in the number of sites dominated by each Plant Functional Type for 1986 to 1995, as modelled by SDGVM.

PFT	*1986*	*1987*	*1988*	*1989*	*1990*	*1991*	*1992*	*1993*	*1994*	*1995*
BG	-0.89	-0.52	-0.92	-2.39	-1.23	-1.57	3.07	3.19	-0.92	2.20
C3	-0.03	-0.08	-0.05	0.37	0.09	-0.03	0.03	-0.20	0.00	-0.11
C4	0.87	0.73	0.99	1.92	1.10	1.55	-2.92	-2.98	0.87	-2.13
EvBl	-0.03	-0.09	0.02	0.05	0.05	0.08	-0.03	-0.01	-0.03	-0.01
DcBl	0.08	-0.03	-0.03	0.05	-0.01	-0.03	-0.15	-0.01	0.08	0.05

Table 6.2b: The annual variation in the number of sites dominated by each Plant Functional Type for 1986 to 1995, in comparison to the previous year (i.e. 1987 vs. 1986, 1988 vs. 1987, etc.).

PFT	*1986*	*1987*	*1988*	*1989*	*1990*	*1991*	*1992*	*1993*	*1994*	*1995*
BG	0	0.3683	-0.3966	-1.4731	1.1615	-0.3399	4.6459	0.1133	-4.1076	3.1161
C3	0	-0.0567	0.0283	0.4249	-0.2833	-0.1133	0.0567	-0.2266	0.1983	-0.1133
C4	0	-0.1416	0.255	0.9348	-0.8215	0.4533	-4.4759	-0.0567	3.8527	-3.0028
EvBl	0	-0.0567	0.1133	0.0283	0	0.0283	-0.1133	0.0283	-0.0283	0.0283
DcBl	0	-0.1133	0	0.085	-0.0567	-0.0283	-0.1133	0.1416	0.085	-0.0283

The small inter-annual variations in the distribution of the PFTs, as modelled by SDGVM, suggest that a comparison of SDGVM output for a particular year with any other dataset will at most be 5% different in comparison to any other year. It was therefore decided to use the average distribution of PFTs for the 10-year period (1986-1995) for comparison with the three datasets available. This average was calculated using the following steps:

- Calculate average percentage of each PFT covering each site for the 10 years.
- Calculate which PFT is dominant at each site using these averages.

6.3. Comparison with Available Databases

6.3.1. The GIS database

The validation dataset has been prepared for Africa south of the equator and was based on datasets that contain three additional land-use types (urban areas,

savannah and inland water bodies) that are not predicted by SDGVM. These will therefore appear as differences in the maps. Further details on this dataset can be found in Chapter 4.

The SDGVM predicts the occurrence of Evergreen Broadleaf Forests further south in the interior of the region (Figure 6.3) and some Deciduous Broadleaf Forests are predicted where the validation dataset shows Evergreen Broadleaf Forests along the coast of the Democratic Republic of Congo (DRC). The validation dataset shows Deciduous Broadleaf Forests further south than predicted by SDGVM, especially over northern Namibia, Botswana and Zimbabwe. SDGVM also predicts an overabundance of forests along the South African southern coast, in comparison to the validation dataset. The Deciduous Broadleaf Forests predicted by SDGVM in the Western Cape should rather be C_3 Grassland/Shrublands, which most accurately reflect the Fynbos vegetation found in reality in this area (shrubland in the validation dataset).

In the areas classified as savannah in the validation dataset, SDGVM generally predicts C_4 Grasslands. This can be seen as a fairly accurate prediction, as savannahs are known to be a dynamic mix of C_4 Grasslands and Deciduous Broadleaf Trees. Along the edge of the Namib Desert, savannah and grasslands are found in the validation dataset. SDGVM only predicts Bare Ground for this area. SDGVM does not model any succulent vegetation types, so areas that in reality may be covered in succulents tend to be classified as Bare Ground by SDGVM.

The validation dataset shows that Madagascar is covered mainly by savannah vegetation, with some small areas of mixed forest and evergreen broadleaf forest along the eastern coast. SDGVM predicts more extensive forests over the island, including both Evergreen and Deciduous Broadleaf forests (Figure 6.3). A small area of C_4 Grassland is predicted by SDGVM along the south eastern coastal area. Generally, SDGVM does not appear to capture the true nature of vegetation in

Madagascar when compared to this dataset, doubtlessly reflecting the intense impact of human land transformation on this island, which has acted to replace forest cover with fire prone grasslands in many areas, and caused extensive deforestation on its eastern seaboard.

6.3.2. The SPOT-VGT data

The SPOT-VGT dataset is the result of the classification of 14 months of SPOT-VGT satellite imagery, as described in Chapter 4. This dataset contains vegetation types that are not modelled by SDGVM, namely Savannah, Nama Karoo and Succulent Karoo. These areas will therefore show up as different from the SDGVM predictions.

SDGVM predicts an area of Evergreen Broadleaf Forests in the north west of this region, with C_4 Grassland in the northeast corner (Figure 6.4). Moving south, the vegetation becomes Deciduous Broadleaf Forests, which extend in a narrow band down the east coast of the region. C_4 Grasslands dominate the central region, with Bare Ground along the west coast and southern interior. C_3 Grassland/Shrubland is found in the south western corner of the region. The Evergreen Broadleaf Forests on the SPOT-VGT classification are not as extensive as SDGVM predicts, but the SPOT and SDGVM Deciduous Broadleaf Forests more or less cover the same region, as do the grasslands. SDGVM predicts C_4 Grasslands in areas classified as savannah by SPOT, which can again be considered as fairly accurate, due to the mixed nature of savannahs. SDGVM predicts mainly Bare Ground over the Karoo region, which is a semi-desert and dominated by succulents. The Namib Desert on the SPOT-VGT classification is not as extensive as predicted by SDGVM, but these results are the dominant vegetation type, and therefore do not indicate the amount of other PFTs at a site. SDGVM also predicts an overabundance of forests in the western Cape region of South Africa, which is dominated by the Fynbos vegetation (shrublands in the SPOT-VGT classification).

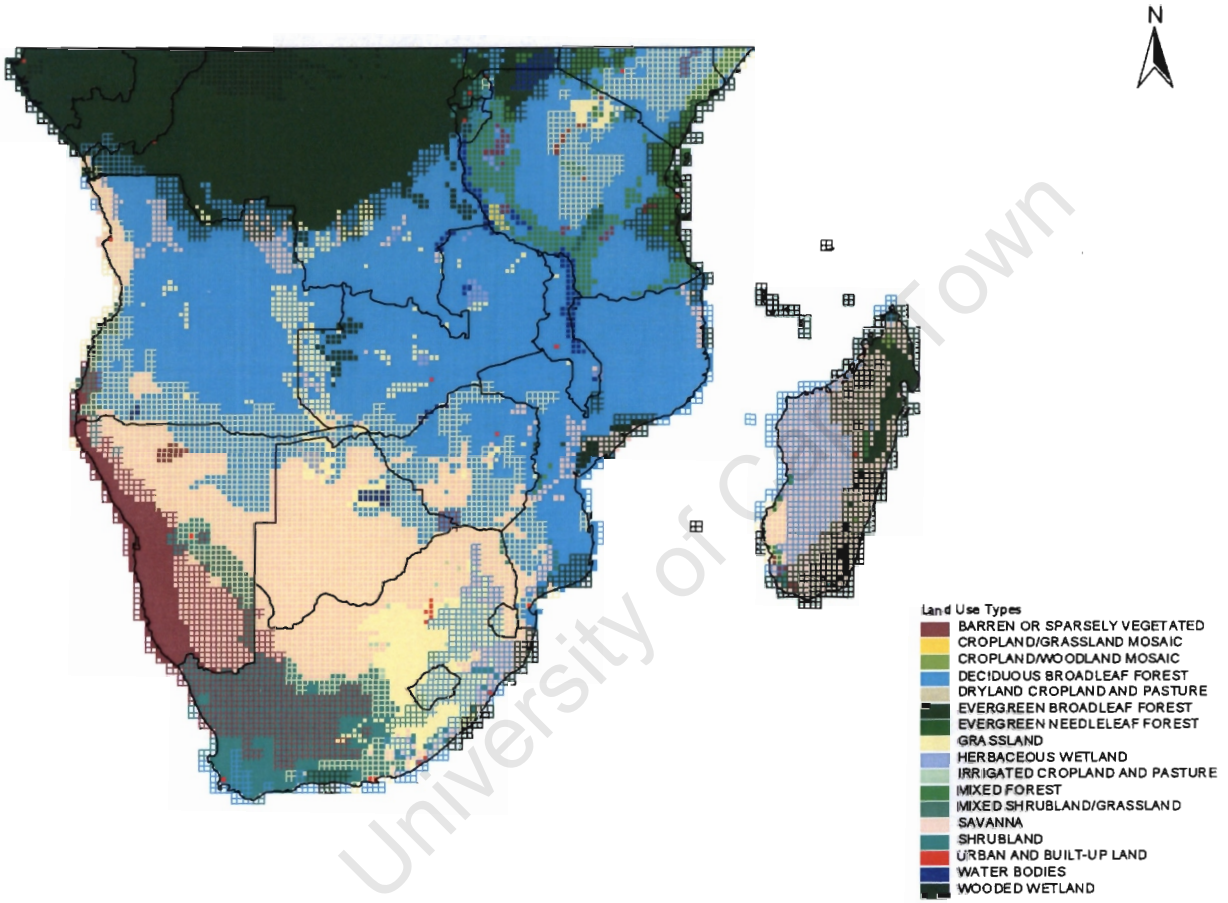

Figure 6.3: The difference between vegetation from the NBI validation dataset and vegetation predicted by SDGVM for southern Africa. (The hatched areas show where the two datasets do not agree; with the hatches representing the SDGVM modelled vegetation, and the areas underneath the NBI validation dataset. This pattern holds for all the maps shown.)

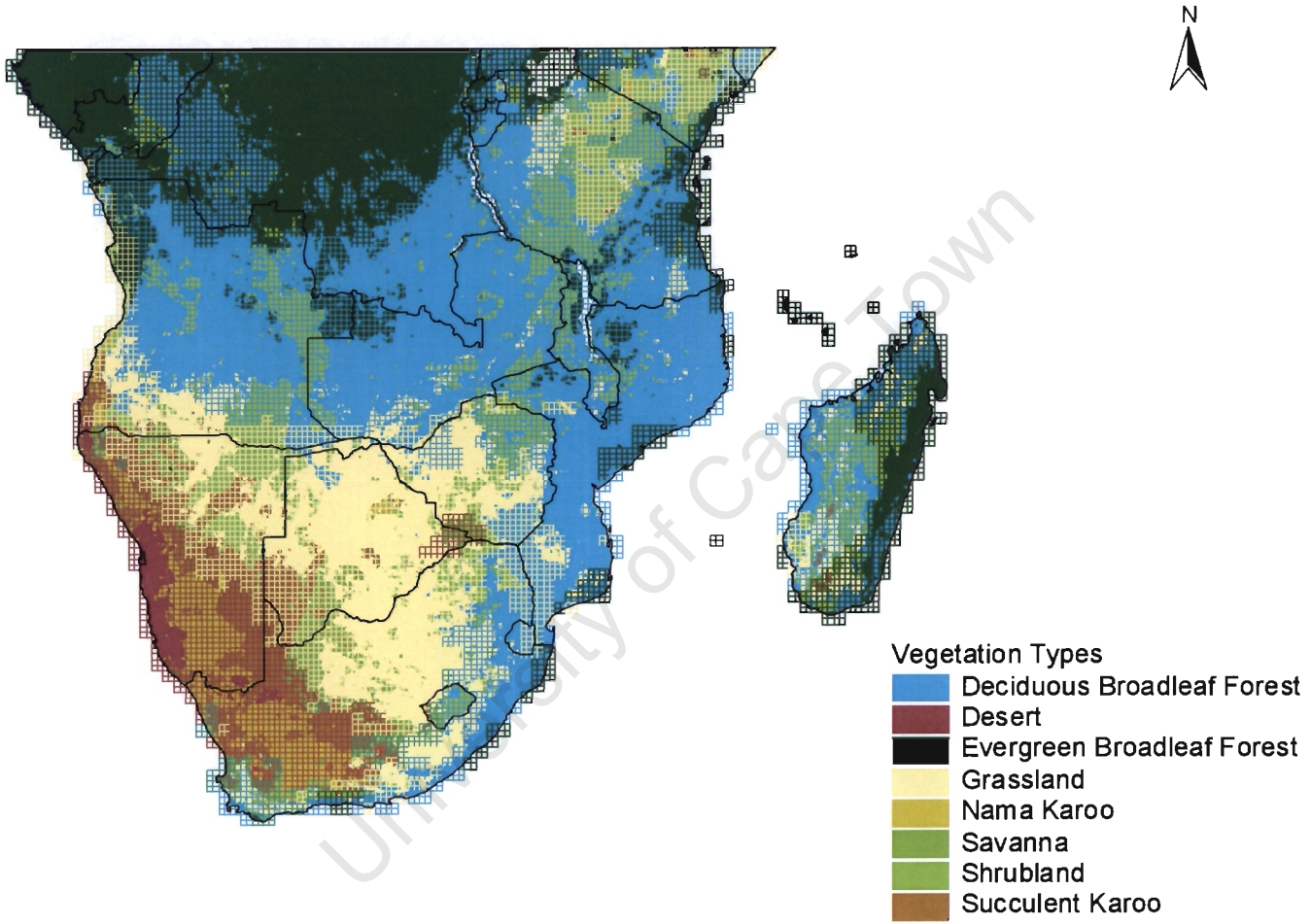

Figure 6.4: The difference between vegetation from the SPOT-VGT classification and vegetation predicted by SDGVM for Southern Africa.

The SDGVM and SPOT-VGT classification both predict a band of Evergreen Broadleaf Forest along the east coast of Madagascar (Figure 6.4), but this is again more extensive in the SDGVM output. A small area of C_4 Grassland is predicted near the south west coast by SDGVM. The SPOT-VGT classification shows a similar area of grassland, but it is further inland. Between the grasslands and the Evergreen Broadleaf Forest, both SPOT-VGT and SDGVM predict Deciduous Broadleaf Forests, but the SPOT-VGT classification also predicts patches of shrublands and grassland within these forests. These areas in the SPOT-VGT classification may be the result of human activities, which would not be predicted by SDGVM (which predicts only potential natural vegetation).

6.3.3. The ISLSCP data

The ISLSCP vegetation dataset is based on a satellite-derived Normalised Difference Vegetation Index (NDVI) (DeFries and Townshed, 1994). The data set has 15 vegetation classes, with 10 of these classes occurring in southern Africa. The data set does include a cultivation class, which SDGVM does not predict. Further details on the ISLSCP data were discussed in chapter 3.

The grassland areas of the ISLSCP data agree closely with the area of C_4 Grassland predicted by SDGVM (Figure 6.5), but SDGVM predicts a large area of Deciduous Broadleaf Forest, which is classified as savannah (mixed C_4 Grassland and Deciduous Broadleaf Trees) by ISLSCP. The Evergreen Broadleaf Forests are also more extensive on the SDGVM output than shown on the ISLSCP data. The area predicted by SDGVM to be Bare Ground corresponds closely to the combined area of the Desert class and the Shrubs and Bare Ground class in the ISLSCP data.

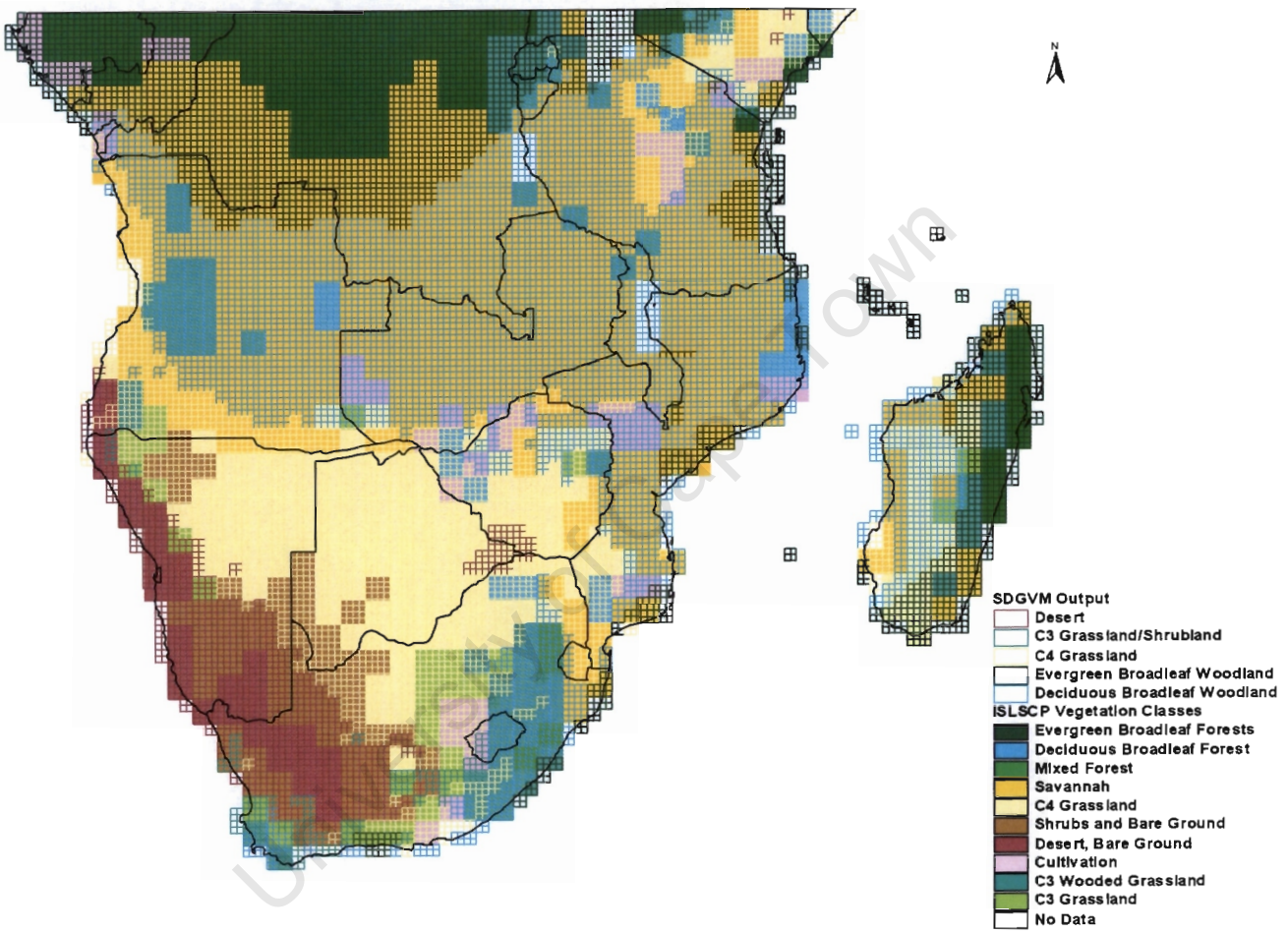

Figure 6.5: The difference between vegetation from the ISLSCP data and vegetation predicted by SDGVM for Southern Africa.

The comparison between SDGVM and the ISLSCP data reveals that SDGVM is fairly accurate in its predicted vegetation distribution. The largest difference between the two datasets is in the occurrence of the Deciduous Broadleaf Forests. SDGVM predicts a far greater range for Deciduous Broadleaf Forests than is shown on the ISLSCP map. However, these regions on the ISLSCP map are classified as savannah, which is, by definition, a mixture of C_4 Grassland and Deciduous Broadleaf trees. It can therefore be said that SDGVM is not totally inaccurate in its predictions, but more that it is under-estimating the occurrence of C_4 Grassland in these regions, when compared to the ISLSCP data. However, these results have only showed the dominant PFT, with no indication of the difference between PFTs or the possibility of co-dominance.

6.4. Reclassification of SDGVM Output

The validation of the vegetation model so far has focussed on the dominant PFT at each site. Another useful output from the model is the percentage of each site that each PFT occupies, also known as the fractional cover. This is particularly useful when comparing to datasets that contain transitional vegetation types, for example, savannah, which is composed mainly of grasses and deciduous broadleaf forests. An attempt was made to use these data to reclassify SDGVM output in terms of the International Geosphere-Biosphere Programme Data and Information System (IGBP-DIS) land cover classification (Table 6.3). However, as the current version of SDGVM does not produce height as an output, the ISLSCP classification was used and modified to more accurately reflect the vegetation of the region (see Chapter 4 for a full explanation). This classification includes some of the vegetation classes found in the three validation data sets (Table 6.4). The reclassified SDGVM output was then compared to the three datasets (validation, SPOT-VGT and ISLSCP), as was done with the original SDGVM output. The analysis below is based on the average of the last 10 years of the control run, specifically 1986 to 1995.

Table 6.3: The IGBP-DIS land cover classification.

Classification	Description
Evergreen Needleleaf forests	Dominated by trees with a percent canopy cover >60% and height exceeding 2m. Almost all trees remain green all year. Canopy is never without green foliage.
Evergreen Broadleaf forests	Dominated by trees with a percent canopy cover >60% and height exceeding 2m. Almost all trees remain green all year. Canopy is never without green foliage.
Deciduous Needleleaf forests	Dominated by trees with a percent canopy cover >60% and height exceeding 2m. Consists of seasonal needleleaf tree communities with an annual cycle of leaf-on and leaf-off periods.
Deciduous broadleaf forests	Dominated by trees with a percent canopy cover >60% and height exceeding 2m. Consists of seasonal broadleaf tree communities with an annual cycle of leaf-on and leaf-off periods.
Mixed forests	Dominated by trees with a percent canopy cover >60% and height exceeding 2m. Consists of tree communities with interspersed mixtures or mosaics of the other four forest cover types. None of the forest types exceeds 60% of landscape.
Closed shrublands	Lands with woody vegetation less than 2m tall and with shrub canopy cover is >60%. The shrub foliage can be either evergreen or deciduous.
Open shrublands	Lands with woody vegetation less than 2m tall and with shrub canopy cover between 10 and 60%. The shrub foliage can be either evergreen or deciduous.
Woody savannahs	Herbaceous and other understorey systems, with forest canopy cover between 30 and 60%. The forest cover height exceeds 2m.
Savannahs	Herbaceous and understorey systems, with forest canopy cover between 10 and 30%. The forest cover height exceeds 2m.
Grassland	Herbaceous types of cover. Tree and shrub cover is less than 10%.

Table 6.4: The Modified Classification of SDGVM output.

CLASS	NAME
1	Bare ground, desert
2	C3 grassland/shrubland
3	C4 grassland
4	Evergreen broadleaf forest
5	Deciduous broadleaf forest
6	Savannah
7	Mixed forest
8	Woody savannah
9	Arid shrubland

The validation dataset contain several classes that occupy only very small areas of the study region (Table 6.5). This dataset was based on the USGS classification (discussed in Chapter 3) and therefore has a northern hemisphere bias. Out of the original 24 classes in this classification, only 17 occur in southern Africa, and only 10 of those occupy more than 1% of the area. This supports the suggestion that this classification may not be suitable for the southern African region.

Table 6.5: The percentage area occupied by the vegetation classes in the validation data, the ISLSCP and the SDGVM output.

Vegetation Class	Validation Data	ISLSCP	SDGVM	SDGVM Reclass
Urban	0.18	0.00	0.00	0.00
Dry Cultivation	0.02	4.93	0.00	0.00
Irrigated Cultivation	0.10	0.00	0.00	0.00
Cropland/Grassland	0.08	0.00	0.00	0.00
Cropland/Woodland	0.04	0.00	0.00	0.00
C4 Grassland	5.94	16.71	26.23	21.81
C3 Grassland/Shrubland	6.22	7.57	1.61	0.99
Woody Savanna	1.13	3.37	0.00	3.20
Savanna	21.55	44.83	0.00	8.60
Deciduous Broadleaf Forest	39.98	2.16	39.20	27.32
Evergreen Broadleaf Forest	15.00	9.01	24.86	18.54
Evergreen Needleleaf Forest	0.13	0.00	0.00	0.00
Mixed Forest	3.54	0.48	0.00	10.49
Water Bodies	1.24	0.00	0.00	0.00
Herbaceous Wetland	0.36	0.00	0.00	0.00
Wooded Wetland	1.93	0.00	0.00	0.00
Bare Ground	2.54	3.61	8.10	3.97
Arid Shrubland	0.00	7.33	0.00	5.07

The graph in Figure 6.6 shows the percentage of the area occupied by each vegetation class for the validation data, the ISLSCP data, the SDGVM output and the SDGVM reclassified output. The relationship between C_4 Grasslands, Deciduous Broadleaf trees and savannas is clearly visible in these results. For example, the ISLSCP data has very low C_4 grassland and deciduous broadleaf

forests, but it has a very high percentage of savannahs. On the other hand, the SDGVM output has high C_4 grasslands and deciduous broadleaf forests, because it does not predict savannah, which is a mixed biome. The SDGVM reclassified data has lower C_4 grasslands and deciduous broadleaf forests than the unclassified output, due to the inclusion of the savannah class.

6.4.1. Comparison with the GIS Database

The comparison of the reclassified SDGVM output with the GIS database does not reveal any great differences from the original SDGVM output over southern Africa (Figure 6.7). The reclassified output shows a transition from Evergreen Broadleaf Forests to Mixed Forest, and then into Deciduous Broadleaf Forests. The GIS database has a direct transition from Evergreen Broadleaf Forests to Deciduous Broadleaf Forest. At the southern border of the Deciduous Broadleaf Forests, SDGVM predicts a change to a small belt of savannah type vegetation and then into C_4 Grasslands. The GIS database shows a far greater expanse of savannah vegetation, with only small areas of grassland further south. The areas of savannah and grassland do not correspond at all on these two datasets. The areas of SDGVM output classified as Arid Shrubland correspond to Shrubland in the validation dataset, but the agreement between the areas classified as desert is still not very good.

The reclassification of SDGVM output also fails to improve the distribution of vegetation over Madagascar (figure 6.7). The only change is that a small area in the south west of the island is now classified as savannah, which does correspond to the GIS database.

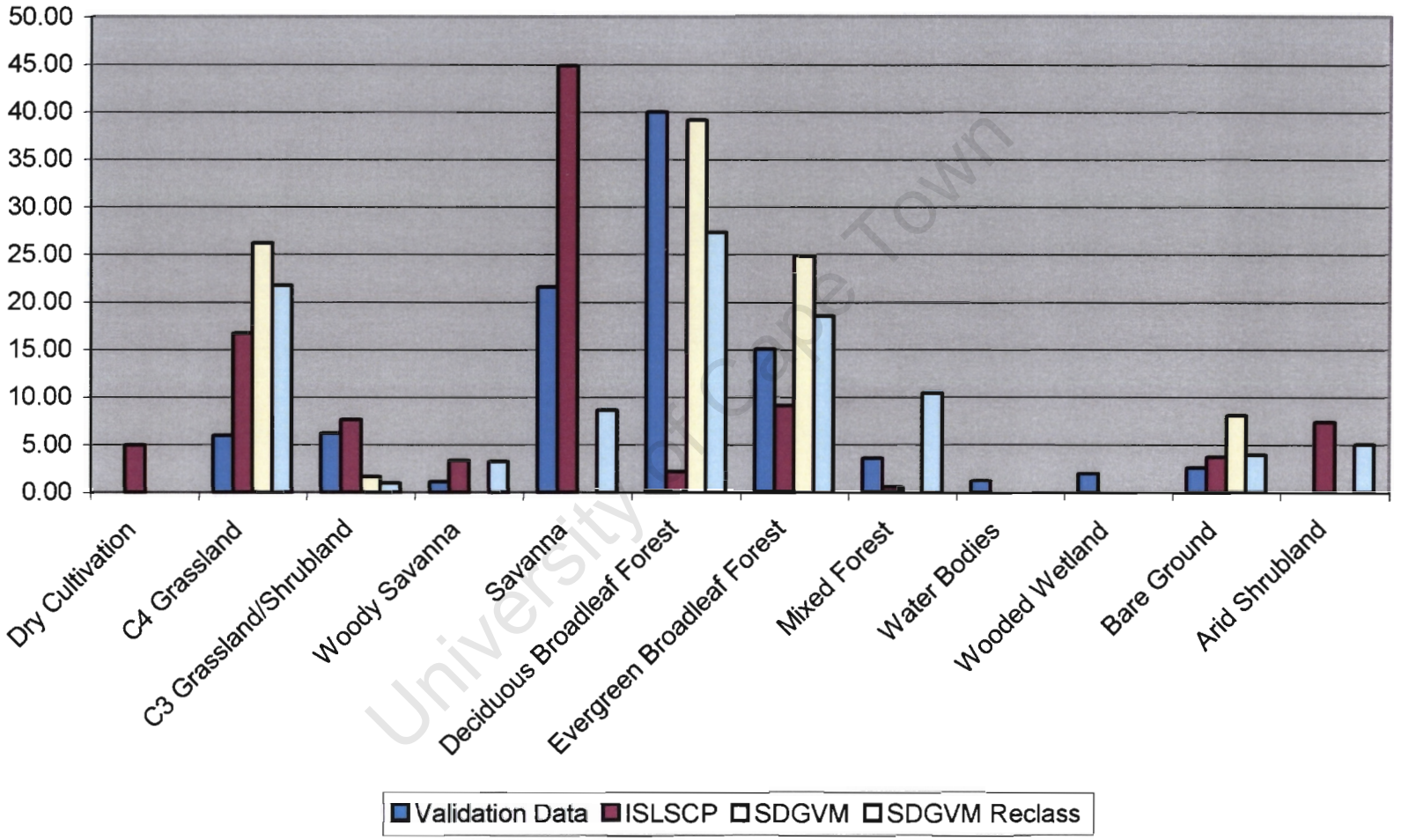

Figure 6.6: The percentage area occupied by the vegetation types for the validation datasets and the SDGVM output.

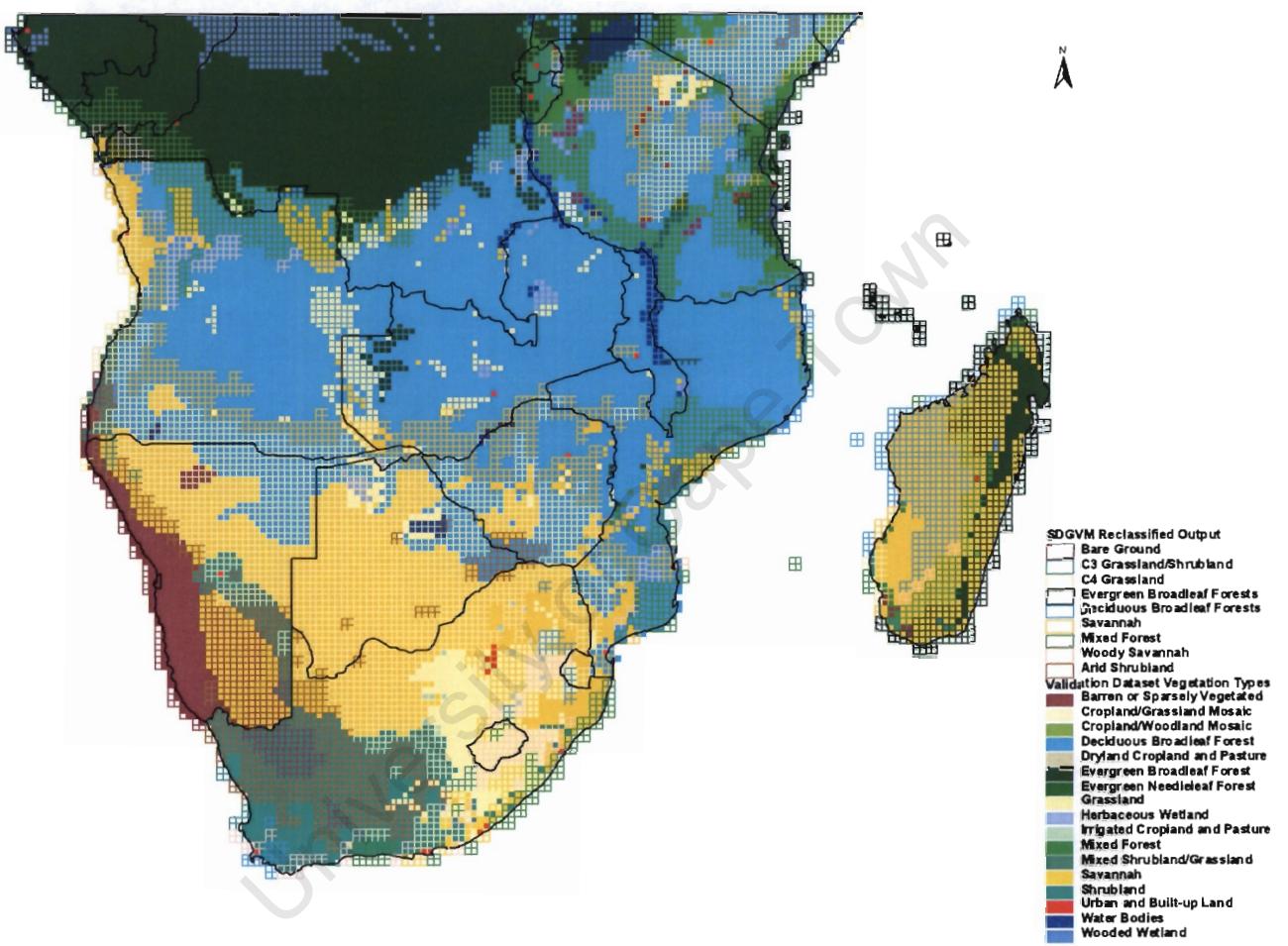

Figure 6.7: The difference between the reclassified SDGVM output and the NBI validation database for southern Africa.

6.4.2. Comparison with the SPOT-VGT Data

In southern Africa, the reclassified SDGVM output shows several transitional vegetation types (Figure 6.8). For example, the border between the Deciduous Broadleaf Forests and Evergreen Broadleaf Forests now consists of an area of Mixed Forest. The SPOT-VGT data, however, shows a sharp change from Evergreen Broadleaf to Deciduous Broadleaf Forest. The transition from Deciduous Broadleaf Forest to Grassland or Shrubland in the SPOT-VGT database is also a direct change, whereas SDGVM predicts a transitional vegetation type (savannah) along this border. The inclusion of the Arid Shrubland class in the reclassified SDGVM output has improved the comparison between the datasets in the Namib Desert and Karoo areas.

The reclassification of SDGVM output also fails to improve the comparison with the SPOT-VGT dataset over Madagascar (Figure 6.8). The area of savannah predicted by SDGVM in the south west of the island, is classified as a mix of grassland and shrubland in the SPOT-VGT dataset. SDGVM again predicts a far greater expanse of all types of forest than this validation dataset.

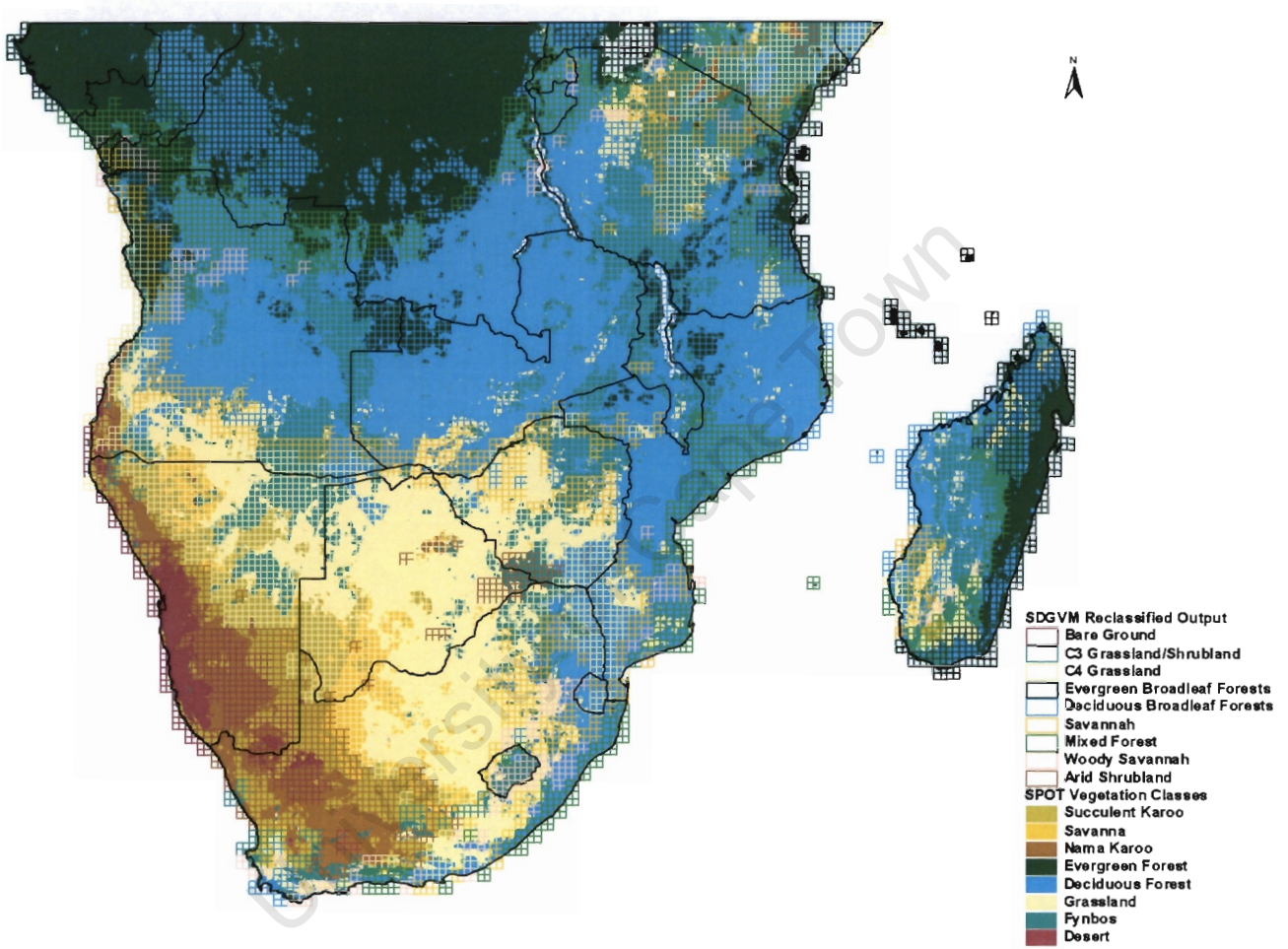

Figure 6.8: The comparison between the reclassified SDGVM output and the SPOT-VGT classification for the region.

6.4.3. Comparison with the ISLSCP Data

The most striking change in the comparison of the reclassified SDGVM output with the ISLSCP dataset is the agreement on the desert and arid shrubland classes between these two datasets (Figure 6.9). SDGVM does predict slightly less extensive areas of arid shrubland, but the borders between the desert and the arid shrubland are fairly well captured by the reclassification procedure. Further north, there is also greater agreement between the two datasets on the occurrence of savannah vegetation, although the savannah is still far more extensive in the ISLSCP data than in the SDGVM output. SDGVM also fails to capture the vegetation distribution over Madagascar in comparison to this dataset, and we must conclude that there is some process responsible for vegetation distribution over the island that is not modelled by SDGVM. The conclusion, as stated above, is therefore drawn that the vegetation of Madagascar has been greatly modified by anthropogenic activities, and no longer supports the natural vegetation that SDGVM predicts for the island. This conclusion is supported by studies in Madagascar that have revealed that more than 80% of the original vegetation on the island has been removed and replaced by secondary grassland[1].

[1] http://www.rbgkew.org.uk/gis/projects/madagascar/veg_mappping.html

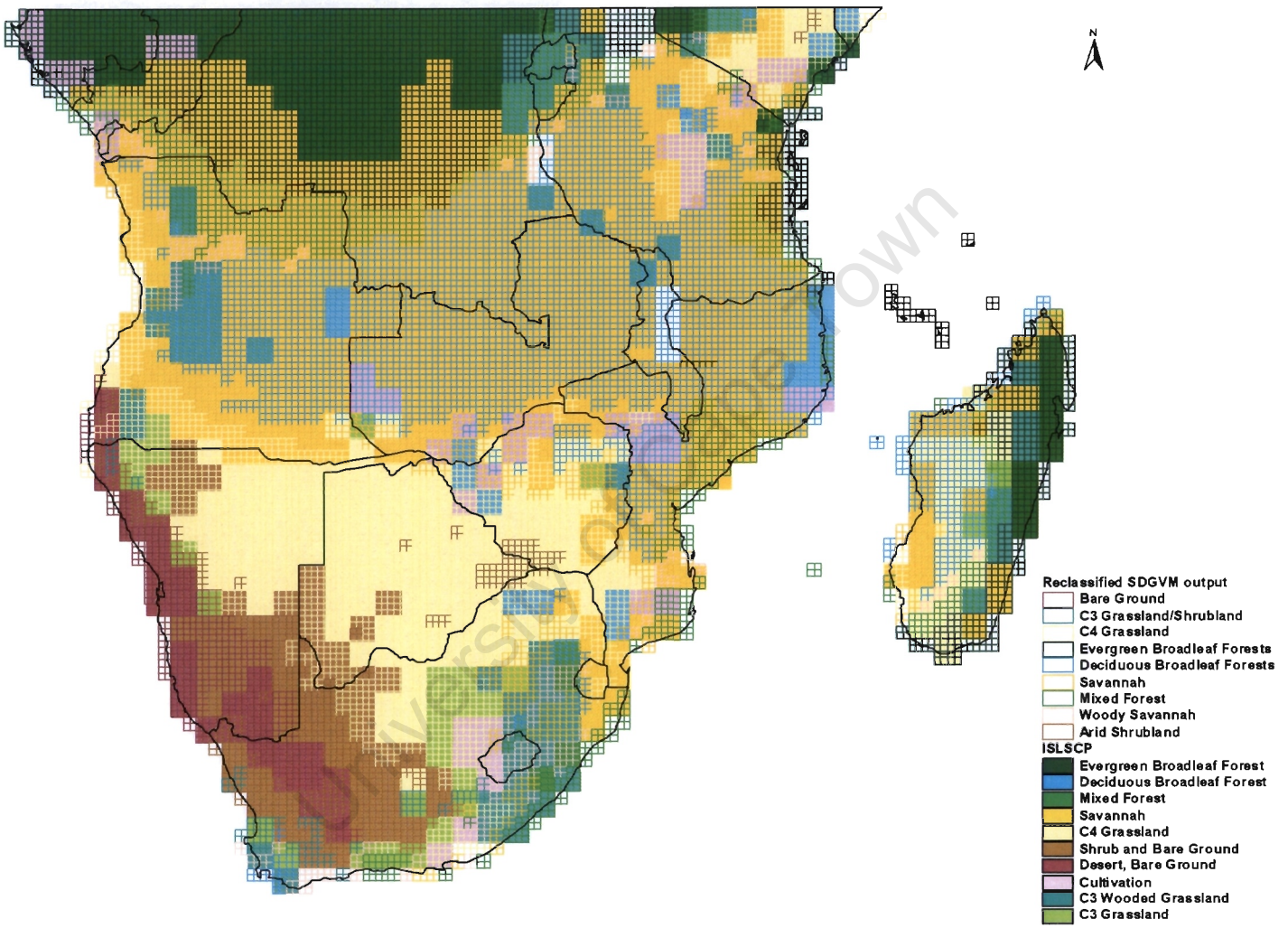

Figure 6.9: The comparison between the reclassified SDGVM output and the ISLSCP data for the region.

6.5. Conclusion

The decadal and inter-annual variation of the PFTs was found to display similar patterns. There is a strong correlation between Bare Ground and C_4 Grasslands, with one increasing while the other decreases. The variation in the other PFTs can be considered to be quite small, particularly at an annual scale. An average of the last 10 years (1986-1995) of the control run period was therefore used for the analysis.

The general patterns displayed by the validation set appear to be captured by SDGVM, except for over Madagascar. The main differences occur where the validation dataset shows vegetation types composed of transitional or mixed vegetation, which SDGVM cannot model.

Overall, there appears to be a fairly close relationship between the vegetation distribution predicted by SDGVM and that shown by the SPOT-VGT classification. Many of the differences can be explained by the differences in the number of classes between the two datasets, and also by remembering that SDGVM does not predict human influences on vegetation, which would be picked up by the SPOT-VGT classification.

The reclassification of SDGVM output was an attempt to simulate transitional types of vegetation, in order to produce better correspondence with the validation datasets. This did not greatly improve the agreement between SDGVM results the GIS database or the SPOT-VGT classification. However, both of these databases include areas where the natural vegetation has been destroyed or altered by human activities, and this may account for many of the differences noted, as SDGVM only models potential natural vegetation. SDGVM does compare more successfully with the ISLSCP dataset. The inaccuracies of the reclassified SDGVM output could also be related to the method of classification. For example, the savannah class is based on the co-dominance of C_4 Grasslands and Deciduous Broadleaf Forests, but the

ratio of the two plant functional types varies greatly between the different types of savannah. Scholes (1997) suggests that the tree canopy can range from 5% to 90% cover and that savannah are part of a continuum of biomes, that ranges from arid shrublands, to lightly wooded grasslands, deciduous woodlands and finally to dry forests. These biomes are also strongly affected by local variations in disturbances, such as fire, herbivory and anthropogenic land use change (Campbell *et al*, 1996). It was not feasible in the current study to undertake experiments investigating combined interactions between fire regime, temperature and moisture availability, but these are certain to provide useful and interesting results for future similar studies.

It has been shown that SDGVM is capable of predicting the distribution of vegetation for the present day, over Africa south of the equator, with the differences being mainly due to anthropogenic land use change, which is not simulated by SDGVM. An investigation of the impact of parameter uncertainty on SDGVM outputs for the subcontinent is beyond the scope of the present work and was not undertaken. Current and future developments to SDGVM include examining the possibility of using satellite imagery to incorporate anthropogenic landscapes (Lomas, *pers. comm.*). However, the complex driving forces of human economic and social development make it extremely difficult to predict future anthropogenic land use changes. The following chapter will examine how SDGVM responds to changes in its input data. Any changes in vegetation distribution modelled by SDGVM will therefore represent a "best estimate", in the absence of suitable techniques to model future anthropogenic land use changes.

SECTION 4:

POSSIBLE FUTURE EFFECTS OF CLIMATE ON VEGETATION

CHAPTER 7: SENSITIVITY EXPERIMENTS II: SDGVM

7.1. Introduction

Three major variables, namely temperature, precipitation and CO_2, have driven vegetation response to past climate change, and will continue to determine vegetation change in response to anthropogenic climate change (Woodward, 1987a; Harrison and Prentice, 2003). These three variables are known to have impacts on the structure of vegetation in southern Africa (e.g. Bond *et al*, 2003a), and these impacts may be large enough to affect vegetation-climate feedbacks, through their effects on surface albedo, roughness length and moisture fluxes.

Rainfall input has long been recognised as a driver of vegetation albedo and leaf area index in most vegetation types of the world on a seasonal timescale, and may also influence plant functional type distribution on longer time scales (Woodward and Williams, 1987; Jones, 1992). The availability of moisture also affects the growth of the plant, with more moisture allowing more growth (Woodward, 1987a). Precipitation directly influences the amount of soil moisture, which determines the ability of plants to survive drought periods, and will therefore affect the type of vegetation in a region (Woodward, 1987a).

The effects of temperature are possibly more complex than those of precipitation, as temperature impacts the process of photosynthesis directly, but also controls the development of plant phenology, and is known to affect leaf production and leaf fall (Jones, 1992). Minimum and maximum temperatures may also be critical in defining the limits of plant survival (Woodward, 1987a). Harrison and Prentice (2003) have shown how lower tropical temperature during the last glacial maximum (LGM, *c.* 21 kyr BP) coupled with increased aridity shifted the margins between forests and more drought-tolerant vegetation, such as savannahs and grasslands.

Fire is an important disturbance mechanism in several southern African biomes, notably in grasslands, fynbos and savannah. For trees less than 2m tall, fire is more likely to reduce their biomass than to cause mortality (Scholes, 1997). Older trees will recover from fires by resprouting, often near from their base, which results in a more "bushy" appearance. However, young trees or trees that have been weakened by repeated fire events may eventually be killed by fires, suggesting that the time between fires, or the fire return interval, is a significant variable in the determination of the amount of tree cover (Scholes, 1997). Heisler *et al* (2003) showed that an increase in the fire return interval resulted in an increase in total shrub cover.

However, if the fire return interval is long enough, young trees will escape to a height at which they are less susceptible to mortality by fire. The age at which this occurs varies, depending on the speed at which individual species grow. SDGVM currently includes a function that controls the age at which trees escape from fire. This function needs to be tested, as there is very little data available on current fire escape ages. The fire escape age will be tested through a series of experiments with SDGVM, and the results will be compared to current vegetation distributions.

Futhermore, the effects of CO_2 change on the growth of young trees are still uncertain, but recent studies suggest that increasing CO_2 could enhance the growth of young trees, which would allow them to escape from fire at a younger age (Bond and Midgley, 2000; Bond *et al*, 2003b). This is particularly relevant to the savannah regions of southern Africa, which are inherently unstable ecosystems determined by a number of competing factors (Scholes, 1997), and where C_4 grasses in these mixed tree/grass ecosystems provide the ideal fuel for fires. It is therefore important to understand how SDGVM responds to fire escape ages under current CO_2 and climate conditions, in order to provide a baseline comparison for future CO_2 and climate change experiments.

A series of experiments was undertaken to determine the sensitivity of the SDGVM outputs to these selected climate parameters, namely precipitation and temperature, as well as to the age at which trees will escape from fire episodes. Precipitation was increased and decreased by 5%, 10%, 15% and 20%, due to the uncertainties in direction of future regional precipitation changes (IPCC, 2001). Temperature was increased by 1ºC through to 5ºC, in order to encompass the predicted increases in temperature over the region (IPCC, 2001). As there is very little published information of current fire escape ages, a range of values were selected to encompass all possibilities. Fire escape age was therefore set to 0, 10, 15, 20, 25, 50, 75, 100 and 1000. All other parameters were set to the default, and the model was run for a period from 1901 to 1995, with annual results. The domain for these experiments covers Africa south of the equator at a resolution of 0.5º x 0.5º.

The results from these experiments presented below are the averages of the last 10 years of the simulations, i.e. the simulated period of 1986 – 1995. The percentage change in vegetation distribution with each of the perturbation experiments was calculated as the percentage of sites (0.5º x 0.5º) where the dominant vegetation type has changed.

7.2. SDGVM Sensitivity to Temperature

Changes in palaeovegetation over Africa have been largely attributed to changes in temperature, with precipitation exerting only a secondary influence (Olago, 2001). Temperatures are generally expected to increase globally under future climates (IPCC, 2001). The graph in figure 7.1 shows the total number of sites that have changed their denomination with increasing temperature for southern Africa. A 1°C increase in temperature results in a change in vegetation distribution of almost 3%, while a 5°C increase in temperature results in a 13% change in vegetation distribution. The change in the frequency of occurrence of each PFT for a temperature increase of 1°-5°C shows a linear response (Figure 7.2). It can be seen from the figure that C_3 Grassland/Shrublands and Deciduous Broadleaf Forests

show a gradual decline with increasing temperature. Bare Ground, C_4 Grasslands and Evergreen Broadleaf Forests all show a positive correlation with increasing temperature. The Deciduous Broadleaf Forests show the greatest change, with a decline of almost 10% with a 5°C increase in temperature. The C_3 Grassland/Shrublands show a maximum decline of only 1.5%, but since they cover such a small area (only about 3% of all the sites in the study region), this is significant. This PFT also represents the species-rich Fynbos biome, and these results therefore suggest an almost total loss of Fynbos with a 5°C increase in temperature. This interesting result concurs with the prediction of a substantial loss of species in the characteristic Fynbos family, the *Proteaceae*, under a mid range climate scenario for 2050 by Thomas *et al* (2004)

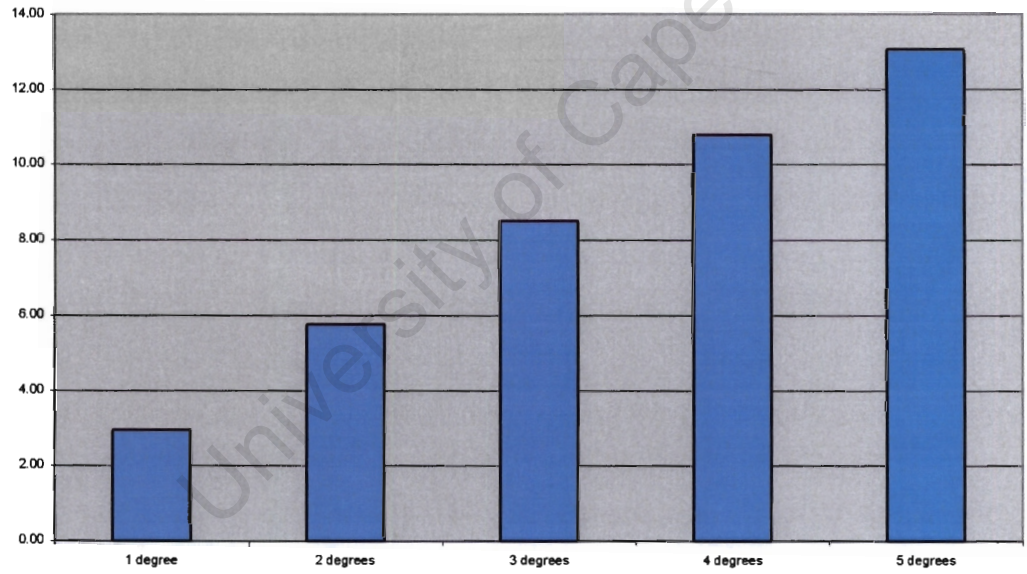

Figure 7.1: The percentage of sites that changed their cover type with a 1° – 5°C increase in temperature.

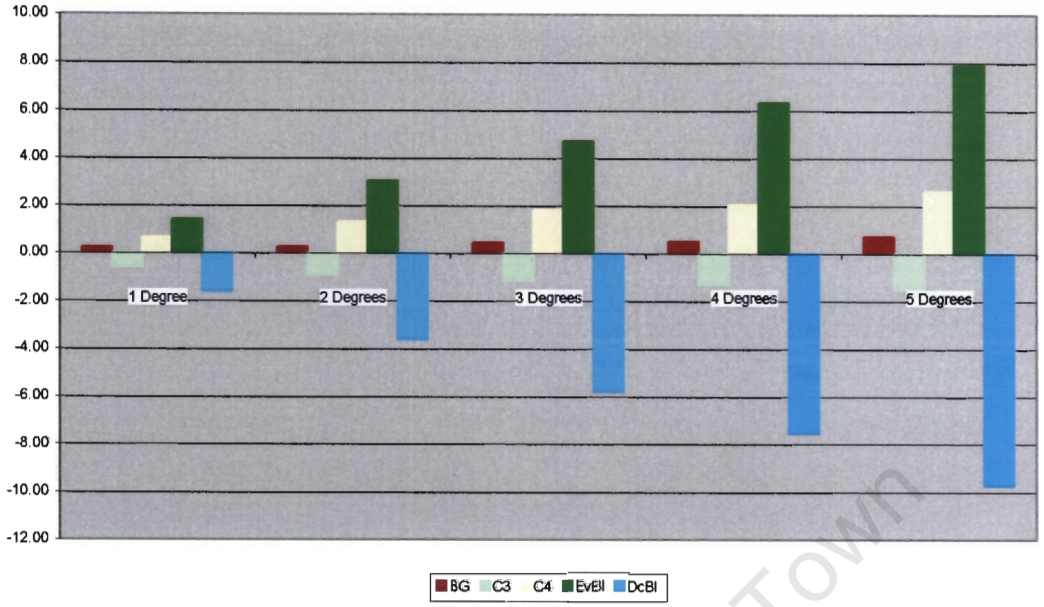

Figure 7.2: The percentage change in the frequency of occurrence of each PFT for a temperature increase of 1° – 5°C.

The maps in Figure 7.3 show the change in vegetation distribution with increasing temperature. The increase in Evergreen Broadleaf Forests evident in Figure 7.2 is also reflected in the maps (Figure 7.3). The expansion of Evergreen Broadleaf Forests occurs along the border with the Deciduous Broadleaf Forests, thereby decreasing the Deciduous Broadleaf Forests and is accentuated with each increase in temperature.

Along the border of the Namib Desert and the Karoo region of South Africa, changes can be seen in the distribution of Bare Ground and C_4 Grasslands. With increasing temperature, the area classified as Bare Ground expands into the C_4 Grasslands, particularly along the border of southern Namibia and Botswana. However, in some places, the C_4 Grasslands expand into the areas of Bare Ground.

Along the border between the C_4 Grasslands and the Deciduous Broadleaf Forests, some changes can be seen, particularly with the greater temperature changes. The

C_4 Grasslands can be seen to gradually expand into the areas that were classified as Deciduous Broadleaf Forests.

The most noticeable change occurs in the Western Cape region of South Africa. This region is currently characterised by the valuable Fynbos biome, represented mainly by the C_3 Grassland/Shrubland PFT. With increasing temperature, the C_3 Grassland/Shrubland PFT dwindles quite drastically, until it is almost non-existent at 5°C. Initially, the Deciduous Broadleaf Forests expand in the region, but with higher temperatures, the C_4 Grasslands and even Bare Ground replace the C_3 Grassland/Shrublands.

The Knysna Forest, which is situated along the southern coast of South Africa, and is one of the few remaining natural indigenous forests in the area, also undergoes a change. It is modelled by SDGVM as Evergreen Broadleaf Forests, but with increasing temperatures, Deciduous Broadleaf Forests start to encroach on the Evergreen Broadleaf Forests.

These findings suggest that an increase in temperature, as is predicted by most climate change scenarios, will have a detrimental effect on the ecologically sensitive region of the Western Cape, South Africa. There will also be a shift in the ratio of grasses to trees in the inherently unstable savannah ecosystems of southern Africa.

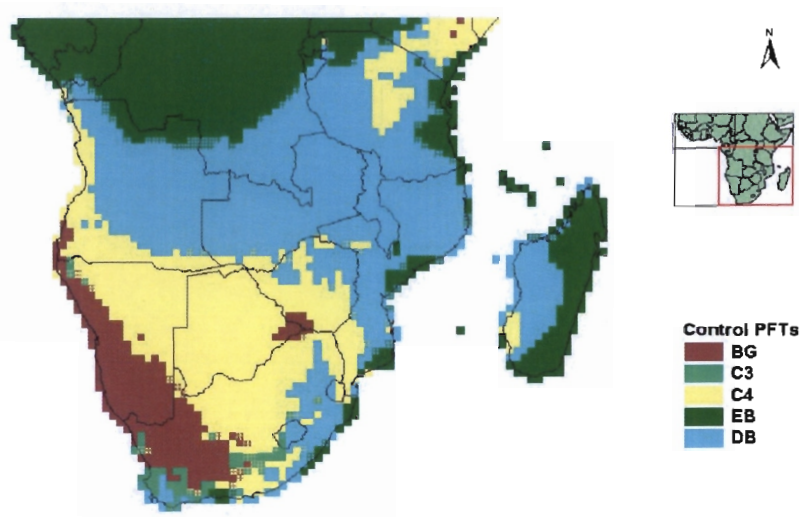

a)

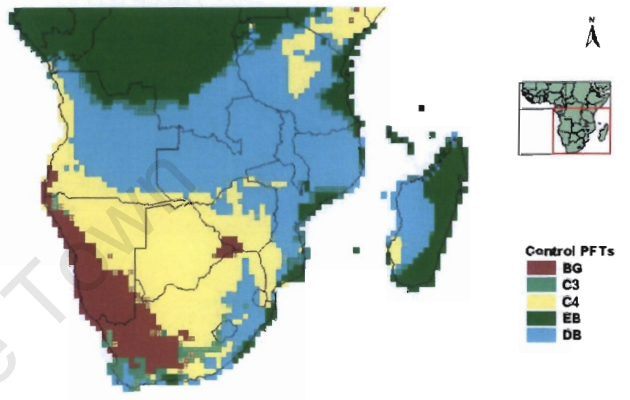

b)

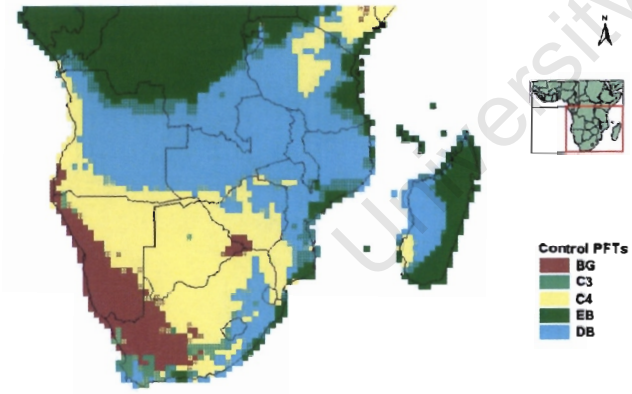

c)

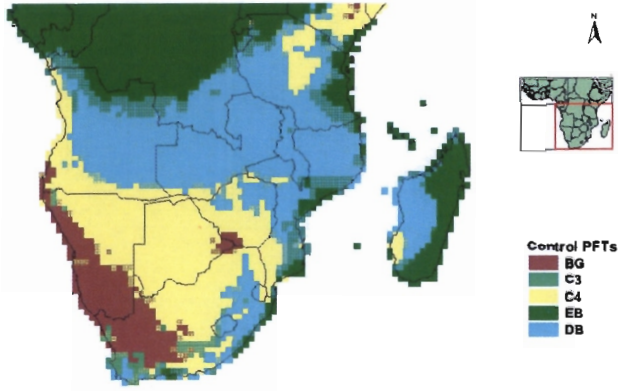

d)

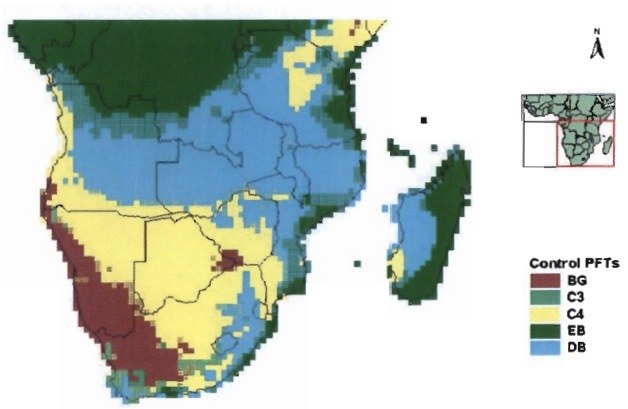

e)

Figure 7.3: The change in vegetation distribution in comparison to the control run with each increase in temperature. a) 1°C increase; b) 2°C increase; c) 3°C increase; d) 4°C increase; and e) 5°C increase. (The hatched areas show where the two datasets do not agree; with the hatches representing the SDGVM modelled vegetation under the increased temperature, and the areas underneath the control experiment modelled vegetation.)

7.3. SDGVM Sensitivity to Precipitation

The graph in figure 7.4 shows that vegetation responds most to an increase in precipitation, where about 16% of the sites changed their designation. For a 20% decrease in precipitation, approximately 12% of the sites responded with changes in vegetation. This is approximately equivalent to the amount of sites that changed with a 15% increase in precipitation. A 5% increase has approximately the same effect as a 5% decrease in precipitation (both changes caused around 3.8% of the sites to change their designation).

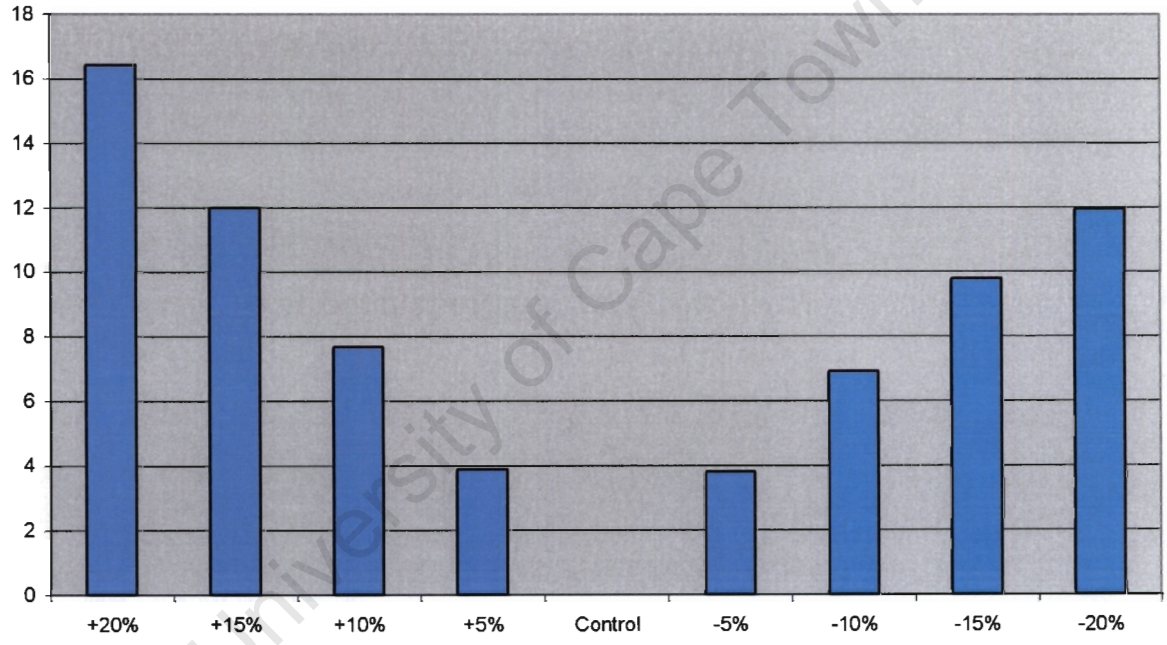

Figure 7.4: The percentage of sites that changed their denomination with a each change in precipitation.

Figure 7.5 shows the change in each Plant Functional Type for each change in precipitation. Bare Ground responds most to a decrease in precipitation, increasing by almost 3% with a 20% decrease in precipitation. A 20% increase in precipitation only causes a 1.5% decrease in Bare Ground. The C_3 Grassland/Shrublands show very little response to precipitation, with all changes being less than 1%. The C_4 Grasslands show the greatest response to precipitation, increasing by 6% with a

20% decrease in precipitation. A 20% increase in precipitation caused a decrease of over 4% in the C_4 Grasslands. In contrast to the C_4 Grasslands, both the Evergreen Broadleaf and Deciduous Broadleaf Forests decrease with a decrease in precipitation (both approximately 4% decrease for a 20% in precipitation), and increase with increasing precipitation.

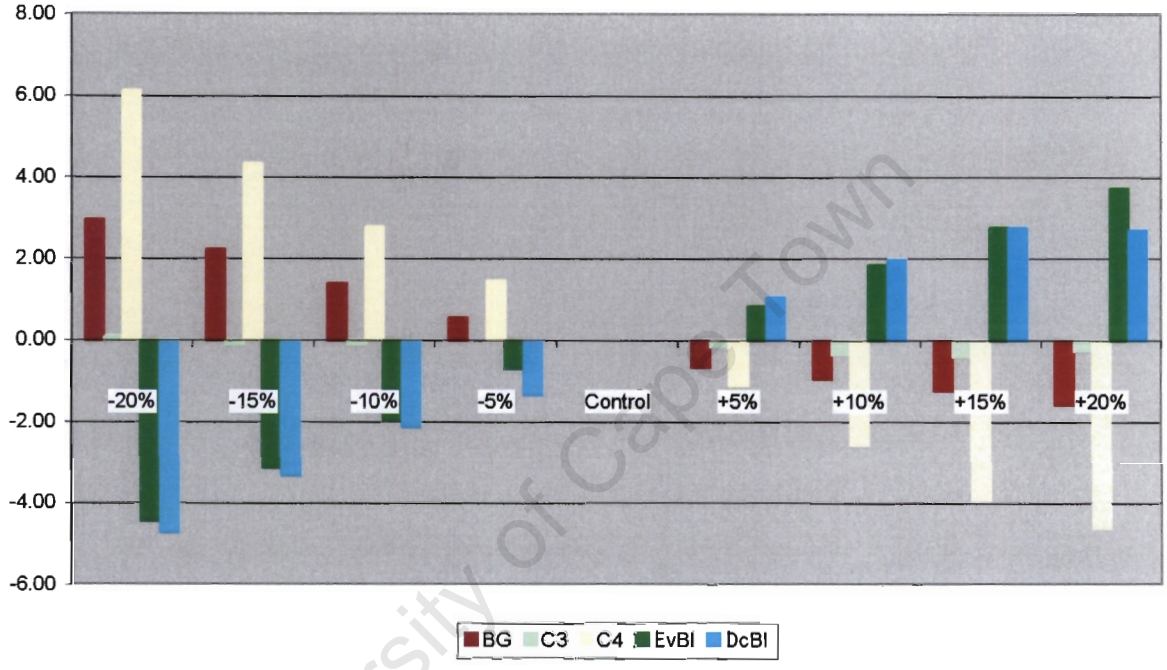

Figure 7.5: The percentage change in the frequency of occurrence of each PFT for each precipitation change.

7.3.1. Precipitation Increase

The increase in the Forests seen in Figure 7.5 is also seen in the maps in Figure 7.6. The Evergreen Broadleaf Forests gradually expand southwards into the Deciduous Broadleaf Forests, and the Deciduous Broadleaf Forests expand into the C_4 Grasslands. The Evergreen Broadleaf Forests can also be seen expanding along the south east coast of South Africa and in the Knysna Forest. The Deciduous Broadleaf Forests expand into the C_3 Grassland/Shrubland in the Western Cape, suggesting that the Fynbos Biome is also sensitive to increasing precipitation, although this change is less drastic than was seen with increasing temperatures.

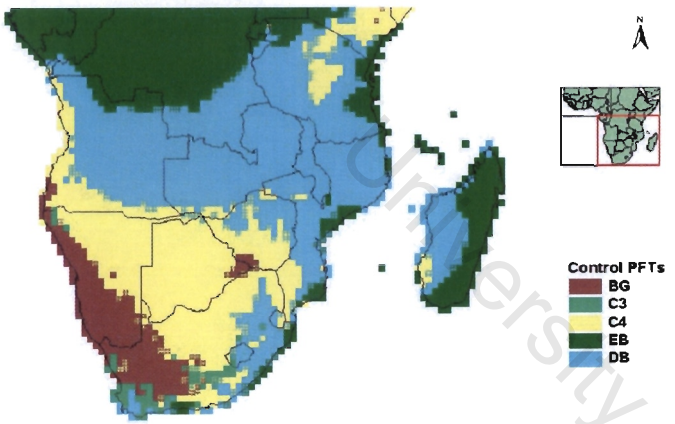

a)

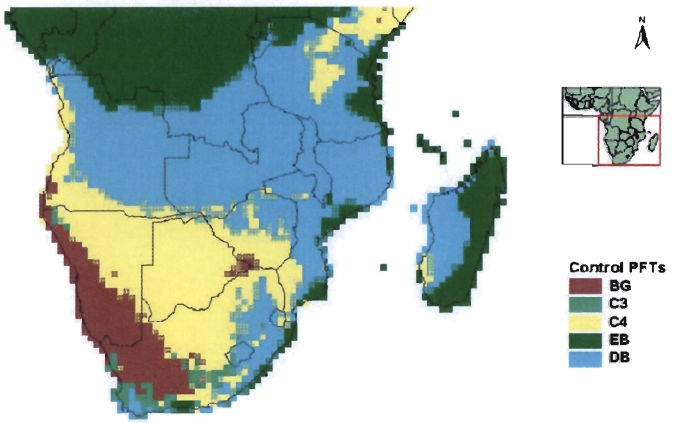

b)

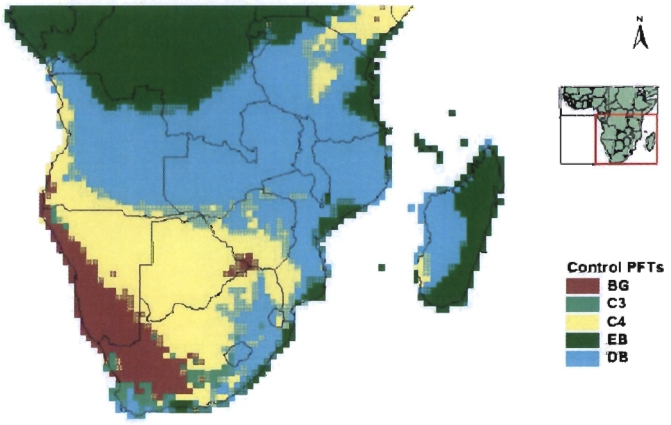

c)

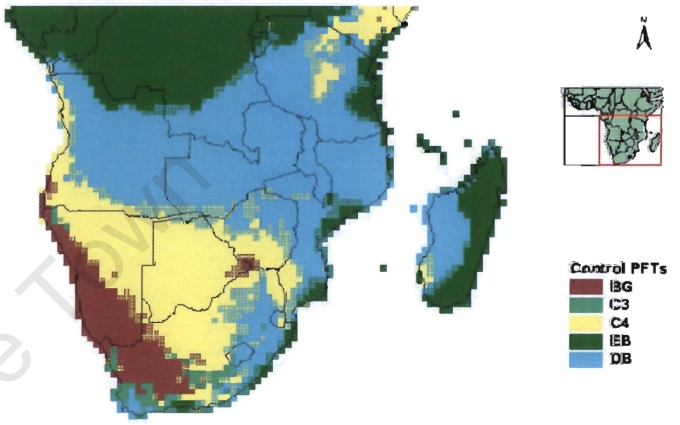

d)

Figure 7.6: The change in vegetation distribution in comparison to the control run with each increase in precipitation. a) 5% increase; b) 10% increase; c) 15% increase; and d) 20% increase. (The hatched areas show where the two datasets do not agree; with the hatches representing the SDGVM modelled vegetation under the increased precipitation, and the areas underneath the control experiment modelled vegetation.)

The areas of Bare Ground all decrease with increasing rainfall, as suggested by the graphs (Figure 7.5). A small area of Bare Ground in the northeast corner of the study region disappears with only a 5% increase in precipitation. The Bare Ground region predicted in south-eastern Botswana by SDGVM shrinks with each increase in precipitation. C_4 Grassland and C_3 Grassland/Shrubland can be seen encroaching into the borders of the Namib Desert and the semi-desert area of the Karoo, suggesting that the dynamics of the arid shrublands in this region are sensitive to precipitation increases.

7.3.2. Precipitation Decrease

The maps in Figure 7.7 show the changes in the distribution of the Plant Functional Types with each decrease in precipitation. In general, many of these patterns are the opposite of what is seen in the increased precipitation experiments, as would be expected. The Deciduous Broadleaf Forests gradually expand into the Evergreen Broadleaf Forest regions, and the C_4 Grasslands expand into the Deciduous Broadleaf Forests, with the main areas of change along the boundaries between these PFTs. The Evergreen Broadleaf Forests along the southern and eastern coasts are reduced by the expansion of Deciduous Broadleaf Forests, especially in the Knysna Forest. The Bare Ground expands in all regions that it is present. With a 20% decrease in precipitation, a new area of Bare Ground appears in the Northern Province of South Africa, in the area of the Kruger National Park. The C_3 Grassland/Shrublands, in contrast to previous findings, are seen to expand, replacing Deciduous Broadleaf Forests in the Western Cape of South Africa.

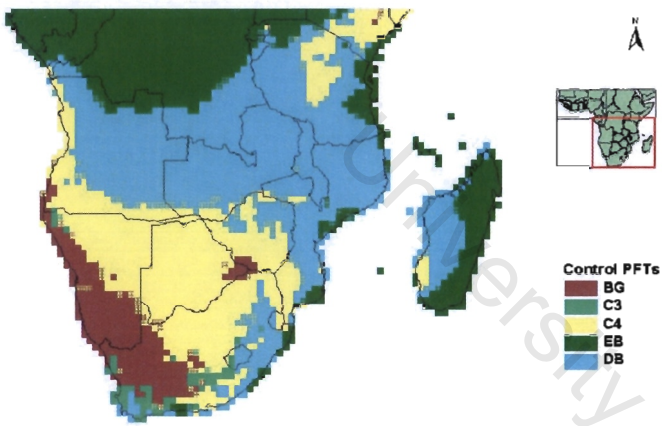

a)

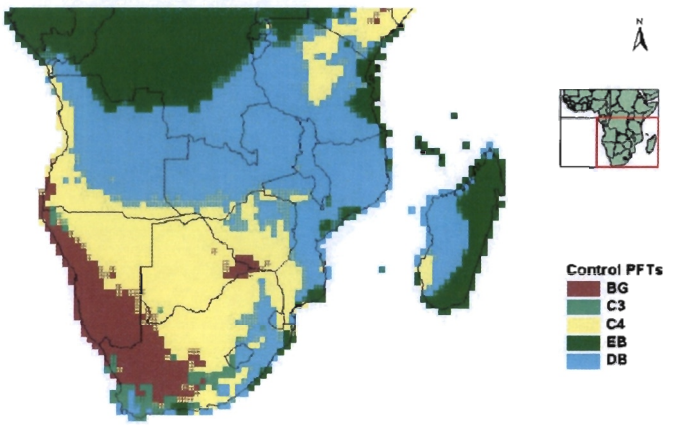

b)

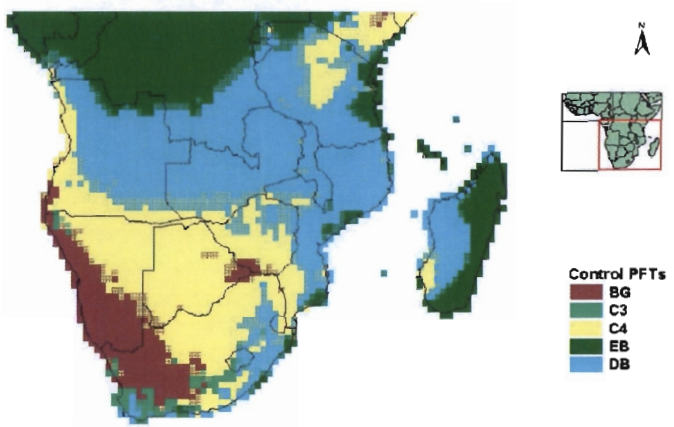

c)

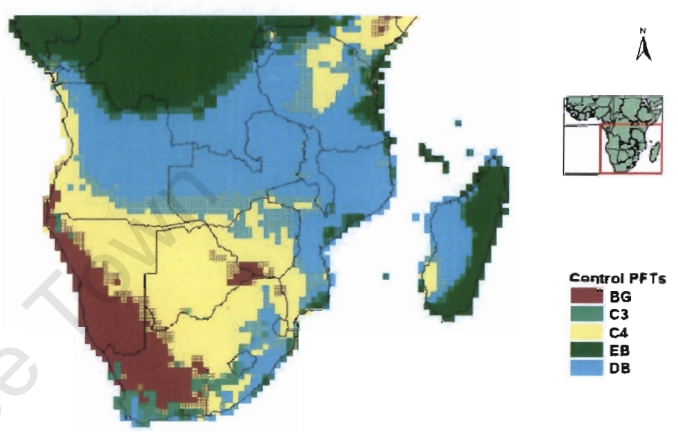

d)

Figure 7.7: The change in vegetation distribution in comparison to the control run with each decrease in precipitation. a) 5% decrease; b) 10% decrease; c) 15% decrease; and d) 20% decrease. (The hatched areas show where the two datasets do not agree; with the hatches representing the SDGVM modelled vegetation under the decreased precipitation, and the areas underneath the control experiment modelled vegetation.)

The most notable vegetation changes occur at the intersections of bare ground, C_4 Grasslands and C_3 Grassland/Shrubland in the deserts and semi-deserts. These areas are often classes as arid shrubland and are shown by these results to be sensitive to precipitation changes, which cause a change in the amount of cover. Precipitation is therefore a very important factor here. Precipitation has also been shown to have an influence on the savannah regions of southern Africa, but temperature appears to be the more dominant climate factor in determining savannah composition, as well as in the Fynbos region of South Africa.

7.4. SDGVM Sensitivity to Fire Escape Age

The grassland, savannah and fynbos biomes of southern Africa are strongly influenced by the occurrence of fire episodes (Cowling *et al*, 1997). The ratio of grassland to shrubs or trees is frequently determined by fire. Grasses provide the fuel for the fire, and will therefore determine the frequency of the fire return interval. Shrubs and trees are not annual plants like vegetation, and persist for many years. They may therefore experience many fire episodes in their life times, provided that they first reach an age at which they can escape the damage fire causes, as many young trees will be killed by fires. Therefore, the higher the age at which trees escape fires, the fewer trees there are. This is demonstrated by the graph in Figure 7.8, which shows the change in biomass with each of the fire escape experiments. The average biomass decreases with an increase in the fire escape age. Leaf area index (LAI) also decreases with fire escape age, but the NPP increases slightly. The decrease in LAI and biomass with an increase in the fire escape age indicates a decrease in the amount of trees, and an increase in the grasses. This is reflected in the maps in Figure 7.9 and Table 7.1, which both show the increase (decrease) in grasses (trees) with increase fire escape age. The Deciduous Broadleaf Forests are particularly sensitive to fire, decreasing from 60% (0 years) of all sites to about 20% (1000 years) with an increase in the fire escape age. There is a corresponding large increase in the C_4 grasses, while the C_3 grasses show only a small increase. Bare ground and Evergreen Broadleaf Forests remain more or less constant.

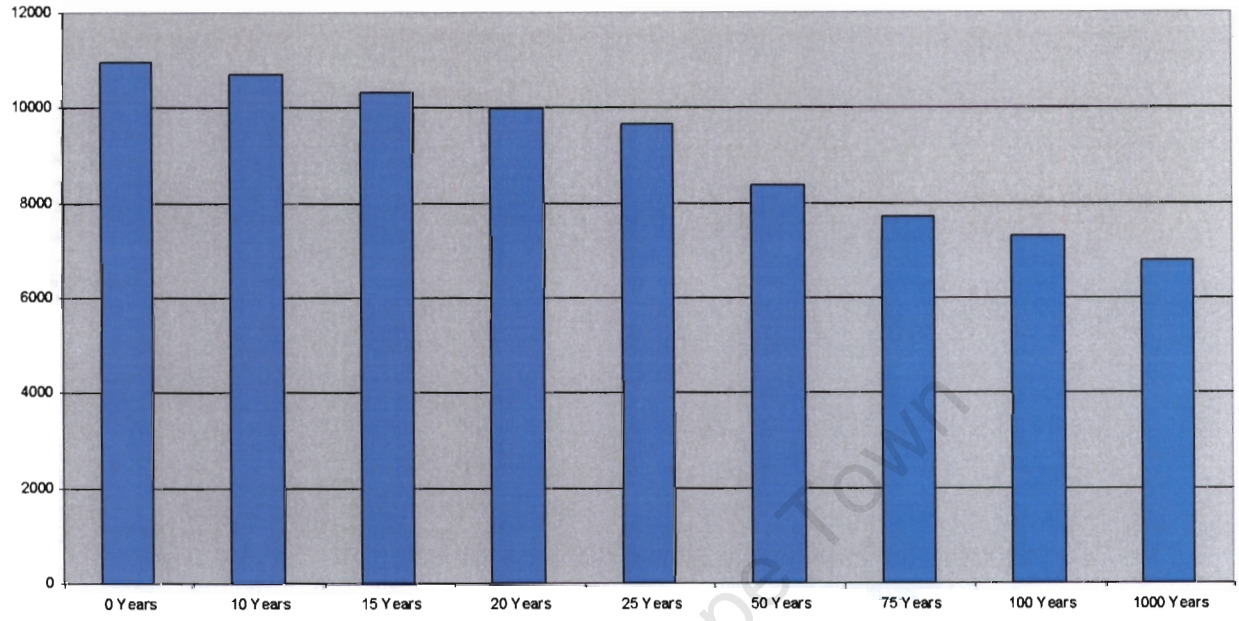

Figure 7.8: The average biomass (g/m^2) for each of the fire escape age experiments.

Table 7.1: The change in the percentage of sites dominated by the PFTs for selected fire escape ages.

	0 Years	25 Years	100 Years	1000 Years
BG	8.19	8.10	8.16	8.16
C_3	0.57	1.61	2.69	2.75
C_4	5.38	26.23	44.67	45.89
EvBl	24.93	24.87	23.85	23.51
DcBl	60.93	39.18	20.62	19.69

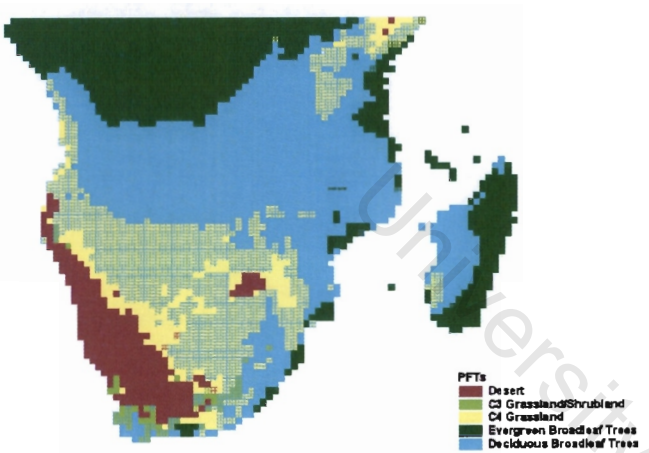

a)

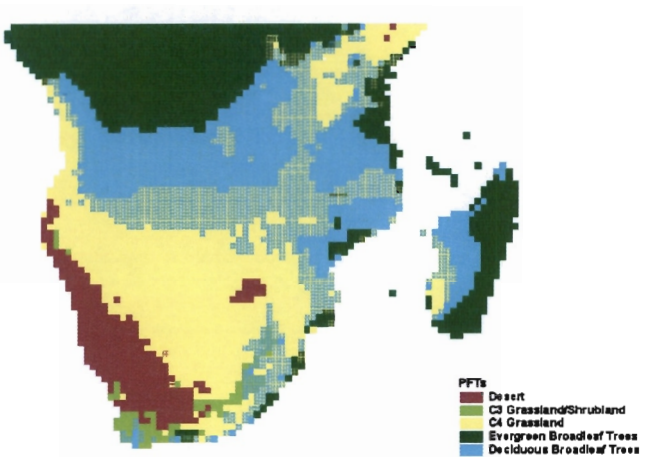

b)

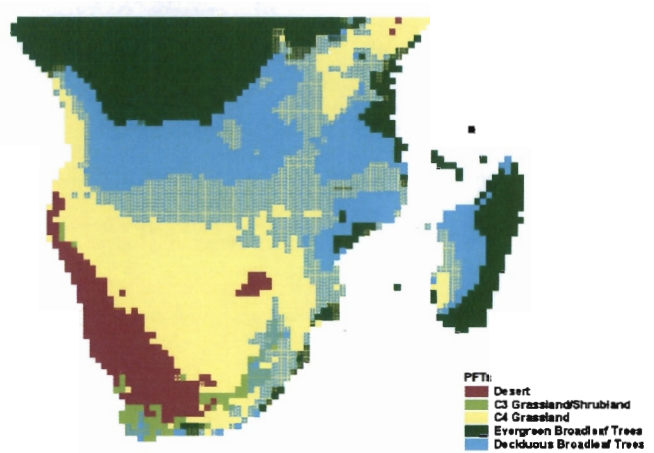

c)

Figure 7.9: The change in vegetation distribution in with a change in the fire escape years, shown in comparison to a fire escape age of 25 years. a) 0 years; b) 100 years; and c) 1000 years. (The hatched areas show where the two datasets do not agree; with the hatches representing the SDGVM modelled vegetation under the changed fire escape age, and the areas underneath represent the modelled vegetation with a fire escape age of 25 years.)

The graphs in figures 7.10 to 7.13 show transects of biomass, LAI and NPP across the domain, at 10.25ºS, 30.25ºS, 20.25ºE and 30.25ºE. The transect at 10.25ºS (Figure 7.10) shows that changes in biomass for various fire escape ages. The differences between the simulations of the range of fire escape ages is not as obvious on the LAI and NPP graphs.

Figure 7.11 shows the change in biomass, LAI and NPP at 30.25ºS. The change from the semi-desert Karoo region to the wetter regions of eastern South Africa are clearly visible on these graphs, although only the biomass graph shows the change with increased fire escape age.

Figure 7.12 is a north-south transect, which passes through the semi-desert Karoo, into the Namib desert and then northwards into the rain forests of central Africa. These changes are reflected in the graphs, with an initial small productivity, followed by a drop to zero and then slowly increasing northwards.

In contrast, the graphs in figure 7.13 are north-south transects along a region of relatively high productivity. A drop in productivity occurs in southern Zimbabwe, which corresponds to a region modelled as bare ground by SDGVM. Once again, the differences between the fire escape ages is best seen on the biomass graph.

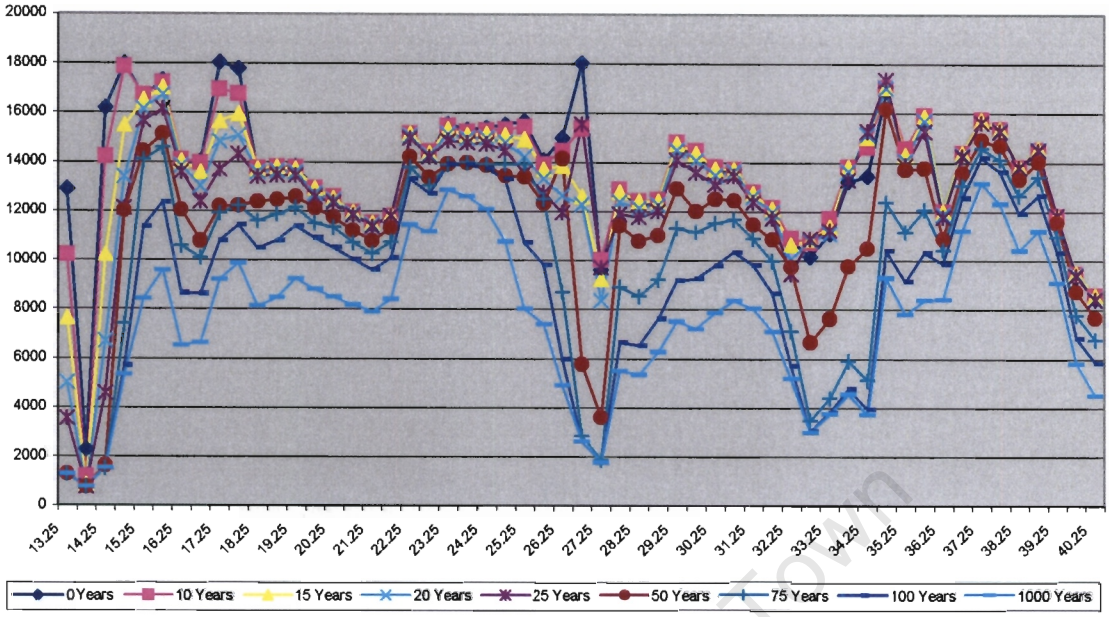

Figure 7.10: The change in biomass associated with the changes in the fire escape age, for an east-west transect at 10.25ºS.

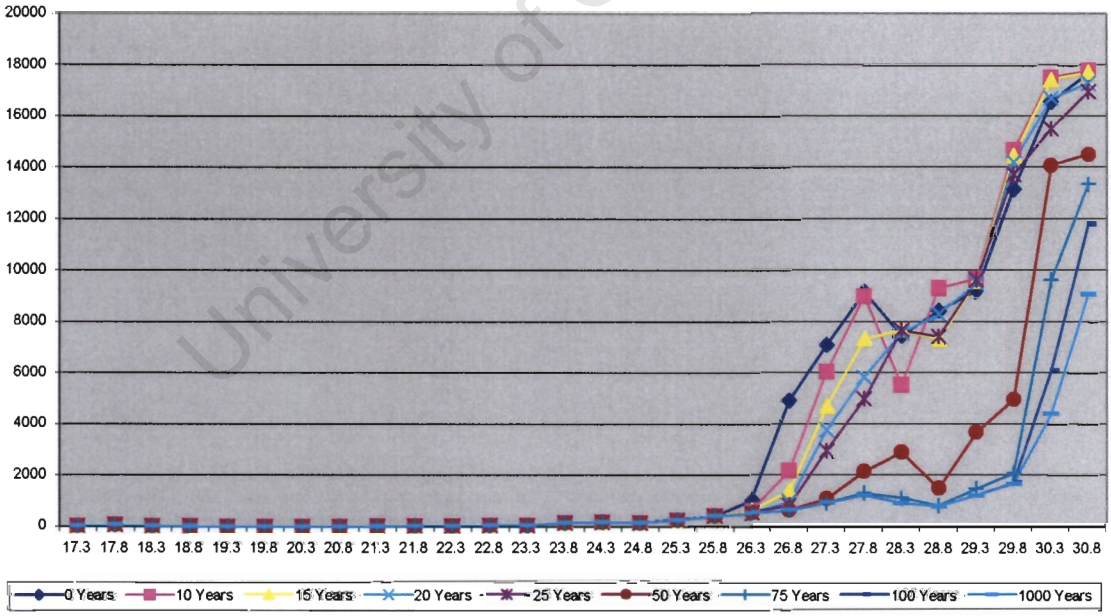

Figure 7.11: The change in biomass associated with the changes in the fire escape age, for an east-west transect at 30.25ºS.

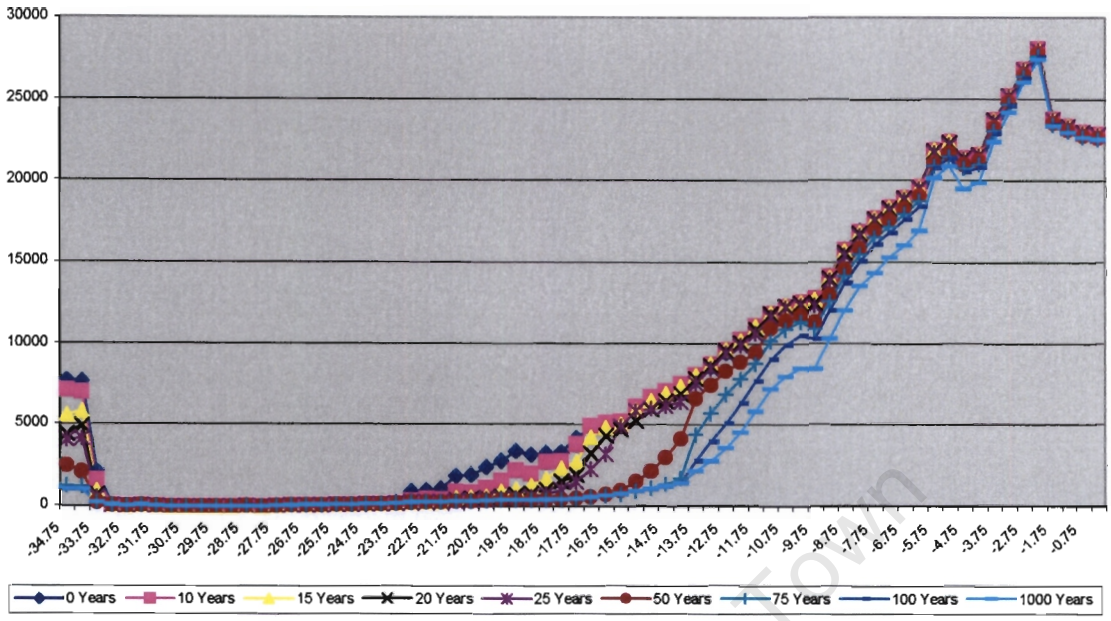

Figure 7.12: The change in biomass associated with the changes in the fire escape age, for a north-south transect at 20.25ºE.

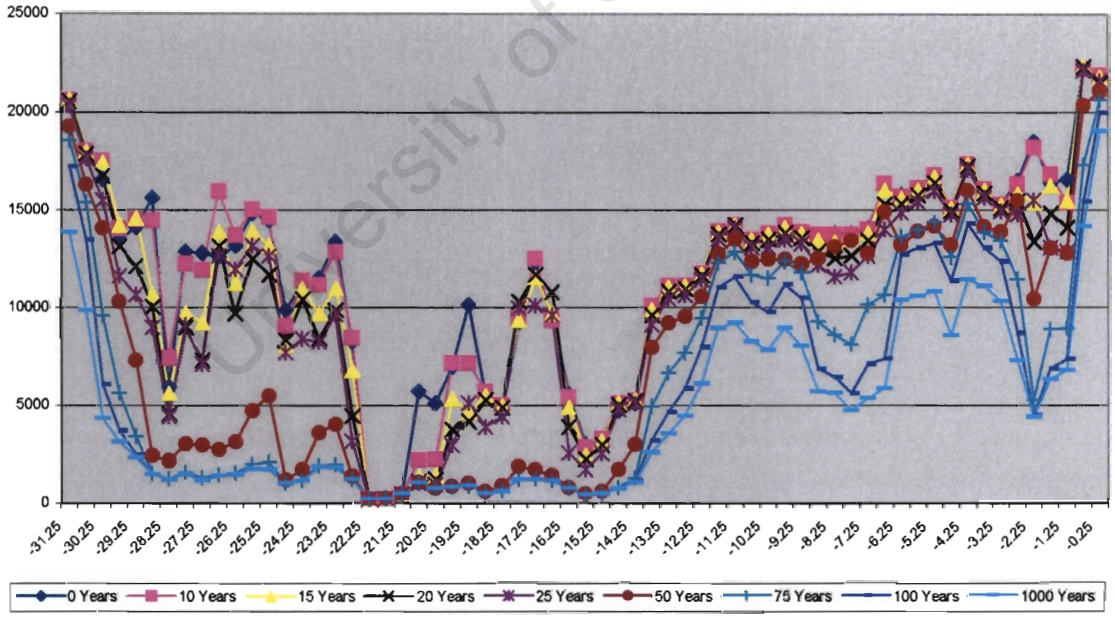

Figure 7.13: The change in biomass associated with the changes in the fire escape age, for a north-south transect at 30.25ºE.

7.5. Conclusion

Very few studies are currently available that simulate the sensitivity of vegetation to a range of environmental scenarios at a regional scale in Africa. Temperature and precipitation have been shown to have an influence on savannahs and the shifting ratio of C_4 grasses to Deciduous Broadleaf trees. Hotter and drier conditions result in more open savannahs, while wetter conditions cause an increase in the canopy cover. Arid shrublands are similarly affected, but precipitation appears to be slightly more important than temperature. There is a positive correlation between precipitation and the amount of cover, in other words, as precipitation increase, so does the amount of vegetation cover, but precipitation decreases result in decreased cover.

Furthermore, the fire escape age experiments revealed that C_4 grasses and Deciduous Broadleaf Forests are the PFTs most sensitive to fire. This is in line with other studies that have indicated the importance of fire in savannah ecosystems (e.g. Scholes, 1997; Bond and Midgley, 2000; Bond et al, 2003a). C_4 grasses and Deciduous Broadleaf trees are the main components of savannah vegetation. The sensitivity of these PFTs to fire escape age therefore has important implications for the future are the large savannahs of Africa, which are important ecosystems for tourism and biodiversity. Although it is possible that fire regimes will be affected by climate change, the nature of these changes are not known as the possible impacts of climate change on fire regimes are still relatively under-studied.

One of the important caveats of this kind of experiment is that the changes forced on the climate data are constant across the entire study region, and may therefore not preserve expected relationships between climate variables, as pointed out by Warrick *et al* (1986). It is far more likely that changes will vary across a region. However, they do highlight some areas of potential change that can be ear-marked for further studies, and the relative importance of climate variables in different ecosystems in southern Africa. In general, most of the changes occur along the

boundaries between Plant Functional Types. These are the regions where the dominant PFT may only be dominant by a small percentage, so even minor changes will affect which PFT is dominant.

In addition, several sensitive areas have been highlighted by these experiments, which may require further studies. The most sensitive area appears to be the Western Cape region, which currently supports the Fynbos Biome (C_3 Grassland/Shrubland PFT). The C_3 Grasslands/Shrublands almost totally disappear with increasing temperatures, and increases in precipitation result in more trees in the region. The Knysna Forest was affected by all the experiments as well. Increasing temperatures and decreasing rainfall, a scenario predicted for the region under future climate changes, results in a change from Evergreen to Deciduous Broadleaf Forest. As this is one of the last remaining indigenous forests in South Africa, the loss of this forest would be disastrous. Finally, the Kruger National Park in northern South Africa has already been experiencing decreasing rainfall over the last 50 years, with declining vegetation levels. As this is the largest natural park in the region, any change to the vegetation could have serious environmental and economic consequences.

These results have highlighted the sensitivity of southern African vegetation to the enforcement of a uniform change in individual climate variables and to changes in the fire escape age variable. It is therefore expected that significant changes will be seen when climate change predictions are used to drive the SDGVM. These predictions represent the combined changes in climate variables, which could result in different changes being observed. The following chapter will examine the response of SDGVM to a range of future climate change scenarios.

CHAPTER 8: CLIMATE CHANGE EXPERIMENTS

8.1. Introduction

Changing climate is very likely to alter the functioning and geographic location of major vegetation types at the sub-continental and continental scale, as was seen in the sensitivity experiments with the SDGVM (Chapter 7), and as has been revealed by modelling at the global level (e.g. Cox *et al,* 2000). The concept of using plant functional types (PFTs), as opposed to species, in vegetation modelling is a useful way of exploring this response, as it simplifies vegetation to a few structural types that respond to changes. Major changes in vegetation can thus be seen primarily through a change in the relative proportion of functional types.

The potential responses of vegetation to climate change have investigated by many authors, for example, Cox *et al* (2000), Betts *et al* (1997) and Harrison and Prentice (2003). Cramer *et al* (2001) presented the possible change in future global vegetation predicted by six different Dynamic Global Vegetation Models (DGVMs) with output from one climate model (HadCM2-SUL) and the IS92a scenario. The results showed the conversion of some tropical forests to grasslands, which resulted in a decline in the terrestrial carbon sink after 2050 as a direct result of climate change. Cox *et al* (2000) obtained similar results using the TRIFFID DGVM driven by the HadCM3 climate model. A hotter and drier climate over South America results in large losses of Amazonian forest, even without any consideration of anthropogenic deforestation. Furthermore, the warming climate also influences plant productivity and soil respiration, resulting in less terrestrial carbon storage, and the conversion of the terrestrial biosphere from a net carbon sink to a net carbon source after 2050.

The ability of vegetation to store carbon is also limited by the availability of other nutrients, such as nitrogen. Hungate *et al* (2003) have questioned the ability of DGVMs to adequately simulate vegetation response to increased CO_2, and in

particular, increased growth in response to elevated CO_2. The ability of several DGVMs to simulate future vegetation is questioned because of the inadequate modelling of nitrogen limitation by these models. Clearly, the nitrogen feedback limitation is critical in estimates of vegetation response. However, the SDGVM has a well accepted nitrogen and carbon cycle model, CENTURY (Parton *et al*, 1993), and Hungate *et al* (2003) are therefore incorrect in stating that SDGVM does not include a nitrogen feedback. Thus the Sheffield Dynamic Global Vegetation Model (SDGVM) is an excellent candidate to investigate regional response of vegetation to future change.

Beerling and Woodward (2001) examined the response of global vegetation to future climate change using the SDGVM driven by a future climate simulated by the HadCM2 climate model. The increase in atmospheric CO_2 concentration resulted in a steady increase in vegetation productivity until 2100, but showed a decline after that, when terrestrial ecosystems switched from being a net carbon sink to a net carbon source. The distribution of vegetation functional types was also predicted to change. The abundance of C_3 shrubs and grasses increased, particularly over the Sahel and southern Africa, in response to increased CO_2 concentrations and at the expense of C_4 grasslands. Other simulated vegetation changes included changes to the forests of Europe and an increased extent of desert ecosystems in Australia and India.

Far fewer studies have simulated vegetation response at the regional scale in Africa. Shannon (2000) used the Integrated Biosphere Simulator (IBIS) of Foley *et al* (1996) driven by results from the Hadley Centre HadCM2 transient GCM simulator to examine future vegetation change over southern Africa. However, this work was limited by several caveats. The climate data used to drive the IBIS model was based on the outdated IS92a scenario and was only available at a resolution of 2.5° latitude by 3.75° longitude, which would limit the results to broad spatial scale changes only. Furthermore, the IBIS model does not take into account the effect of

CO_2 fertilisation and fire disturbance, both of which have a strong impact on the dominance of C_3 versus C_4 grasses.

The positive role of CO_2 in increasing leaf level carbon uptake and water use efficiency is now well understood, especially with regard to different photosynthetic types. CO_2 appears to affect particularly the composition of mixed C_3/C_4 grasslands, and vegetation assemblages comprising both of these photosynthetic types. High CO_2 favours the C_3 pathway, but many of the studies of CO_2 impacts on vegetation have been confined to single plants or species, due to the inherent difficulties involved in changing the CO_2 composition for large areas of mixed ecosystems. However, the role of CO_2 in controlling the balance of different functional types is currently being reassessed (Bond and Midgley, 2000; Bond *et al* 2003a, 2003b).

Ehleringer *et al* (1997) present evidence for the recent evolution of the C_4 photosynthetic pathway, in response to lowered CO_2 concentrations during the last glacial maximum. Plants using the C_4 photosynthetic pathway use a CO_2 concentrating mechanism, which allows them to be more efficient at photosynthesis at low CO_2 concentrations that C_3 plants (Jones, 1992). The temperature during the growing season is also important in determining whether C_3 or C_4 plants will be dominant (Teeri and Stowe, 1976). Ehleringer *et al* (1997) suggest that where the daytime growing season temperature is less than 22°C, C_3 plants are favoured, and where the temperature exceeds 30°C, C_4 plants will be favoured. There is also evidence that greater C_3 growth occurs in winter and spring, whereas C_4 growth preferentially occurs in the summer months (Ehleringer *et al*, 1997). It can therefore be concluded that C_4 plants prefer warmer conditions with low CO_2 concentrations, and C_3 plants prefer cooler conditions with higher CO_2 concentrations. This presents an interesting debate in the context of future climate conditions - increasing CO_2 levels should favour C_3 plants, but the increase in temperature will favour C_4 plants. A modelling approach is essential in teasing apart the relative impact of these competing effects in the diverse environments found in southern Africa.

Although temperature and CO_2 appear to be the most dominant factors in control C_3/ C_4 plant dominance, precipitation also plays a role, with C_4 plants requiring more than 25mm of precipitation a month during the growing season for successful growth (Ehleringer *et al*, 1991; Collatz *et al*, 1998). It should also be noted that other factors, such as soil moisture and fire are likely to have an impact on the dynamics of C_3/ C_4 plant dominance. Recent studies suggest that the increase in atmospheric CO_2 concentrations will enhance young tree growth and allow them to escape from fire damage (Bond and Midgley, 2000; Bond *et al*, 2003a, 2003b), suggesting that the interactions between CO_2, climate, fire and vegetation are more likely to influence plant dominance in the future than any of the variables on their own.

In modelling these potential impacts on vegetation, it is important to take account of the uncertainty in climate projections. There is a broad range of climate change projections currently available, from many different models and scenarios, all of which could be equally plausible. The main body involved in climate change research is the Intergovernmental Panel on Climate Change (IPCC), which has developed a series of plausible climate change scenarios based on assumption of future population growth and resource use (Nakićenović *et al*, 2000). These scenarios have been used to drive a number of global climate models, to produce a range of future climate change predictions.

Most of these projections are based on output from global climate models, which limits the applicability of these results to regional impact studies. New methods of climate data downscaling (e.g. Hewitson and Joubert, 1998), as well as the improvement of regional climate models are producing improved regional predictions. This makes is possible to begin examining the impacts of future climate change on a regional scale. Future studies of vegetation change will need to make use of regional climate model outputs, which are currently too computationally expensive to run for the long time periods required for climate change studies. The

process of downscaling or regridding global climate model output to a finer resolution is therefore used to produce regional scale climate data to drive the SDGVM.

This chapter describes the possible change in vegetation distribution for Africa south of the Equator modelled by one DGVM (the Sheffield Dynamic Global Vegetation Model (SDGVM)), but based on sixteen different modelled future climates. The SDGVM includes both CO_2 effects and a disturbance generator that models the impact of fire regimes. The climate data used were from four General Circulation Models (GCMs), namely the HadCM3, the CCCMA CGCM2, the NCAR PCM and the ECHAM4/OPYC3. Two climate change scenarios from the new SRES societal development scenarios were available for each model and the data were regridded to a finer resolution (0.5° latitude by 0.5° longitude). The GCMs used and the climate change scenarios are described in Chapter 2.

Furthermore, in order to remove the inherent biases within the GCM outputs and to examine the importance of inter-annual variability in vegetation change, it was decided to use the anomalies to drive SDGVM. Two methods were used to calculate these anomalies, as described earlier in Chapter 4. Anomaly 1 assumes current observed inter-annual variability and Anomaly 2 assumes future modelled inter-annual variability. Table 8.1 describes each of the sixteen experiments and the abbreviations used to refer to each.

It is likely that increased atmospheric CO_2 concentration in the future experiments will favour C_3 plants over C_4 plants, due to CO_2 fertilisation effects (Ehleringer *et al*, 1997). In order to establish where the any increases in C_3 Grassland/Shrubland seen in these results is related to atmospheric CO_2, the anomaly 1 climates were used to drive SDGVM initialised with current CO_2 values. These runs therefore reflect the vegetation response to a change in climate only.

Table 8.1: An explanation of the experiment abbreviations.

ABBREVIATION	MODEL	SCENARIO	ANOMALY
CTL	Observed Climate Data		
CA2An1	CCCMa CGCM2	A2	1
CA2An2	CCCMa CGCM2	A2	2
CB2An1	CCCMa CGCM2	B2	1
CB2An2	CCCMa CGCM2	B2	2
EA2An1	ECHAM4/OPYC3	A2	1
EA2An2	ECHAM4/OPYC3	A2	2
EB2An1	ECHAM4/OPYC3	B2	1
EB2An2	ECHAM4/OPYC3	B2	2
HA2An1	HadCM3	A2	1
HA2An2	HadCM3	A2	2
HB2An1	HadCM3	B2	1
HB2An2	HadCM3	B2	2
NA2An1	NCAR PCM	A2	1
NA2An2	NCAR PCM	A2	2
NB2An1	NCAR PCM	B2	1
NB2An2	NCAR PCM	B2	2

8.2. The Modelled Climates

This section describes the changes in the three climate variables used by the Sheffield Dynamic Global Vegetation Model (SDGVM) to determine vegetation characteristics. These variables are relative humidity, precipitation and temperature. The changes described are the averages of thirty years of future model output in comparison to thirty years of current observed climate, for the months of December, January and February (DJF) and for June, July and August (JJA), which represent austral summer and winter respectively. The differences between the four general circulation models (GCMs) as well as between the two climate change scenarios (A2 and B2) and the two anomaly methods (An1 and An2) are discussed. The maps of these changes can be found in Appendix 8.1. An interesting result, which is common to all three of the climate variables, is that the similarities between the two scenarios are greater than the similarities between the two anomalies.

8.2.1. Humidity

The average monthly humidity graphs show that the perturbed climate (Figure 8.1a) monthly averages are similar to those shown by the control (CTL) climate, with high humidity in the summer months and low humidity in the winter. Two CCCMa climates, namely CA2An1 and CB2An1, show higher monthly average humidity values than the control climate for all months. The May and June humidity averages for these two future climates are also far higher than for any of the other future climates. The two ECHAM Anomaly 1 climates (EA2An1 and EB2An1) show lower humidity averages in the winter months than any of the other climates. This is also visible in the seasonal average for winter (Figure 8.1b), where the two lowest winter (JJA) humidity values are from these two model climates. Most of the models show lower winter humidity than the control climate, which represents current conditions. The exceptions are the two CCCMa Anomaly 1 climates (CA2An1 and CB2An1), which have higher winter humidity than the control climate. For the summer months, most of the model climates (10 out of the 16) show an increase in humidity in comparison to the control climate, although some of these increases are fairly small (e.g. EB2An1, which increase by 0.31%). Four of the other model climates show only minor decreases in humidity, but the HadCM3 Anomaly 2 climates (HA2An2 and HB2An2) both decrease by about 5%.

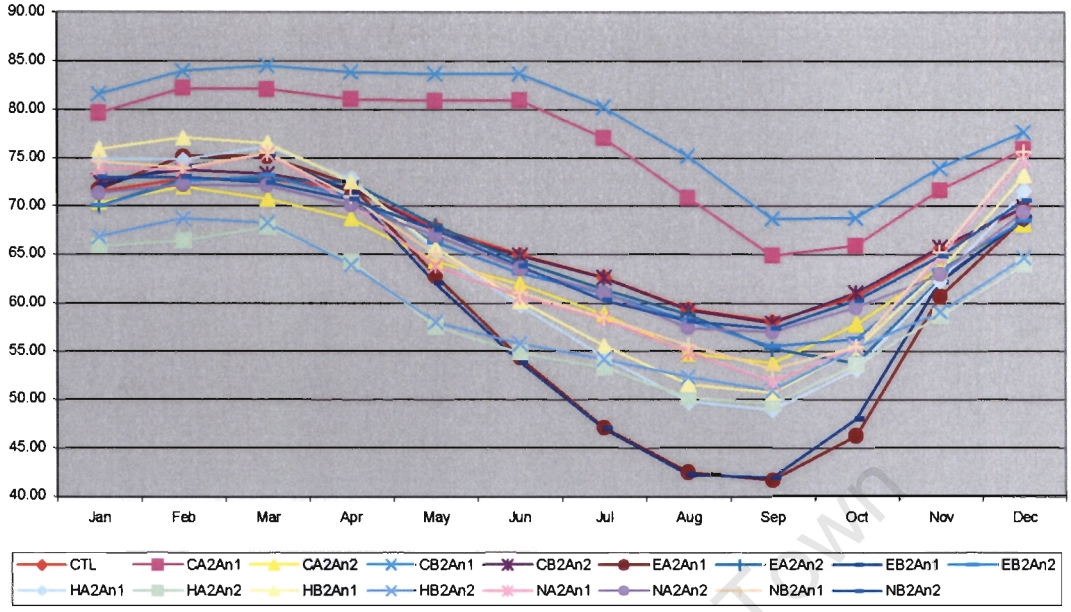

a)

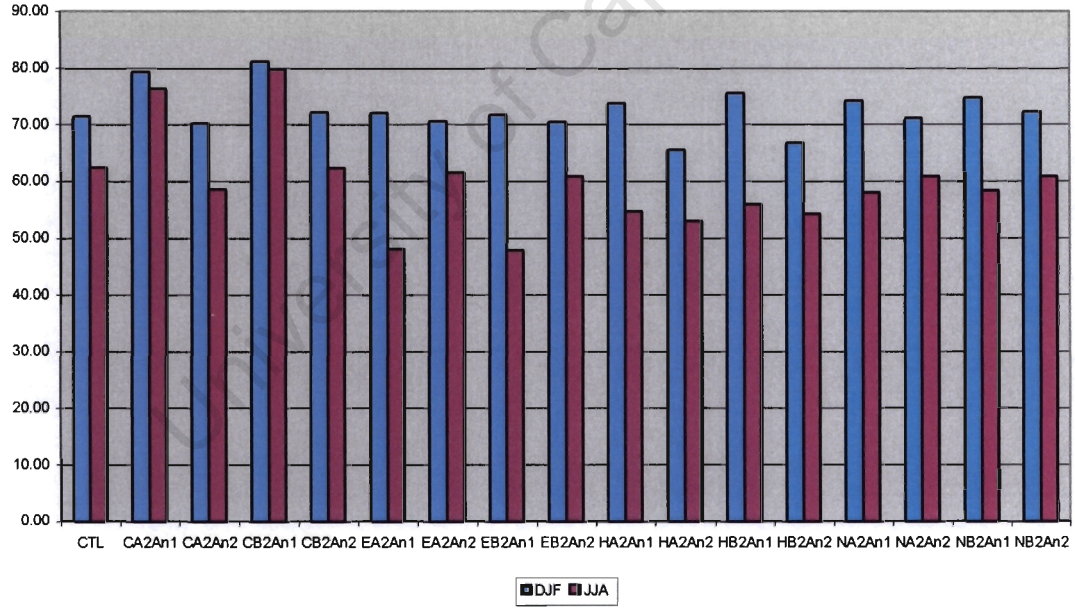

b)

Figure 8.1: The average humidity values for each of the perturbation climates. a) average monthly humidity values; and b) seasonal average humidity.

The spatial patterns of the humidity changes (see Appendix 8.1) show that there are more similarities between the A2 and B2 scenarios, than there are between the two anomalies. For all the models, the range of changes for Anomaly 1 is greater than the range of changes for Anomaly 2. For the CCCMa model, humidity decreases in the central area for all the anomalies and scenarios. Increases are found in the far northeast and the southeastern areas of the study region. The other climate models show greater variation in their results. The ECHAM model summer results display a west-east divide, with humidity decreasing in the western areas and increasing in the southern areas. The ECHAM model winter results generally show a decrease in humidity, with small areas of increased humidity in the south east (Anomaly 1 results), in the north west (EA2An2), as well as in the northeast and along the east coast (EB2An2). The NCAR model results show summertime increases in the south-west and along the west coast, and decreases over the central region for Anomaly 1. The NA2An2 results display increased humidity in the far north-east and north-west, and a general decrease in the southern regions. Humidity increases across Namibia and Botswana and decreases over the northern areas of the study region in the NB2An2 results. The NCAR winter results for Anomaly 2 show a decrease in the south-west and an increase in the north east of the study region. The Anomaly 1 results produce increases in the south and east, with decreases in the north-west.

8.2.2. Precipitation

The graph in Figure 8.2a clearly shows that the majority of the study region is a summer rainfall region, both at present and in the future. The maximum precipitation falls in December or January for most of the models, with June, July and August displaying the minimum values. The rainfall seasonality of the model climates is therefore very similar to that of the current climate. However, the analysis of an average of the entire study domain does exclude areas where the local climate may differ from the overall average, for example, the Western Cape area of South Africa, which is currently a winter rainfall region. The winter (JJA) maps in Appendix 8.1

reveal that 15 out of the 16 model climates show a decrease in winter rainfall over the south Western Cape area of South Africa.

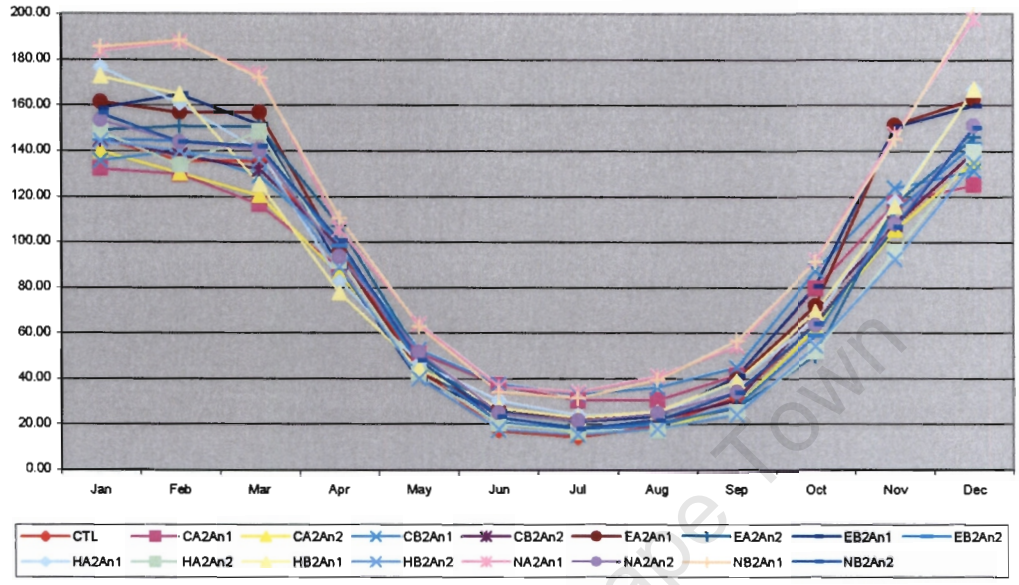

a)

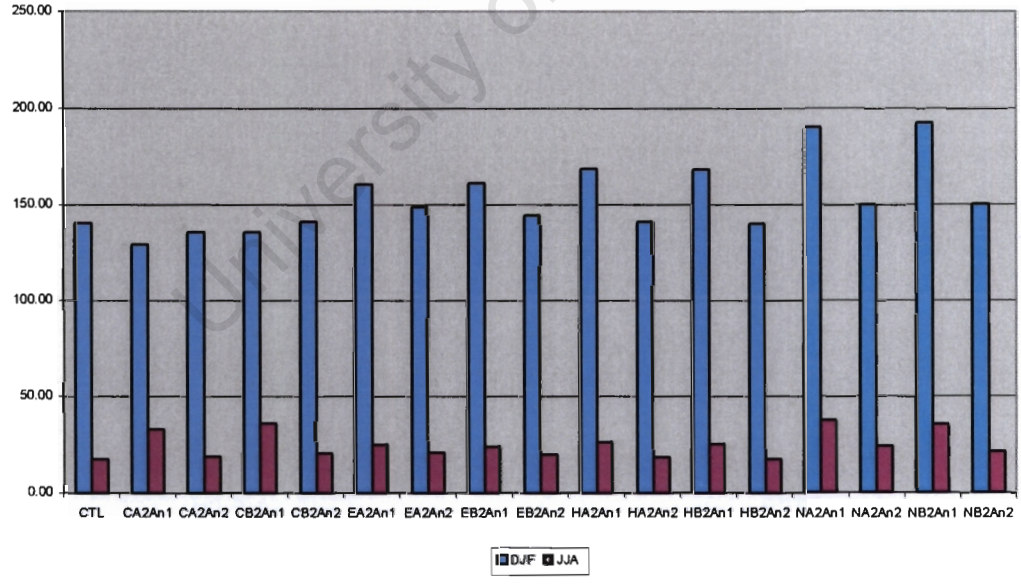

b)

Figure 8.2: The average precipitation values for each of the perturbation climates. a) average monthly precipitation values; and b) seasonal average precipitation.

The seasonal differences in precipitation are clearly obvious in Figure 8.2b, which shows the average precipitation for summer (DJF) and winter (JJA). For the summer months, the majority of the model climates show an increase in precipitation in comparison to the control climate. Only four of the model climates suggest a decrease in future summer precipitation, namely CA2An1, CA2An2, CB2An1 and HB2An2. However, the largest decrease is only 11mm/month for the CA2An1 climate. For the majority of the models, precipitation changes show an east-west divide for the summer months. Ten models show increases in the east and decreases in the west. Four models show the opposite pattern and two models do not show this east-west divide. For the winter months, all the models display an increase in average precipitation, although there is substantial variation in the amount of the increase. However, most of these winter increases occur over what are currently summer rainfall regions.

8.2.3. Temperature

The monthly average temperature graph (Figure 8.3a) clearly shows the seasonal changes, with October to March representing summer and April to September representing the cooler months. It is also apparent from this graph that the majority of the model climates predict an increase in temperature throughout the year, as the average temperature for each month is higher than the average for each month of the control climate. The only exception is NB2An1, which predicts warmer summers and cooler winters than are currently experienced. The two ECHAM Anomaly 1 model climates (EA2An1 and EB2An1) predict a shift in the seasons with shorter winters, and the highest temperatures will occur in October. The seasonal averages for the model climates are all warmer than the control climate, except for the NB2An1 winter temperature, which is slightly cooler than the current average (0.4°C). The highest summer increase is predicted by the EA2An1 climate (just over 4°C) and the lowest summer increase is just 0.2°C, for the NB2An1 climate. The

highest winter increase is also predicted by the EA2An1 climate (almost 8°C!) and the lowest winter increase is just 0.4°C, for the NA2An1 climate.

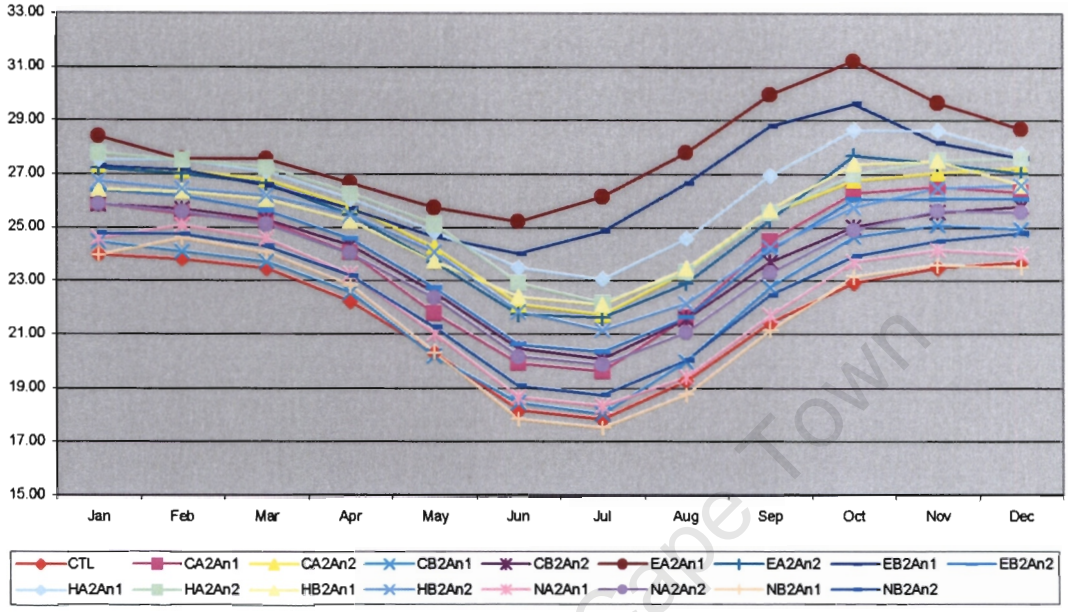

a)

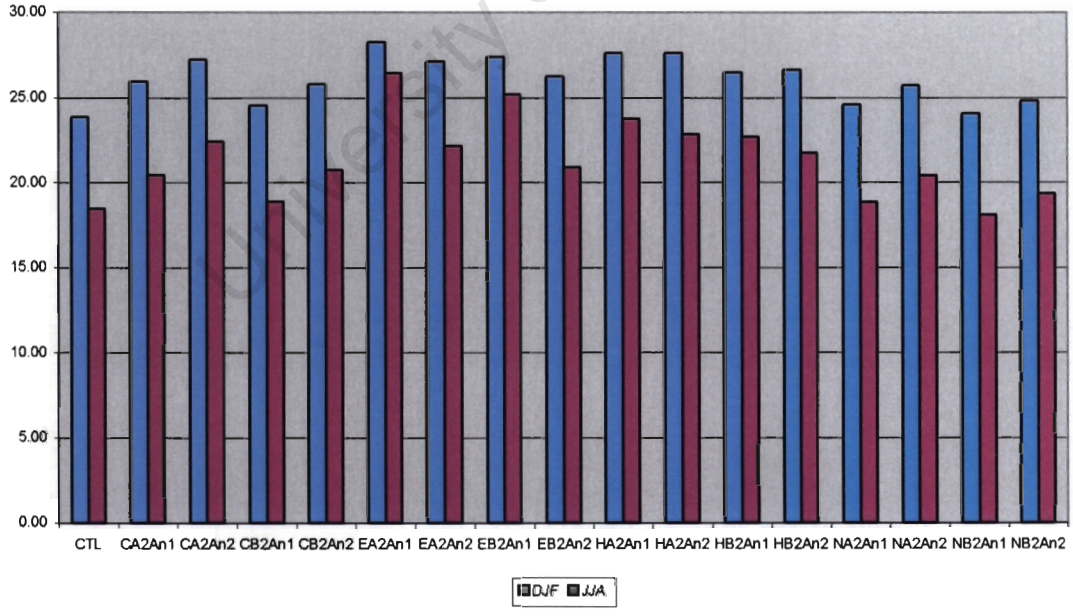

Figure 8.3: The average temperatures for each of the perturbation climates. a) average monthly temperature; and b) seasonal average temperature.

Nine models show a maximum change in temperature in the south and west, with lower temperature changes in the north-east for the summer months (Appendix 8.1). Four models do not show a distinct pattern, namely HA2An1, HB2An1 and NB2An1. The NCAR Anomaly 2 summer results show a maximum increases in the south and smaller changes in the north. For the winter, six Anomaly 2 models (CA2An2, CB2An2, EA2An2, EB2An2, HA2An2 and HB2An2) show maximum increases in the interior, with smaller changes along the coastline of the study region. The NCAR Anomaly 2 models show maximum increases in the south-west and minimum changes in the central eastern areas. The two CCCMa Anomaly 1 models show maximum temperature changes in the south east and north west, with minimum temperature changes in the north east. The ECHAM Anomaly 1 models have maximum increases in the central and western regions, with smaller changes in the north, east and southern regions. The HadCM3 Anomaly 1 models show a decrease in temperature in the south west, with increases over the rest of the region. The NCAR Anomaly 1 results show maximum temperature increases along the west coast, with smaller changes over the rest of the region.

A brief overview of the modelled climates showed that they are predicting a general increase in summer humidity and a decrease in winter humidity. The overall change in humidity is a decrease of between 0.5% and 7.6%. Precipitation is predicted to increase in summer and winter, with the maximum increase of about 38%. The IPCC (2001) predicts that globally, precipitation will increase, but there are large regional differences. East and west Africa will experience a small increase during the summer months, while southern Africa will experience a small decrease during the winter months. There are, however, inconsistent results from the predictions for this region. Temperatures will also increase, with greater increases in the winter months. The maximum average temperature increase is about 6ºC. Global average temperatures are predicted to increase by 1.4 to 5.8ºC over the period 1990 to 2100 (IPCC, 2001), making the average increase for southern Africa very similar to the

global average increase. The influence of climate on vegetation discussed above suggests that these changes will affect vegetation distribution over southern Africa. The results from SDGVM driven by these changed climates are presented below.

8.3. Vegetation Model Responses

8.3.1. Distribution of Cover Types

A series of maps can be found in Appendix 8.2, which show the distribution of the plant functional types for each of the SDGVM experiments. From these maps and the graphs in Figure 8.4 it is clear that vegetation change may be significant, and that atmospheric CO2 is an important moderator of change. The most striking change (in comparison to the control results) is the increase in C_3 Grassland/Shrubland under future atmospheric CO_2 concentration. The change occurs in all of the increased CO_2 model experiments and mainly results in the decline of C_4 Grassland across northern Namibia, Botswana, Zimbabwe northern South Africa, as well as south western Madagascar. This can most likely be attributed to the increase in CO_2, which favours the expansion of C_3 vegetation (Ehleringer *et al*, 1997; Collatz *et al*, 1998). However, many of the climate models show a decrease in humidity over this region, which may also affect the type of grassland, as C_4 Grassland prefers more humid conditions (Collatz *et al*, 1998). Another interesting result is that the Anomaly 2 results for all models show larger increases in C_3 Grassland/Shrubland than the Anomaly 1 results. This is particularly obvious in the NCAR results. This is possibly due to the lower humidity and precipitation values in the Anomaly 2 climates (see section 8.2), as C_4 plants require sufficient growing season precipitation to flourish (Collatz *et al*, 1998). Both the CCCMa anomalies show that the A2 scenario produces more C_3 Grassland/Shrubland than the B2 scenario. This pattern is also seen in the NCAR (both anomalies) and the ECHAM anomaly 2. For all the other experiments, the B2 scenarios show more C_3 Grassland/Shrubland than the A2 scenario. The ECHAM model shows the smallest changes in C_3 Grassland/Shrubland out of the four models.

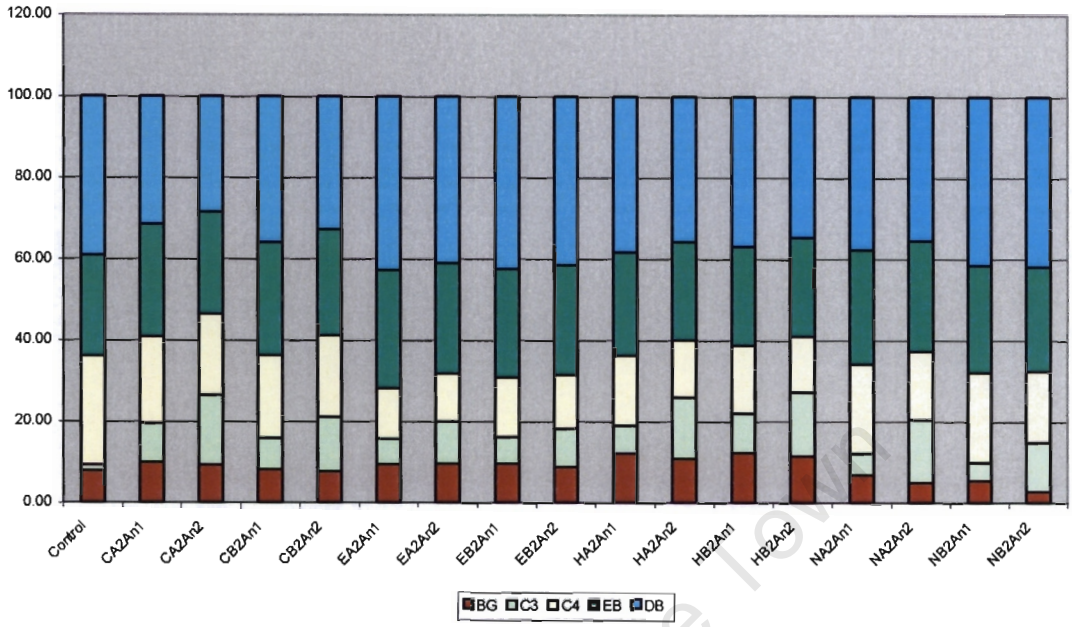

a)

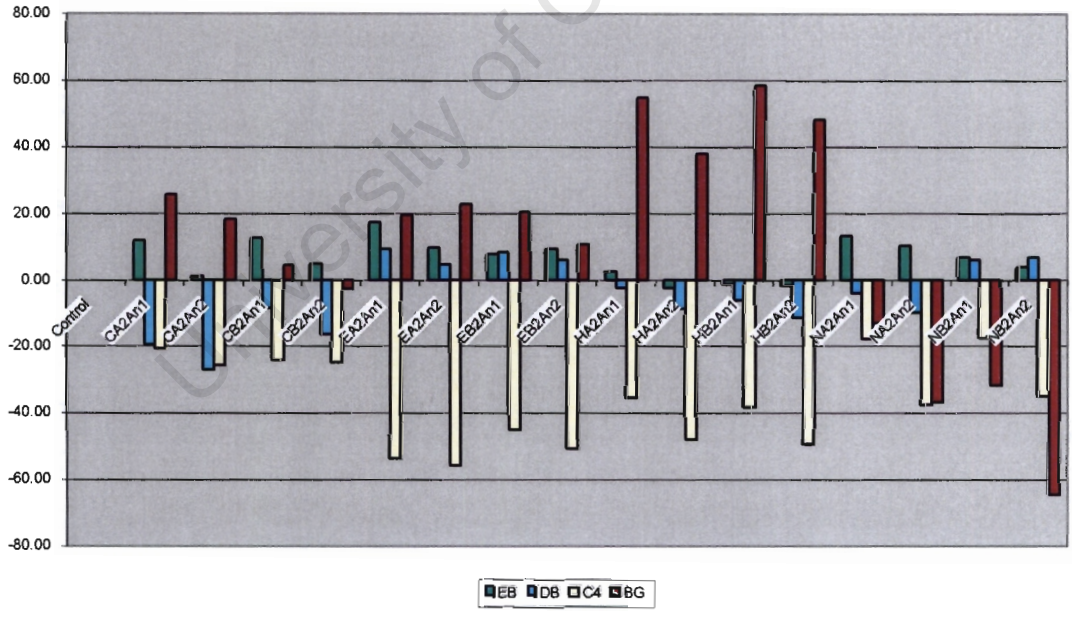

b)

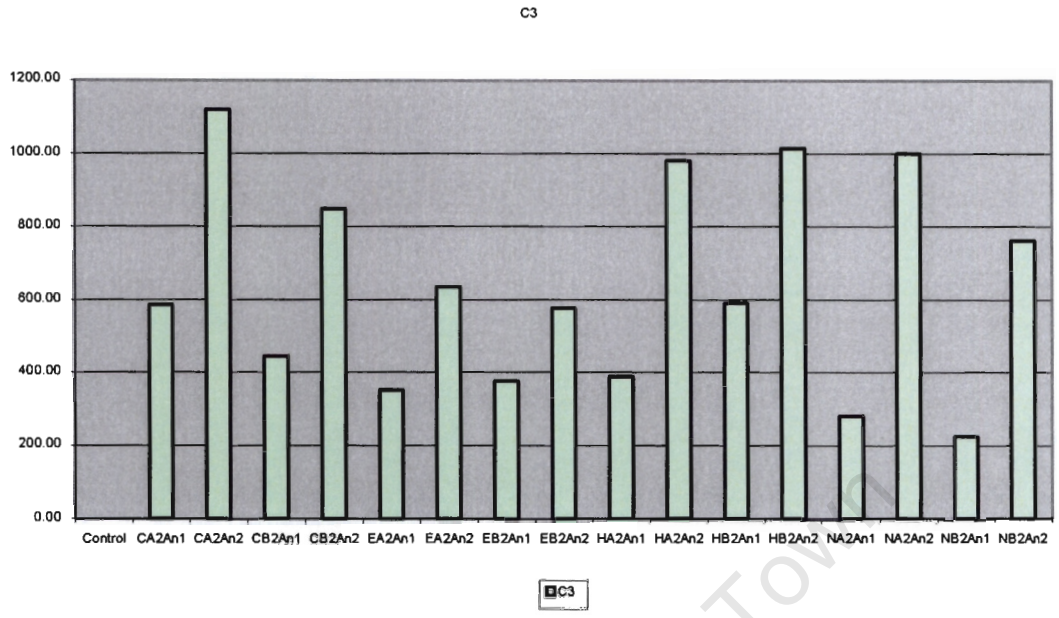

c)

Figure 8.4: Comparison of the dominance of plant functional types for each experiment. a) The percentage of sites dominated by each Plant Functional Type, averaged over the entire study region for each experiment. b) The percentage change in the plant functional types (excluding C3 Grassland/Shrubland) in comparison to the control run. c) The percentage change in the C3 Grassland/Shrubland plant functional types in comparison to the control run.

The result of these increases in C_3 Grassland/Shrubland is the contraction of C_4 Grassland for all the model experiments, as can clearly be seen in Figure 8.4b and the maps in Appendix 8.2. The ECHAM and HadCM3 models show the greatest decline in C_4 Grassland. This is not only due to the expansion of C_3 Grassland/Shrubland, but also due to expansion of Deciduous Broadleaf Forests in central Tanzania, Zimbabwe, southern Mozambique and north eastern South Africa. As for the C_3 Grassland/Shrubland, the Anomaly 1 results show smaller changes than the Anomaly 2 results. The A2 scenario shows greater changes than the B2 scenario for the CCCMa Anomaly 2, both the ECHAM anomalies, and the NCAR anomalies. The B2 scenario changes are greater for all the other experiments. The

increase in CO_2 appears to be more important in these experiments than the temperature increase in controlling the relative dominance of C_3 or C_4 vegetation. The increase in C_3 vegetation confirms the encroachment of woody vegetation into grasslands, as suggested by Bond and Midgley (2000) and Bond *et al* (2003a).

The majority of the experiments show an increase in Bare Ground, with the HadCM3 model showing the greatest increases. Most of this expansion occurs in southern Namibia, but there is also some expansion of Bare Ground in the south and south-west Cape region of South Africa. The four NCAR experiments and the CCCMa B2 anomaly 2 experiment show a decrease in Bare Ground. The NCAR results are quite striking as they show that the Namib Desert declining drastically, and the remaining Bare Ground is largely located in the Karoo region of South Africa and southern Namibia. This is particularly true for the NB2An2 experiment. Both C_4 Grassland and C_3 Grassland/Shrubland mainly replace the Bare Ground. For the HadCM3 model, the anomaly 1 results show greater changes than the anomaly 2 results, but this pattern is reversed for the NCAR model. The CCCMa and ECHAM model do not show a pattern between the anomalies. The majority of the experiments show that the A2 scenario produces more Bare Ground than the B2 scenario, with three exceptions, namely the CCCMa Anomaly 1 and 2, and the ECHAM Anomaly 2 experiments. The affect of CO_2 and climate changes does not show a consistent direction of change in arid shrubland change. The differences between the GCM modelled climates appears to be the dominant signal and causes uncertainties in the prediction of arid shrubland distribution.

In addition, the results for the Deciduous Broadleaf Forests are also rather mixed. All the CCCMa and HadCM3 model experiments show a decrease in Deciduous Broadleaf Forests, the ECHAM model shows an increased and the NCAR model shows both. The decreases in Deciduous Broadleaf Forests mainly occur along the southern border between Deciduous Broadleaf Forests and C_4 Grasslands in Zimbabwe. The increases in Deciduous Broadleaf Forests are found mainly in

central Tanzania and the northern areas of South Africa. The inconsistencies in these results again suggest that there are uncertainties in the predictions of C_4 Grasslands and Deciduous Broadleaf tree dominance in the savannah regions.

With respect to vegetation in regions of higher moisture, there is strong and consistent evidence that the Knysna Forest, which is currently the only remaining indigenous evergreen forest in South Africa, will switch in dominance from evergreen- to deciduous trees. Out of the sixteen model experiments, only two show that the whole southern Cape forest remains evergreen, while 10 of the model experiments suggest that over 50% of the forest will become deciduous. The A2 scenario results for the NCAR model show a decrease while the B2 scenario produces an increase. The actual change is greater for the A2 scenario than the B2 scenario in the anomaly 1 results, but the B2 scenario change is greater for the anomaly 2 results. The A2 scenarios for the CCCMa model and the ECHAM anomaly 1 results show a greater change than the B2 scenario. All the other results show a greater change in the B2 scenario and a smaller change in the A2 scenario. For all the models, apart from the ECHAM model, the anomaly 1 results show a greater change as opposed to the anomaly 2 results.

Most of the results show an increase in Evergreen Broadleaf Forests, apart from HA2An2, HB2An1 and HB2An2. These increases mainly occur along the southern borders of the rainforest in northern Angola, the Democratic Republic of Congo and eastern Tanzania. The decreases seen in the HadCM3 model results occur in northern Angola and the Democratic Republic of Congo, where the Evergreen Broadleaf Forests are replaced by a combination of C_3 Grassland/Shrubland and C_4 Grassland. A comparison between the scenarios shows a greater increase in Evergreen Broadleaf Forests in the A2 scenario than in the B2 scenario for the CCCMa model. For all the other models, the B2 scenario shows a greater increase than the A2 scenario. In the HadCM3 anomaly 1 results, the A2 scenario is positive, but the B2 scenario shows a decrease in Evergreen Broadleaf Forests, however, the

overall change is higher for the A2 scenario. The inter-anomaly comparison reveals that in the majority of experiments, the anomaly 1 results showed a greater change than the anomaly 2 results. The exceptions are the ECHAM and HadCM3 B2 scenarios, where the anomaly 1 results are lower than the anomaly 2 results.

Figure 8.5 shows the distribution of plant functional types that are congruent between the control run and all the GCM experiments. The areas where all the GCM experiments results agree with the control run results reflect areas where there is no predicted change in vegetation. The areas shaded in red show where there is no agreement and accounts for approximately 57% of the study region. The figure shows that the major areas of disagreement are the areas of transition between the forest plant functional types, and most of the grassland areas in the south. This maps suggests substantial and significant changes in the distribution of major vegetation types over southern Africa during the course of this century.

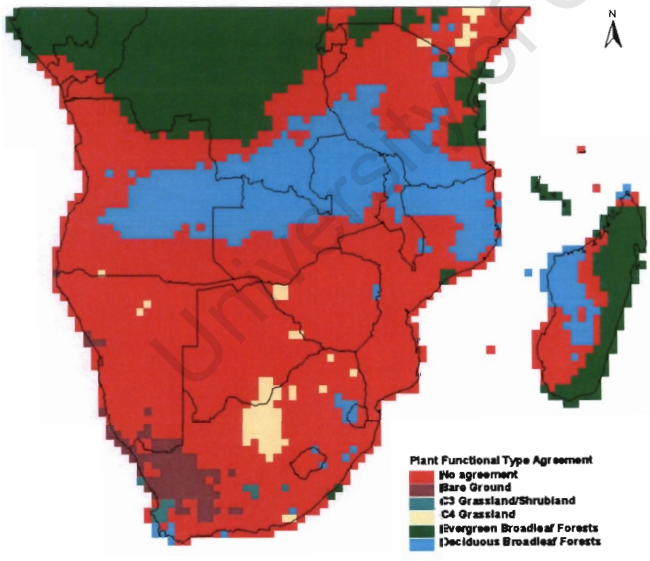

Figure 8.5: The distribution of areas where the control and GCM experiments agree on the dominant plant functional type.

8.3.2. The CO_2 Experiment

The graphs in Figure 8.6 show the percentage of sites dominated by each PFT for the control run, as well as the current and future CO_2 runs. The climate change only experiments (C) all show a drastic reduction in the occurrence of C_3 Grassland/Shrublands, but the climate change runs with future CO_2 values (F) all show large increases in the occurrence of C_3 Grassland/Shrublands. The Deciduous Broadleaf Forests also respond to increased CO_2 and therefore show higher percentages under the future CO_2 experiments than under the current CO_2 experiments. The C_4 Grasslands, on the other hand, increase under climate change with current CO_2 conditions, but decrease under the future, higher CO_2 concentrations.

These results are also reflected in the spatial distribution of the vegetation change (Appendix 8.3). In contrast to the future CO_2 experiments, the current CO_2 experiments do not show the expansion of C_3 Grassland/Shrubland into the central regions. These maps show a southerly expansion of the Evergreen Broadleaf Forests, as well as expansion of the C_4 Grassland and in some cases, the Bare Ground or desert areas expand.

The climate change only (without the CO_2 change) results confirm the importance of the CO_2 fertilisation effect on C_3 vegetation. There is also evidence that climate change and not CO_2 change will favour Evergreen Broadleaf Forests, as this PFT expands with and without CO_2 change. The instability of the co-dominated C_4 grassland and Deciduous Broadleaf tree savannahs is confirmed, as the dominant PFT shifts both with and without CO_2 change.

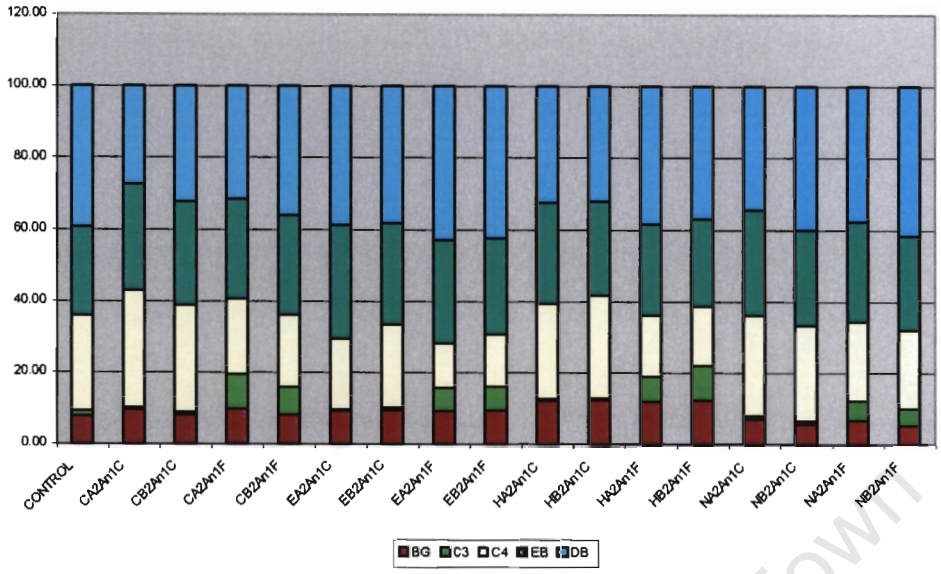

a)

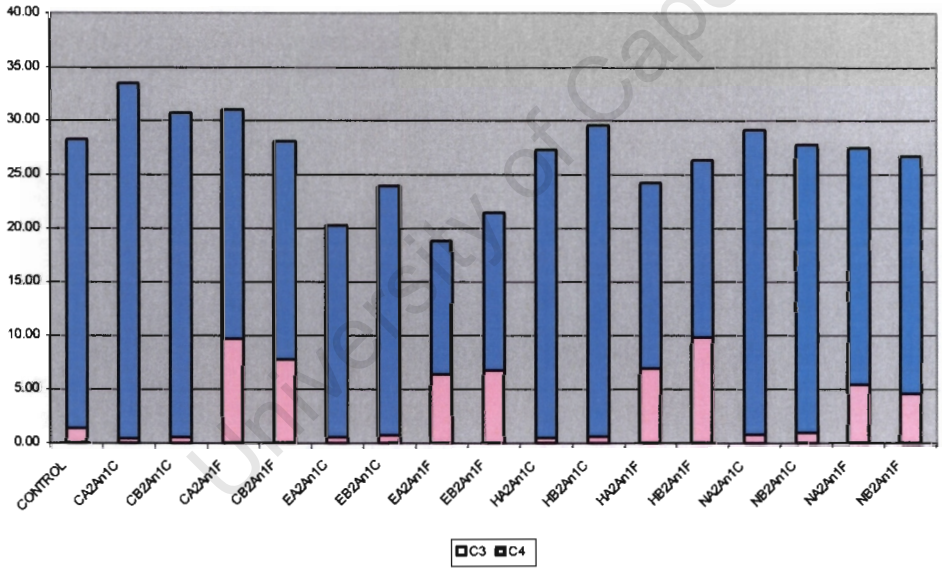

b)

Figure 8.6: The dominance of the plant functional types for the current and future CO_2 experiments. The letters C and F at the end of the experiment names represent current and future CO_2 values, respectively. a) The percentage of sites dominated by each Plant Functional Type. b) The percentage of sites dominated by the C_3 Grassland/Shrubland and the C_4 Grassland Plant Functional Types.

8.3.3. Leaf Area Index and Net Primary Productivity

Leaf Area Index (LAI) and Net Primary Productivity (NPP) are key parameters in modelling of land surface energy exchanges with the atmosphere (Betts *et al*, 1997; Scurlock *et al*, 2001). NPP is defined as the net amount of carbon captured by land plants (Melillo *et al*, 1993). LAI is a dimensionless number that specifies the area of leaf per area of vegetation (Lomas *et al*, 2001), and is particularly useful in calculating evapo-transpiration rates and radiation dispersal within a canopy (Jones, 1992).

The graph in Figure 8.7 shows the average LAI and NPP for each of the experiments, including the control. The graph shows that the current CO_2 and the control experiments have lower LAIs than the future CO_2 experiments. The current CO_2 experiments all have LAIs below 5.8 and all the future CO_2 experiments have an average LAI over 6. The HadCM3 results show the smallest increase in LAI, with the NCAR model showing the greatest increase.

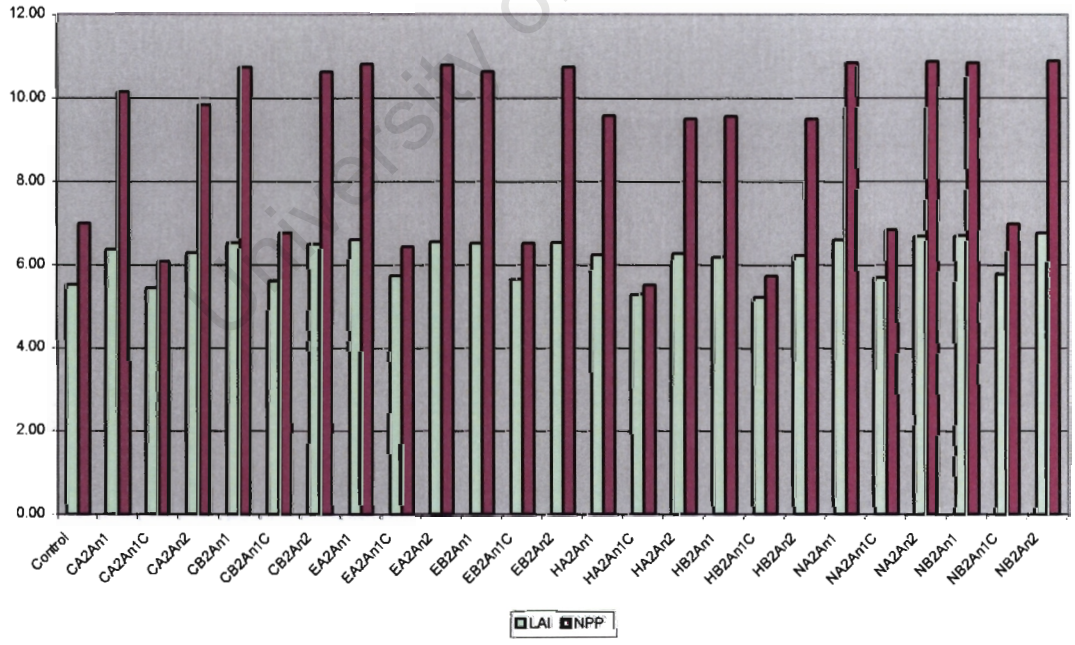

Figure 8.7: The average LAI and NPP for each of the experiments.

The Net Primary Productivity (NPP) shows a much greater response than the LAI. The control and current CO_2 NPP values are just under 7 tons/hectare (or 698 gm^{-2} for the control run), while the lowest model experiment NPP is 9.49 tons/hectare (949 gm^{-2}) for the HB2An2 experiment. This reflects the increase in productivity suggested by the increased LAI. The HadCM3 model again shows the smallest increases in NPP, with the NCAR model showing the greatest increases. Figure 8.8 shows the difference in NPP between the current and the future CO_2 experiments for these two models. These maps show that NPP increases under future CO_2 conditions across almost the entire study region, except for southern Namibia and the north-western areas of South Africa. There is an increase in productivity in the central regions of the study area, which is significant as this area has low productivity, so any change will be large, and this corresponds to the areas where the C_3 Grassland/Shrublands were predicted to increase under future CO_2 conditions.

The increased productivity of vegetation under future climate and CO_2 conditions will have an impact on the carbon cycle, which will affect the feedback mechanisms between the land surface and the atmosphere. Furthermore, the increase in LAI predicted for future conditions will affect evapotranspiration calculations and surface albedo. These results reinforce the necessity of including dynamic vegetation into modelling studies of future climate change.

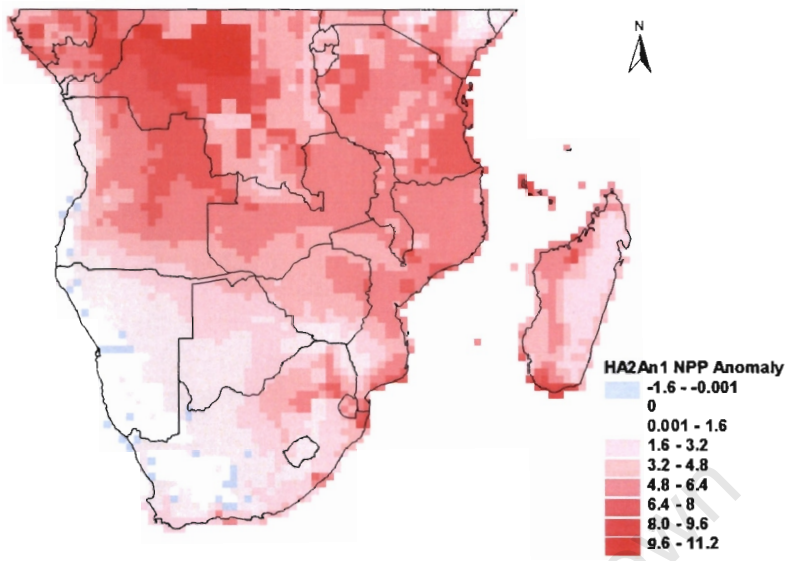

a)

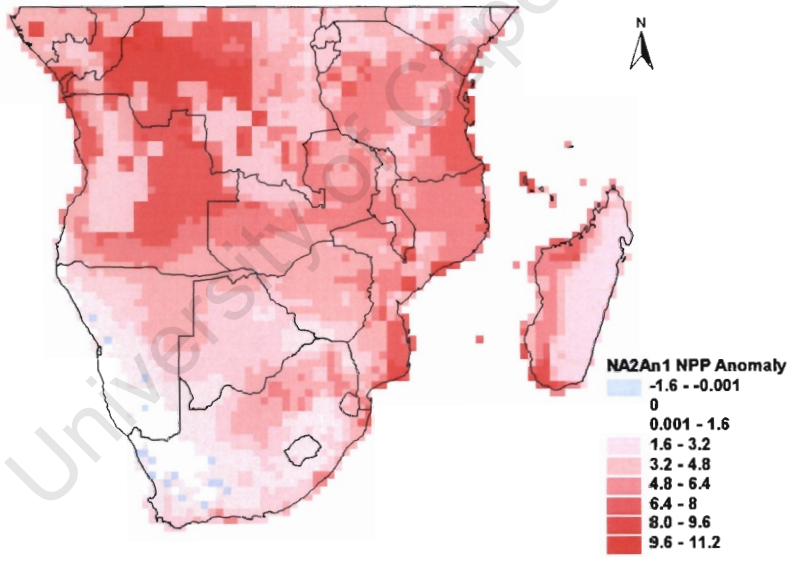

b)

Figure 8.8: The difference between NPP modelled with future CO_2 concentrations and NPP modelled with current CO_2 concentrations driven by a) the HA2An1 climate; and b) the NA2An1 climate.

8.4. Conclusions

The results from the modelled future climate experiments presented here show the range of possible future vegetation changes in response to both climate change and CO_2 change, and to climate change only. The most striking change seen is the expansion of C_3 Grassland/Shrubland under future CO_2 concentrations and climate across eastern Namibia, Botswana and Zimbabwe, at the expense of C_4 Grassland. The comparison with the climate change only experiments shows that this must be mostly due to the increase in carbon dioxide that will occur by the late twenty-first century. Savannahs are inherently unstable systems (Frost, 1996) and are therefore able to respond dynamically to changes in climate, changes in CO_2, and to the combination of these changes. The increase in C_3 Grassland/Shrubland suggests the encroachment of woody vegetation into grasslands. However, this does not take into account any changes in fire regimes, which will most certainly occur under future climate conditions. This region is where the great savannahs of Africa is found, so a change in the vegetation type may have serious implications for the savannah ecosystem and those that depend on it for survival, such as the wildlife and the growing tourism industry. Furthermore, the change to a climate that favours the C_3 photosynthetic pathway has implications for agriculture, as many of the crops currently grown in this region follow the C_4 photosynthesis pathway.

As most tree species also follow the C_3 photosynthetic pathway, increased carbon dioxide favours the rainforests in the north of the study region. This is seen in the expansion of the Evergreen Broadleaf Forests southwards, as well as the increase in Net Primary Productivity and Leaf Area Index that is seen in all the future CO_2 model experiments. However, the Evergreen Broadleaf Forests in the south, which make up the indigenous Knysna forest, do not fare as well. There is strong evidence that this region will not be able to support evergreen forests in the future, and the forest will become deciduous. This would be a great loss to South Africa, as this is the last remaining area of natural indigenous forest left in South Africa.

The changes in Bare Ground for the future CO_2 model experiments are not consistent. The four NCAR model results suggest a decline in Bare Ground or desert areas, particularly in Namibia. The other results all suggest a possible eastward expansion of the desert in southern Namibia, as well as an expansion of the semi-desert Karoo area eastwards and possibly southwards. The areas east of the Karoo are currently some of the most fertile areas of South Africa, producing crops such as maize. This eastward expansion of the semi-desert will result in a change, most likely to sheep farming, which is the dominant agricultural activity in the Karoo. The southern expansion of the Karoo will have implications for the Fynbos regions of the south western Cape. The Fynbos region is one of the most species rich regions in the world, and represents a plant kingdom on it own. Along with the Knysna forest, this is a region of natural beauty, which needs to be preserved. However, the uncertainty in the direction of change does create difficulties in planning for the conservation of these areas.

Although the Sheffield Dynamic Global Vegetation Model (SDGVM) predicts only potential natural vegetation, the results here can be used to infer changes to the actual vegetation that occurs in a region. The areas of southern Africa where vegetation changes are most likely to occur have been highlighted with the regions of possible change covering more than half the study area. This has implications for agriculture and other economic activities in the region. Furthermore, such a large scale change in vegetation is bound to have an influence on the climate of the future, and thereby produces more feedbacks in the atmosphere-biosphere cycle. As there are currently no climate change predictions available that include a dynamic vegetation component, which can feedback to the atmosphere, the current suite of climate change predictions should alter when dynamic vegetation is finally incorporated into climate change predictions.

SECTION 5:

FINAL OUTCOMES

CHAPTER 9: DISCUSSION AND CONCLUSIONS

9.1. Summary of Important Results

There are a growing number climate change studies that have shown the importance of vegetation feedbacks to climate at sub-continental scales, many of which have been discussed throughout this thesis. These emphasise the need for coupled atmosphere-biosphere systems models, and a few experimental coupled systems have now been tested, and more are under development. There is also a growing recognition that regional scale predictions are needed for climate change impact studies. In order to obtain reliable predictions of future climate change at a regional scale, regional climate models will need to incorporate dynamic vegetation components, which allow vegetation to respond to the climate changes, and to feedback to the atmosphere. The results that have been presented here are an initial step towards coupling a Dynamic Global Vegetation Model (the Sheffield Dynamic Global Vegetation Model or SDGVM) with the MM5 regional climate model. The most significant results shown by these modelling studies are summarised below.

9.1.1. Climate Model Sensitivity Experiments

The sensitivity of the MM5 regional climate model to its vegetation parameters was tested by increasing surface roughness length and albedo by 20% each. These would represent significant changes in vegetation structure and cover for well-vegetated regions of higher rainfall, with an increase in roughness length of 20% equivalent to the difference between grassland and shrubland, and albedo changes representing large changes in cover. Vegetation responses to predicted climate change easily fall within this range of land surface transformation, for example, the increase in atmospheric CO_2 concentration expected by 2070 results in the expansion of woody shrubland into grasslands in southern Africa, as modelled by SDGVM. However, a 20% change in roughness length is small if the unperturbed

roughness length is small as is the case for areas of low rainfall with low vegetation cover.

The results from the roughness length run did not reveal a clear signal that could be directly related to the roughness length manipulation, suggesting either that the MM5 model is not overly sensitive to a 20% change in roughness length, or that unperturbed roughness length was small enough over a large enough area to render the manipulation insignificant. Therefore, a larger roughness length perturbation, or an absolute change (as opposed to a relative change), may result in more significant climate responses, but in the context of this initial experiment, no further analysis has been undertaken. Furthermore, as the results indicate, the albedo appears to be the more dominant factor of the two, and is therefore focused on in this study. The albedo increase simulation caused significant meso-climatic responses, including the reduced transport of moisture into the interior of the sub-continent, reducing clouds, and increasing incoming short-wave radiation, which contributed towards increased temperatures over the interior of the subcontinent. Although the applied change was an unlikely uniform increase in albedo across the country, it reflects the sensitivity of the MM5 model to albedo and feedbacks from the land surface, which may result from changing land surface cover characteristics. These are not only predicted to occur with climate change, but also accompany intensive and extensive land use practices such as the conversion of rainforests and other natural ecosystem to agriculture, which occurs frequently in Africa. Such future changes in vegetation are likely to result in a less uniform albedo change, and it is therefore essential that more realistic simulations be carried out, based on future predicted vegetation distribution.

9.1.2. Vegetation Model Sensitivity Experiments

The SDGVM results were compared to several datasets of vegetation distribution for Africa. Overall, there was good agreement between the datasets and the SDGVM output, but two areas of disagreement occurred. Firstly, the SDGVM results did not

show transitional or mixed vegetation types (or biomes), which are commonly defined by published datasets. An attempt was made to rectify this by reclassifying the SDGVM output to reflect the mixed biomes. This improved the comparison between SDGVM and the datasets, but several areas of non-correspondence remained. These areas tended to be found in regions heavily altered by human influences, which are not modelled by SDGVM (such as Madagascar). SDGVM predicts only potential natural vegetation, and will therefore not agree with published datasets that include anthropogenically altered land surfaces.

SDGVM also proved to be sensitive to changes in climate inputs. The modelled C3 Grassland/Shrubland plant functional type (PFT) was particularly sensitive to increasing temperatures and is predicted to decrease under such conditions, which is in line with other studies (e.g. Ehleringer *et al*, 1997; Collatz *et al*, 1998). Increased precipitation favoured the growth of trees, while decreasing precipitation generally resulted in the expansion of C4 Grassland and Bare Ground (apparent desertification) at the expense of C3 Grassland/Shrubland and Deciduous Broadleaf Forests.

The fire escape age sensitivity studies showed the importance of fire and tree regrowth rates in determining the composition of savannah vegetation, as has been suggested by several authors (Scholes, 1997; Bond and Midgley, 2000; Heisler *et al*, 2003; Bond *et al*, 2003a, 2003b). Increasing (decreasing) the fire escape age allows for the expansion of C4 Grasslands (Deciduous Broadleaf Trees). These two vegetation types co-exist in savannah, which has long been suggested to be an inherently unstable system controlled by factors such as fire and herbivory (Scholes, 1997). The SDGVM simulations reveal the possible root cause of that instability.

It was not possible in the scope of this study to explore fully the factorial interactions between fire regime, rainfall and temperature changes, which may develop as

climate change plays itself out over the subcontinent – this will be an interesting and useful future development of this modelling approach.

9.1.3. Vegetation under Possible Future Climates

Inputs from several possible future climate scenarios, generated by a range of GCM's, were used to drive SDGVM, with current and future CO_2 concentrations. A comparison between the current and future CO_2 driven experiments revealed a strong CO_2 fertilisation effect resulting in the increase in C3 Grassland/Shrublands at the expense of C4 Grasslands. This seems to represent a woody shrub encroachment into the savannahs of central southern Africa. The encroachment of some regions by shrubs such as *Lycium* species has indeed been recorded in certain areas (Midgley, *pers. comm.*). Although a change in fire escape years (i.e. tree growth rate) was not simulated, recent studies suggest that the expansion of shrubs into savannah may be strongly influence by CO_2 fertilisation allowing trees and shrubs to escape from fire at a younger age (Bond and Midgley, 2000; Bond *et al*, 2003a).

These experiments show the range of possible future vegetation changes, and therefore examine, to a degree, the uncertainty in future vegetation changes. The results in chapter seven and a number of other studies (e.g. Cramer *et al*, 2001; Woodward *et al*, 2001) give an indication of the sensitivity of SDGVM to a select few of its parameters. Furthermore, Woodward and Lomas (2004) outline some of the many assumptions and uncertainties in the SDGVM. It is not possible to fully examine all the uncertainties associated with the vegetation model, and its underlying assumptions and parameter uncertainty, within the scope of this thesis. Despite this, various studies (e.g. Woodward and Lomas, 2004) have shown that the model can simulate contemporary processes and vegetation properties with reasonable accuracy.

9.2. Important Considerations

To date, none of the climate change scenarios from the IPCC include a dynamic vegetation component, although there is recognition of the need for improved vegetation characterisation in GCMs (IPCC, 2001). However, there are many difficulties inherent in coupling atmospheric and vegetation models at regional scales. Most of the current dynamic vegetation models are designed to run on a global scale (hence the name Dynamic Global Vegetation Models or DGVMs). An even greater problem is the difference in time scales between regional climate models and vegetation models. A vegetation model, such as SDGVM, may take hundreds of years to reach an initial equilibrium state and needs a minimum of 20 years of climate data as input. Most of the vegetation processes modelled by SDGVM currently run on a monthly scale and the model produces annual averages as its output. However, a regional model, such as MM5, will only take approximately one month to spin-up (with prescribed boundary conditions) and outputs data every six hours. Due to the vast number of processes included in MM5 it is computationally expensive, and to produce the 20 years of data required to initialise SDGVM would take several months of continuous computing power.

Despite these difficulties, scientists are progressing with fully coupled dynamic vegetation-atmosphere modelling studies (e.g. Cox *et al*, 2000). The study described here has examined the likely impacts of climate change on vegetation and its feedbacks to the atmosphere for southern Africa, and is a first step towards coupling a DGVM with a regional climate model for southern Africa. The selected DGVM (the Sheffield Dynamic Global Vegetation Model or SDGVM) has been validated for the region, and its sensitivities to temperature, precipitation and CO_2, as well as to climate change scenarios have been tested. An initial test of the regional model's sensitivity to its vegetation parameters has been undertaken, and has proved to be an important consideration. Currently, experiments are underway to examine the sensitivity of the regional model (the MM5) to changes in other vegetation parameters, and also to a change in vegetation distribution (Hewitson,

pers. comm.). Once the sensitivity and validity of the MM5 model have been proved, it should be possible to couple the MM5 with the SDGVM.

The modelling approach has provided a set of possible future vegetation distributions, and has also emphasised the importance of role of carbon dioxide in determining vegetation structure over southern Africa. Future vegetation change predictions can only be made with a model, and by testing the SDGVM extensively prior to making such predictions, we have increased the confidence level of the predictions. It is not possible to observe the effect of carbon dioxide in field experiments over large areas, due to the impracticalities of increasing carbon dioxide over regions. Most studies of the effects of carbon dioxide are therefore either accomplished within a small, controlled environment, or with the use of models. The use of the vegetation model has therefore shown the importance of carbon dioxide in the invasion of grasslands by woody shrubs over a region that is too large for field studies.

The vegetation changes predicted under future climate in Chapter 8, and the response of the MM5 regional model to even a small change in only one vegetation parameter, suggest that vegetation-atmosphere feedbacks and the changes in those feedbacks may significantly affect future climate predictions. Given that current climate change predictions do not include vegetation changes and dynamic feedbacks, policy makers should remember that climate change predictions might change with continued research and development of climate change models. Policy makers and other users of climate change predictions should therefore continually review their decisions based on the most up-to-date predictions available. Furthermore, institutions involved in creating climate change predictions, such as the IPCC, should ensure that future research incorporates dynamic vegetation feedbacks into climate change predictions.

9.3. Caveats

The study of vegetation-atmosphere interactions is by its very nature a complex issue. Some of the important issues that have not been fully explored in this study, mainly due to these complexities and due to time constraints include:

Soil moisture: There has been no attempt made to quantify the direct effects of changing soil moisture on vegetation in this study, except where SDGVM itself simulates soil moisture change as an emerging component of climate change. Soil moisture represents the water storage that is essential for vegetation survival, and also interacts with the atmosphere through evaporation. It is essential that future studies examine the role of soil moisture in land surface – atmosphere interactions over southern Africa.

Soil depth: In addition to the inadequacies mentioned above, the soil depth used within SDGVM is globally uniform. Clearly this inadequacy may influence the vegetation type modelled, particularly where soil depth is especially deep or shallow. Although this issue has been discussed as a possible future development to SDGVM (Lomas, *pers. comm.*), it has as yet not been addressed. Therefore, a programme of future experiments examining vegetation response to climate change should attempt to address both the issues of soil moisture and soil depth.

The atmosphere: Although this has been a study of vegetation-atmosphere interactions, there has been very little study of how the atmosphere responds to changing vegetation, and this should be a priority for future studies.

The SDGVM has been shown to be able simulate the vegetation over southern Africa under current and future climates. However, several inadequacies of the model have been highlighted. Firstly, the model predicts only the potential natural vegetation that could occur under the prescribed climate conditions, and therefore does not take into account any human land use changes. Attempts are underway to include the use of satellite imagery, which will be used to prescribe anthropogenic surfaces (Lomas, *pers. comm.*), but this will still not consider future changes in human land use patterns. Secondly, the temporal scale of SDGVM currently

provides only annual average output, and this will need to be improved if it is going to be coupled with MM5, which runs at a much finer temporal scale. A new daily version of the SDGVM is currently under construction (Lomas, *pers. comm.*), but this version will still need to be extensively tested before it can be coupled with the MM5 regional climate model. SDGVM does not model the performance of plants with the CAM photosynthesis pathway, which is used by plants in arid environments. Although this does mean that many areas classified as bare ground by SDGVM do in fact have some plant life, vegetation within the arid areas is sparse and should therefore be of secondary importance in terms of feedback mechanisms to the atmosphere. SDGVM does also not distinguish between grasses and shrubs in C3 Grassland/Shrubland PFT, due to the complexities involved in defining shrubs. However, SDGVM does still manage to predict vegetation distribution and characteristics over southern Africa with acceptable fidelity, as long as interpretation of the meaning of the C3 category is broad enough.

9.4. Implications and Future Research

The suggestion by Charney *et al* (1975, 1977) that increasing albedo and the resulting decrease in precipitation becomes a cyclical process has some importance for southern Africa, in light of the results presented here. The increase in albedo over southern Africa simulated in chapter 5 also resulted in decreased rainfall, as predicted by Charney *et al* (1975) for the Sahel. There is therefore the implication that should albedo increase over southern Africa, the cyclical process could be started over this region. Most (11 out of 16) of the simulations of future vegetation based on the GCM output and future CO_2 concentrations showed an increase in Bare Ground over Namibia and central South Africa. This change would result in an albedo increase over these regions. Should this change in albedo result in decreased precipitation for the region, this will exacerbate the need for adequate planning of future water resource management.

The predictions of future vegetation change suggest that changing CO_2 concentrations is a dominant factor in controlling vegetation change. This will affect the carbon cycle. The results suggest that southern African vegetation will be more productive, and should therefore fix more carbon. This has implications for the implementation of the Kyoto Protocol and carbon accounting procedures. However, should anthropogenic land use changes result in a land surface that is dramatically different from the potential natural vegetation, the existence of a carbon sink in the region could be threatened.

The predicted changes in vegetation are significant, even when considered apart from the context of vegetation-climate interactions (Cowling *et al*, 1997). The diversified nature of southern African vegetation and the high species endemism that are characteristic of the region also mean that the vegetation is highly susceptible to localised extinctions (Thomas *et al,* 2004). Impacts at species level are not at all simulated by SDGVM, and are unlikely to be realistically simulated by such a mechanistic model. Additional modelling methods that quantify species responses are therefore important as an adjunct to SDGVM-type simulations. This is particularly important in cases where significant migration of plant species is required to achieve a switch in dominant vegetation cover as predicted by the DGVM approach.

The need for more research into vegetation-atmosphere interactions, and the appropriateness of a modelling approach to these studies over southern Africa has been confirmed. The long-term goal of these studies should be the incorporation of a dynamic vegetation component into a regional climate model, with the aim of producing credible regional scale future climate change predictions for southern Africa. However, future research should also take into account the possibility that a dynamic vegetation component within a regional climate model may produce a large feedback effect. As a common technique for providing lateral boundary fields to the regional climate model (RCM) is a "one-way" nesting of the RCM within the general

circulation model, the regional model may become unstable due to its inability to propagate the vegetation feedback back to the general circulation model.

The results presented here are only an initial assessment of possible future changes and their feedbacks, but there is still a vast amount of research that needs to be undertaken in this area. The Sheffield Dynamic Global Model has proved to be a valuable and accurate tool for predicting both current and future vegetation distribution over southern Africa. The new daily version of the SDGVM that is currently being developed needs to be validated and tested, as the smaller temporal scale will improving coupling with the regional climate model. There is an even greater need for sensitivity analyses of the MM5 model, and in particular, the response of the MM5 model to changing vegetation and the incorporation of a dynamic vegetation component in this regional model. At present, there are no predictions of future climate change for southern Africa based on the MM5 regional model. These climate change predictions should be seen as a matter of priority for two reasons. Firstly, these results will be vital for climate change impact studies over southern Africa and the response of the SDGVM to future change predicted by a regional climate model needs to be assessed. Secondly, the aim of all future research should be to couple SDGVM with MM5 to predict future climate change for the southern African region. This will provide the plausible regional scale climate predictions that are essential for impact assessments and for policy decisions.

REFERENCES

REFERENCES

Acocks J.P.H. (1988) *Veld Types of South Africa.* Memoirs of the Botanical Survey of South Africa, 57. (An update of the first edition, published in 1953).

Allan R.J. (2000) ENSO and climatic variability in the past 150 years. In Diaz H.F. and V. Markgraf (eds.) *El Nino and the Southern Oscillation.* Cambridge University Press, Cambridge, p.3-55.

Barry R.G. and R.J. Chorley (2003) *Atmosphere, Weather and Climate.* Eighth Edition. Routledge, London, 421pp.

Beerling D.J. and F.I. Woodward (2001) *Vegetation and the Terrestrial Carbon Cycle. Modelling the first 400 million years.* Cambridge University Press, Cambridge, 405pp.

Behera S.K. and T. Yamagata (2001) Subtropical SST dipole events in the southern Indian Ocean. *Geophysical Research Letters*, 28, p.327-330.

Betts R.A. (2000) Offset of the potential carbon sink from boreal forestation by decreases in surface albedo. *Nature*, 408, p. 187-190.

Betts R.A., P.M. Cox, S.E. Lee and F.I. Woodward (1997) Contrasting physiological and structural vegetation feedbacks in climate change simulations. *Nature*, 387, p.796-799.

Bolin B., J. Jager and B.R. Doos (1986) The greenhouse effect, climatic change and ecosystems: A synthesis of present knowledge. In Bolin B., B.R. Doos, J. Jager and R.A. Warwick (eds.) *The Greenhouse Effect, Climatic Change and Ecosystems (SCOPE 29)*, John Wiley and Sons, Chichester, p.363-392.

Bonan G.B. (1996) *A land surface model (LSM version 1) for ecological, hydrological, and atmospheric studies: technical description and user's guide.* NCAR Technical Note NCAR/TN-417+STR. National Center for Atmospheric Research, Boulder, 1150pp.

Bonan G.B., S. Levis, L. Kergoat and K.W. Oleson (2002) Landscapes as patches of plant functional types: An integrating concept for climate and ecosystem models. *Global Biogeochemical Cycles*, 16 (2).

Bond W.J. and G.F. Midgley (2000) A proposed CO_2-controlled mechanism of woody plant invasion in grasslands and savannas. *Global Change Biology*, 6, p1-5.

Bond W.J., G.F. Midgley and F.I. Woodward (2003a) What controls South African vegetation – climate or fire? *South African Journal of Botany*, 69 (1), p.1-13.

Bond W.J., G.F. Midgley and F.I. Woodward (2003b) The importance of low atmospheric CO2 and fire in promoting the spread of grasslands and savannas. *Global Change Biology*, 9, p.973-982.

Box E.O. (1981) *Macroclimate and plant forms: an introduction to predictive modelling in phytogeography*. Tasks for Vegetation Science, Volume 1, Junk, The Hague.

Box E.O. (1996) Plant functional types and climate at the global scale. *Journal of Vegetation Science*, 7, p.309-320.

Breigleb B.P. and D.H. Bromwich (1998) Polar radiation budgets of the NCAR CCM3. *Journal of Climate*, 11, p.1246-1269.

Campbell B., P. Frost and N. Byron (1996) Miombo woodlands and their use: Overview and key issues. In Campbell B. (ed.) *The Miombo in Transition: Woodlands and Welfare in Africa*. Center for International Forestry Research (CIFOR), Bogor, Indonesia, p.1-10.

Cao M. and F.I. Woodward (1998) Dynamic responses of terrestrial ecosystem carbon cycling to global climate change. *Nature*, 393, p.249-252.

Cao M., Q. Zhang and H.H. Shugart (2001) Dynamic responses of African ecosystem carbon cycling to climate change. *Climate Research*, 17, p.183-193.

Chapin F.S. III (2003) Effects of plant traits on ecosystem and regional processes: a conceptual framework for predicting the consequences of global change. *Annals of Botany*, 91, p.455-463.

Charney J., P.H. Stone and W.J. Quirk (1975) Drought in the Sahara: a biophysical feedback mechanism. *Science*, 187, p.434-435.

Charney J. (1975) Dynamics of deserts and drought in the Sahel. *Quarterly Journal of the Royal Meteorological Society*, 101, p.193-202.

Charney J.F., W.J. Quirk, S.H. Chow and J. Kornfield (1977) A comparative study of the effects of albedo change on drought in semi-arid regions. *Journal of Atmospheric Sciences*, 34, p.1366-1385.

Chase T.N., R.A. Pielke Sr, T.G.F. Kittel, R.R. Nemani and S.W. Running (1996) Sensitivity of a general circulation model to global changes in leaf area index. *Journal of Geophysical Research*, 101(D3), p.7393-7408.

Chase T.N., R.A. Pielke Sr, T.G.F. Kittel, J.S. Baron and T.J. Stohlgren (1999) Potential impacts on Colorado Rocky Mountain weather due to land use changes on the adjacent Great Plains. *Journal of Geophysical Research*, 104(D14), p.16673-16690.

Chase T.N., R.A. Pielke Sr, T.G.F. Kittel, R.R. Nemani and S.W. Running (2000) Simulated impacts of historical land cover changes on global climate in northern winter. *Climate Dynamics*, 16, p.93-105.

Chase T.N. and R.G. Barry (2003) Numerical models of the general circulation, climate and weather prediction. In Barry R.G. and R.J. Chorley (eds.) *Atmosphere, Weather and Climate*. Eighth Edition. Routledge, London, p.162-176.

Chen F. and J. Dudhia (2001a) Coupling and advanced land surface-hydrology model with the Penn State-NCAR MM5 Modeling System. Part I: Model implementation and sensitivity. *Monthly Weather Review*, 129, p.569-585.

Chen F. and J. Dudhia (2001b) Coupling and advanced land surface-hydrology model with the Penn State-NCAR MM5 Modeling System. Part II: Preliminary model validation. *Monthly Weather Review*, 129, p.587-604.

Chidumayo E.N. (2001) Climate and phenology of savanna vegetation in southern Africa. *Journal of Vegetation Science*, 12, p.347-354.

CI (1999) *Priorities for Biodiversity Conservation in Madagascar CD-ROM.* Conservation International, Washington.

Claussen M., U. Lohmann, E. Roeckner and U. Schulzweida (1994) A global dataset of land-surface parameters. Max Planck Institut fur Meteorologie, Report No. 135, Hamburg, Germany, 23pp.

Collatz G.J., J.A. Berry and J.S. Clark (1998) Effects of climate and atmospheric CO_2 partial pressure on the global distribution of C_4 grasses: present, past, and future. *Oecologia*, 114, p.441-454.

Copeland J.H., R.A. Pielke and T.G.F. Kittel (1996) Potential climatic impacts of vegetation change: a regional modeling study. *Journal of Geophysical Research*, 101(D3), p.7409-7418.

Cowling R.M., D.M. Richardson and S.M. Pierce (eds.) (1997) *Vegetation of Southern Africa*. Cambridge University Press, Cambridge, 615pp.

Cox, P. M., C. Huntingford and R.J. Harding (1998) A canopy conductance and photosynthesis model for use in a GCM land surface scheme. *J Hydrology*, 212-213, p.79-94.

Cox, P. and M. Best (1999) Implementation of MOSES in the mesoscale model. *NWP Gazette*, December 1999, UK Meteorological Office. http://www.meto.gov.uk/research/nwp/publications/nwp_gazette/dec99/moses.html

Cox P., R. Betts, C. Bunton, R. Essery, P.R. Rowntree and J. Smith (1999) The impact of new land surface physics on the GCM simulation of climate and climate sensitivity. *Climate Dynamics*, 15, p.183-204.

Cox P.M., R.A. Betts, C.D. Jones, S.A. Spall and I.J. Totterdell (2000) Acceleration of global warming due to carbon-cycle feedbacks in a coupled climate model. *Nature*, 408, p.184-187.

Cramer W., A. Bondeau, F.I. Woodward, I.C. Prentice, R.A. Betts, V. Brovkin, P.M. Cox, V. Fisher, J.A. Foley, A.D. Friend, C. Kucharik, M.R. Lomas, N. Ramankutty, S. Sitch, B. Smith, A. White and C. Young-Molling (2001) Global response of terrestrial ecosystem structure and function to CO_2 and climate change: results from six dynamic global vegetation models. *Global Change Biology*, 7, p.357-373.

D'Antonio C.M. and P.M. Vitousek (1992) Biological invasions by exotic grasses, the grass-fire cycle, and global change. *Annual Review of Ecology and Systematics*, 23, p.63-87.

DeFries R.S. and J.R.G. Townshend (1994) NDVI-derived land cover classification at global scales. *International Journal of Remote Sensing*, 15, p.3567-3586. Special Issue on Global Data Sets.

DEAT (1997) The Environmental Potential Atlas (ENPAT) CD-Rom. Department of Environmental Affairs and Tourism, South Africa.

Denis B., R. Laprise, D. Caya and J. Côté (2002) Downscaling ability of one-way nested regional climate models: the Big-Brother Experiment. *Climate Dynamics*, 18, p.627-646.

Desanker P.V. and C.O. Justice (2001) Africa and global climate change: critical issues and suggestions for further research and integrated assessment modelling. *Climate Research*, 17, p.93-103.

Dickinson R.E. (1984) Modeling Evapotranspiration for Three-Dimensional Global Climate Models. *Climate Processes and Climate Sensitivity*, Geophysical Monograph 29, Maurice Ewing Volume 5, p.58-72.

Dickinson R.E. (1986) The climate system and modelling of future climate. In Bolin B., B.R. Doos, J. Jager and R.A. Warwick (eds.) *The Greenhouse Effect, Climatic Change and Ecosystems (SCOPE 29)*, John Wiley and Sons, Chichester, p.363-392.

Dickinson R.E. (1992) Land surface. In Trenberth K.E. (ed.) *Climate System Modeling*. Cambridge University Press, Cambridge, p.149-172.

Dickinson R.E., A. Henderson-Sellers, P.J. Kennedy and M.F. Wilson (1986) *Biosphere-Atmosphere Transfer Scheme (BATS) for the NCAR Community Climate Model*. NCAR Technical Note, NCAR/TN-275+STR, Bouder, 69pp.

Dickinson R.E., A. Henderson-Sellers, P.J. Kennedy and F. Giorgi (1992) Biosphere-Atmosphere Transfer Scheme (BATS), Version 1e as Coupled to the NCAR Community Climate Model. NCAR Technical Note, in prep.

Dirmeyer P.A. and J. Shukla (1994) Albedo as a modulator of climate response to tropical deforestation. *Journal of Geophysical Research*, 99(10), p.863-877.

Dorman J.L. and P.J. Sellers (1989) A global climatology of albedo, roughness length and stomatal resistance for atmospheric general circulation models as represented by the Simple Biosphere Model (SiB). *Journal of Applied Meteorology*, 28, p.833-855.

Dudhia J., D. Gill, Y.-R. Guo, K. Manning, W. Wang and J. Chiszar (2000) *PSU/NCAR Mesoscale Modelling System Tutorial Class Notes and User's Guide: MM5 Modelling System Version 3*. Mesoscale and Microscale Meteorology Division, National Center for Atmospheric Research, Boulder.

Dukowicz J.K. and R.D. Smith (1994) Implicit free-surface method for the Bryan-Cox-Semtner Ocean model. *Journal of Geophysical Research*, 99, p.7991-8014.

Eastman J.L., M.B. Coughenour and R.A. Pielke Sr. (2001) The regional effects of CO2 and landscape change using a coupled plant and meteorological model. *Global Change Biology*, 7, p.797-815.

Edwards J.M. and A. Slingo (1996) Studies with a flexible new radiation code. I: Choosing a configuration for a large scale model. *Quarterly Journal of the Royal Meteorological Society*, 122, p.689-719.

Ehleringer J.R., R.F. Sage, L.B. Flanagan and R.W. Pearcy (1991) Climate change and the evolution of C_4 photosynthesis. *Tree*, 6(3), p.95-99.

Ehleringer J.R., T.E. Cerling and B.R. Helliker (1997) C_4 photosynthesis, atmospheric CO_2, and climate. *Oecologia*, 112, p.285-299.

Flato G.M., G.J. Boer, W.G. Lee, N.A. McFarlane, D. Ramsden, M.C. Reader and A.J. Weaver (2000) The Canadian Centre for Climate Modelling and Analysis Global Coupled Model and its Climate. *Climate Dynamics*, 16, p.451-467.

Foley J.A., J.E. Kutzbach, M.T. Coe and S. Levis (1994) Feedbacks beteen climate and boreal forests during the Holocene epoch. *Nature*, 371, p.52-54.

Foley J.A., I.C. Prentice, N. Ramankutty, S. Levis, D. Pollard, S. Sitch and A. Haxeltine (1996) An integrated biosphere model of land surface processes, terrestrial carbon balance, and vegetation dynamics. *Global Biogeochemical Cycles*, 10, p.603-628.

Foley J.A., S. Levis, I.C. Prentice, D. Pollard and S.L. Thompson (1998) Coupling dynamic models of climate and vegetation. *Global Change Biology*, 4, p.561-579.

Foster P. (2001) The potential negative impacts of global climate change on tropical montane cloud forests. *Earth-Science Reviews*, 55, p.73-106.

Fouquart Y. and B. Bonnel (1980) Computation of solar heating of the Earth's atmosphere: A new parameterization. *Beitr. Phys. Atmos.*, 53, p.35-62.

Frost P. (1996) The ecology of Miombo woodlands. In Campbell B. (ed.) *The Miombo in Transition: Woodlands and Welfare in Africa*. Center for International Forestry Research (CIFOR), Bogor, Indonesia, p.1-10.

Giorgi F., B.C. Hewitson, J. Christensen, M. Hulme, H. von Storch, P. Whetton, R. Jones, L. Mearns and C. Fu (2001) Regional Climate Information – Evaluation and Projections. In Houghton J.T., Y. Ding and M. Nogouer (eds.) *Climate Change 2001: The Scientific Basis*, Cambridge University Press, p.583-638.

Gordon C., C. Cooper, C.A. Senior, H. Banks, J.M. Gregory, T.C. Johns, J.F.B. Mitchell and R.A. Wood (2000) The simulation of SST, sea ice extents and ocean heat transports in a version of the Hadley Centre coupled model without flux adjustments. *Climate Dynamics*, 16, p.147-168.

Grassl H. (2000) Status and Improvements of Coupled General Circulation Models. *Science*, 288, p.1991-1997.

Gregory D. (1995) A consistent treatment of the evaporation of rain and snow for use in large-scale models. *Monthly Weather Review*, 123, p.2716-2732.

Gregory D. and S. Allen (1991) The effect of convective scale downdrafts upon NWP and climate simulations. *Ninth conference on numerical weather prediction*. Denver, Colorado, American Meteorological Society, p.122-123.

Gregory D. and D. Morris (1996) The sensitivity of climate simulations to the specification of mixed phase clouds. *Climate Dynamics* 12, p.641-651.

Gregory D. and P.R. Rowntree (1990) A mass flux convection scheme with representation of cloud ensemble characteristics and stability dependent closure. *Monthly Weather Review,* 118, p.1483-1506.

Grell G., J. Dudhia and D. Stauffer (1994) *A description of the Fifth-Generation Penn State/NCAR Mesoscale Model (MM5).* NCAR Technical Note. NCAR/TN-398+STR, 117pp.

Gutowski W.J. Jr, D.S. Gutzler and W.-C. Wang (1991) Surface energy balances of three general circulation models: implications for simulating regional climate change. *Journal of Climate*, 4, p.121-134.

Hack J.J. (1994) Parametrization of moist convection in the NCAR Community Climate Model (CCM2). *Journal of Geophysical Research*, 99, p.5551-5568.

Hack J.J., J.M. Rosinski, D.L. Williamson, B.A. Boville and J.E. Truesdale (1995) Computational Design of the NCAR community climate model. *Parallel Computing*, 21, p.1545-1569.

Harrison S.P. and C.I. Prentice (2003) Climate and CO_2 controls on global vegetation distribution at the last glacial maximum: analysis based on palaeovegetation data, biome modelling and palaeoclimate simulations. *Global Change Biology*, 9, p. 983-1004.

Henderson-Sellers A. (1993) Continental vegetation as a dynamic component of a global climate model: a preliminary assessment. *Climatic Change*, 23, p.337-377.

Henderson-Sellers A., P. Irannejad, K. McGuffie and A.J. Pitman (2003) Predicting land-surface climates – better skill or moving targets? *Geophysical Research Letters*, 30 (14), p.1777-1780.

Heisler J.L., J.M. Briggs and A.K. Knapp (2003) Long-term patterns of shrub expansion in a C_4-dominated grassland: fire frequency and the dynamics of shrub cover and abundance. *American Journal of Botany*, 9(3), p.423-428.

Hewitson B.C. and B. Joubert (1998) Climate downscaling: current South African projections. http://www.egs.uct.ac.za/fccc/

Holdridge (1947) Determination of world plant formations from simple climatic data. *Science*, 105, p.367-368.

Holtslag A.A.M. and B.A. Boville (1993) Local versus non-local boundary layer diffusion in a global climate model. *Journal of Climate*, 6, p.1825-1842.

Hulme M. (ed.) (1996) *Climate Change and Southern Africa: An exploration of some potential impacts and implications in the SADC region.* CRU/WWF, Norwich.

Hulme M., R. Doherty, T. Ngara, M. New and D. Lister (2001) African climate change: 1900 – 2100. *Climate Research*, 17, p.145-168.

Hurrell J., J.J. Hack, B.A. Boville, D. Williamson and J.T. Kiehl (1998) The dynamical simulation of the NCAR Community Climate Model version 3 (CCM3). *Journal of Climate*, 11, p.1207-1236.

IPCC (1997) *An introduction to simple climate models used in the IPCC Second Assessment Report*. Houghton, J.T., L.G.M. Filho, D.J. Griggs and K. Maskell (eds.), IPCC Technical Paper II.

IPCC (2001) *Climate Change 2001: The Scientific Basis*. Houghton, J.T., Y. Ding and M. Nogouer (eds.), Cambridge University Press, Cambridge, United Kingdom and New York, USA, 881pp.

Johns T.C., R.E. Carnell, J.F. Crossley, J.M. Gregory, J.F.B. Mitchell, C.A. Senior, S.F.B. Tett and R.A. Wood (1997) The second Hadley Centre coupled ocean-atmosphere GCM: Model description, spinup and validation. *Climate Dynamics*, 13, p.103-134.

Jones H.G. (1992) *Plants and Microclimate. A quantitative approach to environmental plant physiology*. Second Edition. Cambridge University Press, Cambridge, 428pp.

Jones P. (1999) First and second-order conservative remapping. *Monthly Weather Review*, 127, p.2204-2210.

Kalnay et al (1996) The NCEP/NCAR 40-year reanalysis project. *Bulletin of the American Meteorological Society*, 77, p.437-471.

Kiehl J.T., J.J. Hack, G.B. Bonan, B.A. Boville, D.L. Williamson and P.J. Rasch (1998) The National Center for Atmospheric Research Community Climate Model: CCM3. *Journal of Climate*, 11, p.1131-1149.

Kutzbach J., G. Bonan, J. Foley and S.P. Harrison (1996) Vegetation and soil feedbacks on the response of the Africa monsoon to orbital forcing in the early to middle Holocene. *Nature*, 384, p.623-626.

Lawton R.O., U.S. Nair, R.A. Pielke Sr. and R.M. Welch (2001) Climatic impact of tropical lowland deforestation on nearby montane cloud forests. *Science*, 294, p.584-587.

Lomas M.R., F.I. Woodward and S. Quegan (2001) *Application of the Sheffield Dynamic Global Vegetation Model (SDGVM) to simulating the carbon balance of Buedingen forest*. Unpublished report, University of Sheffield.

Lomas M.R. and F.I. Woodward (2003) *The role of Dynamic Vegetation Models*. Unpublished draft report, University of Sheffield.

Loveland T.R., B.C. Reed, J.F. Brown, D.O. Ohlen, Z. Zhu, L. Yang and J.W. Merchant (2000) Development of a global land cover characteristics database and IGBP-DISCover from 1 km AVHRR data. *International Journal of Remote Sensing*, 21, p.1303-1330.

Low A.B. and A.G. Rebelo (1996) *Vegetation of South Africa, Lesotho and Swaziland*. Department of Environmental Affairs and Tourism, Pretoria, South Africa.

Manabe S. (1969) Climate and ocean circulation: 1. The atmospheric circulation and the hydrology of the Earth's surface. *Monthly Weather Review*, 97, p.739-774.

Marshall C.H., R.A. Pielke Sr. and L.T. Steyaert (2003) Crop freezes and land-use change in Florida. *Nature*, 426, p.29-30.

Matthews E. (1983) Global vegetation and land use: New high resolution databases for climate studies. *Journal of Climate and Applied Meteorology*, 22, p.474-487.

Maltrud M.E., R.D. Smith, A.J. Semtner and R.C. Malone (1998) Global eddy-resolving ocean simulations driven by 1985-1995 atmospheric winds. *Journal of Geophysical Research*, 30, p.30825-30853.

McAvaney B.J., C. Covey, S. Joussaume, V. Kattsov, A. Kitoh, W. Ogana, A.J. Pitman, A.J. Weaver, R.A. Wood, Z.-C. Zhao (2001) Model Evaluation. In Houghton J.T., Y. Ding and M. Nogouer (eds.) *Climate Change 2001: The Scientific Basis*, Cambridge University Press, p.471-524.

McFarlane N.A., G.J. Boer, J.-P. Blanchet and M. Lazare (1992) The Canadian Climate Centre second-generation general circulation model and its equilibrium climate. *Journal of Climate*, 5(10), p.1013-1044.

Meehl G.A., P. Gent, J.M. Arblaster, B. Otto-Bliesner, E. Brady and A. Craig (2000) Factors that affect the amplitude of El Nino in global coupled climate models. *Climate Dynamics*, 17 (7), p. 515-526.

Meeson B.W., F.E. Corprew, J.M.P. McManus, D.M. Myers, J.W. Closs, K.-J. Sun, D.J. Sunday and P.J. Sellers (1995) ISLSCP Initiative I – Global Data Sets for Land-Atmosphere Models, 1987-1988. Volumes 1-5, published on CD by NASA.

Melillo J.M., A.D. McGuire, D.W. Kicklighter, B. Moore III, C.J. Vorosmary and A.L. Schloss (1993) Global climate change and terrestrial net primary productivity. *Nature*, 363, p.234-240.

Midgley G., M. Rutherford and W. Bond (2001) *The heat is on…impacts of climate change on plant diversity in South Africa*. National Botanical Institute, Cape Town.

Moorcroft P.R. (2003) Recent advances in ecosystem-aatmosphere interactions: an ecological perspective. *Proceedings of the Royal Society of London B*, 270, p.1215-1227.

Morcrette, J.-J. (1991) Radiation and cloud radiative properties in the ECMWF operational weather forecast model. *Journal of Geophysical Research*, 96, p.9121-9132.

Nakićenović N, J. Alcamo, G. Davis, B. de Vries, J. Fenhann, S. Gaffin, K. Gregory, A. Grubler, T.Y. Jung, T. Kram, E.L. La Rovere, L. Michaelis, S. Mori, T. Morita, W. Pepper, H. Pitcher, L. Price, K. Raihi, A. Roehrl, H.-H. Rogner, A. Sankovski, M. Schlesinger, P. Shukla, S. Smith, R. Swart, S. van Rooijen, N. Victor and Z. Dadi (2000) *IPCC Special Report of Emissions Scenarios*, Cambridge University Press, Cambridge, United Kingdom and New York, USA, 599pp.

Nepstad D.C., A. Verissimo, A. Alencar, C. Nobre, E. Lima, P. Lefebvre, P. Schlesinger, C. Potter, P. Moutinho, E. Mendoza, M. Cochrane and V. Brooks (1999) Large-scale impoverishment of Amazonian forests by logging and fire. *Nature*, 398, p.505-508.

New M., M. Hulme and P. Jones (1999) Representing twentieth-century space-time climate variability. Part II: Development of 1901-1996 monthly grids of terrestrial surface climate. *Journal of Climate*, 13(13), p.2217-2238.

Nicholson S.E. (1997) An analysis of the ENSO signal in the tropical Atlantic and western Indian Oceans. *International Journal of Climatology*, 17, p.345-375.

Nicholson S.E. (2001) Climatic and environmental change in Africa during the last two centuries. *Climate Research*, 17, p.123-144.

de Noblet N.I., I.C. Prentice, S. Joussaume, D. Texier, A. Botta and A. Haxeltine (1996) Possible role of atmosphere-biosphere interactions in triggering the last glaciation. *Geophysical Research Letters*, 23(22), p.3191-3194.

Oberhuber J.M. (1993) The description of a coupled snow, sea-ice, mixed layer and isopycnal ocean model. DKRZ-Model Users Support Group, Hamburg, Germany, 130pp. Available at http://cera-www.dkrz.de/IPCC-DDC/SRES/ECHAM4/echam4opyc3.html

Olago D.O. (2001) Vegetation changes over palaeo-time scales in Africa. *Climate Research*, 17, p.105-121.

Olson J.S. and J.A. Watts (1982) *Major World Ecosystem Complex Map*. Oak Ridge National Laboratory, Oak Ridge.

Pacala S.W., G.C. Hurtt, D. Baker, P. Peylin, R.A. Houghton, R.A. Birdsey, L. Heath, E.T. Sundquist, R.F. Stallard, P. Ciais, P. Moorcroft, J.P. Caspersen, E. Shevliakova, B. Moore, G. Kohlmaier, E. Holland, M. Gloor, M.E. Harmon, S.-M. Fan, J.L. Sarmiento, C.L. Goodale, D. Schimel and C.B. Field (2001) Consistent land and atmosphere-based US carbon sink estimates. *Science*, 292, p.2316-2320.

Pacanowski R.C., K. Dizon and A. Rosati (1993) *The GFDL modular ocean model users guide*. GFDL Ocean Group Technical Report 2. Geophysical Fluid Dynamics Laboratory, Princeton, 46pp.

Page S.E. et al (2002) The amount of carbon released from peat and forest fires in Indonesia during 1997. *Nature*, 420, p.61-65.

Parton W.J., J. Scurlock, D. Ojima, T. Gilmanov, R. Scholes, D. Schimel, T. Kirchner, J.C. Menaut, T. Seastedt, D. Moya, A. Kamnalrut and J. Kinyamario (1993) Observations and modeling of biomass and soil organic matter dynamics for the grassland biome worldwide. *Global Biogeochemical Cycles*, 7, p.785-809.

Pielke R.A. (2001) Influence of the spatial distribution of vegetation and soils on the prediction of cumulus convective rainfall. *Review of Geophysics*, 39, p.151-177.

Pielke R.A. Sr. (2001) Carbon sequestration – the need for an integrated climate system approach. *Bulletin of the American Meteorological Society*, p.2021.

Pielke R.A., G.A. Dalu, J.S. Snook, T.J. Lee and T.G.F. Kittel (1991) Nonlinear influence of mesoscale land use on weather and climate. *Journal of Climate*, 4, p.1053-1069.

Pielke R.A. Sr., R. Avissar, M. Raupach, A.J. Dolman, X. Zeng and A.S. Denning (1998) Interactions between the atmosphere and terrestrial ecosystems: influence on weather and climate. *Global Change Biology*, 4, p.461-475.

Pope V.D., M.L. Gallani, P.R. Rowntree and R.A. Stratton (2000) The impact of new physical parametrizations in the Hadley Centre climate Model – HadAM3. *Climate Dynamics*, 16, 123-146.

Potter C., S. Klooster, V. Genovese and R. Myneni (2003) Satellite data help predict terrestrial carbon sinks. *EOS*, 84 (46), p.508.

Prentice I.C., W. Carmer, S.P. Harrison, R. Leemans, R.A. Monserud and A.M. Solomon (1992) A global biome model based on plant physiology and dominance, soil properties and climate. *Journal of Biogeography*, 19, p.117-134.

Pronk J. (2002) Opening Address. In Steffen W., J. Jager, D.J. Carson and C. Bradshaw (eds.) *Challenges of a Changing Earth. Proceedings of the Global Change Open Science Conference, Amsterdam, The Netherlands, July 2001.* Springer-Verlag, Berlin, p.3-5.

Reason C.J.C. (2001) Subtropical Indian Ocean SST dipole events and southern African rainfall. *Geophysical Research Letters*, 28 (11), p.2225-2227.

Roberts L. (1989) How fast can trees migrate? *Science*, 243, p.735-737.

Roeckner, E., J.M. Oberhuber, A. Bacher, M. Christoph and I. Kirchner (1996a) ENSO variability and atmospheric response in a global couple atmosphere-ocean GCM. *Climate Dynamics*, 12, p.737-754.

Roeckner, E., K. Arpe, L. Bengtsson, M. Christoph, M. Claussen, L. Dümenil, M. Esch, M. Giorgetta, U. Schlese, and U. Schulzweida (1996b) *The atmospheric general circulation model ECHAM4: Model description and simulation of present-day climate*. Max Planck Institut für Meteorologie, Report No. 218, Hamburg, Germany, 90 pp.

Rutherford M.C. and R.H. Westfall (1994) *Biomes of southern Africa – an objective categorisation. Second Edition*. Memoirs of the Botanical Survey of South Africa, Number 63.

Schefuss E., S. Schouten, J.H.F. Jansen, S. Damsté and S. Jaap (2003) African vegetation controlled by tropical sea surface temperatures in the mid-Pleistocene period. *Nature*, 422, p.359-454.

Schindler D.W. (1999) Carbon Cycling: The mysterious missing sink. *Nature*, 398, p.105-106.

Scholes R.J. (1997) Savannah. In Cowling R.M., D.M. Richardson and S.M. Pierce (eds.) *Vegetation of Southern Africa*. Cambridge University Press, Cambridge, p.258-277.

Scholes R.J., G. Pickett, W.N. Ellery and A.C. Blackmore (1997) Plant functional types in African savannas and grasslands. In Smith T.M., H.H. Shugart and F.I. Woodward (eds.) *Plant Functional Types*, Cambridge University Press, Cambridge, p.255-268.

Schulze R.E. (1990) Climate change and hydrological response in southern Africa: heading towards the future. *South African Journal of Science*, 86, p.373-381.

Scurlock J.M.O., G.P. Asner and S.T. Gower (2001) *Worldwide Historical Estimates of Leaf Area Index, 1932–2000.* ORNL/TM-2001/268, Oak Ridge National Laboratory, Oak Ridge. Available online at http://daac.ornl.gov/global_vegetation/HistoricalLai/comp/LAI_TM.pdf

Sellers P.J. (1987) Modeling effects of vegetation on climate. In Dickinson R.E. (ed.) *The Geophysiology of Amazonia*. Wiley and Sons, p.244-264.

Sellers P. (1991) Modeling and observing land-surface-atmosphere interactions on large scales. In Wood E.F. (ed.) *Land Surface – Atmosphere Interactions for Climate Modeling. Observations, Models and Analysis*. Kluwer Academic Publishers, Dordrecht, p.85-114

Sellers P.J., Y. Mintz, Y.C. Sud and A. Dalcher (1986) A Simple Biosphere Model (SiB) for use within General Circulation Models. *Journal of the Atmospheric Sciences*, 43 (6), p.505-531.

Sellers P.J, D.A. Randall, G.J. Collatz, J.A. Berry, C.B. Field, D.A. Dazlich, C. Zhang, G.D. Collelo, and L. Bounoua (1996a) A revised land surface parameterization (SiB2) for atmospheric GCMs. Part I: Model Formulation. *Journal of Climate*, 9, p.676-705.

Sellers P.J., S.O Los, C.J. Tucker, C.O. Justice, D.A. Dazlich, G.J. Collatz and D.A. Randall (1996b) A revised land surface parameterization (SiB2) for atmospheric GCMs. Part II: The generation of global fields of terrestrial biophysical parameters from satellite data. *Journal of Climate*, 9, p.706-737.

Semazzi F.H.M. and Y. Song (2001) A GCM study of climate change induced by deforestation in Africa. *Climate Research*, 17, p.169-182.

Senior C. and J.F.B. Mitchell (1993) CO2 and climate: The impact of cloud parametrization. *Journal of Climate*, 6, p.393-418.

Shannon D.A. (2000) *Land surface response to climate change forcing over southern Africa.* Unpublished PhD thesis, University of Cape Town.

Shukla J. and Y. Mintz (1982) Influence of land-surface evapotranspiration on the Earth's climate. *Science*, 215, p.1498-1501.

Sitch S., B. Smith, I.C. Prentice, A. Arneth, A. Bondeau, W. Cramer, J.O. Kaplan, S. Levis, W. Lucht, M.T. Sykes, K. Thonicke and S. Venevsky (2002) Evaluation of ecosystem dynamics, plant geography and terrestrial carbon cycling in the LPJ Dynamic Global Vegetation Model. *Global Change Biology*, 9, p.161-185.

Smith R.D., S. Kortas and B. Meltz (1995) *Curvilinear co-ordinates for global ocean models.* LA-UR-95-1146, Los Alamos National Laboratory, Los Alamos, New Mexico, 38pp.

Smith R.N.B (1990) A scheme for predicting layer clouds and their water content in a general circulation model. *Quarterly Journal of the Royal Meteorology Society*, 116, p.435-460.

Smith T.M., H.H. Shugart, F.I. Woodward and P.J. Burton (1993) Plant Functional Types. In Solomon A.M. and H.H. Shugart (eds.) *Vegetation Dynamics and Global Change*. Chapman and Hall, New York, p.272-292.

Smith T.M., H.H. Shugart and F.I. Woodward (eds.) (1997) *Plant Functional Types*. Cambridge University Press, Cambridge, 369pp.

Stocker T.F., G.K.C. Clarke, H. Le Treut, R.S. Lindzen, V.P. Meleshko, R.K. Mugara, T.N. Palmer, R.T. Pierrehumbert, P.J. Sellers, K.E. Trenberth, J. Willebrand (2001) Physical Climate Processes and Feedbacks. In Houghton J.T., Y. Ding and M. Nogouer (eds.) *Climate Change 2001: The Scientific Basis*, Cambridge University Press, p.417-470.

Stohlgren T.J., T.N. Chase, R.A. Pielke Snr., T.G.F. Kittel and J.S. Baron (1998) Evidence that local land use practices influence regional climate, vegetation, and stream flow patterns in adjacent natural areas. *Global Change Biology*, 4, p.495-504.

Sundquist E.T. (1993) The global carbon dioxide budget. *Science*, 259, p.934-940.

Teeri J.A. (1988) Interaction of temperature and other environmental variables influencing plant distribution. In Long S.P. and F.I. Woodward (eds.) *Plants and Temperature*, Society for Experimental Biology, Cambridge, p.77-89.

Teeri J.A. and L.G. Stowe (1976) Climatic patterns and the distribution of C_4 grasses in North America. *Oecologia*, 23, p.1-12.

Thomas C. D., A. Cameron, R. E. Green, M. Bakkenes, L. J. Beaumont, Y. C. Collingham, B. F. N. Erasmus, M. Ferreira De Siqueira, A. Grainger, L. Hannah, L. Hughes, B. Huntley, A. S. Van Jaarsveld, G. F. Midgley, L. Miles, M. A. Ortega-Huerta, A. Townsend Peterson, O. L. Phillips And S. E. Williams (2004) Extinction risk from climate change. *Nature*, 427, p.145 - 148

Tyson P.D. (1986) *Climatic Change and Variability in Southern Africa*. Oxford University Press, Cape Town, 220pp.

Tyson P.D. and R.A. Preston-Whyte (2000) *The Weather and Climate of Southern Africa*. Oxford University Press, Cape Town, 396pp.

Tyson P.D., E. Odada, R. Schulze and C. Vogel (2002) Regional-Global Change Linkages: Southern Africa. In Tyson P.D., R. Fuchs, C. Fu, L. Lebel, A.P. Mitra, E. Odada, J. Perry, W. Steffen and H. Virji (eds.) *Global-Regional Linkages in the Earth System*, Springer-Verlag, Berlin, p.3-73.

Vaughan D.G., G.J. Marshall, W.M. Connolley, J.C. King and R. Mulvaney (2001) Devil in the Detail. *Science*, 293, p.1777-1779.

Vazquez A., B. Perez, F. Fernandez-Gonzalez and J.M. Moreno (2002) Recent fire regime characteristics and potential natural vegetation relationships in Spain. *Journal of Vegetation Science*, 13, p.663-676.

Verseghy D.L. (1991) CLASS – A Candian Land Surface Scheme for GCMs. I. Soil Model. *International Journal of Climatology*, 11, p.111-133.

Verseghy D.L., N.A. McFarland and M. Lazare (1993) CLASS – A Canadian land surface scheme for GCMs, II. Vegetation model and coupled runs. *International Journal of Climatologyf*, 13, p.347-370.

Warrick R.A., H.H. Shugart, M.J.A. Anotonovsky, J.R. Tarrant and C.J. Tucker (1986) The effects of increased CO_2 and climatic change on terrestrial ecosystems: Global perspectives, aims and issues. In Bolin B., B.R. Doos, J. Jager and R.A. Warwick (eds.) *The Greenhouse Effect, Climatic Change and Ecosystems (SCOPE 29)*, John Wiley and Sons, Chichester, p.363-392.

Washington W.M., J.W. Weatherly, G.A. Meehl, A.J. Semtner, Jr., T.W. Bettge, A.P. Craig, W.G. Strand, Jr., J.M. Arblaster, V.B. Wayland, R. James, Y. Zhang, (2000) Parallel climate model (PCM) control and transient simulations. *Climate Dynamics*, 16(10/11), p.755-774.

Wells P.V. (1965) Scarp woodlands, transported grassland soils and the concept of grassland fire in the Great Plains region. *Science*, 148, p.246-249.

White F. (1983) The *Vegetation of Africa*. Unesco, Paris.

Williamson D.L., and P.J. Rasch (1994) Water vapor transport in the NCAR CCM2. *Tellus*, 46A, p.34-51.

Wilson M.F. and A. Henderson-Sellers (1985) A global archive of land cover and soils data for use in general circulation climate models. *Journal of Climate*, 5, p.119-143.

Woodward F.I. (1987a) *Climate and plant distribution*. Cambridge University Press, Cambridge.

Woodward F.I. (1987b) Stomatal numbers are sensitive to increases in CO_2 from preindustrial levels. *Nature*, 327, p.617-618.

Woodward F.I. (1988) Temperature and the distribution of plant species. In Long S.P. and F.I. Woodward (eds.) *Plants and Temperature*, Society for Experimental Biology, Cambridge, p.59-75.

Woodward F.I. and B.G. Williams (1987) Climate and plant distribution at global and local scales. *Vegetatio*, 69, p.189-197.

Woodward F.I., T.M. Smith and W.R. Emanuel (1995) A global land primary productivity and phytogeography model. *Global Biogeochemical Cycles*, 9(4), p.471-490.

Woodward F.I., M.R. Lomas and S.E. Lee (2001) Predicting the future productivity and distribution of global terrestrial vegetation. In Jacques R., B. Saugier and H. Mooney (eds.) *Terrestrial Global Productivity*, Academic Press, New York, p.521-541.

Woodward F.I. and M.R. Lomas (2004) Vegetation dynamics – simulating responses to climatic change. *Biol Rev*, 79, p.643-670.

Woolhouse H.W. (1988) Overview: Problems and proposals for the understanding of temperature responses in plants. In Long S.P. and F.I. Woodward (eds.) *Plants and Temperature*, Society for Experimental Biology, Cambridge, p.411-415.

Zeng N., J.D. Neelin, K.-M. Lau and C.J. Tucker (1999) Enhancement of interdecadal climate variability in the Sahel by vegetation interaction. *Science*, 286, p.1537-1540.

Zhang G.J. and N.A. McFarlane (1995) Sensitivity of climate simulations to the parameterization of cumulus convection in the Canadian Climate Centre general circulation model. *Atmosphere-Ocean*, 33, p.407-446.

Zhang J.L. and W.D. Hibler III (1997) On an efficient numerical method for modeling sea ice dynamics. *Journal of Geophysical Research*, 102, p.8691-8702.

Zhao M., A.J. Pitman and T. Chase (2001) The impact of land cover change on the atmospheric circulation. *Climate Dynamics*, 17, p.467-477.

APPENDICES

APPENDIX 6.1

The following 11 pictures show the decadal variation of SDGVM output from 1901 to 1995 (SDGVM with CRU data).

A.1901

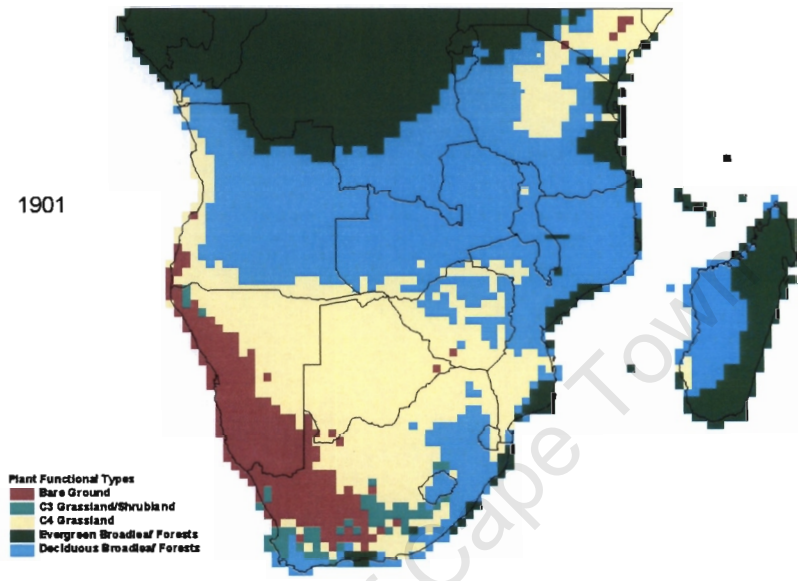

B. 1910

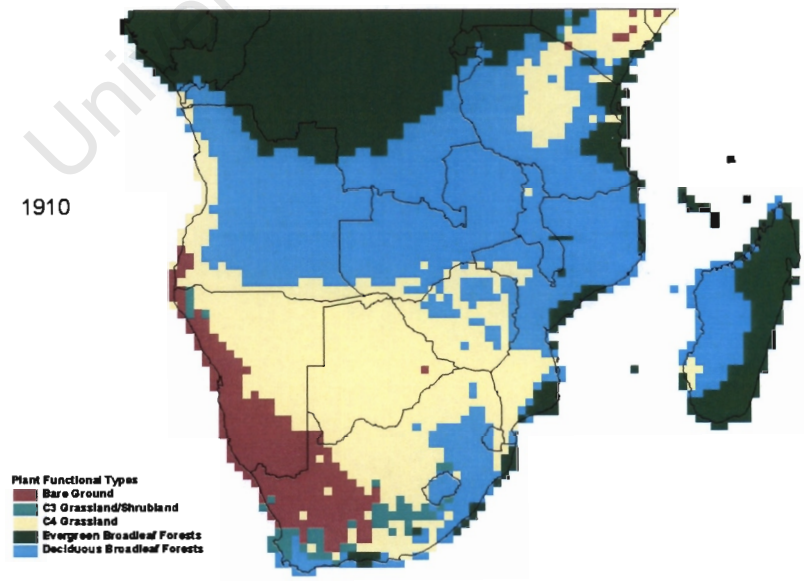

C. 1920

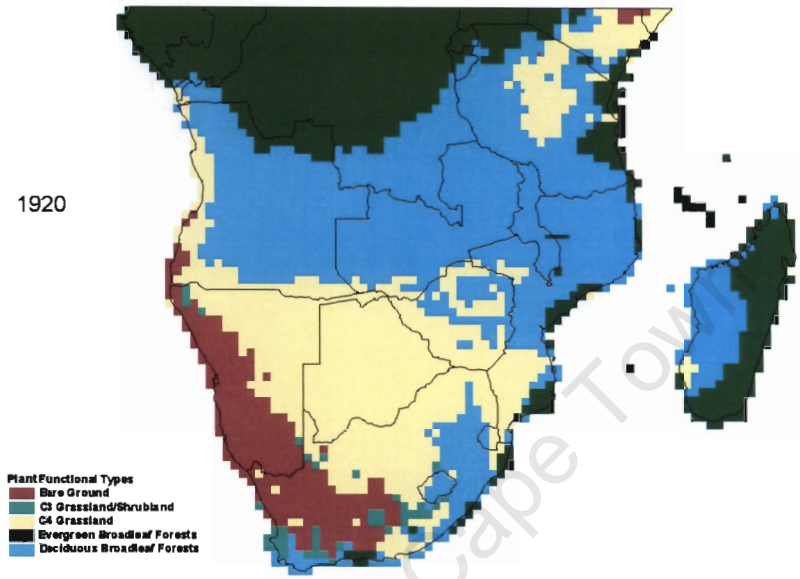

D. 1930

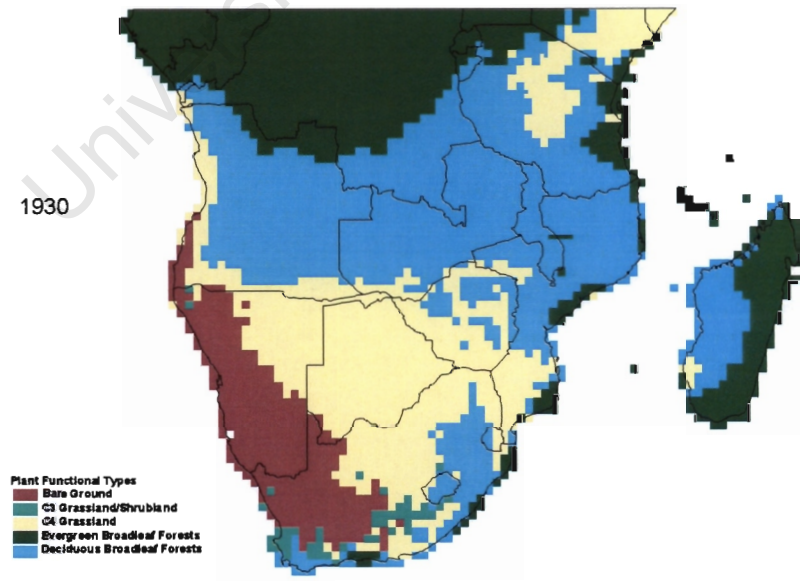

E. 1940

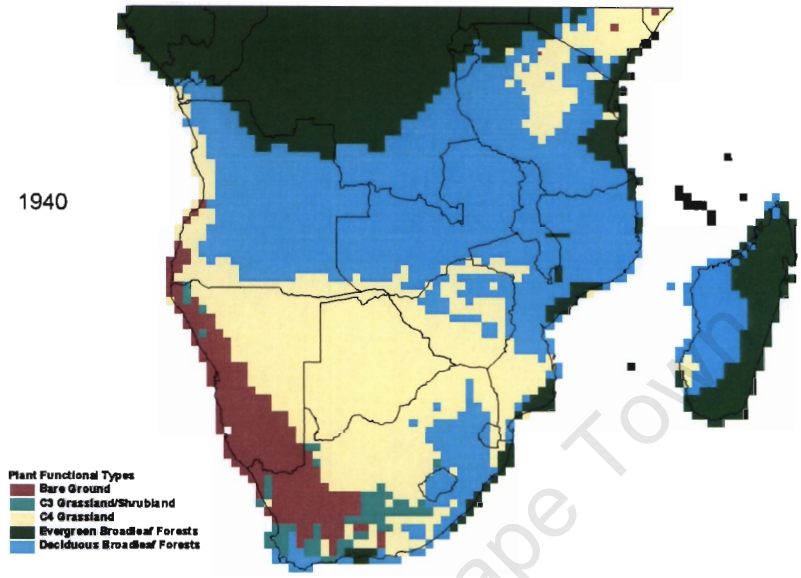

F. 1950

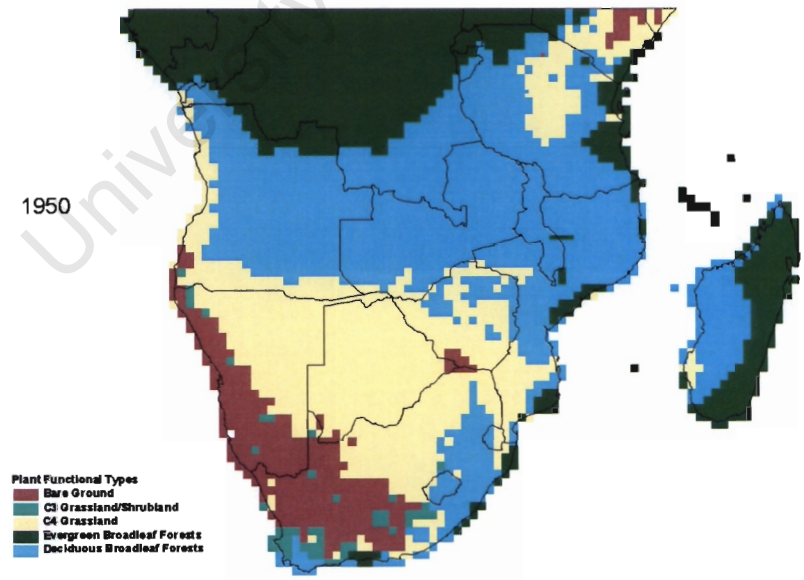

G. 1960

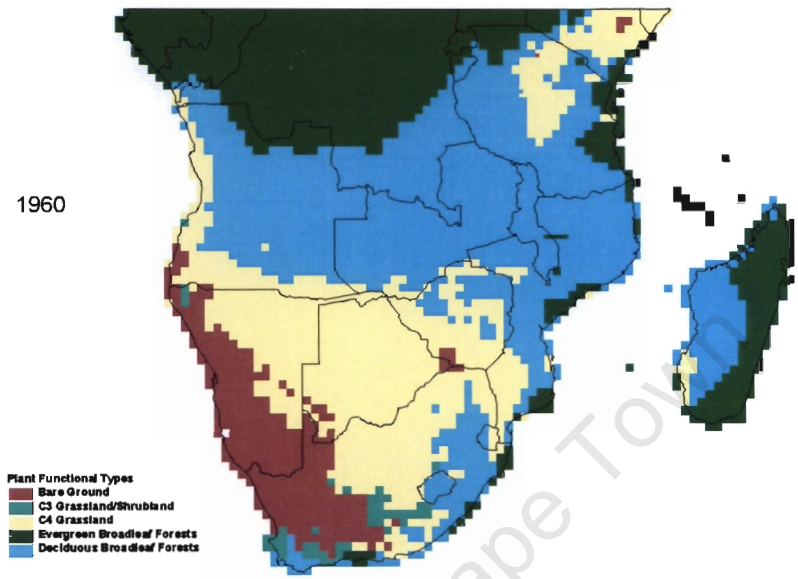

H. 1970

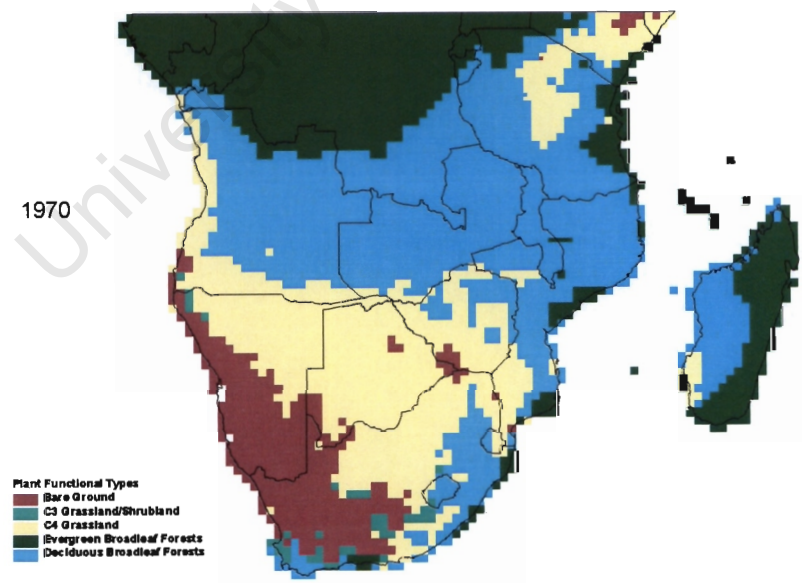

I. 1980

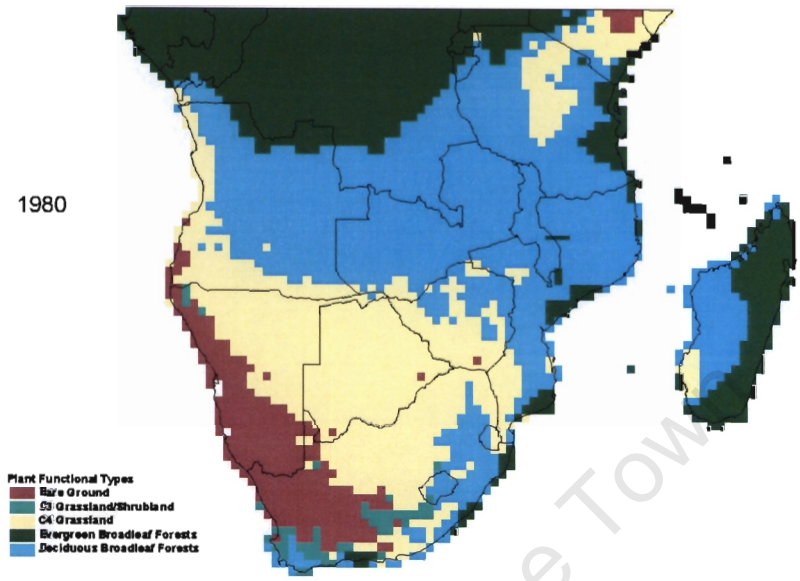

J. 1990

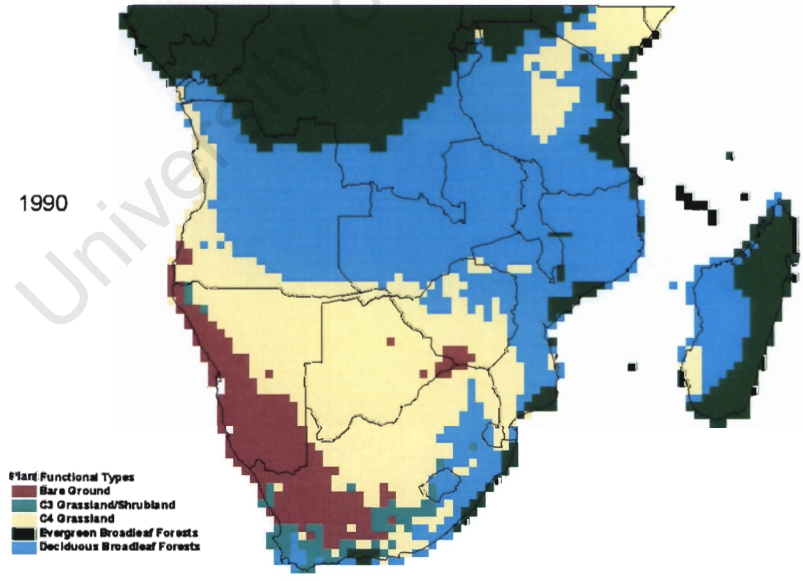

K. 1995

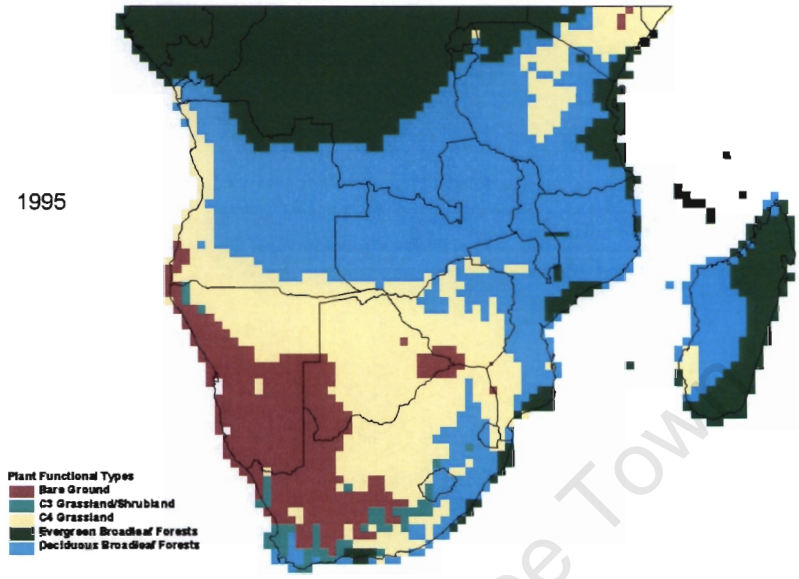

APPENDIX 8.1: THE MODELLED CLIMATE VARIABLES

These images show the control climate, as well as the difference between the control and the future climate, and therefore provide some idea of the magnitude of the changes that are predicted to occur. However, it should be remembered that these data are based on regridded global climate model data, which has a fairly coarse data. There may therefore be artefacts in the data that reflect the original resolution of the data. The relative humidity, precipitation and temperature data for the austral summer and winter are presented, in that order. The images on the left are the average of December, January and February (DJF), representing the austral summer. The right hand images are the averages of June, July and August (JJA), representing winter.

8.1.1. RELATIVE HUMIDITY

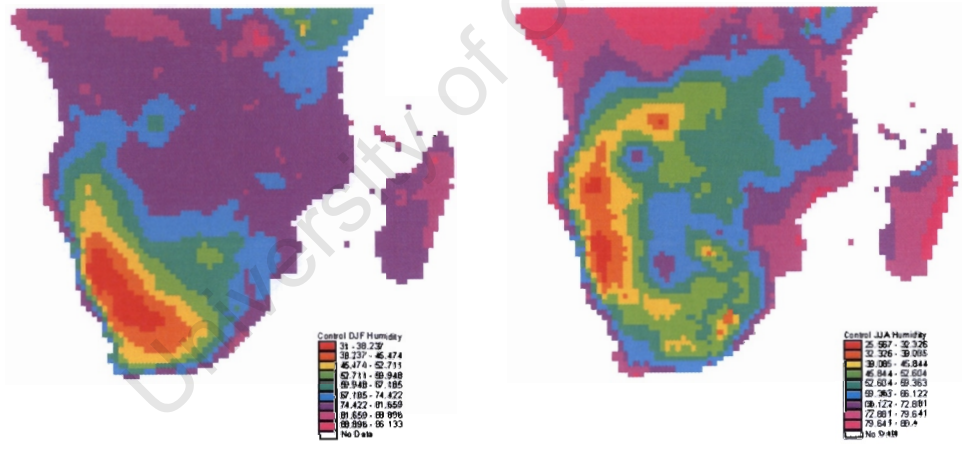

1. Control Relative Humidity (%)

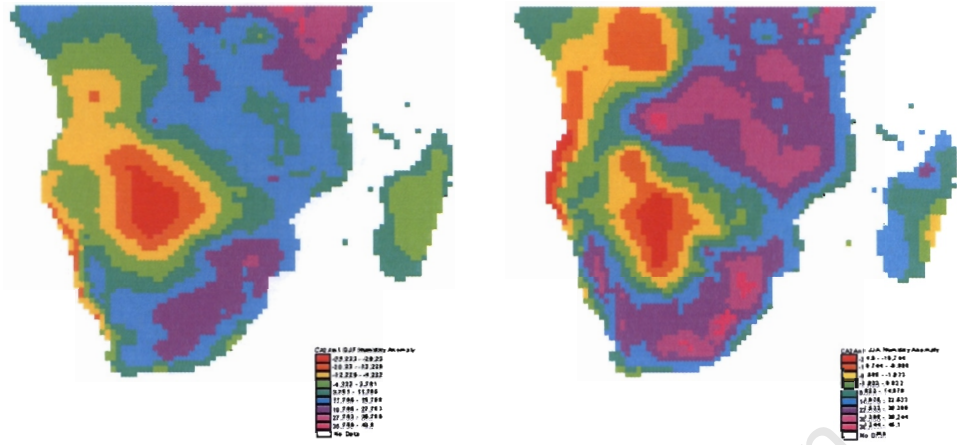

2. CCCMa A2 Anomaly 1

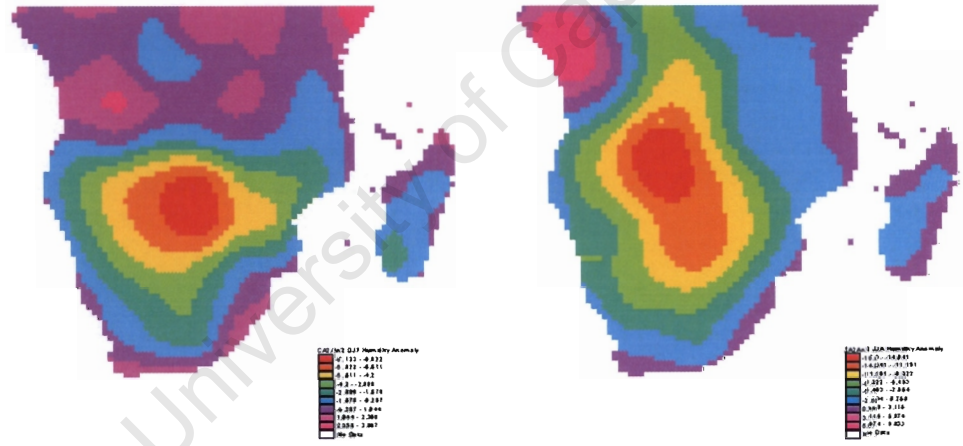

3. CCCMa A2 Anomaly 2

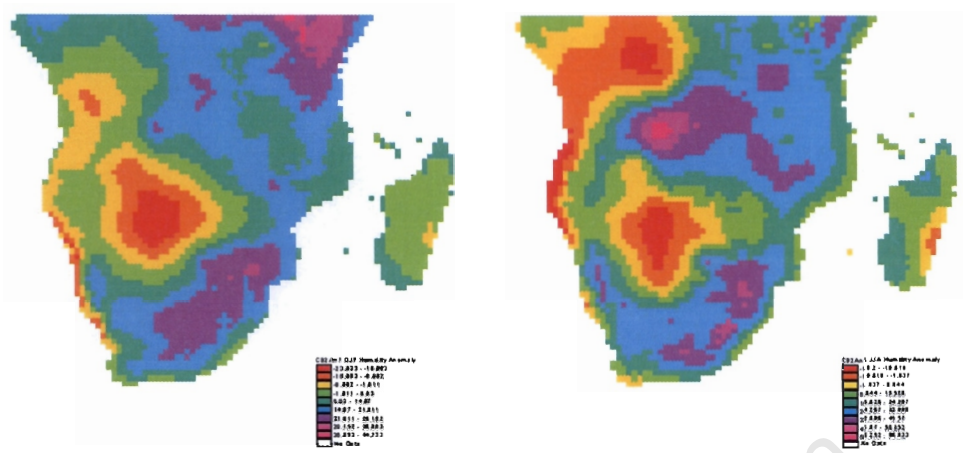

4. CCCMa B2 Anomaly 1

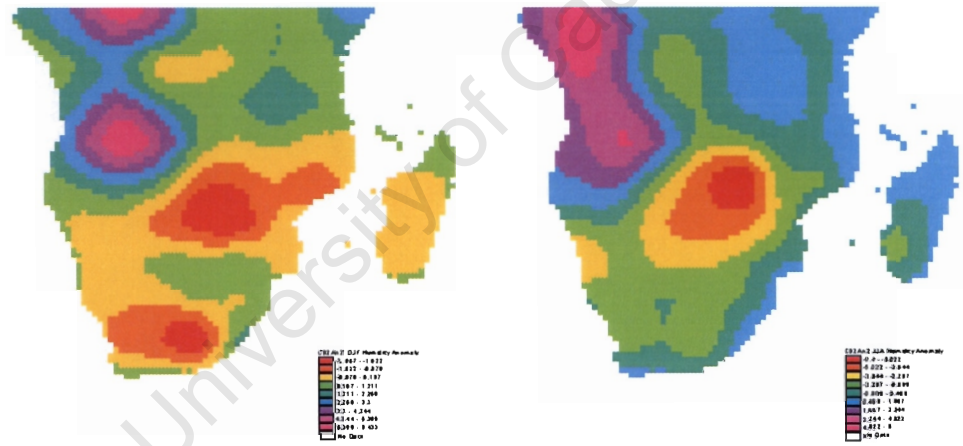

5. CCCMa B2 Anomaly 2

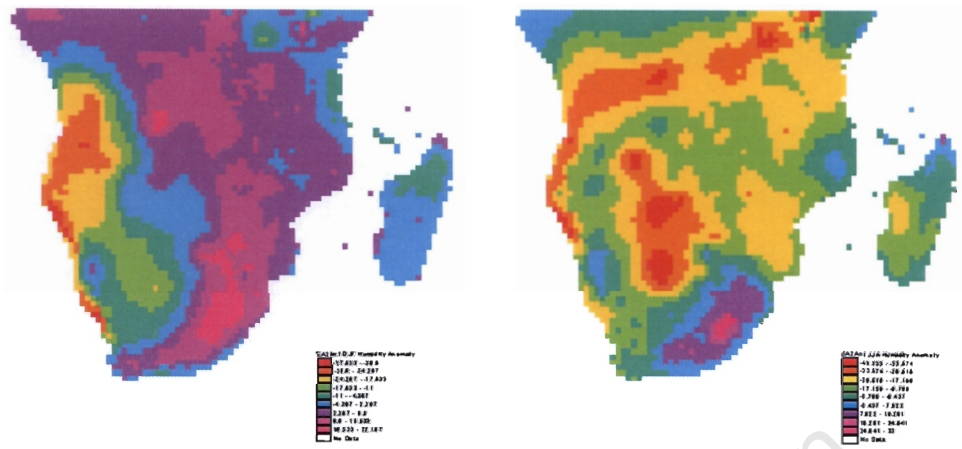

6. ECHAM A2 Anomaly 1

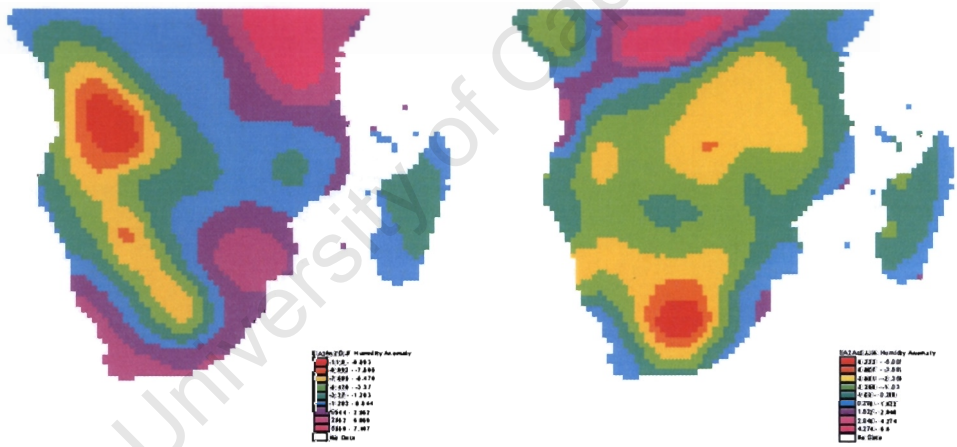

7. ECHAM A2 Anomaly 2

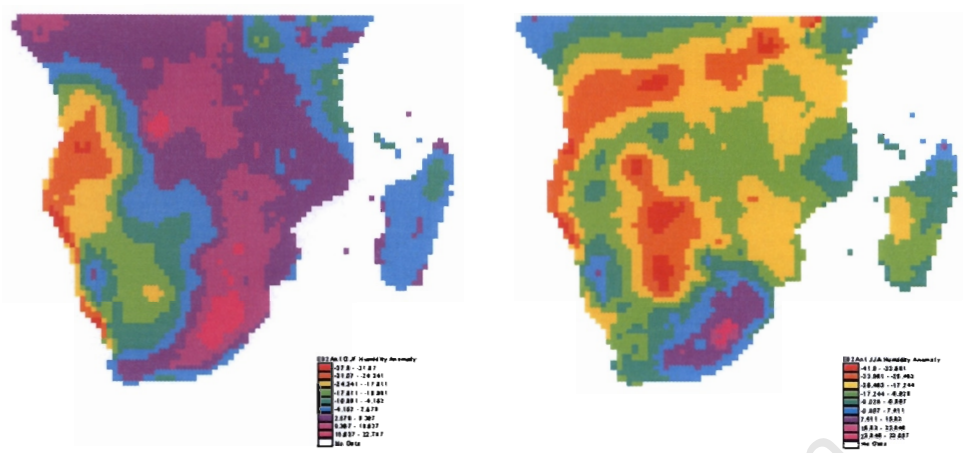

8. EHAM B2 Anomaly 1

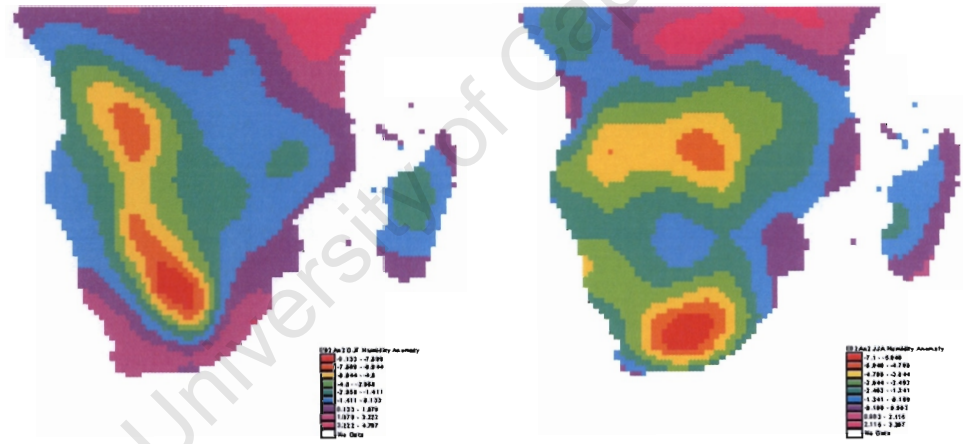

9. ECHAM B2 Anomaly 2

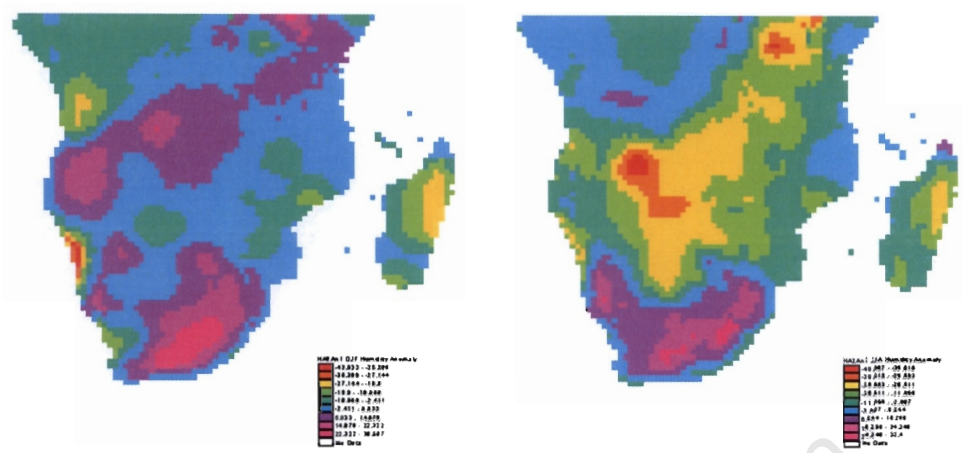

10. HadCM3 A2 Anomaly 1

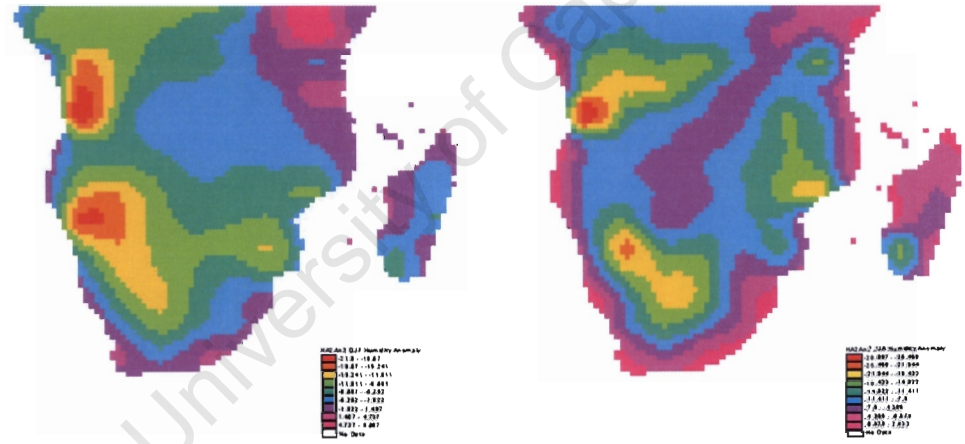

11. HadCM3 A2 Anomaly 2

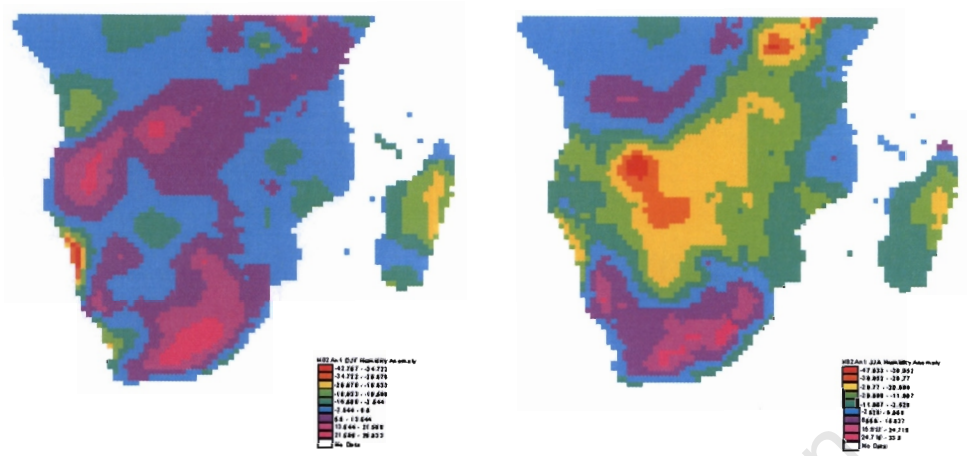

12. HadCM3 B2 Anomaly 1

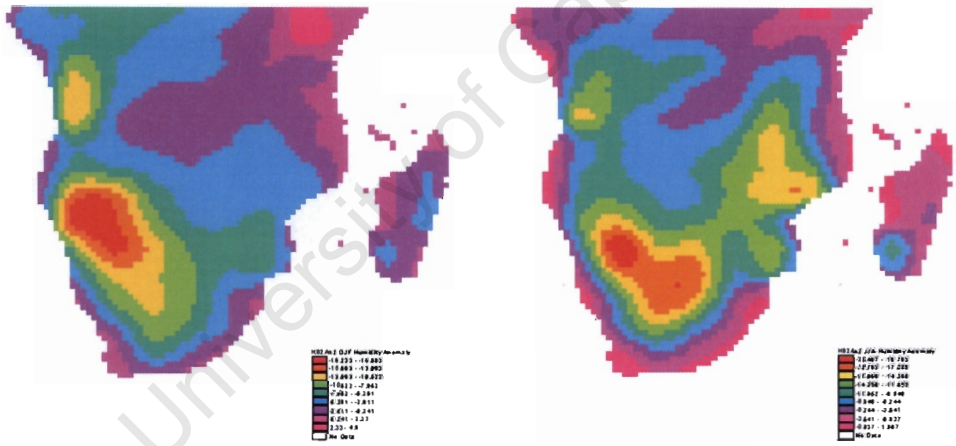

13. HadCM3 B2 Anomaly 2

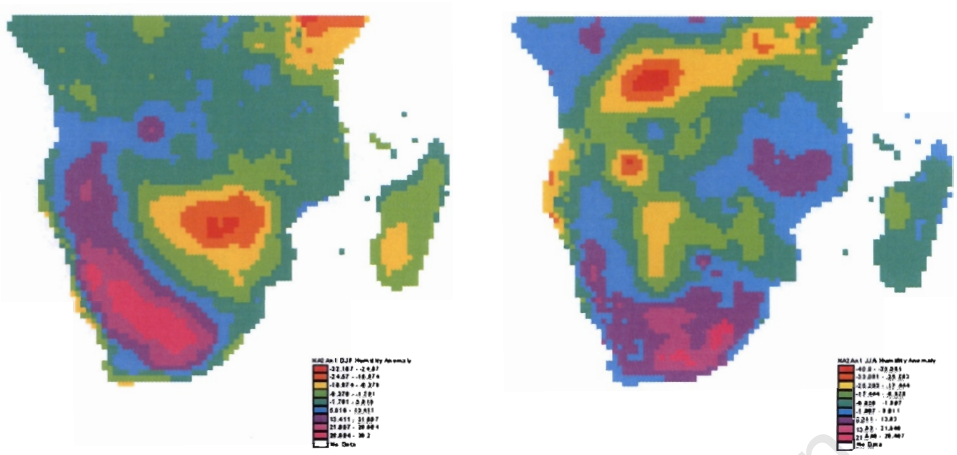

14. NCAR A2 Anomaly 1

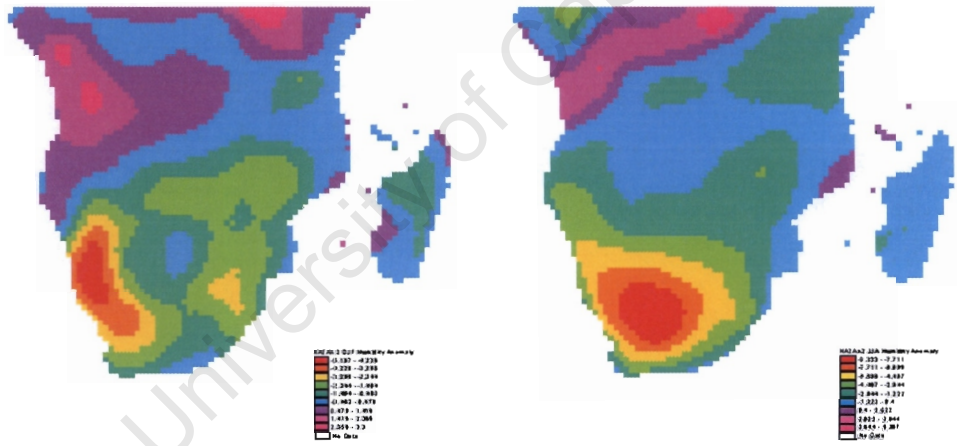

15. NCAR A2 Anomaly 2

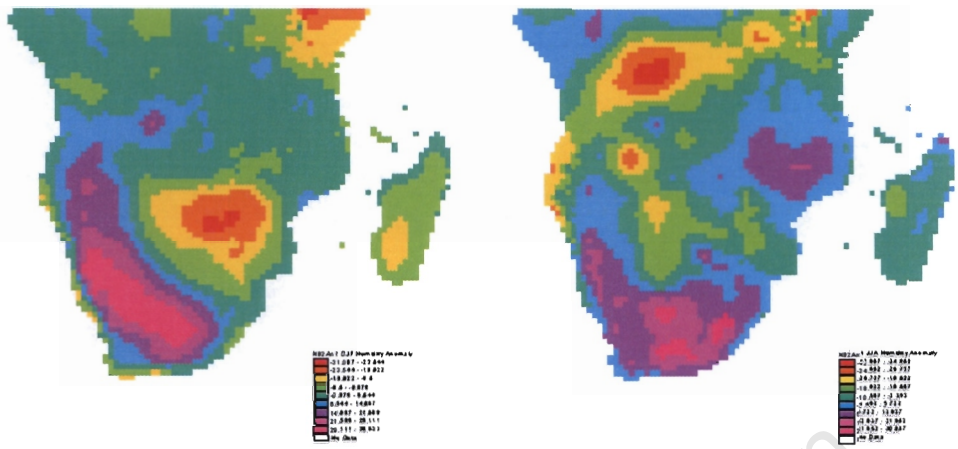

16. NCAR B2 Anomaly 1

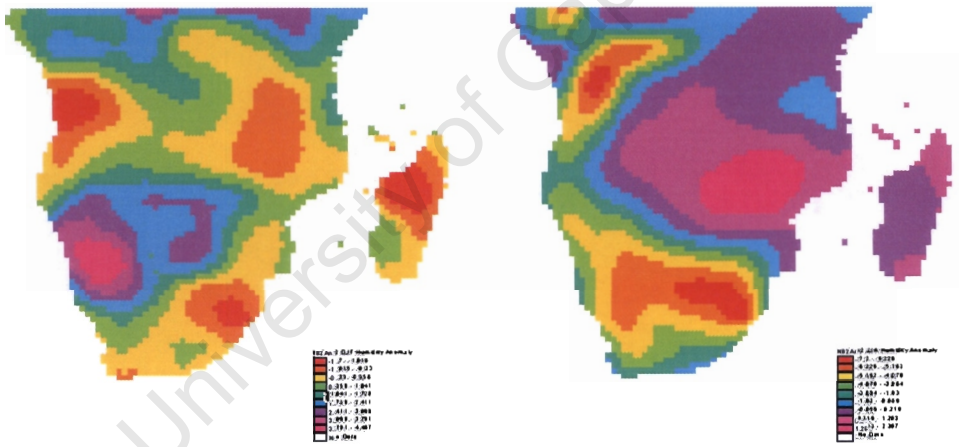

17. NCAR B2 Anomaly 2

8.1.2. PRECIPITATION

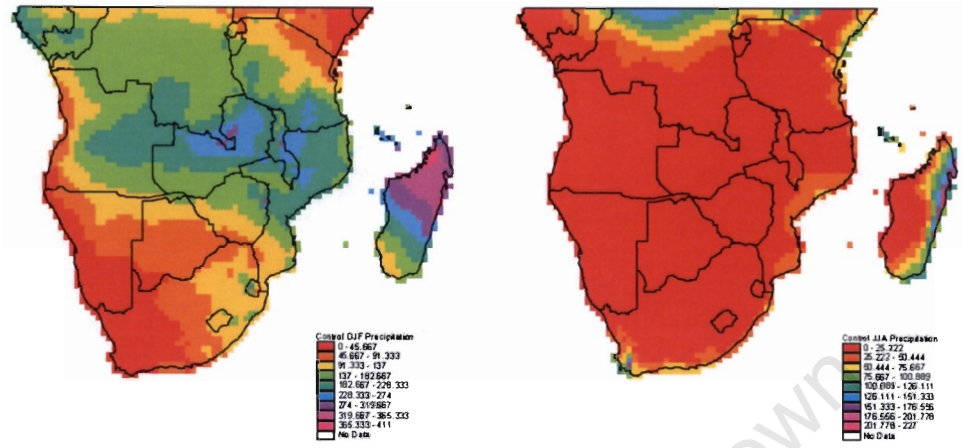

1. Control Precipitation (mm/month)

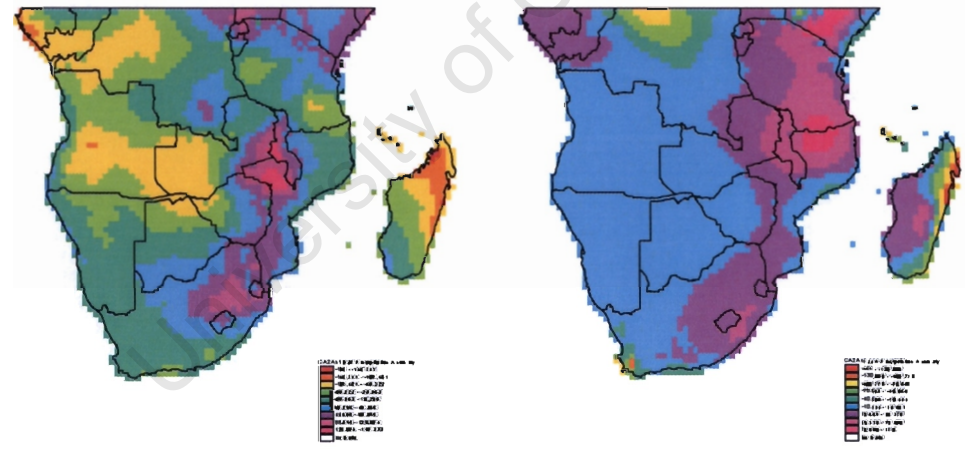

2. CCCMa A2 Anomaly 1

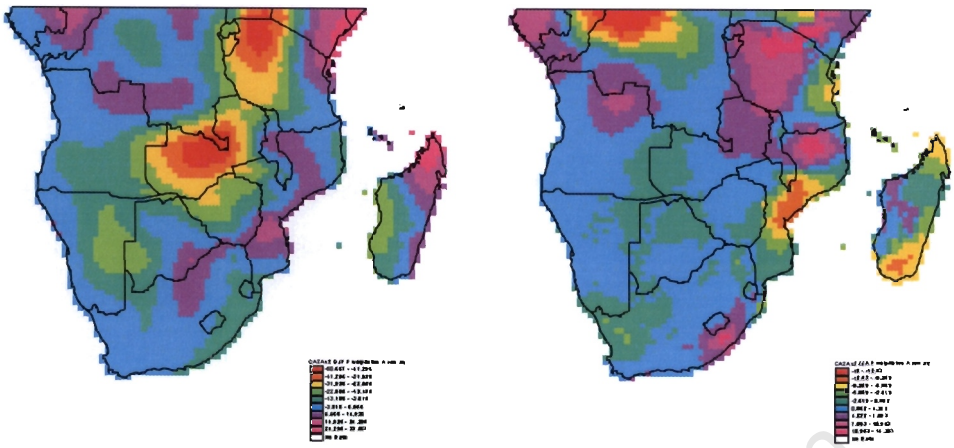

3. CCCMa A2 Anomaly 2

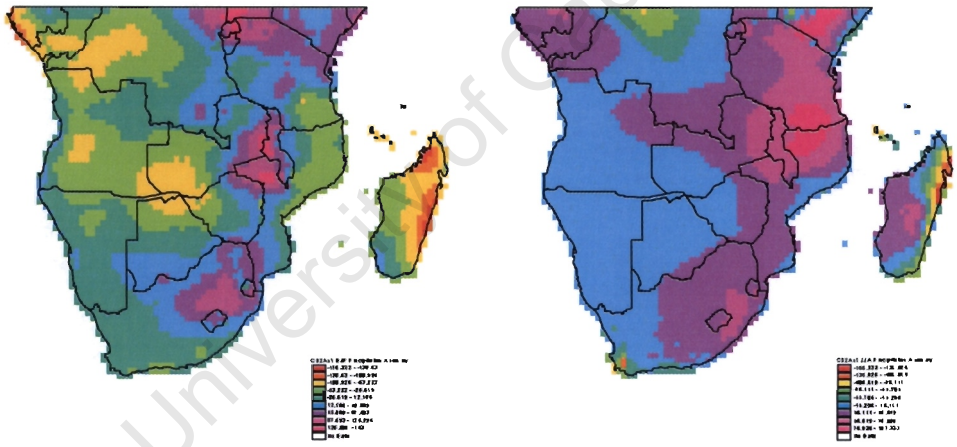

4. CCCMa B2 Anomaly 1

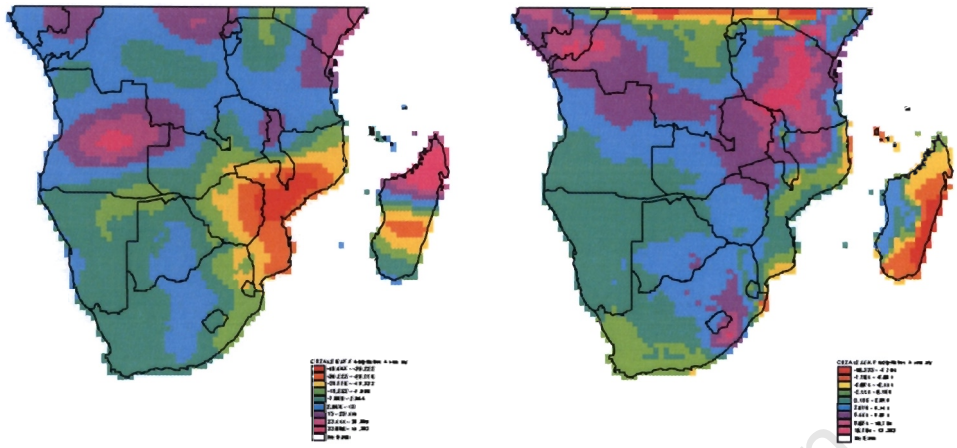

5. CCCMa B2 Anomaly 1

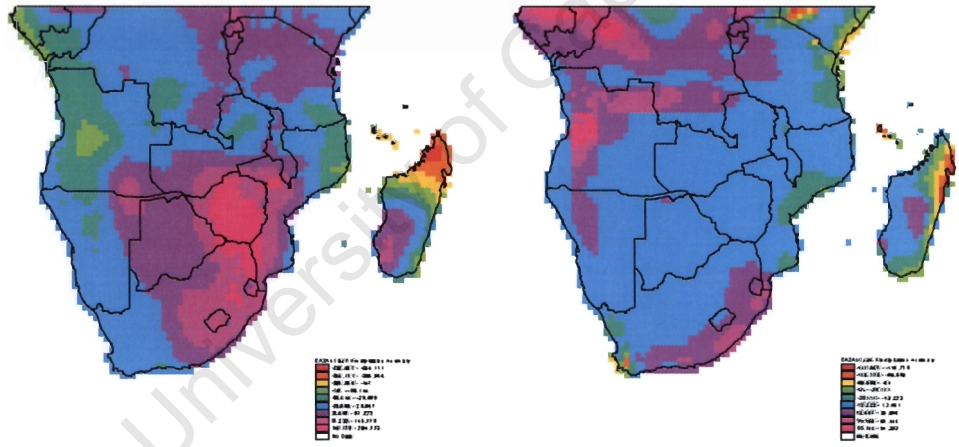

6. ECHAM A2 Anomaly 1

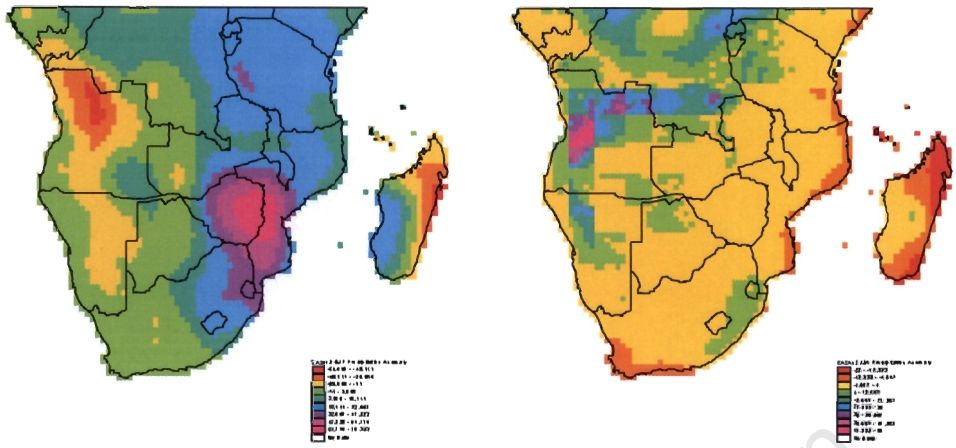

7. ECHAM A2 Anomaly 2

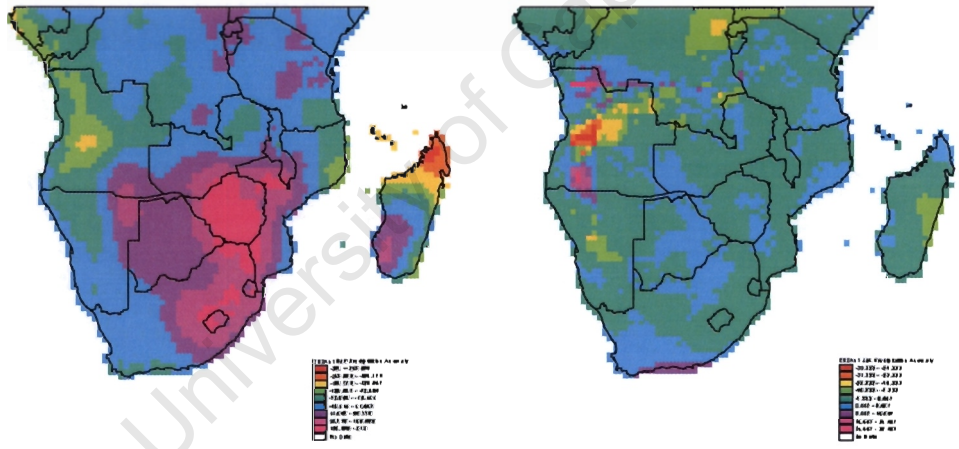

8. ECHAM B2 Anomaly 1

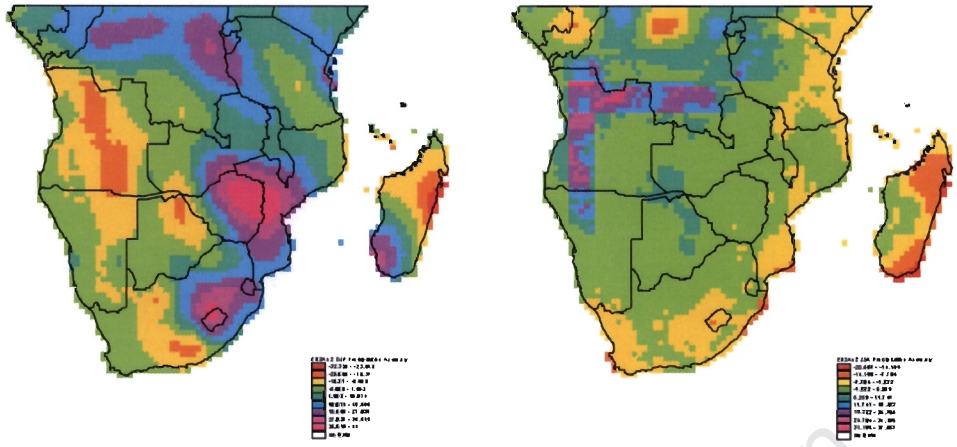

9. ECHAM B2 Anomaly 2

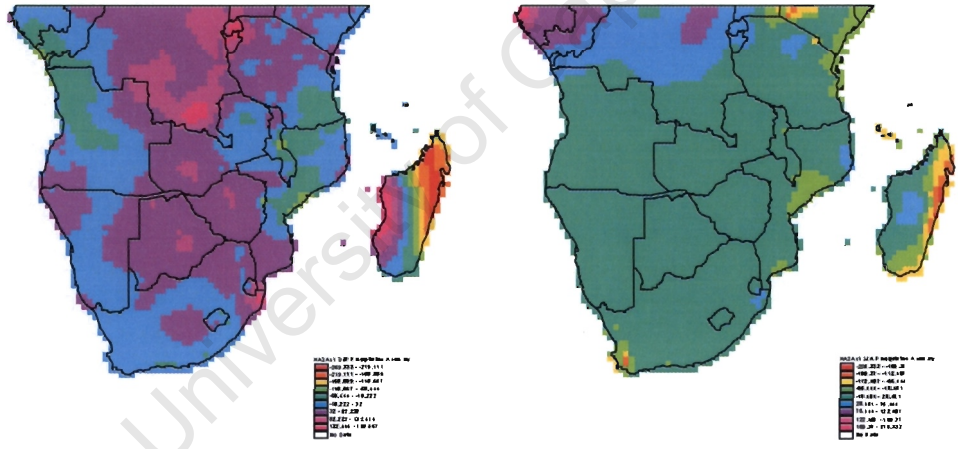

10. HadCM3 A2 Anomaly 1

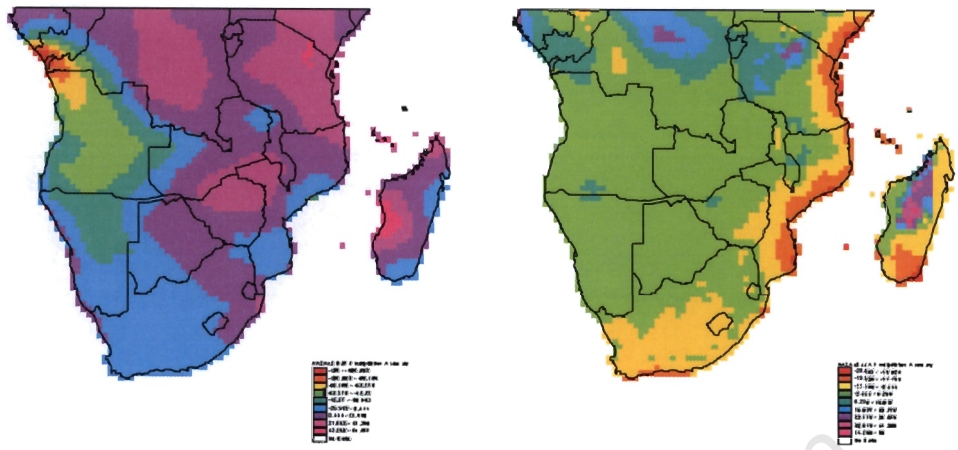

11. HadCM3 A2 Anomaly 2

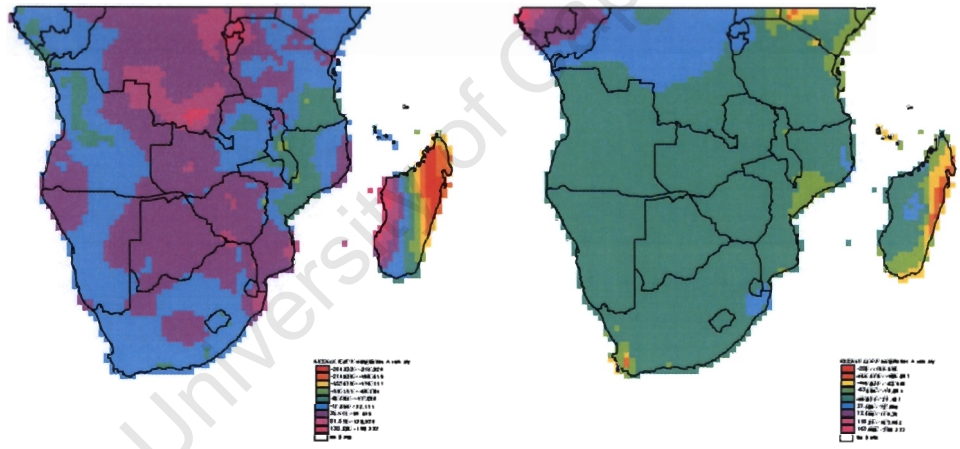

12. HadCM3 B2 Anomaly 1

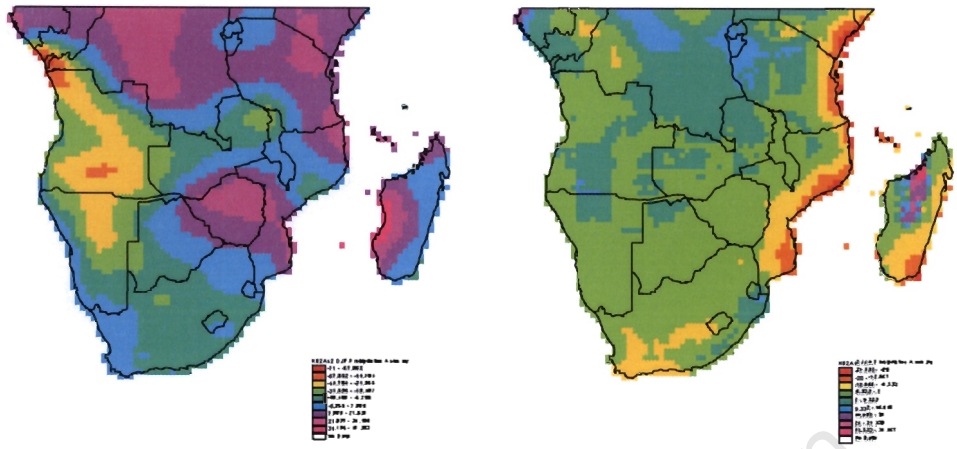

13. HadCM3 B2 Anomaly 2

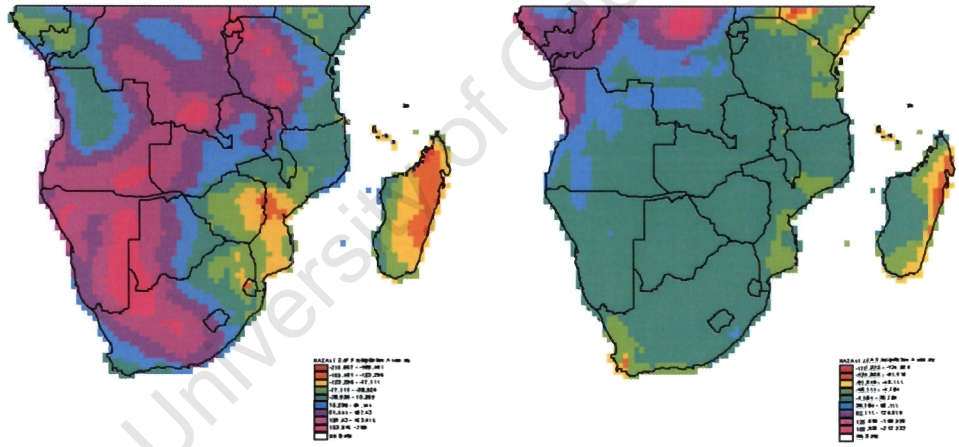

14. NCAR A2 Anomaly 1

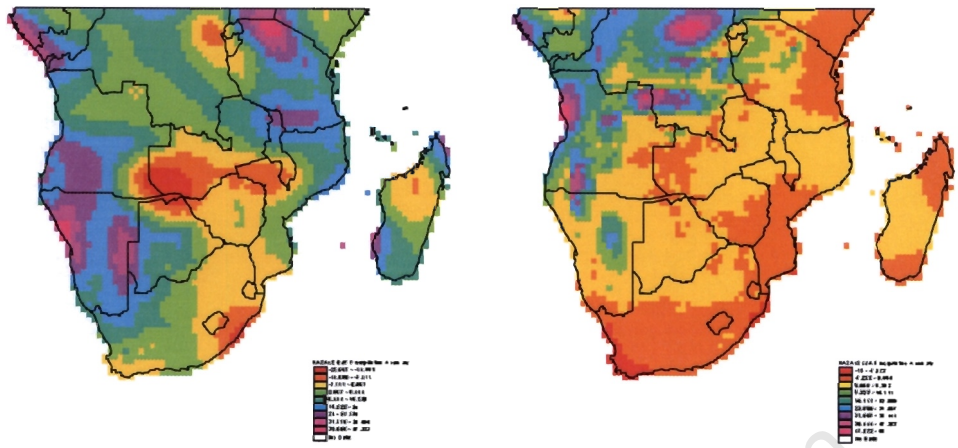

15. NCAR A2 Anomaly 2

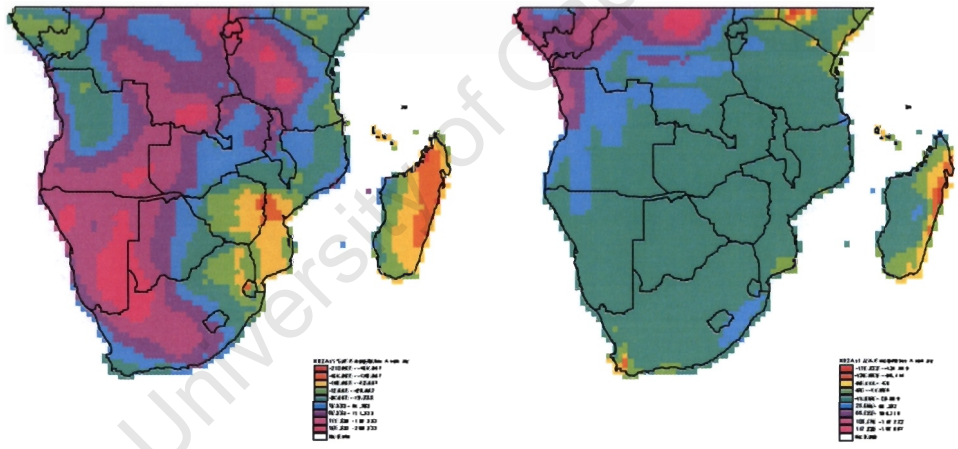

16. NCAR B2 Anomaly 1

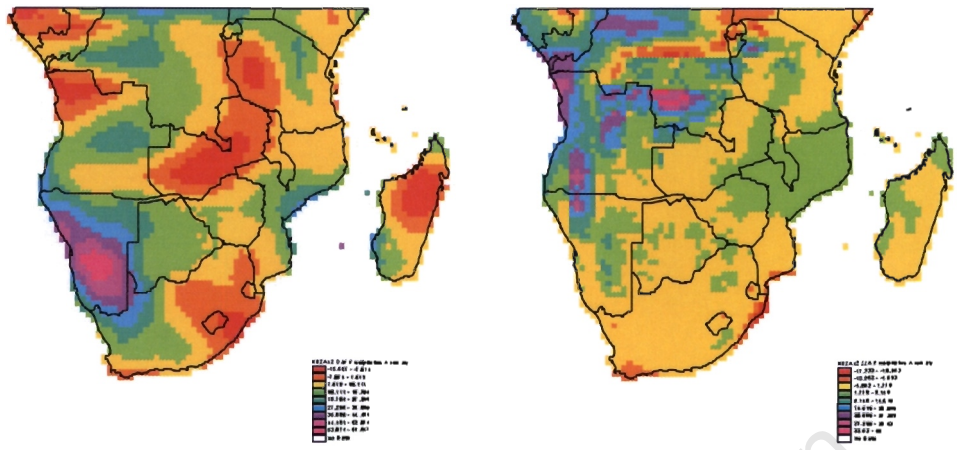

17. NCAR B2 Anomaly 2

8.1.3. TEMPERATURE

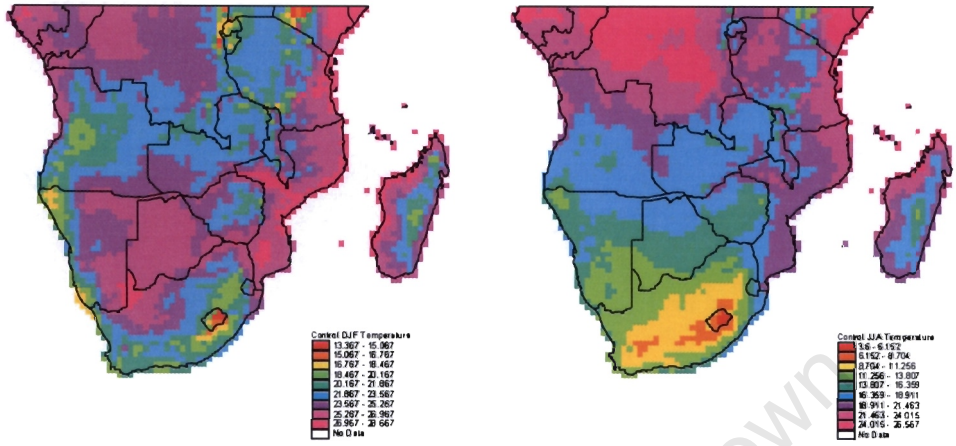

1. Control Temperature (ºC)

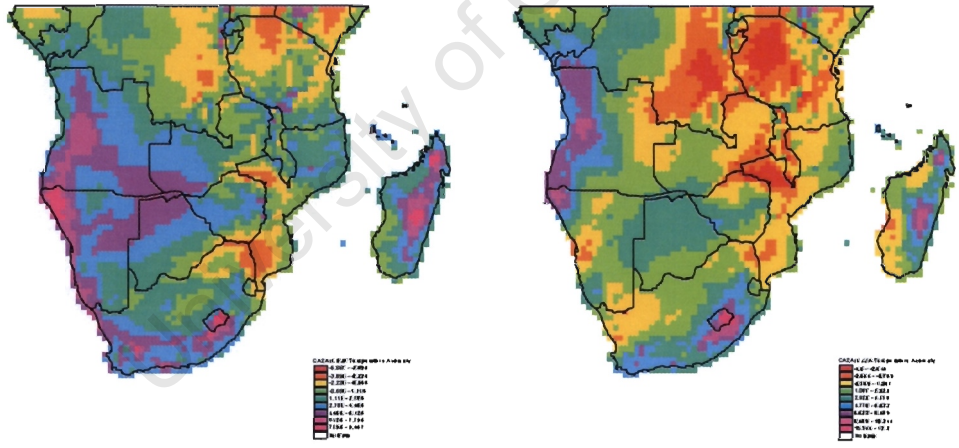

2. CCCMa A2 Anomaly 1

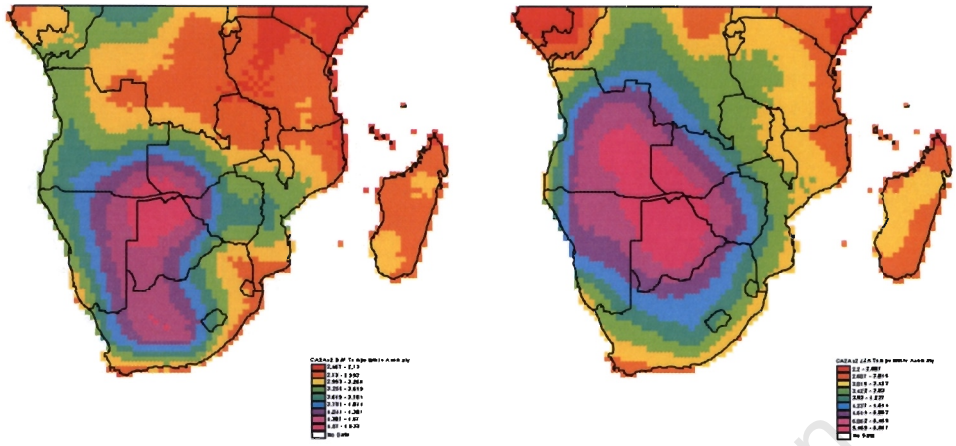

3. CCCMa A2 Anomaly 2

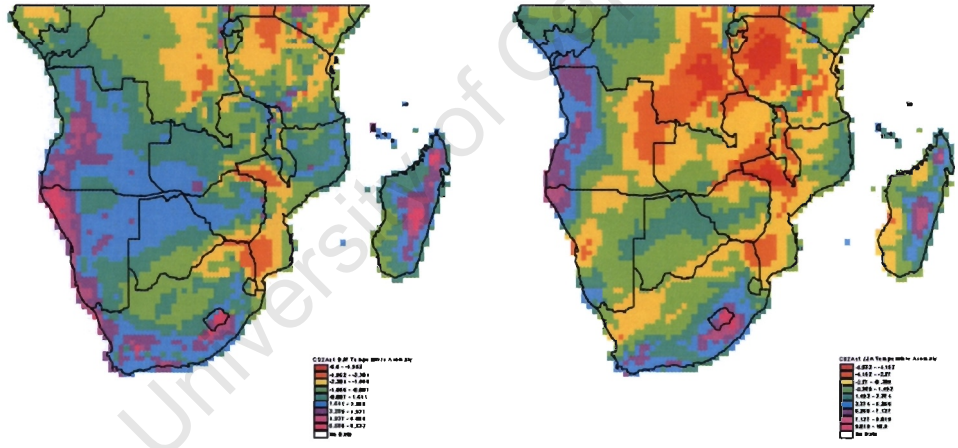

4. CCCMa B2 Anomaly 1

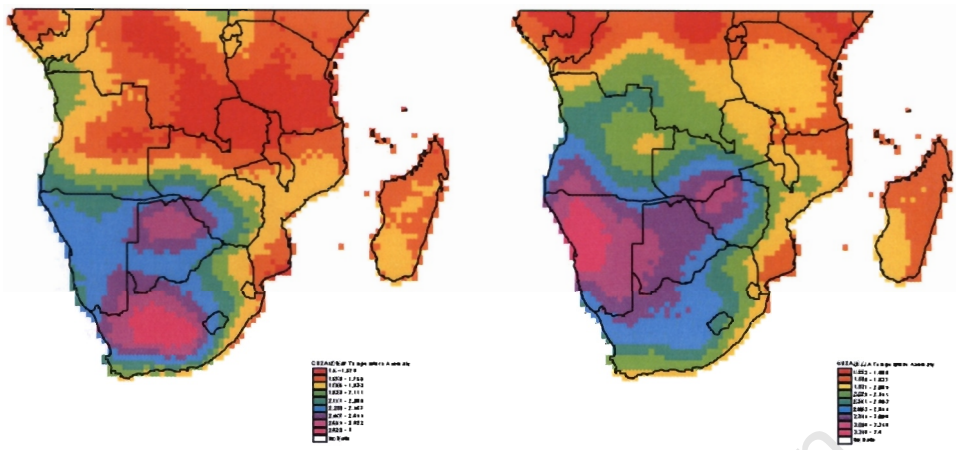

5. CCCMa B2 Anomaly 1

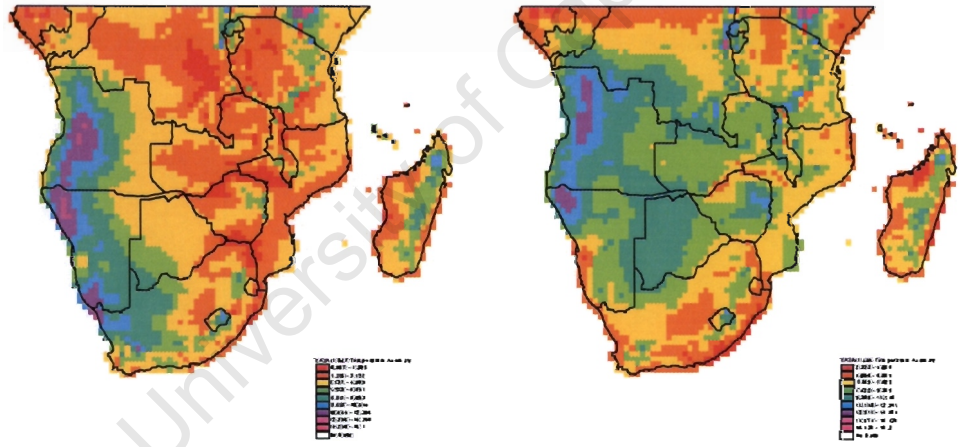

6. ECHAM A2 Anomaly 1

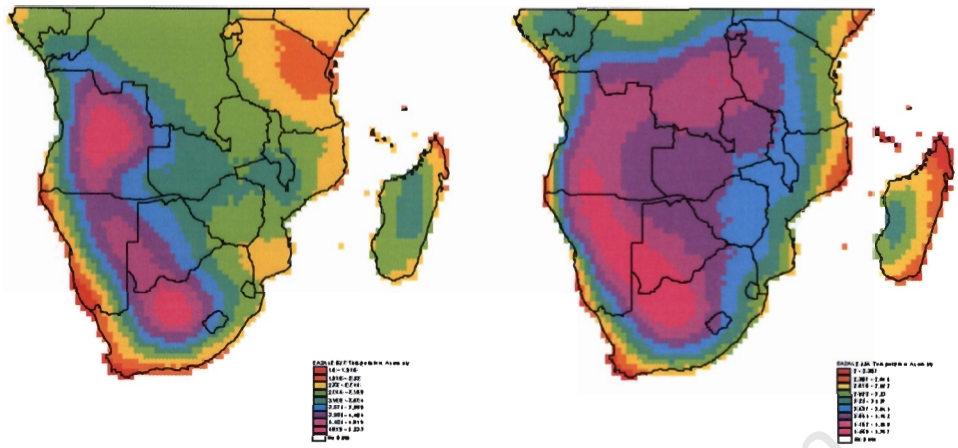

7. ECHAM A2 Anomaly 2

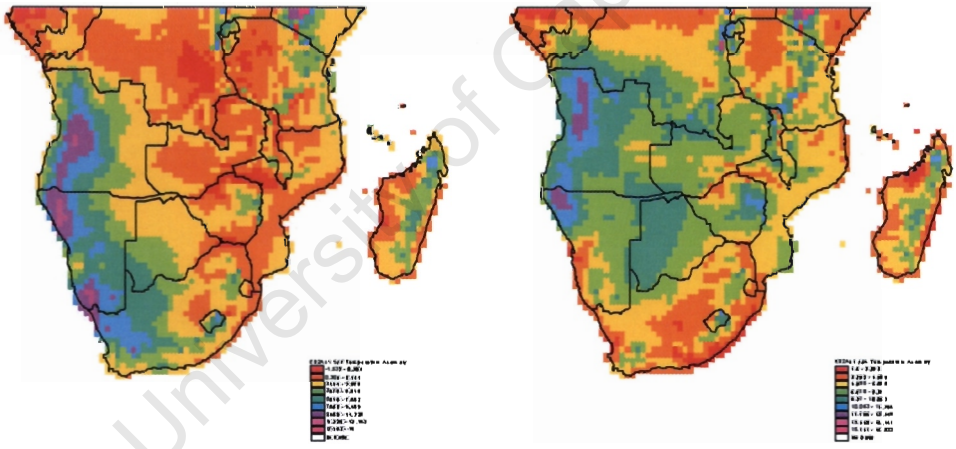

8. ECHAM B2 Anomaly 1

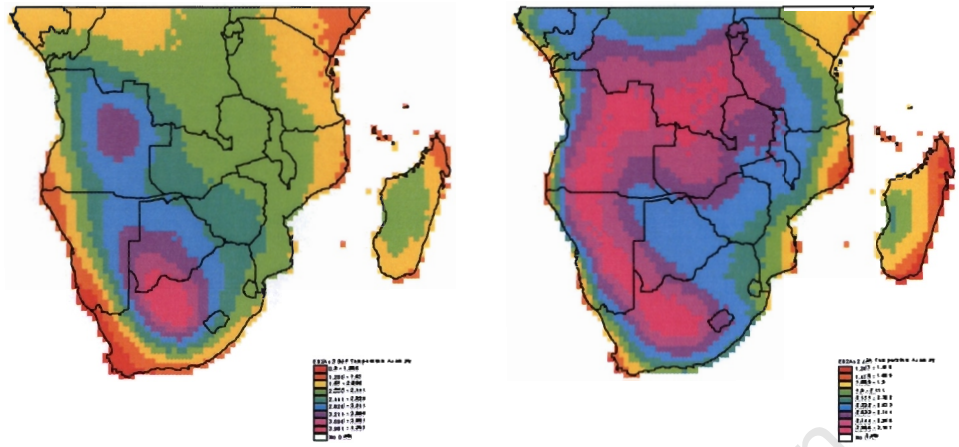

9. ECHAM B2 Anomaly 2

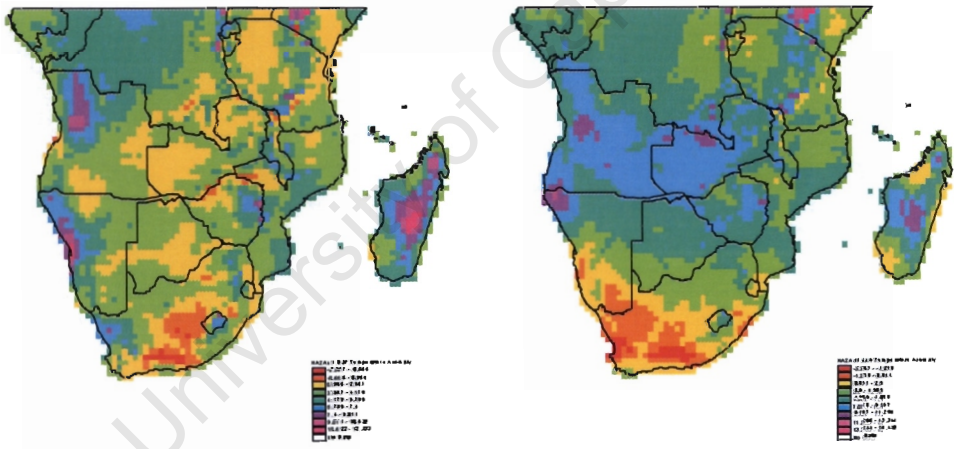

10. HadCM3 A2 Anomaly 1

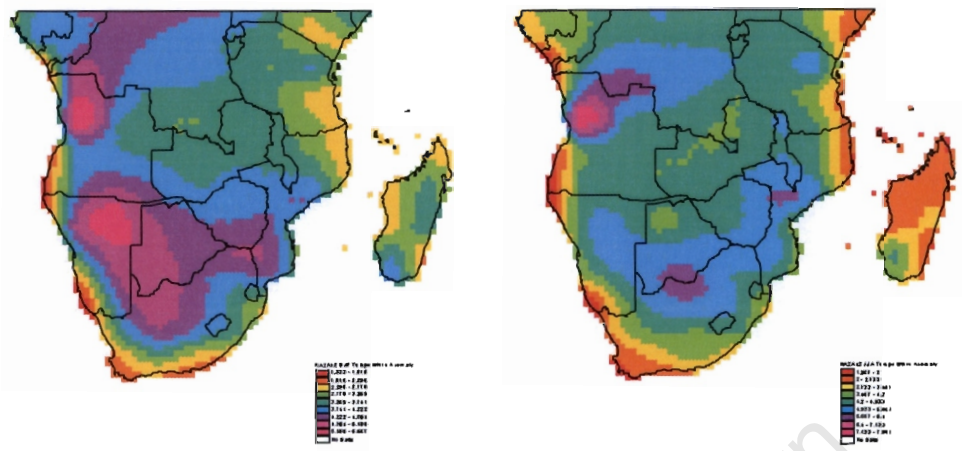

11. HadCM3 A2 Anomaly 2

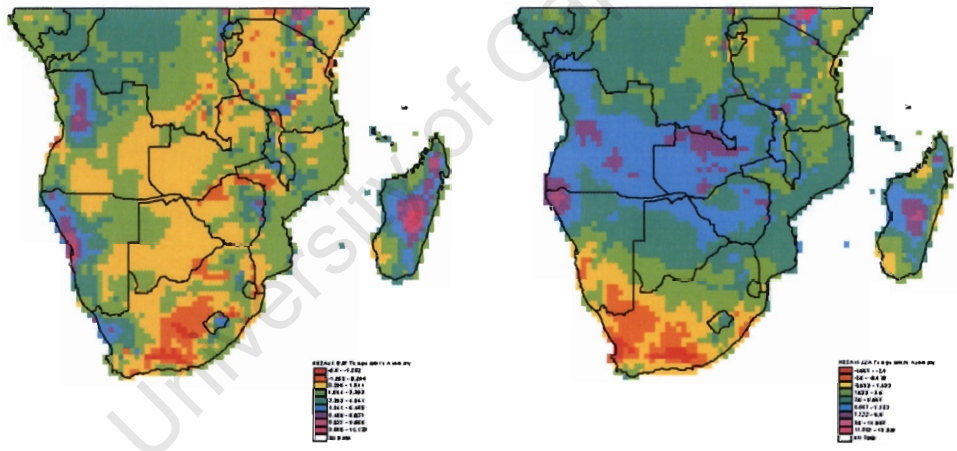

12. HadCM3 B2 Anomaly 1

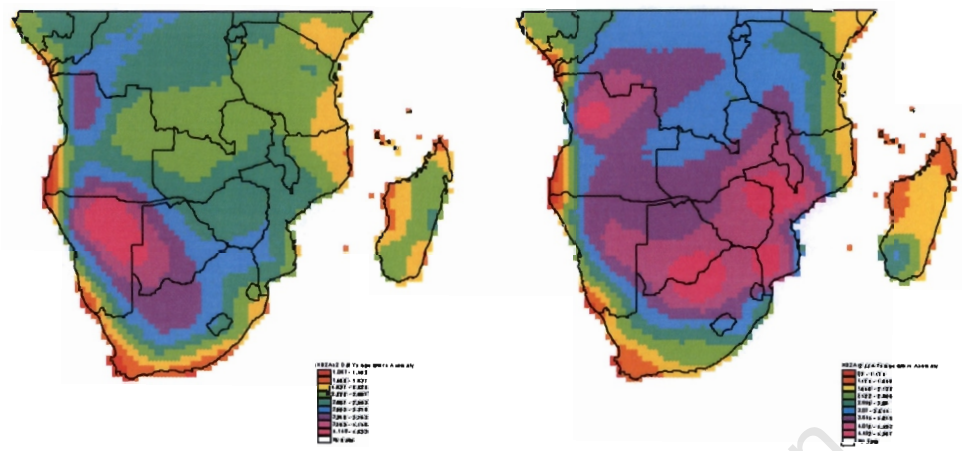

13. HadCM3 B2 Anomaly 2

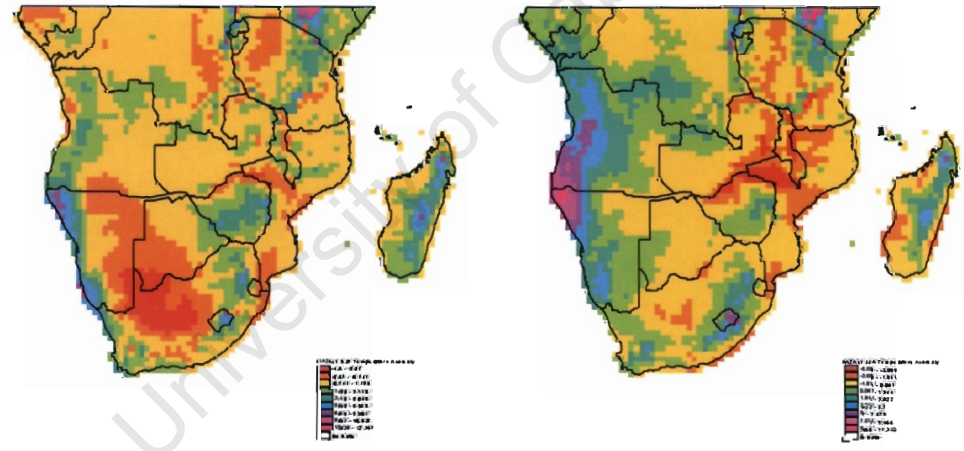

14. NCAR A2 Anomaly 1

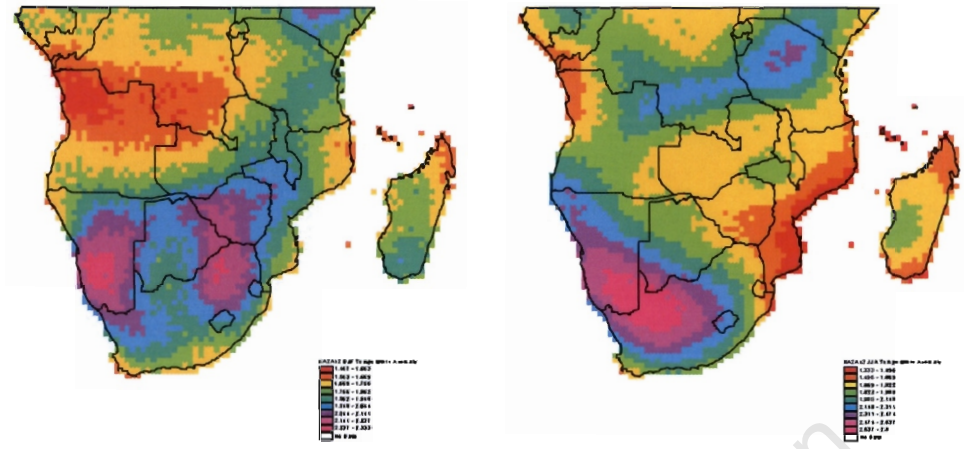

15. NCAR A2 Anomaly 2

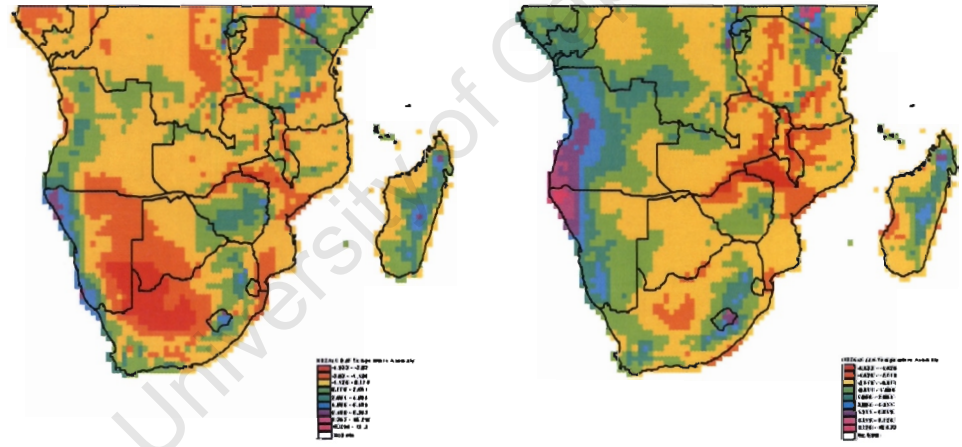

16. NCAR B2 Anomaly 1

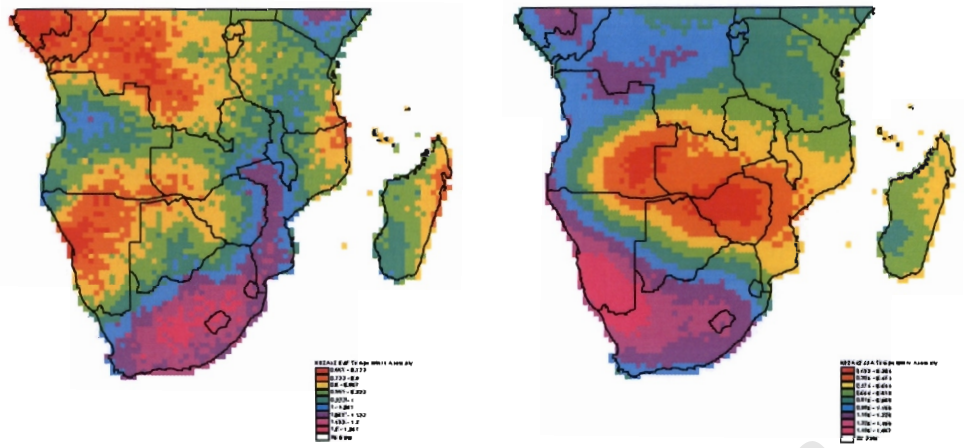

17. NCAR B2 Anomaly 2

APPENDIX 8.2: THE VEGETATION DISTRIBUTION UNDER FUTURE CLIMATE CHANGE AND FUTURE CO_2 CONCENTRATIONS

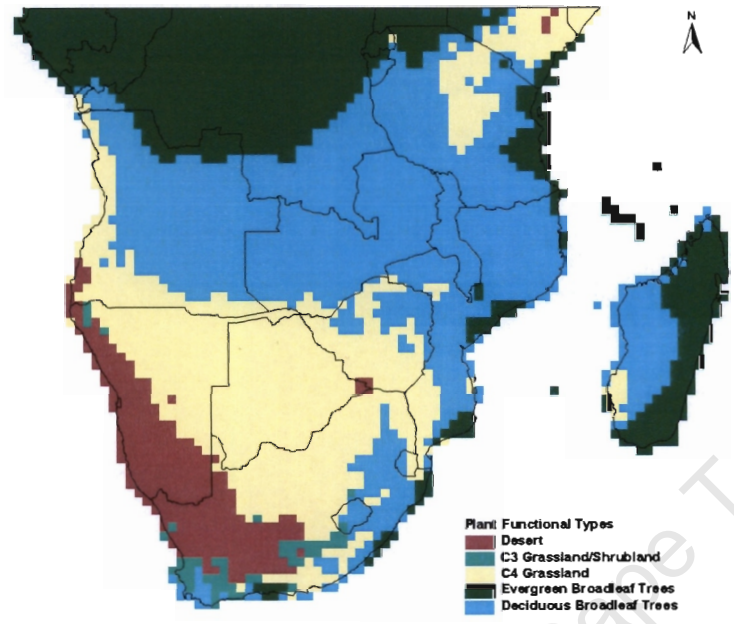

1. Control

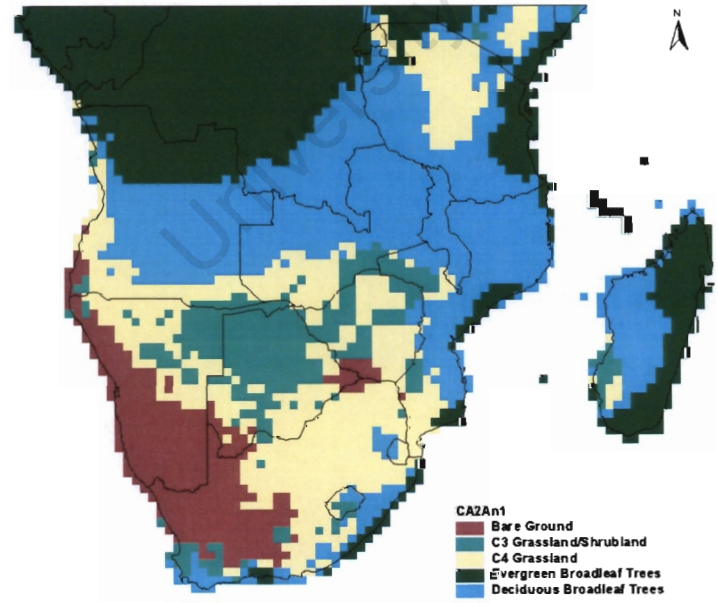

2. CCCMa A2 Anomaly 1

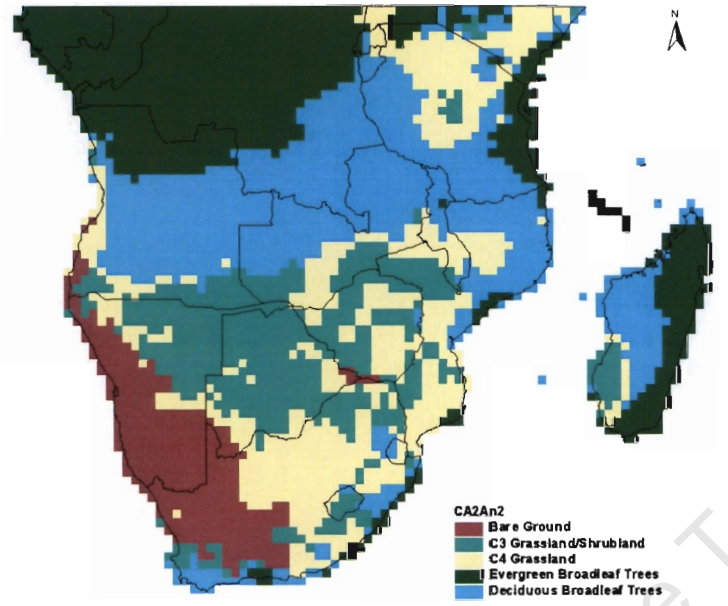

3. CCCMa A2 Anomaly 2

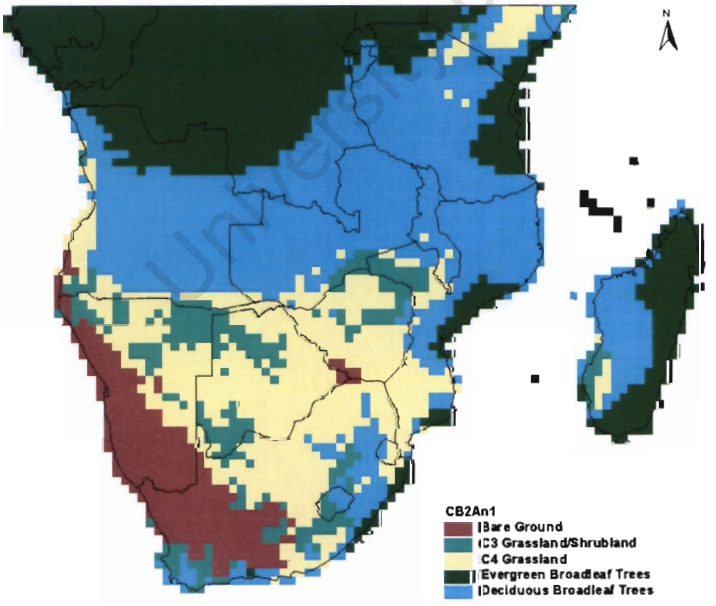

4. CCCMa B2 Anomaly 1

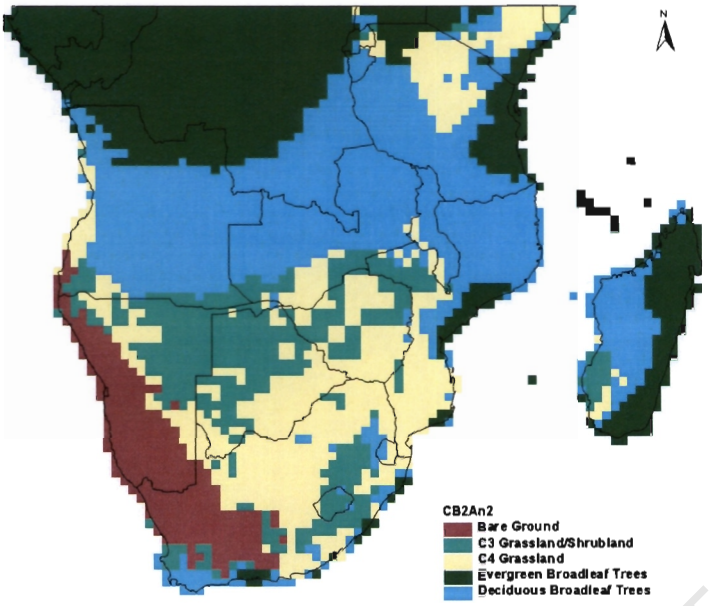

5. CCCMa B2 Anomaly 2

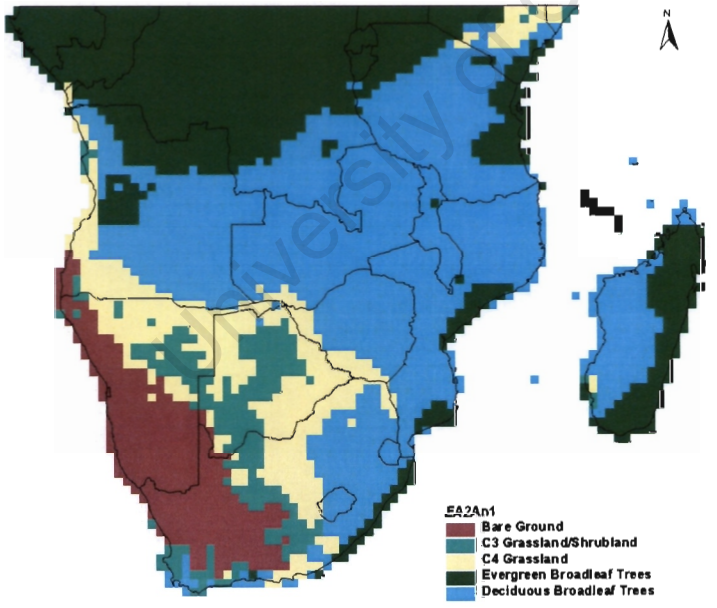

6. ECHAM A2 Anomaly 1

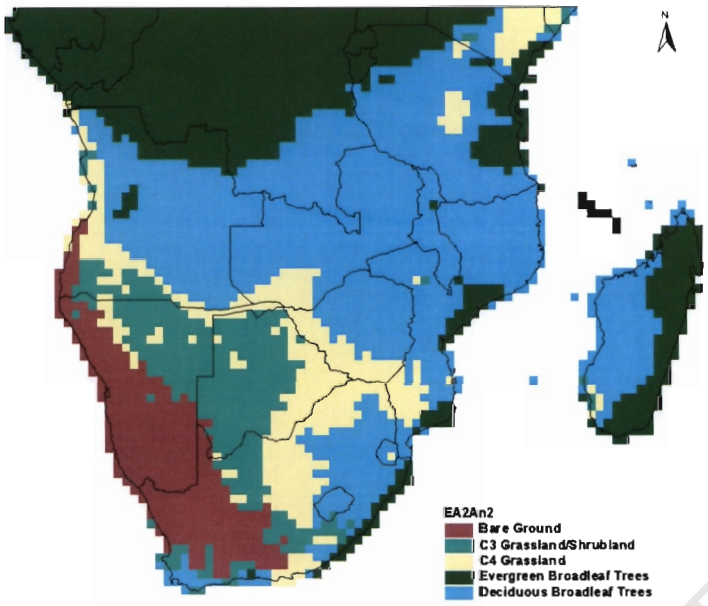

7. ECHAM A2 Anomaly 2

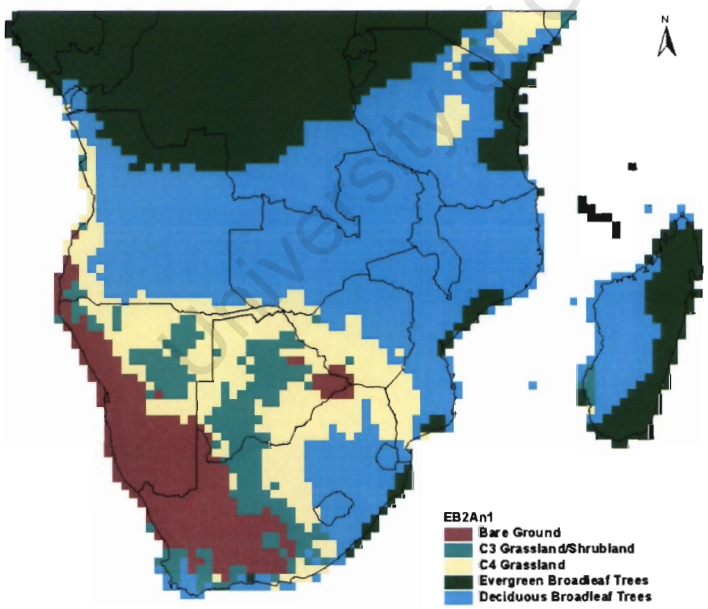

8. ECHAM B2 Anomaly 1

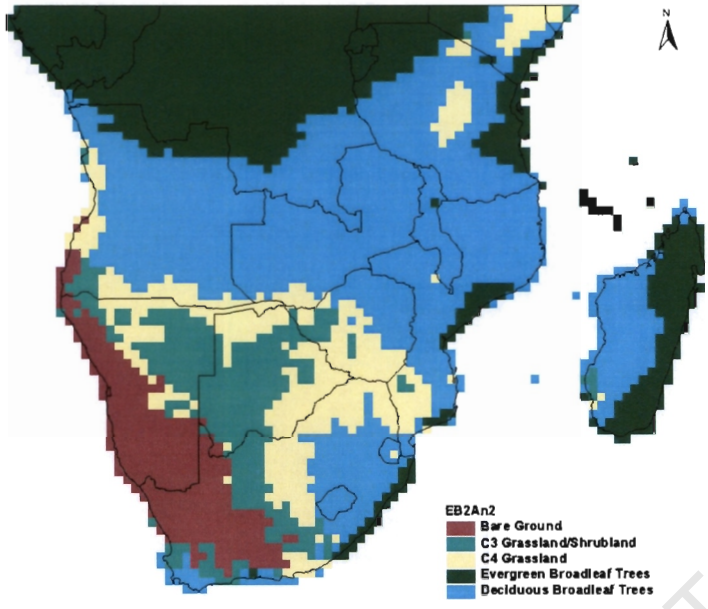

9. ECHAM B2 Anomaly 2

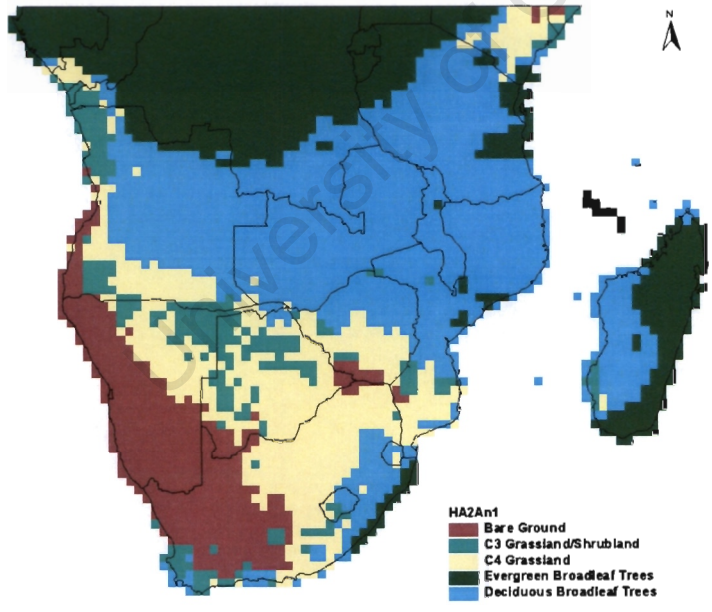

10. HadCM3 A2 Anomaly 1

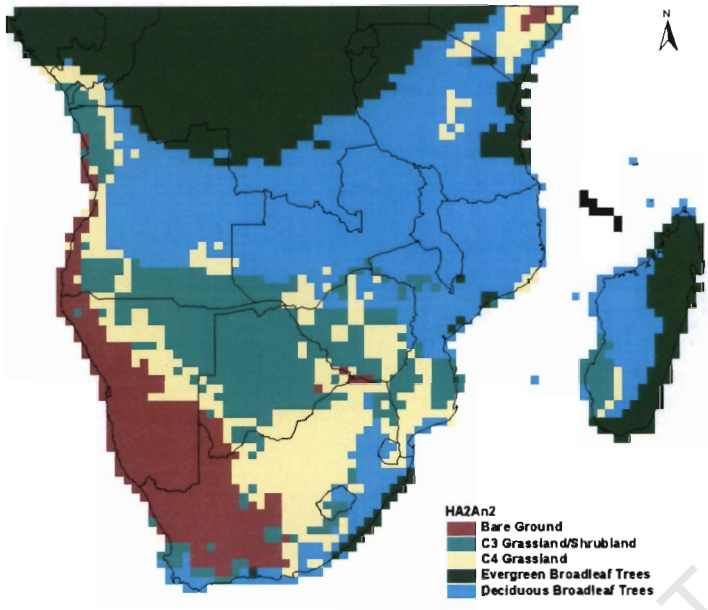

11. HadCM3 A2 Anomaly 2

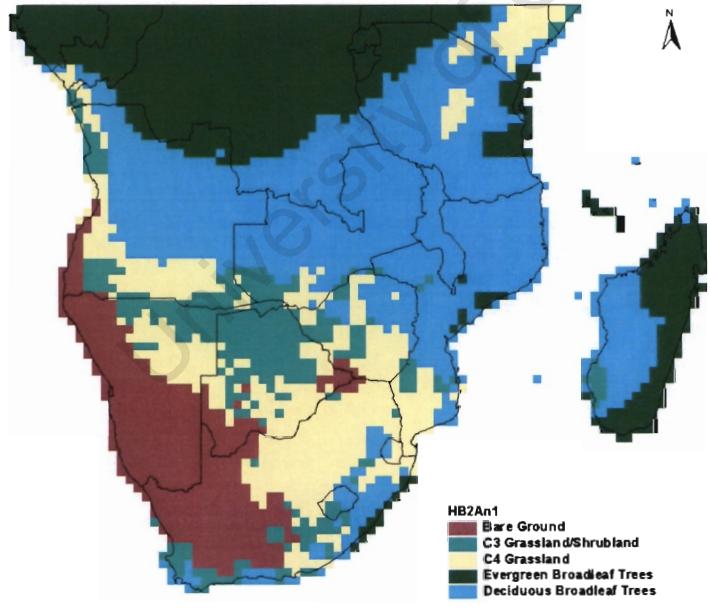

12. HadCM3 B2 Anomaly 1

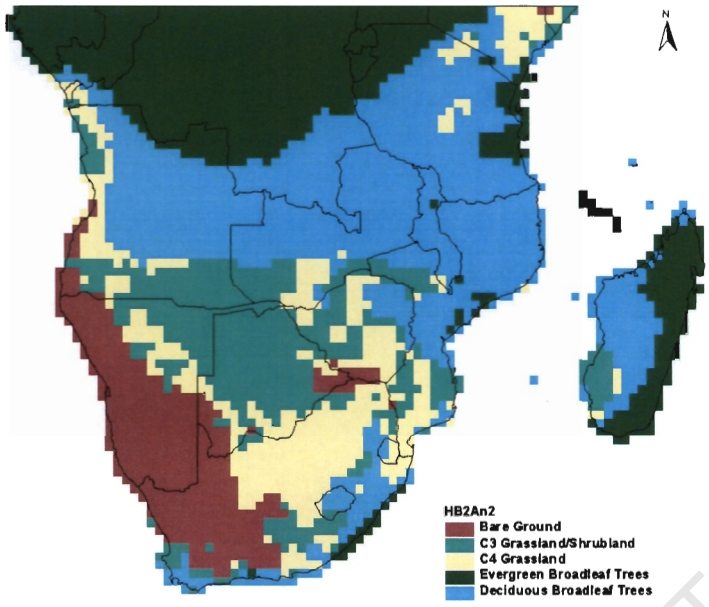

13. HadCM3 B2 Anomaly 2

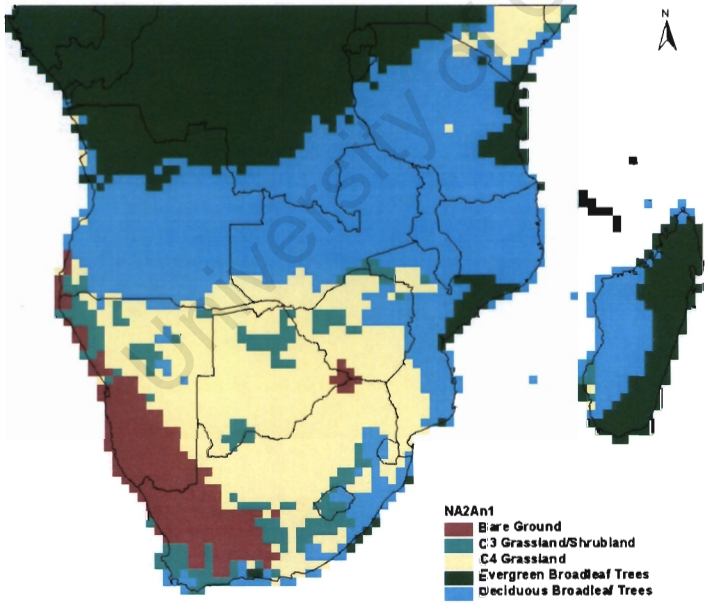

14. NCAR A2 Anomaly 1

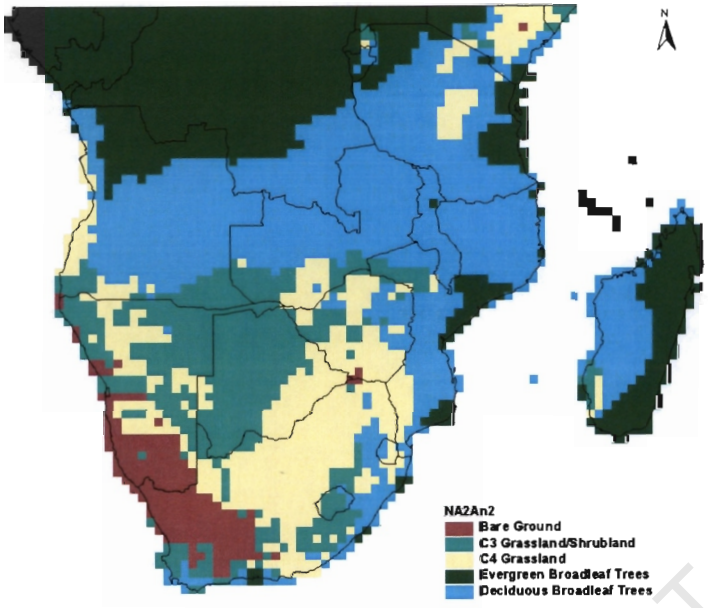

15. NCAR A2 Anomaly 2

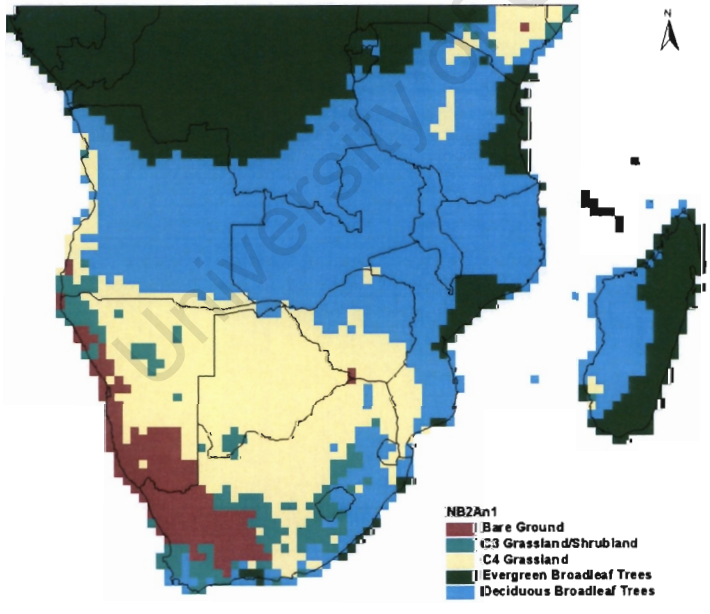

16. NCAR B2 Anomaly 1

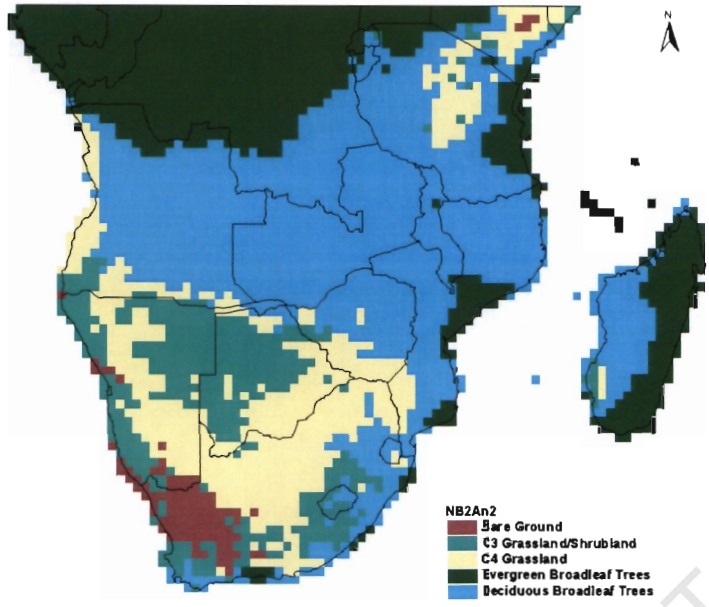

17. NCAR B2 Anomaly 2

APPENDIX 8.3: THE VEGETATION DISTRIBUTION UNDER FUTURE CLIMATE CHANGE AND CURRENT CO_2 CONCENTRATIONS FOR ANOMALY 1 ONLY

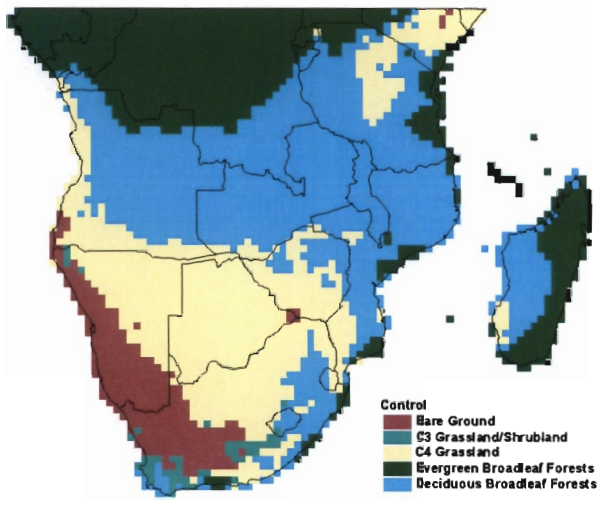

1. Control

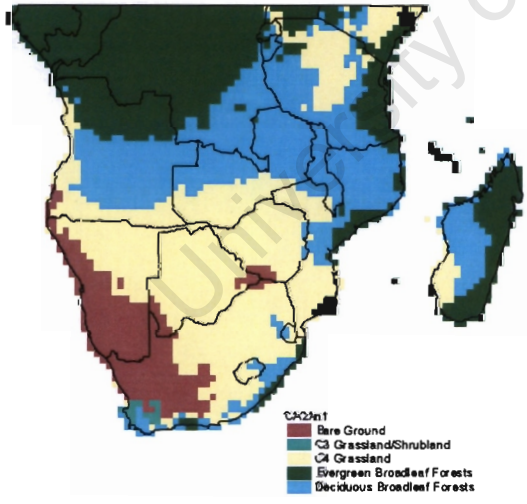

2. CCCMa A2

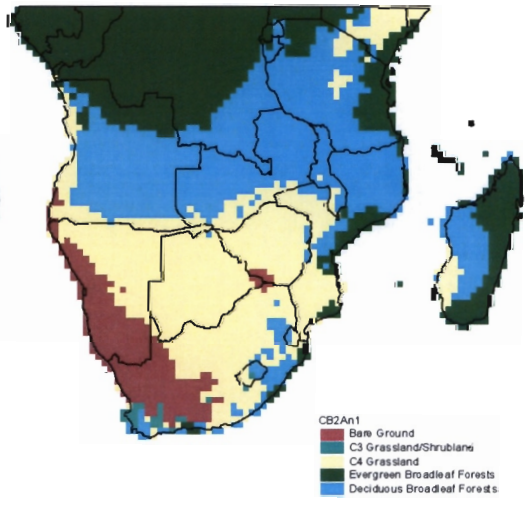

3. CCCMa B2

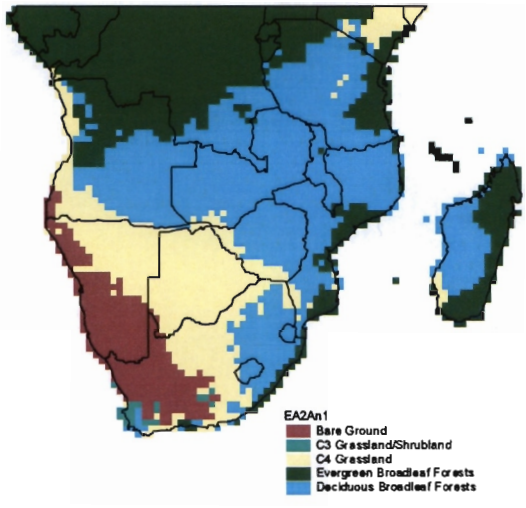

4. ECHAM A2

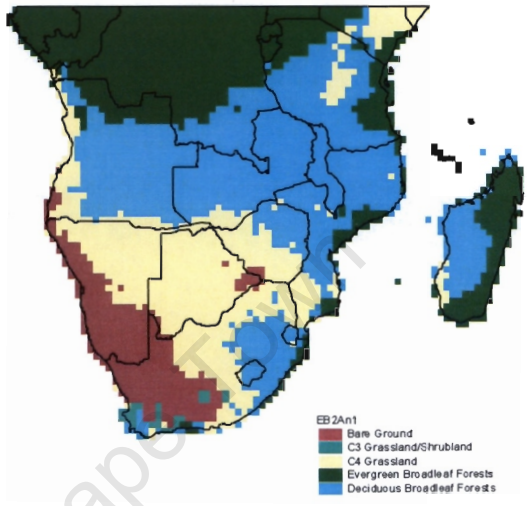

5. ECHAM B2

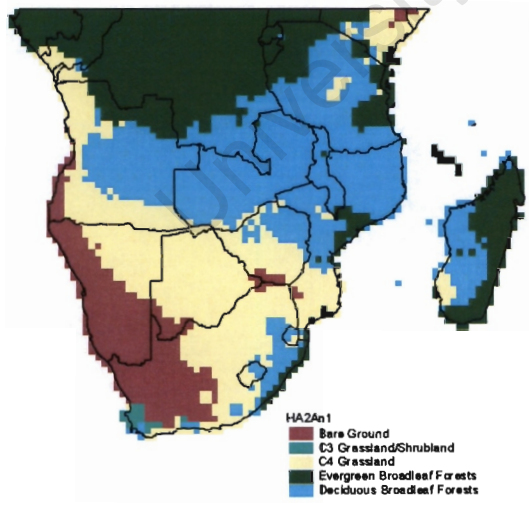

6. HadCM3 A2

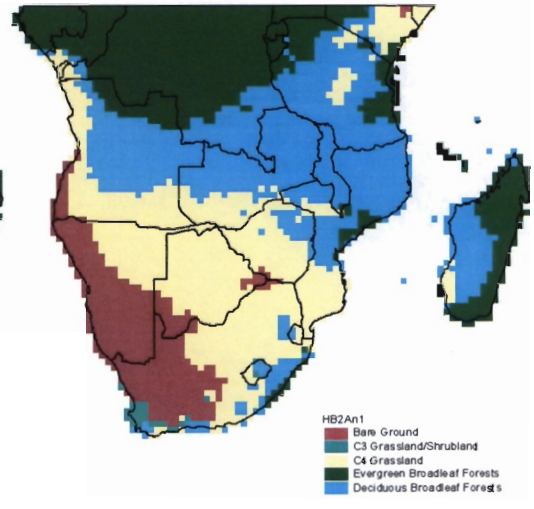

7. HadCM3 B2

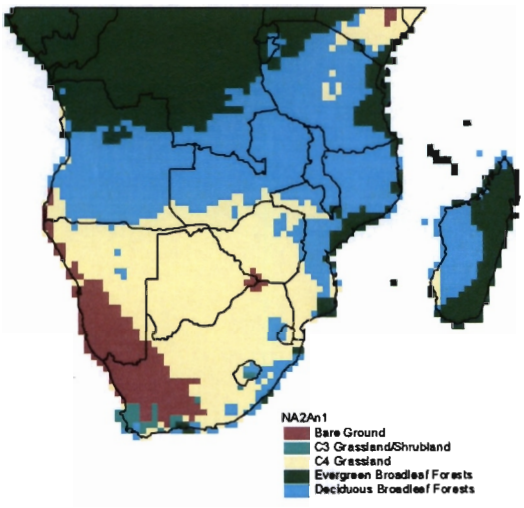

8. NCAR A2

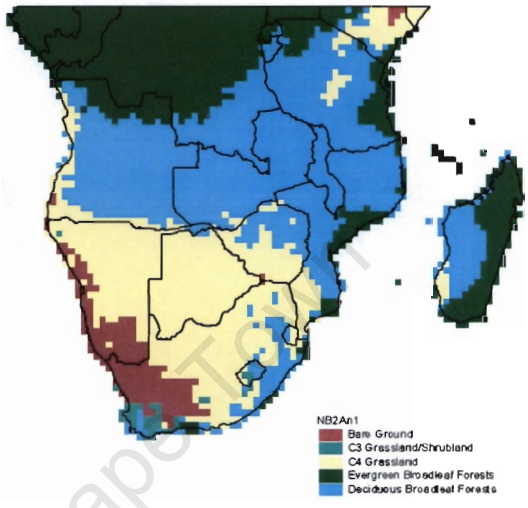

9. NCAR B2